

# IRANIAN JOURNAL



University of Kashan

## OF MATHEMATICAL CHEMISTRY

### Editor-in-Chief:

A R Ashrafi (University of Kashan, Iran)

### Managing Director:

B Bazigaran (University of Kashan, Iran)

### Language Editor:

S Mosazadeh (University of Kashan, Iran)

### Technical Manager:

M Pourbabaee (University of Kashan, Iran)

### Editorial Board:

A R Ashrafi (University of Kashan, Iran)

B Bazigaran (University of Kashan, Iran)

M R Darafsheh (University of Tehran, Iran)

M Deza (École Normale Supérieure, France)

M Diudea (Babes-Bolyai University, Romania)

T Došlić (University of Zagreb, Croatia)

A Gholami (University of Qom, Iran)

I Gutman (University of Kragujevac, Serbia)

A Iranmanesh (Tarbiat Modares University, Iran)

M A Iranmanesh (Yazd University, Iran)

P E John (Technical University of Ilmenau, Germany)

S Klavžar (University of Maribor, Slovenia)

X Li (Nankai University, China)

H R Maimani (Shahid Rajaee Teacher Training University, Iran)

O Ori (Actinum Chemical Research, Italy)

M V Puts (West University of Timisoara, Romania)

M Salavati-Niasari (University of Kashan, Iran)

B Shareghi-Boroujeni (University of Shahrkord, Iran)

B Taeri (Isfahan University of Technology, Iran)

H Yousefi-Azari (University of Tehran, Iran)

S Yousefi (Malek-Ashtar University Of Technology, Iran)

B Zhou (South China Normal University, China)

### Past Editor

A Graovac (Ruder Boskovic institute, Croatia)

<http://IJMC.Kashanu.ac.ir>

## Iranian Journal of Mathematical Chemistry

Iranian Journal of Mathematical Chemistry (IJMC) publishes quality original research papers and survey articles in Mathematical Chemistry and related areas that are of the highest possible quality.

Research papers and review articles are selected through a normal refereeing process by a member of editorial board.

It is intended that the journal may act as an interdisciplinary forum for publishing chemically important mathematical papers. Papers published in this journal must have a clear connection to chemistry with non-trivial mathematics.

**Aims and Scopes:** Iranian Journal of Mathematical Chemistry is a bi publication of the University of Kashan. It contains research and expository papers as well as short communications on chemically important mathematical problems.

**Preparation of Manuscripts:** An abstract of 150 words or less and keywords clarifying the subject of the manuscripts are required. Authors should submit the paper electronically in word file to [ijmc@kashanu.ac.ir](mailto:ijmc@kashanu.ac.ir).

The language of the journal is English. Authors who are less familiar with English language are advised to seek assistance from proficient scholars to prepare manuscripts that are grammatically and linguistically free from errors. Manuscripts should be typed with double spacing and wide margins. Papers submitted for consideration for publication have to be prepared concisely and must not exceed 30 typewritten pages, (font 12, 1.15 spacing, including tables & graphs). Diagrams and figures should be submitted as original drawings. Figures and tables are to be numbered in the sequence in which they are cited in the manuscript. Every table must have a caption that explains its content. Tables and diagrams are to be prepared in separate pages and placed at the end of the manuscript. References to the literature should be numbered in square brackets in the order in which they appear in the text. A complete list of references should be presented in numerical order at the end of the manuscript. References to journals, books, proceedings and patents must be presented in accordance with the following examples:

**Journals:** I. Gutman, B. Zhou and B. Furtula, The Laplacian-energy like invariant is an energy like invariant MATCH Commun. Math. Comput. Chem., 64(1) (2010), 85-96.

**Patents:** Primack, H.S.; Method of Stabilizing Polyvalent Metal Solutions, U.S. patent No. 4, 373, 104(1983).

**Indexing/ Abstracting:** The Iranian Journal of Mathematical Chemistry is indexed/abstracted in the following:

- Islamic World Science Citation Center (ISC)
- Zentralblatt für Mathematik
- Web of Science (ISI)

# EditorialBoard

<b>ARAshrafi</b>	University of Kashan, IR Iran E-mail: <a href="mailto:ashrafi@kashanu.ac.ir">ashrafi@kashanu.ac.ir</a>
<b>BBazigaran</b>	University of Kashan, IR Iran E-mail: <a href="mailto:bazigaran@kashanu.ac.ir">bazigaran@kashanu.ac.ir</a>
<b>MRDarafsheh</b>	University of Tehran, IR Iran E-mail: <a href="mailto:darafsheh@ut.ac.ir">darafsheh@ut.ac.ir</a>
<b>MDeza</b>	École Normale Supérieure, France E-mail: <a href="mailto:Michel.Deza@ens.fr">Michel.Deza@ens.fr</a>
<b>MDiudea</b>	Babes–Bolyai University, Romania E-mail: <a href="mailto:diudea@chem.ubbcluj.ro">diudea@chem.ubbcluj.ro</a>
<b>TDošlić</b>	University of Zagreb, Croatia E-mail: <a href="mailto:doslic@faust.irb.hr">doslic@faust.irb.hr</a>
<b>AGholami</b>	University of Qom, IR Iran E-mail: <a href="mailto:a.gholami@qom.ac.ir">a.gholami@qom.ac.ir</a>
<b>IGutman</b>	University of Kragujevac, Serbia E-mail: <a href="mailto:gutman@kg.ac.yu">gutman@kg.ac.yu</a>
<b>AIranmanesh</b>	Tarbiat Modares University, IR Iran E-mail: <a href="mailto:iranmanesh@modares.ac.ir">iranmanesh@modares.ac.ir</a>
<b>MAIranmanesh</b>	Yazd University, IR Iran E-mail: <a href="mailto:iranmanesh@yazduni.ac.ir">iranmanesh@yazduni.ac.ir</a>
<b>PEJohn</b>	Technical University of Ilmenau, Germany E-mail: <a href="mailto:peter.john@tu-ilmenau.de">peter.john@tu-ilmenau.de</a>
<b>SKlavžar</b>	University of Maribor, Slovenia E-mail: <a href="mailto:sandi.klavzar@fmf.uni-lj.si">sandi.klavzar@fmf.uni-lj.si</a>
<b>XLi</b>	Nankai University, Tianjin 300071, Tianjin, P.R. China E-mail: <a href="mailto:lxl@nankai.edu.cn">lxl@nankai.edu.cn</a>
<b>H R Maimani</b>	Shahid Rajaei Teacher Training University, IR Iran E-mail: <a href="mailto:maimani@ipm.ir">maimani@ipm.ir</a>
<b>O Ori</b>	Actinum Chemical Research, Rome, Italy E-mail: <a href="mailto:ottorino.ori@gmail.com">ottorino.ori@gmail.com</a>
<b>MV Putz</b>	West University of Timisoara, Timisoara, Romania E-mail: <a href="mailto:mv_putz@yahoo.com">mv_putz@yahoo.com</a>
<b>MSalavati–Niasar</b>	University of Kashan, IR Iran E-mail: <a href="mailto:Salavati@kashanu.ac.ir">Salavati@kashanu.ac.ir</a>
<b>BShareghi–Boroujeni</b>	Shahrekord University, IR Iran E-mail: <a href="mailto:share.beh@sci.sku.ac.ir">share.beh@sci.sku.ac.ir</a>
<b>BTaeri</b>	Isfahan University of Technology, IR Iran E-mail: <a href="mailto:b.taeri@cc.iut.ac.ir">b.taeri@cc.iut.ac.ir</a>
<b>H Yousefi-Azari</b>	University of Tehran, IR Iran E-mail: <a href="mailto:hyousefi@ut.ac.ir">hyousefi@ut.ac.ir</a>
<b>SYousefi</b>	Malek–Ashtar University of Technology, IR Iran E-mail: <a href="mailto:yousefi100@yahoo.com">yousefi100@yahoo.com</a>
<b>BZhou</b>	South China Normal University, P.R. China E-mail: <a href="mailto:zhoubo@scnu.edu.cn">zhoubo@scnu.edu.cn</a>
<b>AGraovac</b>	<b>Past Editors</b> Ruđer Bošković Institute, Croatia E-mail: <a href="mailto:graovac@irb.hr">graovac@irb.hr</a>

## Editor-in-Chief:

Ali Reza Ashrafi  
Department of Pure Mathematics, Faculty of Mathematical Sciences, University of Kashan, Kashan 87317-53153, IR IRAN  
mail: [ashrafi@kashanu.ac.ir](mailto:ashrafi@kashanu.ac.ir)

## Technical Manager:

Marzieh Pourbabaee  
Department of Applied Mathematics, Faculty of Mathematical Sciences, University of Kashan, Kashan 87317-53153, IR IRAN  
Email: [m.pourbabaee@kashanu.ac.ir](mailto:m.pourbabaee@kashanu.ac.ir)

## Managing Director:

Behnam Bazigaran  
Department of Pure Mathematics, Faculty of Mathematical Sciences, University of Kashan, Kashan 87317-53153, IR IRAN  
E-mail: [bazigaran@kashanu.ac.ir](mailto:bazigaran@kashanu.ac.ir)

## Editorial office:

Somayeh Madani  
Department of Pure Mathematics, Faculty of Mathematical Sciences, University of Kashan, Kashan 87317-53153, IR IRAN  
E-mail: [ijmc@kashanu.ac.ir](mailto:ijmc@kashanu.ac.ir)

## Language Editor:

Seyfollah Mosazadeh  
Department of Pure Mathematics, Faculty of Mathematical Sciences, University of Kashan, Kashan 87317-53153, IR IRAN  
E-mail: [s.mosazadeh@kashanu.ac.ir](mailto:s.mosazadeh@kashanu.ac.ir)





Special Issue On  
Applications of  
Group Theory in  
Chemistry



# Iranian Journal of Mathematical Chemistry

Vol. 7, No. 2 October 2016

CONTENTS	pages
<b>Autobiography of Shinsaku Fujita</b> <i>S. Fujita</i>	111
<b>Type-Itemized Enumeration of RS-Stereoisomers of Octahedral Complexes</b> <i>S. Fujita</i>	113
<b>Half-Century Journey from Synthetic Organic Chemistry to Mathematical Stereochemistry through Chemoinformatics</b> <i>S. Fujita</i>	155
<b>Enumeration of Conformers of Octahedral [M(ABC)<sub>6</sub>] Complex on the Basis of Computational Group Theory</b> <i>H. Sakiyama and K. Waki</i>	223
<b>QSPR Modeling of Heat Capacity, Thermal Energy and Entropy of Aliphatic Aldehydes by using Topological Indices and MLR Method</b> <i>A. Alaghebandi and F. Shafiei</i>	235
<b>On the Mark and Markaracter Tables of Finite Groups</b> <i>M. Ghorbani</i>	253
<b>Weak Algebraic Hyperstructures as a Model for Interpretation of Chemical Reactions</b> <i>B. Davvaz</i>	267



## ***Autobiography of Shinsaku Fujita***



Shinsaku Fujita was born in Kita-Kyushu City (at that time, Tobata City), Japan in 1944. He received his undergraduate training at Kyoto University. After earning a Master's degree in 1968, he started as a research instructor and received a Dr. Eng. degree at Kyoto University in 1972 under the guidance of Prof. Hitosi Nozaki. In 1972, he joined Ashigara Research Laboratories, Fuji Photo Film Co., Ltd., where he was engaged in the R&D of organic compounds for instant color photography and in the R&D of the organic reaction database until 1997. From 1997 to 2007, he has been Professor of Information Chemistry and Materials Technology at the Kyoto Institute of Technology. In 2007, he has started Shonan Institute of Chemoinformatics and Mathematical Chemistry as a private laboratory.

He was awarded the Synthetic Organic Chemistry Japan Award in 1982 and the Society of Computer Chemistry Japan Award in 2002.

His research interests have included reactive intermediates (nitrenes), synthetic organic chemistry (cyclophanes, strained heterocycles, and organic compounds for photography), organic photochemistry, organic stereochemistry (theoretical approach such as Fujita's stereoisogram approach), mathematical organic chemistry (combinatorial enumeration such as Fujita's USCI approach and Fujita's proligand method), and the organic reaction database (the concept of imaginary transition structures). His activities will be described in his account article of the present issue of

this journal under the title “Half-Century Journey from Synthetic Organic Chemistry to Mathematical Stereochemistry through Chemoinformatics”.

He is a member of the Chemical Society of Japan, the Society of Synthetic Organic Chemistry, Japan, the Kinki Chemical Society, Japan, the Society of Computer Chemistry, Japan, the American Chemical Society, and the International Academy of Mathematical Chemistry.

He is the developer of the XYMTEx system for drawing chemical structural formulas in TEX/LATEX documents (1993–). The present version (Version 5.01) is available from his homepage (<http://xymtex.com/>) with an on-line manual of 780 pages (<http://xymtex.com/fujitas3/xymtex/xym501/manual/xymtex-manualPS.pdf>). He is also the developer of LATEX utilities for typesetting Japanese classical literature (e.g., furigana, warigaki, and kanbun). He is the author of the on-line series of essays entitled “Jintan no Chomei-Kanban wo Yosuga ni Kyo-Meguri (Time-Space Trips in Kyoto by Jintan’s Guideposts)”, which has been written as a sample of using the LATEX utilities developed by himself (<http://xymtex.com/kyomeguri/index.html>).

He is the sole author of *Symmetry and Combinatorial Enumeration in Chemistry* (Springer–Verlag, Berlin–Heidelberg, 1991), *XYMTEx — Typesetting Chemical Structural Formulas* (Addison–Wesley Japan, Tokyo, 1997), *Computer–Oriented Representation of Organic Reactions* (Yoshioka Shoten, Kyoto, 2001), *Organic Chemistry of Photography* (Springer–Verlag, Berlin–Heidelberg, 2004), *Diagrammatical Approach to Molecular Symmetry and Enumeration of Stereoisomers, Mathematical Chemistry Monographs Series Vol. 4* (Kragujevac University, Kragujevac, 2007), *Combinatorial Enumeration of Graphs, Three-Dimensional Structures, and Chemical Compounds, Mathematical Chemistry Monographs Series Vol. 15* (Kragujevac University, Kragujevac, 2013), *Mathematical Stereochemistry* (Walter de Gruyter, Berlin–Boston, 2015), and several books on TEX/LATEX. His homepage on World Wide Web is located at <http://xymtex.com/>.

# Type–Itemized Enumeration of *RS*–Stereoisomers of Octahedral Complexes

SHINSAKU FUJITA

Shonan Institute of Chemoinformatics and Mathematical Chemistry, Kaneko 479-7  
Ooimachi, Ashigara-Kami-Gun, Kanagawa-Ken, 258-0019 Japan

Correspondence should be addressed to SHINSAKU FUJITA (EMAIL: shinsaku\_fujita@nifty.com)

Received 16 November 2015; Accepted 24 November 2015

ACADEMIC EDITOR: ALI REZA ASHRAFI

**ABSTRACT** Stereoisograms of octahedral complexes are classified into five types (type I–type V) under the action of the corresponding *RS*-stereoisomeric group. Their enumeration is accomplished in a type-itemized fashion, where Fujita’s proligand method developed originally for combinatorial enumeration under point groups (S. Fujita, *Theor. Chem. Acc.*, 113, 73–79 (2005)) is extended to meet the requirement of Fujita’s stereoisogram approach. The cycle index with chirality fittingness (CI-CF) of the point group  $O_h$  is modulated by taking account of the CI-CF for calculating type-V quadruplets contained in stereoisograms. The modulated CI-CF is combined with a CI-CF of the maximum chiral point group (O), a CI-CF of the maximum *RS*-permutation group, a CI-CF of the maximum ligand-reflection group, and a CI-CF of the *RS*-stereoisomeric group, so as to generate CI-CFs for evaluating type-I to type-V quadruplets. By introducing ligand-inventory functions into the CI-CFs, the numbers of quadruplets of octahedral complexes are obtained and shown in tabular forms. Several stereoisograms for typical complexes are depicted. Their configuration indices and *C/A*-descriptors are discussed on the basis of Fujita’s stereoisogram approach.

**KEYWORDS** enumeration • stereoisogram • octahedral complex • *RS*–stereoisomeric group.

## 1. INTRODUCTION

Fujita’s stereoisogram approach has been developed by defining *RS*-stereoisomeric groups as algebraic formulations [1, 2] and *stereoisograms* as their diagrammatic expressions [3, 4, 5]. Diagrammatically speaking, the vertical direction of a stereoisogram is concerned with the chiral aspect for supporting Le Bel’s way (dissymmetry, chirality) [6, 7] and the horizontal direction of a stereoisogram is concerned with the *RS*-stereogenic aspect for



supporting van't Hoff's way (asymmetry, stereogenicity) [8, 9]. Thereby, these two ways have been integrated to reach Aufheben, so that the theoretical foundations of modern stereochemistry and the terminology of stereochemical nomenclature (e.g., the Cahn-Ingold-Prelog system [10, 11] and the *pro-R/pro-S* system [12, 13, 14]) have been thoroughly revised, as discussed in recent articles [15, 16, 17, 18].

A quadruplet of *RS*-stereoisomers contained in a stereoisogram can be regarded as an equivalence class under the action of an *RS*-stereoisomeric group. This means that the number of inequivalent quadruplets can be combinatorially enumerated by extending Fujita's unit-subducedcycle- index (USCI) approach [19, 20] to meet the requirement of Fujita's stereoisogram approach, if the data of the *RS*-stereoisomeric group (e.g., mark tables, inverse mark tables, and subduction tables) are available. According to this guideline, symmetry-itemized enumerations of quadruplets of *RS*-stereoisomers have been reported by starting from a tetrahedral skeleton [21, 22], an allene skeleton [23, 24], and an oxirane skeleton [25, 26, 27]. It is to be noted, however, that mark tables, inverse mark tables, and subduction tables for the *RS*-stereoisomeric groups have been obtained by rather tedious procedures even in the enumerations based on the above-mentioned skeletons of ligancy 4.

As for the action of point groups, derivatives to be counted can be classified into two categories, i.e., chiral and achiral derivatives. According to this classification, chirality-itemized enumeration for aiming at itemization into chiral and achiral derivatives has been accomplished by using Fujita's proligand method [28], which has been developed as a simpler method for gross enumeration than those supported by Fujita's USCI approach for symmetry-itemized enumeration [19, 20]. Note that Fujita's proligand method applied to such chirality-itemized enumeration does not require mark tables, inverse mark tables, and subduction tables, which are not always available.

In a similar way to chirality-itemized enumeration under the action of point groups, it is desirable to investigate type-itemized enumeration of inequivalent quadruplets under the action of an *RS*-stereoisomeric group, because such quadruplets of *RS*-stereoisomers as represented by stereoisograms have been proven to be categorized into five types (type I to type V) [2]. Type-itemized enumerations of quadruplets of *RS*-stereoisomers based on inclusion-exclusion procedures [29, 30] and on more systematic procedures [31, 32] have been reported by using tetrahedral and allene derivatives as probes of ligancy 4.

Because the more systematic procedures [31, 32] are expected to have wide applicability, they should be examined extensively by being applied to more complicated derivatives. The present article is devoted to the application of one of the procedures (using cycle indices with chirality fittingness modulated by type-V quadruplets [32]) to octahedral complexes of ligancy 6.

## 2. RS-STEREISOMERIC GROUPS FOR OCTAHEDRAL COMPLEXES

### 2.1. ALGEBRAIC FORMULATION OF RS-STEREISOMERIC GROUPS

Although the algebraic formulation of an *RS*-stereoisomeric group  $O_{h\tilde{i}}$  for characterizing an octahedral skeleton **1** has been described in a previous report [33], a minimal set of data should be cited here for the sake of convenience.

By starting from the point group  $O_h$  for characterizing an octahedral skeleton **1**, the *RS*-stereoisomeric group  $O_{h\tilde{i}}$  is represented by the following coset decomposition:

$$O_{h\tilde{i}} = O + Oi + O\tilde{l} + O\hat{I} \quad (1)$$

where the group  $O$  is the maximal chiral subgroup of the point group of  $O_h$ , the first representative  $I$  (omitted for the sake of simplicity) is an identity operation, the second representative  $i$  is an inversion operation, the third representative  $\tilde{l}$  is an *RS*-permutation operation, and the fourth representative  $\hat{I}$  is a ligand-reflection operation.

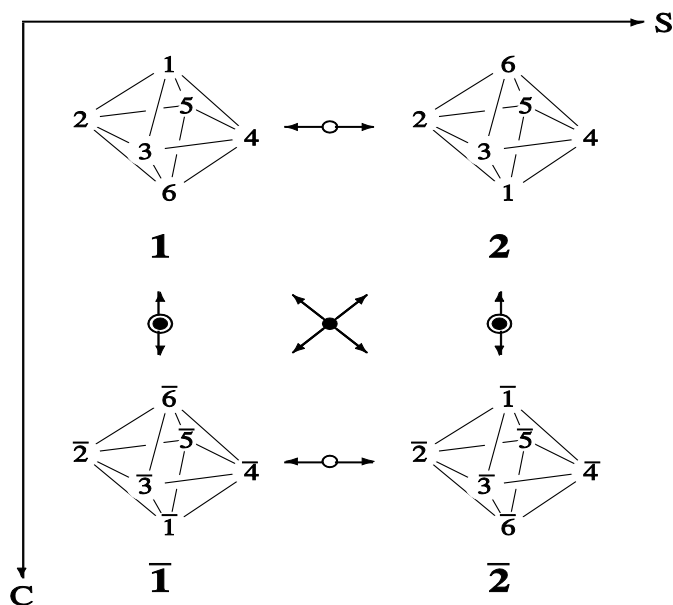


**Figure 1.** Elementary stereoisogram of an octahedral skeleton [33].

The 96 elements of the *RS*-stereoisomeric group  $O_{h\tilde{i}}$  (Eq. 1) are collected in Figure 2. According to the coset decomposition represented by Eq. 1, they are categorized into four parts, as denoted by large gray letters (A, B, C, and D):

1. The upper left part denoted by a gray letter A in Figure 2 corresponds to the coset  $O$  ( $= OI$ ). When the representative of this coset is selected to the identity element  $I$  which is assigned to the representative skeleton 1, the other operations contained in the coset  $O(= OI)$  generate respective homomers of 1. The operations collected in the upper left part (A) are called *rotations*.
2. The lower left part denoted by a gray letter B in Figure 2 corresponds to the coset  $Oi$ . When the representative of this coset is selected to a reflection  $\sigma_{h(1)}$  in place of  $i$ , a mirror-image skeleton  $\bar{1}$  is generated as a representative (Figure 1). The other operations contained in the coset  $Oi$  ( $= O\sigma_{h(1)}$ ) generate respective homomers of  $\bar{1}$ . The operations collected in the lower left part (B) are called *reflections*, which connote roto reflections (e.g.,  $S_{4(1)}$ ) and an inversion ( $i$ ) in addition to mirror-image operations.
3. The upper right part denoted by a gray letter C in Figure 2 corresponds to the coset  $O\tilde{l}$ . When the representative of this coset is selected to an  $RS$ -permutation in place of  $\tilde{l}$ , an  $RS$ -permuted skeleton 2 is generated as a representative (Figure 1). The other operations contained in the coset  $O\tilde{l}$  ( $= O\tilde{\sigma}_{h(1)}$ ) generate respective homomers of 2. The operations collected in the upper right part (C) are called *RS-permutations*.
4. The lower right part denoted by a gray letter D in Figure 2 corresponds to the coset  $O\hat{l}$ . When the representative of this coset is selected to a ligand reflection  $\hat{l}$ , an  $RS$ -ligand reflected skeleton  $\bar{2}$  is generated as a representative (Figure 1). The other operations contained in the coset  $O\hat{l}$  generate respective homomers of  $\bar{2}$ . The operations collected in the lower right part (D) are called *ligand reflections*.

The  $RS$ -stereoisomeric group  $O_{h\tilde{l}\hat{l}}$  collected in Figure 2 has 96 elements (order 96) and contains the following subgroups of order 48.

The maximum point group (A + B):

$$O_h = O + Oi \quad (2)$$

The maximum  $RS$ -permutation group (A + C):

$$O_{\tilde{l}} = O + O\tilde{l}, \quad (3)$$

The maximum ligand-reflection group (A + D):

$$O_{\hat{l}} = O + O\hat{l}, \quad (4)$$

<b>O</b>	<i>I</i>	(1)(2)(3)(4)(5)(6)	$b_1^6$	$\bar{i}$	(1 6)(2 4)(3 5)	$b_2^3$	<b>O<math>\bar{i}</math></b>
	<i>C</i> <sub>2(1)</sub>	(1)(2 4)(3 5)(6)	$b_1^2 b_2^2$	$\bar{\sigma}_h(3)$	(1)(2 4)(3)(5)(6)	$b_1^4 b_2$	
	<i>C</i> <sub>2(2)</sub>	(1 6)(3 5)(2)(4)	$b_1^2 b_2^2$	$\bar{\sigma}_h(2)$	(1)(2)(3 5)(4)(6)	$b_1^4 b_2$	
	<i>C</i> <sub>2(3)</sub>	(1 6)(2 4)(3)(5)	$b_1^2 b_2^2$	$\bar{\sigma}_h(1)$	(1 6)(2)(3)(4)(5)	$b_1^4 b_2$	
	<i>C</i> <sub>3(1)</sub>	(1 3 2)(4 6 5)	$b_3^2$	$\bar{S}_6^5(1)$	(1 4 3 6 2 5)	$b_6$	
	<i>C</i> <sub>3(3)</sub>	(1 4 5)(2 3 6)	$b_3^2$	$\bar{S}_6^5(3)$	(1 3 4 6 5 2)	$b_6$	
	<i>C</i> <sub>3(2)</sub>	(1 4 3)(2 5 6)	$b_3^2$	$\bar{S}_6^5(2)$	(1 5 4 6 3 2)	$b_6$	
	<i>C</i> <sub>3(4)</sub>	(1 2 5)(3 6 4)	$b_3^2$	$\bar{S}_6^5(4)$	(1 3 2 6 5 4)	$b_6$	
	<i>C</i> <sub>3(1)</sub>	(1 2 3)(4 5 6)	$b_3^2$	$\bar{S}_6(1)$	(1 5 2 6 3 4)	$b_6$	
	<i>C</i> <sub>3(3)</sub>	(1 5 4)(2 6 3)	$b_3^2$	$\bar{S}_6(4)$	(1 4 5 6 2 3)	$b_6$	
	<i>C</i> <sub>3(2)</sub>	(1 3 4)(2 6 5)	$b_3^2$	$\bar{S}_6(3)$	(1 2 5 6 4 3)	$b_6$	
	<i>C</i> <sub>3(4)</sub>	(1 5 2)(3 4 6)	$b_3^2$	$\bar{S}_6(2)$	(1 2 3 6 4 5)	$b_6$	
	<i>C</i> <sub>2(6)</sub>	(1 6)(2 5)(3 4)	$b_2^3$	$\bar{\sigma}_d(1)$	(1)(2 3)(4 5)(6)	$b_1^2 b_2^2$	
	<i>C</i> <sub>2(1)</sub>	(1 6)(2 3)(4 5)	$b_2^3$	$\bar{\sigma}_d(6)$	(1)(2 5)(3 4)(6)	$b_1^2 b_2^2$	
	<i>C</i> <sub>2(4)</sub>	(1 2)(3 5)(4 6)	$b_2^3$	$\bar{\sigma}_d(2)$	(1 3)(2)(4)(5 6)	$b_1^2 b_2^2$	
	<i>C</i> <sub>2(2)</sub>	(1 5)(2 4)(3 6)	$b_2^3$	$\bar{\sigma}_d(4)$	(1 5)(2)(4)(3 6)	$b_1^2 b_2^2$	
	<i>C</i> <sub>2(5)</sub>	(1 4)(2 6)(3 5)	$b_2^3$	$\bar{\sigma}_d(3)$	(1 4)(2 6)(3)(5)	$b_1^2 b_2^2$	
	<i>C</i> <sub>2(3)</sub>	(1 3)(2 4)(5 6)	$b_2^3$	$\bar{\sigma}_d(5)$	(1 2)(4 6)(3)(5)	$b_1^2 b_2^2$	
	<i>C</i> <sub>4(3)</sub>	(1)(2 3 4 5)(6)	$b_1^2 b_4$	$\bar{S}_4(3)$	(1 6)(2 3 4 5)	$b_2 b_4$	
	<i>C</i> <sub>4(3)</sub>	(1)(2 5 4 3)(6)	$b_1^2 b_4$	$\bar{S}_4^3(3)$	(1 6)(2 5 4 3)	$b_2 b_4$	
<i>C</i> <sub>4(1)</sub>	(1 5 6 3)(2)(4)	$b_1^2 b_4$	$\bar{S}_4(1)$	(1 3 6 5)(2 4)	$b_2 b_4$		
<i>C</i> <sub>4(1)</sub>	(1 3 6 5)(2)(4)	$b_1^2 b_4$	$\bar{S}_4^3(1)$	(1 5 6 3)(2 4)	$b_2 b_4$		
<i>C</i> <sub>4(2)</sub>	(1 4 6 2)(3)(5)	$b_1^2 b_4$	$\bar{S}_4(2)$	1 2 6 4(3 5)	$b_2 b_4$		
<i>C</i> <sub>4(2)</sub>	(1 2 6 4)(3)(5)	$b_1^2 b_4$	$\bar{S}_4^3(2)$	(1 4 6 2)(3 5)	$b_2 b_4$		
<b>O<math>i</math></b>	<i>i</i>	(1 6)(2 4)(3 5)	$c_2^3$	$\hat{i}$	(1)(2)(3)(4)(5)(6)	$a_1^6$	<b>O<math>\hat{i}</math></b>
	$\bar{\sigma}_h(3)$	(1)(2 4)(3)(5)(6)	$a_1^4 c_2$	$\hat{C}_2(1)$	(1)(2 4)(3 5)(6)	$a_1^2 c_2^2$	
	$\bar{\sigma}_h(2)$	(1)(2)(3 5)(4)(6)	$a_1^4 c_2$	$\hat{C}_2(2)$	(1 6)(3 5)(2)(4)	$a_1^2 c_2^2$	
	$\bar{\sigma}_h(1)$	(1 6)(2)(3)(4)(5)	$a_1^4 c_2$	$\hat{C}_2(3)$	(1 6)(2 4)(3)(5)	$a_1^2 c_2^2$	
	$\bar{S}_6^5(1)$	(1 4 3 6 2 5)	$c_6$	$\hat{C}_3(1)$	(1 3 2)(4 6 5)	$a_3^2$	
	$\bar{S}_6^5(3)$	(1 3 4 6 5 2)	$c_6$	$\hat{C}_3(3)$	(1 4 5)(2 3 6)	$a_3^2$	
	$\bar{S}_6^5(2)$	(1 5 4 6 3 2)	$c_6$	$\hat{C}_3(2)$	(1 4 3)(2 5 6)	$a_3^2$	
	$\bar{S}_6^5(4)$	(1 3 2 6 5 4)	$c_6$	$\hat{C}_3(4)$	(1 2 5)(3 6 4)	$a_3^2$	
	$\bar{S}_6(1)$	(1 5 2 6 3 4)	$c_6$	$\hat{C}_3^2(1)$	(1 2 3)(4 5 6)	$a_3^2$	
	$\bar{S}_6(4)$	(1 4 5 6 2 3)	$c_6$	$\hat{C}_3^2(3)$	(1 5 4)(2 6 3)	$a_3^2$	
	$\bar{S}_6(3)$	(1 2 5 6 4 3)	$c_6$	$\hat{C}_3^2(2)$	(1 3 4)(2 6 5)	$a_3^2$	
	$\bar{S}_6(2)$	(1 2 3 6 4 5)	$c_6$	$\hat{C}_3^2(4)$	(1 5 2)(3 4 6)	$a_3^2$	
	$\bar{\sigma}_d(1)$	(1)(2 3)(4 5)(6)	$a_1^2 c_2^2$	$\hat{C}_2(6)$	(1 6)(2 5)(3 4)	$c_3^2$	
	$\bar{\sigma}_d(6)$	(1)(2 5)(3 4)(6)	$a_1^2 c_2^2$	$\hat{C}_2(1)$	(1 6)(2 3)(4 5)	$c_3^2$	
	$\bar{\sigma}_d(2)$	(1 3)(2)(4)(5 6)	$a_1^2 c_2^2$	$\hat{C}_2(4)$	(1 2)(3 5)(4 6)	$c_3^2$	
	$\bar{\sigma}_d(4)$	(1 5)(2)(4)(3 6)	$a_1^2 c_2^2$	$\hat{C}_2(2)$	(1 5)(2 4)(3 6)	$c_3^2$	
	$\bar{\sigma}_d(3)$	(1 4)(2 6)(3)(5)	$a_1^2 c_2^2$	$\hat{C}_2(5)$	(1 4)(2 6)(3 5)	$c_3^2$	
	$\bar{\sigma}_d(5)$	(1 2)(4 6)(3)(5)	$a_1^2 c_2^2$	$\hat{C}_2(3)$	(1 3)(2 4)(5 6)	$c_3^2$	
	$\bar{S}_4(3)$	(1 6)(2 3 4 5)	$c_2 c_4$	$\hat{C}_4^3(3)$	(1)(2 3 4 5)(6)	$a_1^2 c_4$	
	$\bar{S}_4^3(3)$	(1 6)(2 5 4 3)	$c_2 c_4$	$\hat{C}_4(3)$	(1)(2 5 4 3)(6)	$a_1^2 c_4$	
$\bar{S}_4(1)$	(1 3 6 5)(2 4)	$c_2 c_4$	$\hat{C}_4^3(1)$	(1 5 6 3)(2)(4)	$a_1^2 c_4$		
$\bar{S}_4^3(1)$	(1 5 6 3)(2 4)	$c_2 c_4$	$\hat{C}_4(1)$	(1 3 6 5)(2)(4)	$a_1^2 c_4$		
$\bar{S}_4(2)$	(1 2 6 4)(3 5)	$c_2 c_4$	$\hat{C}_4(2)$	(1 4 6 2)(3)(5)	$a_1^2 c_4$		
$\bar{S}_4^3(2)$	(1 4 6 2)(3 5)	$c_2 c_4$	$\hat{C}_4^3(2)$	(1 2 6 4)(3)(5)	$a_1^2 c_4$		

**Figure 2.** RS-Stereoisomeric group  $O_{h\bar{i}}$  for an octahedral skeleton. The elements of the coset O (= OI) are called *rotations*, the elements of the coset Oi are called (*roto*) *reflections*, the elements of the coset  $O\bar{i}$  are called *RS-permutations*, and the elements of the coset  $O\hat{i}$  are called *ligand reflections*. [33]

where these subgroups of order 48 contain the point group  $O$  of order 24 commonly. It should be noted that the  $RS$ -stereoisomeric group  $O_{h\bar{i}i}$  contains other subgroups of order 48, which do not contain the point group  $O$  of order 24. For example, the  $RS$ -stereoisomeric group  $T_{d\bar{\sigma}i}$  derived from the point group  $T_d$  (cf. Table 1 of [21]) is of order 48 and does not contain  $O$ , although it is a subgroup of  $O_{h\bar{i}i}$ .

According to Eqs. 1, 2, 3, and 4 in addition to the common chiral subgroup  $O$ , a subgroup  $G$  of the  $RS$ -stereoisomeric group  $O_{h\bar{i}i}$  is classified into one of the following five types:

- type I:  $G \subset O_i$  ( $G \not\subset O$ )
  - type II:  $G \subset O_{\bar{i}}$  ( $G \not\subset O$ )
  - type III:  $G \subset O$
  - type IV:  $G \subset O_{h\bar{i}i}$  ( $G \not\subset O$ ,  $G \not\subset O_{\bar{i}}$ ,  $G \not\subset O_i$ ,  $G \not\subset O_h$ )
  - type V:  $G \subset O_h$  ( $G \not\subset O$ )
- (5)

## 2.2. STEREOISOGRAMS AS DIAGRAMMATIC EXPRESSIONS OF $RS$ -STEREOISOMERIC GROUPS

The four skeletons collected in Figure 1 are interchanged into one another on the action of the  $RS$ -stereoisomeric group  $O_{h\bar{i}i}$  (Eq. 1) and its subgroups listed in Eqs. 2, 3, and 4. In general, a quadruplet of four skeletons linked with double-headed arrows (e.g., Figure 1) is called an *elementary stereoisogram*. The elementary stereoisogram of octahedral skeletons (Figure 1) is a basic diagram for giving stereoisograms of octahedral derivatives as promolecules, where a set of proligands (abstract ligands with chirality/achirality, e.g. A, B, C, X, Y, and Z for achiral proligands, as well as  $p/\bar{p}$ ,  $q/\bar{q}$ ,  $r/\bar{r}$ , and  $s/\bar{s}$  for a pair of chiral proligands of opposite chirality senses) is placed on the six positions of each of the skeletons, as exemplified in Figure 3. Note that an achiral proligand (e.g., A) on a position with an overlined number (e.g., 1) remains unchanged, because  $\bar{A}$  is identical with A itself. On the other hand, a chiral proligand (e.g., p or  $\bar{p}$ ) on a position with an overlined number (e.g.,  $\bar{1}$ ) is changed into its mirror-image proligand (e.g.,  $\bar{p}$  or p), where  $\bar{\bar{p}} = p$ .

Each of the resulting quadruplets of promolecules (octahedral derivatives) belongs to a subgroup  $G$  of the  $RS$ -stereoisomeric group  $O_{h\bar{i}i}$ , so that it is characterized to be one of five types (type I to type V). In other words, each stereoisogram can be categorized into one of type I to type V, as shown in Figure 3.

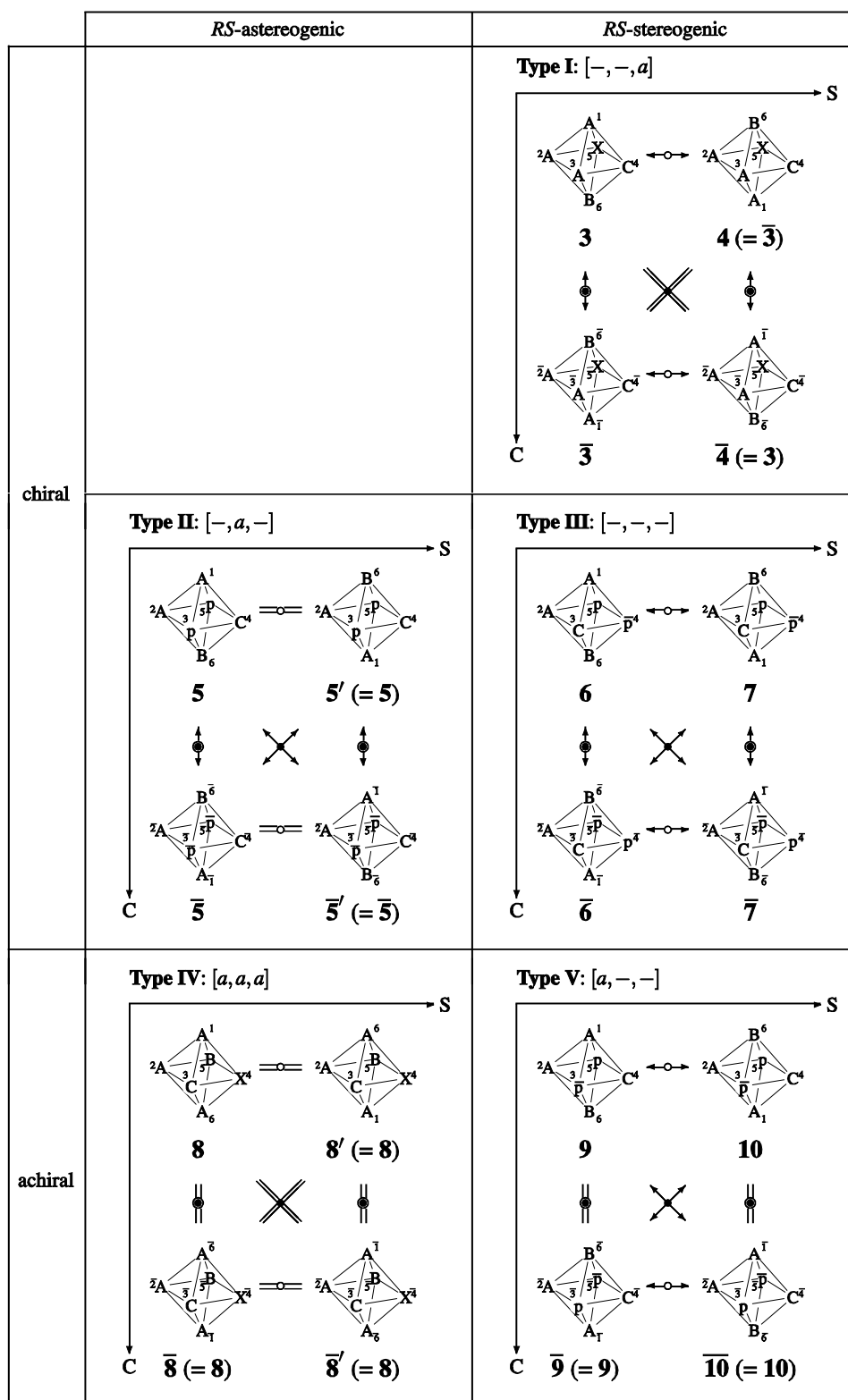


Figure 3. Stereoisograms for representing RS-stereoisomers of five types [4].

For the purpose of applying *RS*-stereoisomeric groups to qualitative discussions, the following terminology based on stereoisograms is adopted [34].

1. The relationship between 1 and  $\bar{1}$  (or between 2 and  $\bar{2}$ ) in the vertical direction of Figure 1 is called a (self-)enantiomeric relationship, where the corresponding attribute is called chirality (or achirality). The interconversion between 1 and  $\bar{1}$  (or between 2 and  $\bar{2}$ ) is brought about by reflections contained in the point group  $O_h$ ,
2. The relationship between 1 and 2 (or between  $\bar{1}$  and  $\bar{2}$ ) in the horizontal direction of Figure 1 is called a (self-)*RS*-diastereomeric relationship, where the corresponding attribute is called *RS*-stereogenicity (or *RS*-astereogenicity). The interconversion between 1 and 2 (or between  $\bar{1}$  and  $\bar{2}$ ) is brought about by *RS*-permutations contained in the *RS*-permutation group  $O_{\bar{7}}$ .
3. The relationship between 1 and  $\bar{2}$  (or between 2 and  $\bar{1}$ ) in the diagonal direction of Figure 1 is called a (self-)holantimeric relationship, where the corresponding attribute is called sclerality (or asclerality). The interconversion between 1 and  $\bar{2}$  (or between 2 and  $\bar{1}$ ) is brought about by ligand reflections contained in the ligand-reflection group  $O_{\bar{7}}$ .

A type-I stereoisogram is characterized by equality symbols in the diagonal direction, so that the enantiomeric relationship is coincident with the *RS*-diastereomeric relationship in the type-I stereoisogram (cf. Figure 3). This means that the quadruplet of promolecules contained in the type-I stereoisogram belongs to a type-I subgroup shown in Eq. 5. For example, the promolecule 3 is identical with its holantimer  $\bar{4}$  ( $= 3$ ), so that it is self-holantimeric and exhibits asclerality. According to the terminology described above, the type-I stereoisogram is chiral, *RS*-stereogenic, and ascleral, so that it is characterized by a type index  $[-,-,a]$ .

A type-II stereoisogram is characterized by equality symbols in the horizontal direction, so that the enantiomeric relationship is coincident with the holantimeric relationship in the type-II stereoisogram (cf. Figure 3). This means that the quadruplet of promolecules contained in the type-II stereoisogram belongs to a type-II subgroup shown in Eq. 5. For example, the promolecule 5 is identical with its *RS*-diastereomer  $5'$  ( $= 5$ ) so that it is self-*RS*-diastereomeric and exhibits *RS*-astereogenicity. According to the terminology described above, the type-II stereoisogram is chiral, *RS*-astereogenic, and scleral, so that it is characterized by a type index  $[-,a,-]$ .

A type-III stereoisogram is characterized by the absence of equality symbols in all directions, so that it belongs to a type-III subgroup shown in Eq. 5. For example, the



promolecules 6, 7,  $\bar{6}$ , and  $\bar{7}$  are different from one another (Figure 3). Hence, the type-III stereoisogram is chiral, *RS*-stereogenic, and scleral, so that it is characterized by a type index  $[-,-,-]$ .

A type-IV stereoisogram is characterized by the presence of equality symbols in all directions, so that it belongs to a type-IV subgroup shown in Eq. 5. For example, the promolecules 8, 8',  $\bar{8}$  and  $\bar{8}'$  are identical with one another (Figure 3). Hence, the type-IV stereoisogram is achiral, *RS*-astereogenic, and ascleral, so that it is characterized by a type index  $[a,a,a]$ .

A type-V stereoisogram is characterized by equality symbols in the vertical direction, so that the *RS*-diastereomeric relationship is coincident with the holantimeric relationship in the type-V stereoisogram (cf. Figure 3). This means that the quadruplet of promolecules contained in the type-V stereoisogram belongs to a type-V subgroup shown in Eq. 5. For example, the promolecule 9 (or 10) is identical with its enantiomer  $\bar{9}$  (= 9) (or  $\bar{10}$  (= 10)), so that it is self-enantiomeric and exhibits achirality. The relationship between 9 and 10 is an *RS*-diastereomeric relationship. According to the terminology described above, the type-V stereoisogram is achiral, *RS*-stereogenic, and scleral, so that it is characterized by a type index  $[a,-,-]$ . Such a pair of *RS*-diastereomers is referred to under the term 'pseudoasymmetry' in the conventional terminology of stereochemistry.

### 3. GROSS ENUMERATION

#### 3.1. ACTION OF THE MAXIMUM POINT GROUP $O_h$

The symmetry-itemized enumeration of octahedral complexes has been conducted by Fujita's USCI approach [35]. Because the inverse mark table and the USCI-CF table of  $O_h$  has been reported in [36, 28], Def. 16.1 of [19] for gross enumeration can be applied to the gross enumeration of octahedral complexes. According to Section 2.6 of [28], the procedure of gross enumeration can be simplified by using a gross enumeration matrix (GEM), where the column sum  $\hat{N}$  of the inverse mark table is beforehand evaluated (Theorem 2.8 of [28]). Thus, the column sum  $\hat{N}$  for  $O_h$  is calculated as follows:

$$T_{\hat{N}} = \left( \frac{1}{48}, \frac{1}{16}, \frac{1}{8}, \frac{1}{16}, \frac{1}{8}, \frac{1}{48}, \frac{1}{6}, \frac{1}{8}, \frac{1}{8}, 0, 0, 0, 0, 0, 0, \right. \\ \left. 0, 0, 0, \frac{1}{6}, 0, 0, 0, 0, 0, 0, 0, 0, 0, 0, 0, 0 \right), \quad (6)$$

which is cited from Table 3 of [36] or Table 2.4 of [28].

The six positions of the octahedral skeleton construct an orbit governed by the coset representation  $O_h/C_{4v}$ , which is listed as products of cycles in the left parts (A and B) of

Figure 2. Hence, the  $O_h(/C_{4v})$ -row of the USCI-CF table of  $O_h$  (Tables 4 and 5 of [36] or Tables 2.5 and 2.6 of [28]) is adopted and aligned to form a formal row vector as follows:

$$\begin{aligned} \text{USCI-CF}_{O_h(/C_{4v})} = & (b_1^6, b_1^2 b_2^2, b_2^3, a_1^4 c_2, a_1^2 c_2^2, c_2^3, b_3^2, b_1^2 b_4, c_2 c_4, b_2^3, \\ & b_2 b_4, a_1^2 a_2^2, a_1^2 c_4, a_2^3, a_2^2 c_2, a_2 c_4, b_6, a_3^2, c_6, b_2 b_4, \\ & a_1^2 a_4, c_2 a_4, a_2 c_4, a_2 a_4, a_2^3, a_2 a_4, b_6, a_6, a_2 a_4, b_6, a_6, a_6, a_6). \end{aligned} \quad (7)$$

According to Corollary 1.3 of [37], the formal row vector  $\text{USCI-CF}_{O_h(/C_{4v})}$  (Eq. 7) is multiplied by the column vector (Eq. 6), so as to give the corresponding CI-CF as follows:

$$\begin{aligned} \text{CI-CF}_{O_h(/C_{4v})} = & \text{USCI-CF}_{O_h(/C_{4v})} \times \hat{N} \\ = & \frac{1}{48} b_1^6 + \frac{1}{16} b_1^2 b_2^2 + \frac{1}{8} b_2^3 + \frac{1}{16} a_1^4 c_2 + \frac{1}{8} a_1^2 c_2^2 \\ & + \frac{1}{48} c_2^3 + \frac{1}{6} b_3^2 + \frac{1}{8} b_1^2 b_4 + \frac{1}{8} c_2 c_4 + \frac{1}{6} c_6. \end{aligned} \quad (8)$$

The CI-CF can be alternatively obtained according to Fujita's proligand method [38, 39,40], which has been introduced in a book (Chapter 7 of [28]). Let us start from the coset representation  $O_h(/C_{4v})$  listed as products of cycles in the left parts (A and B) of Figure 2. Each cycle is classified into one of three categories, i.e., homospheric, enantiospheric, and hemispheric cycles, where the concept of sphericities for cycles is introduced in a similar way to the concept of sphericities for orbits. Then, a product of sphericity indices (PSI) is calculated for characterizing each product of cycles, where a sphericity index  $a_d$  is assigned to a homospheric  $d$ -cycle, a sphericity index  $c_d$  is assigned to an enantiospheric  $d$ -cycle, and a sphericity index  $b_d$  is assigned to a hemispheric  $d$ -cycle.

For example, the two-fold rotation  $C_{2(1)}$  represented by a product of cycles (1)(2 4)(3 5)(6) (Figure 2) is characterized by a PSI  $b_1^2 b_2^2$ , because each of the two 1-cycles is hemispheric and takes SI  $b_1$ , while each of the two 2-cycles is hemispheric and takes SI  $b_2$ . The reflection  $\sigma_{h(3)}$  represented by a product of cycles (1)(2 4)(3)(5)(6) is characterized by a PSI  $a_1^4 c_2$ , because each of the four 1-cycles is homospheric and takes SI  $a_1$ , while the one 2-cycles is enantiospheric and takes SI  $c_2$ . The resulting PSIs are listed in the rightmost column of each part of Figure 2.

According to Fujita's proligand method [38, 39, 40], all of the PSIs for the point group  $O_h$  (the parts A and B of Figure 2) are summed up. The resulting sum is divided by the order of  $O_h$  (48), so as to give the following CI-CF (Def. 7.20 of [28]):



correspond to the terms  $A^6$ ,  $B^6$  ...;  $A^5B$ ,  $A^5C$ , ...; and so on.

### 3.2. ACTION OF THE MAXIMUM CHIRAL SUBGROUP O

Enumeration under the action of the maximum chiral subgroup is referred to as enumeration of promolecules as steric isomers in Chapter 7 of [28]. The enumeration of octahedral promolecules as steric isomers is conducted under the point group O, so that the CI-CF for is calculated by using the PSIs collected in the upperleft part of Figure 2 according to Def. 7.23 of [28] as follows:

$$\text{CI - CF(O)} = \frac{1}{24}(b_1^6 + 3b_1^2b_2^2 + 8b_3^2 + 6b_2^3 + 6b_1^2b_4). \quad (17)$$

A general treatment of CI-CFs for maximum chiral subgroups has been reported (Eq. 17 of [29]).

The ligand-inventory function represented by Eq. 13 is introduced into Eq. 17. The resulting equation is expanded to give a generating function. Note that the enumeration under the maximum chiral point group O (using Eq. 17) counts each promolecule of an enantiomeric pair (or each achiral promolecule) just once.

### 3.3 ACTION OF THE MAXIMUM RS-PERMUTATION GROUP $O_{\bar{7}}$

The point group  $T_d$  and the symmetric group of degree 4  $S^{[4]}$  are compared by applying them to a tetrahedral skeleton [41], although the concept of *RS*-stereoisomeric groups was not developed at that time. Note that the symmetric group of degree 4  $S^{[4]}$  is regarded as an *RS*-permutation group  $T_{\bar{6}}$  from the viewpoint of Fujita's stereoisogram approach [3, 1].

Enumeration under the *RS*-permutation group  $O_{\bar{7}}$  can be conducted in a parallel way. Thus, all of the PSIs for the *RS*-permutation group  $O_{\bar{7}}$  (the parts A and C of Figure 2) are summed up. The resulting sum is divided by the order of  $O_{\bar{7}}$  (48), so as to give the following CI-CF:

$$\begin{aligned} \text{CI - CF}(O_{\bar{7}}) = \frac{1}{48} & (b_1^6 + 3b_1^2b_2^2 + 8b_3^2 + 6b_2^3 + 6b_1^2b_4 \\ & + b_2^3 + 3b_1^4b_2 + 8b_6 + 6b_1^2b_2^2 + 6b_2b_4). \end{aligned} \quad (18)$$

A general treatment of CI-CFs for maximum *RS*-permutation groups has been reported (Eq. 41 of [30]).

The ligand-inventory function represented by Eq. 13 is introduced into Eq. 18. The resulting equation is expanded to give a generating function. Note that the enumeration under the *RS*-permutation group  $O_{\bar{7}}$  (using Eq. 18) counts a pair of *RS*-diastereomers (or each *RS*-astereogenic promolecule) just once.

### 3.4. ACTION OF THE MAXIMUM LIGAND-REFLECTION GROUP $O_{\hat{i}}$

To conduct enumeration under the maximum ligand-reflection group  $O_{\hat{i}}$ , all of the PSIs for  $O_{\hat{i}}$  (the parts A and D of Figure 2) are summed up. The resulting sum is divided by the order of  $O_{\hat{i}}$  (48), so as to give the following CI-CF:

$$\begin{aligned} \text{CI-CF}(O_{\hat{i}}) = \frac{1}{48} & (b_1^6 + 3b_1^2b_2^2 + 8b_3^2 + 6b_2^3 + 6b_1^2b_4 \\ & + a_1^6 + 3a_1^2c_2^2 + 8a_3^2 + 6c_2^3 + 6a_1^2c_4). \end{aligned} \quad (19)$$

A general treatment of CI-CFs for maximum ligand-reflection groups has been reported (Eq. 54 of [30]).

The ligand inventory functions represented by Eqs. 11–13 are introduced into Eq. 19. The resulting equation is expanded to give a generating function. Note that the enumeration under the maximum ligand-reflection group  $O_{\hat{i}}$ , (using Eq. 19) counts a pair of holantimers (or each *RS*-ascleral promolecule) just once.

### 3.5. ACTION OF THE RS-STEREISOISOMERIC GROUP $O_{h\tilde{i}\hat{i}}$

Because products of cycles appearing in the lower parts (B and D) of Figure 2 contain ligand reflections as designated by overbars, they are characterized by products of  $a_d$  and/or  $c_d$  after the concept of sphericities for cycles is extended to meet *RS*-stereoisomeric groups [30]. Thereby, Fujita's proligand method [38, 39, 40] is extended to evaluate the number of quadruplets of *RS*-stereoisomeric promolecules. The following cycle index with chirality fittingness (CI-CF) is obtained:

$$\begin{aligned} \text{CI-CF}(O_{h\tilde{i}\hat{i}}) = \frac{1}{96} & (b_1^6 + 3b_1^2b_2^2 + 8b_3^2 + 6b_2^3 + 6b_1^2b_4 \\ & + c_2^3 + 3a_1^4c_2 + 8c_6 + 6a_1^2c_2^2 + 6c_2c_4 \\ & + b_2^3 + 3b_1^4b_2 + 8b_6 + 6b_1^2b_2^2 + 6b_2b_4 \\ & + a_1^6 + 3a_1^2c_2^2 + 8a_3^2 + 6c_2^3 + 6a_1^2c_4). \end{aligned} \quad (20)$$

A general treatment of CI-CFs for *RS*-stereoisomeric groups has been reported (Eq. 11 of [30]).

The ligand inventory functions represented by Eqs. 11–13 are introduced into Eq. 20. The resulting equation is expanded to give a generating function. Note that the enumeration under the *RS*-stereoisomeric group  $O_{h\tilde{i}\hat{i}}$  (using Eq. 20) counts a quadruplet of *RS*-stereoisomers (type I to type V) just once.

## 4. TYPE-ITEMIZED ENUMERATION

### 4.1. FOUNDATIONS FOR CI-CFs OF FIVE TYPES

Under the *RS*-stereoisomeric group  $O_{h\tilde{l}\hat{i}}$ , a quadruplet of *RS*-stereoisomers contained in a stereoisogram (type I to type V) is an equivalence class, which is counted just once by means of the CI-CF represented by Eq. 20. Let the symbol CI-CF<sup>[K]</sup>( $O_{h\tilde{l}\hat{i}}$ ) (K = I, II, . . . V) be a CI-CF for counting each type. Then, their sum is equal to Eq. 20 as follows:

$$\begin{aligned} \text{CI - CF}(O_{h\tilde{l}\hat{i}}) = & \text{CI - CF}^{\text{[I]}}(O_{h\tilde{l}\hat{i}}) + \text{CI - CF}^{\text{[II]}}(O_{h\tilde{l}\hat{i}}) + \text{CI - CF}^{\text{[III]}}(O_{h\tilde{l}\hat{i}}) + \text{CI - CF}^{\text{[IV]}}(O_{h\tilde{l}\hat{i}}) \\ & + \text{CI - CF}^{\text{[V]}}(O_{h\tilde{l}\hat{i}}) + \text{CI - CF}^{\text{[VI]}}(O_{h\tilde{l}\hat{i}}) \end{aligned} \quad (21)$$

Under the maximum chiral subgroup  $O$ , each promolecule of an enantiomeric pair (or each achiral promolecule) is an equivalence class, which is counted just once by means of the CI-CF represented by Eq. 17. Figure 3 indicates that a type-I stereoisogram contains two promolecules, a type-II stereoisogram contains two promolecules, a type-III stereoisogram contains four promolecules, a type-IV stereoisogram contains one promolecule, and a type-V stereoisogram contains two promolecules. Hence, the CI-CF of Eq. 17 is represented as follows:

$$\begin{aligned} \text{CI - CF}(O) = & 2\text{CI - CF}^{\text{[I]}}(O_{h\tilde{l}\hat{i}}) + 2\text{CI - CF}^{\text{[II]}}(O_{h\tilde{l}\hat{i}}) + 4\text{CI - CF}^{\text{[III]}}(O_{h\tilde{l}\hat{i}}) \\ & + \text{CI - CF}^{\text{[IV]}}(O_{h\tilde{l}\hat{i}}) + 2\text{CI - CF}^{\text{[V]}}(O_{h\tilde{l}\hat{i}}). \end{aligned} \quad (22)$$

Under the maximum point group  $O_h$ , each pair of (self-)enantiomers is an equivalence class, which is counted just once by means of the CI-CF represented by Eq. 9. Note that a pair of self-enantiomers means an achiral promolecule. Figure 3 indicates that a type-I stereoisogram contains one pair of enantiomers, a type-II stereoisogram contains one pair of enantiomers, a type-III stereoisogram contains two pairs of enantiomers, a type-IV stereoisogram contains one pair of self-enantiomers (one achiral promolecule), and a type-V stereoisogram contains two pairs of self-enantiomers (two achiral promolecules). Hence, the CI-CF of Eq. 9 is represented as follows:

$$\begin{aligned} \text{CI - CF}(O_h) = & \text{CI - CF}^{\text{[I]}}(O_{h\tilde{l}\hat{i}}) + \text{CI - CF}^{\text{[II]}}(O_{h\tilde{l}\hat{i}}) + 2\text{CI - CF}^{\text{[III]}}(O_{h\tilde{l}\hat{i}}) \\ & + \text{CI - CF}^{\text{[IV]}}(O_{h\tilde{l}\hat{i}}) + 2\text{CI - CF}^{\text{[V]}}(O_{h\tilde{l}\hat{i}}) \end{aligned} \quad (23)$$

Under the maximum *RS*-permutation group  $O_{\tilde{\gamma}}$ , each pair of (self-)*RS*-diastereomers is an equivalence class, which is counted just once by means of the CI-CF represented by Eq. 18. Note that a pair of self-*RS*-diastereomers means an *RS*-astereogenic promolecule. Figure 3 indicates that a type-I stereoisogram contains one pair of *RS*-diastereomers, a type-II stereoisogram contains two pairs of self-*RS*-diastereomers (two *RS*-astereogenic

promolecules), a type- III stereoisogram contains two pairs of *RS*-diastereomers, a type-IV stereoisogram contains one pair of self-*RS*-diastereomers (one *RS*-astereogenic promolecule), and a type-V stereoisogram contains one pair of *RS*-diastereomers. Hence, the CI-CF of Eq. 18 is represented as follows:

$$\begin{aligned} \text{CI-CF}(\text{O}_{\tilde{\gamma}}) &= \text{CI-CF}^{\text{[I]}}(\text{O}_{h\tilde{\gamma}\hat{\gamma}}) + 2\text{CI-CF}^{\text{[II]}}(\text{O}_{h\tilde{\gamma}\hat{\gamma}}) + 2\text{CI-CF}^{\text{[III]}}(\text{O}_{h\tilde{\gamma}\hat{\gamma}}) \\ &+ \text{CI-CF}^{\text{[IV]}}(\text{O}_{h\tilde{\gamma}\hat{\gamma}}) + \text{CI-CF}^{\text{[V]}}(\text{O}_{h\tilde{\gamma}\hat{\gamma}}). \end{aligned} \quad (24)$$

Under the maximum ligand-reflection group  $\text{O}_{\hat{\gamma}}$ , each pair of (self-)holantimers is an equivalence class, which is counted just once by means of the CI-CF represented by Eq. 19. Note that a pair of self-holantimers means an ascleral promolecule. Figure 3 indicates that a type-I stereoisogram contains two pairs of self-holantimers (two ascleral promolecules), a type-II stereoisogram contains one pair of holantimers, a type-III stereoisogram contains two pairs of holantimers, a type-IV stereoisogram contains one pair of self-holantimers (one ascleral promolecule), and a type-V stereoisogram contains one pair of holantimers. Hence, the CI-CF of Eq. 19 is represented as follows:

$$\begin{aligned} \text{CI-CF}(\text{O}_{\hat{\gamma}}) &= 2\text{CI-CF}^{\text{[I]}}(\text{O}_{h\tilde{\gamma}\hat{\gamma}}) + \text{CI-CF}^{\text{[II]}}(\text{O}_{h\tilde{\gamma}\hat{\gamma}}) + 2\text{CI-CF}^{\text{[III]}}(\text{O}_{h\tilde{\gamma}\hat{\gamma}}) \\ &+ \text{CI-CF}^{\text{[IV]}}(\text{O}_{h\tilde{\gamma}\hat{\gamma}}) + \text{CI-CF}^{\text{[V]}}(\text{O}_{h\tilde{\gamma}\hat{\gamma}}). \end{aligned} \quad (25)$$

Although the five equations (Eqs. 21, 22, 23, 24, and 25) are obtained, they cannot be solved to give  $\text{CI-CF}^{\text{[K]}}(\text{O}_{h\tilde{\gamma}\hat{\gamma}})$  ( $\text{K} = \text{I, II, } \dots \text{ V}$ ).

For the purpose of obtaining  $\text{CI-CF}^{\text{[K]}}(\text{O}_{h\tilde{\gamma}\hat{\gamma}})$  For the purpose of obtaining  $\text{CI-CF}^{\text{[K]}}(\text{O}_{h\tilde{\gamma}\hat{\gamma}})$  ( $\text{K} = \text{I, II, } \dots \text{ V}$ ), the CI-CF of Eq. 23 is modulated according to Def. 1 of [32].) ( $\text{K} = \text{I, II, } \dots \text{ V}$ ), the CI-CF of Eq. 23 is modulated according to Def. 1 of [32].

$$\begin{aligned} \text{CI-CF}''(\text{O}_h) &= \text{CI-CF}(\text{O}_h) - \text{CI-CF}^{\text{[V]}}(\text{O}_{h\tilde{\gamma}\hat{\gamma}}) \\ &= \text{CI-CF}^{\text{[I]}}(\text{O}_{h\tilde{\gamma}\hat{\gamma}}) + \text{CI-CF}^{\text{[II]}}(\text{O}_{h\tilde{\gamma}\hat{\gamma}}) + 2\text{CI-CF}^{\text{[III]}}(\text{O}_{h\tilde{\gamma}\hat{\gamma}}) \\ &+ \text{CI-CF}^{\text{[IV]}}(\text{O}_{h\tilde{\gamma}\hat{\gamma}}) + \text{CI-CF}^{\text{[V]}}(\text{O}_{h\tilde{\gamma}\hat{\gamma}}). \end{aligned} \quad (26)$$

If the modulated  $\text{CI-CF}''(\text{O}_h)$  is evaluated, Eqs. 21, 22, 24, and 25 in addition to Eq. 26 can be solved to give  $\text{CI-CF}^{\text{[K]}}(\text{O}_{h\tilde{\gamma}\hat{\gamma}})$  ( $\text{K} = \text{I, II, } \dots \text{ V}$ ) as follows:

$$\text{CI-CF}^{\text{[I]}}(\text{O}_{h\tilde{\gamma}\hat{\gamma}}) = -\text{CI-CF}''(\text{O}_h) + \text{CI-CF}(\text{O}_{\tilde{\gamma}}) \quad (27)$$

$$\text{CI-CF}^{\text{[II]}}(\text{O}_{h\tilde{\gamma}\hat{\gamma}}) = -\text{CI-CF}''(\text{O}_h) + \text{CI-CF}(\text{O}_{\tilde{\gamma}}) \quad (28)$$

$$\text{CI-CF}^{\text{[III]}}(\text{O}_{h\tilde{\gamma}\hat{\gamma}}) = \text{CI-CF}''(\text{O}_h) - \text{CI-CF}(\text{O}_{h\tilde{\gamma}\hat{\gamma}}) \quad (29)$$

$$\text{CI-CF}^{\text{[IV]}}(\text{O}_{h\tilde{\gamma}\hat{\gamma}}) = -\text{CI-CF}(\text{O}) + 2\text{CI-CF}''(\text{O}_h) \quad (30)$$



$$\begin{aligned} \text{CI-CF}^{[\text{VI}]}(\text{O}_{h\bar{1}\bar{1}}) &= \text{CI-CF}(\text{O}) - \text{CI-CF}''(\text{O}_h) - \text{CI-CF}(\text{O}_{\bar{1}}) \\ &\quad - \text{CI-CF}(\text{O}_{\bar{1}}) + 2\text{CI-CF}(\text{O}_{h\bar{1}\bar{1}}) \end{aligned} \quad (31)$$

Note that the introduction of  $\text{CI-CF}''(\text{O}_h)$  (Eq. 26) into Eq. 31 generates the following equation:

$$\text{CI-CF}(\text{O}) = \text{CI-CF}(\text{O}_h) + \text{CI-CF}(\text{O}_{\bar{1}}) + \text{CI-CF}(\text{O}_{\bar{1}}) - 2\text{CI-CF}(\text{O}_{h\bar{1}\bar{1}}), \quad (32)$$

which is an identical equation.

#### 4.2. EVALUATION OF THE MODULATED CI-CF

The next task is the evaluation of the modulated CI-CF shown in Eq. 26. By starting from Eqs. 22 and 23 and by introducing Eqs. 9 and 17, we obtain the following CI-CF:

$$\begin{aligned} \text{CI-CF}^{[\text{IV}]}(\text{O}_{h\bar{1}\bar{1}}) + 2\text{CI-CF}^{[\text{V}]}(\text{O}_{h\bar{1}\bar{1}}) &= 2\text{CI-CF}(\text{O}_h) - \text{CI-CF}(\text{O}) \\ &= \frac{1}{24}(c_2^3 + 3a_1^4c_2 + 8c_6 + 6a_1^2c_2^2 + 6c_2c_4), \end{aligned} \quad (33)$$

which indicates that achiral promolecules (type IV plus  $2 \times$  type V) are counted under the point group  $\text{O}_h$ . For the purpose of evaluating  $\text{CI-CF}^{[\text{V}]}(\text{O}_{h\bar{1}\bar{1}})$ , let us examine whether or not each term appearing in the right-hand side of Eq. 33 contributes the formation of type-V promolecules.

The term  $c_2^3$  (a PSI) in Eq. 33 is concerned with the generation of such a type-V promolecule as having the composition  $\text{p}\bar{\text{p}}\bar{\text{q}}\bar{\text{q}}\bar{\text{r}}\bar{\text{r}}$ , which is depicted in Figure 4. The generating function which is generated by introducing the ligand-inventory function of Eq. 12 into the PSI  $c_2^3$  is contaminated with terms of type-IV promolecules, which stem from the PSIs such as  $a_2c_2^2, a_2^2c_2, c_2c_4, a_2c_4, a_4c_2, a_2a_4, c_6, a_6$  and  $c_2^3$ , because each  $c_2$  in the PSI  $c_2^3$  behaves independently.

The influences of such contaminated PSIs are excluded by trial-and-error examination of inclusion-exclusion behaviors, so as to leave such necessary terms as  $\text{p}\bar{\text{p}}\bar{\text{q}}\bar{\text{q}}\bar{\text{r}}\bar{\text{r}}$ . The source code based on the GAP system is attached as an appendix, where a simplified examination is executed by using the ligand-inventory functions with A, B, C, X,  $\text{p}/\bar{\text{p}}$ ,  $\text{q}/\bar{\text{q}}$ , and  $\text{r}/\bar{\text{r}}$ . Thereby, the following equation is obtained as a net contribution of  $c_2^3$  to type V:

$$V_1 := \frac{1}{48}(c_2^3 - 3(a_2c_2^2 - a_2^2c_2) - 6(c_2c_4 - a_2c_4 - a_4c_2 + a_2a_4) + 8(c_6 - a_6) - a_2^3), \quad (34)$$

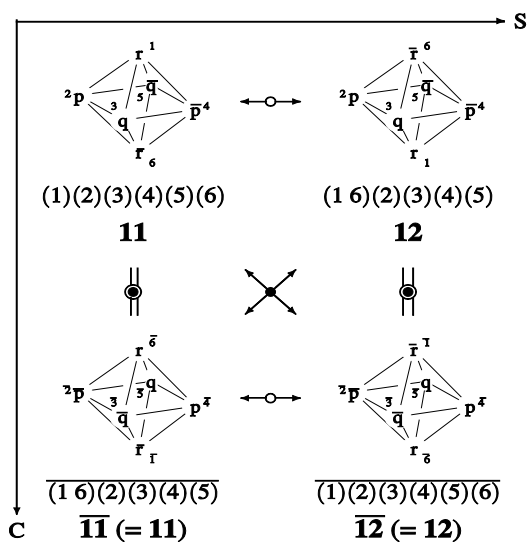


**Figure 4.** Type-V stereoisogram of a promolecule with the composition  $p\bar{p}q\bar{q}r\bar{r}$ , which is evaluated by the PSI  $c_2^3$ .

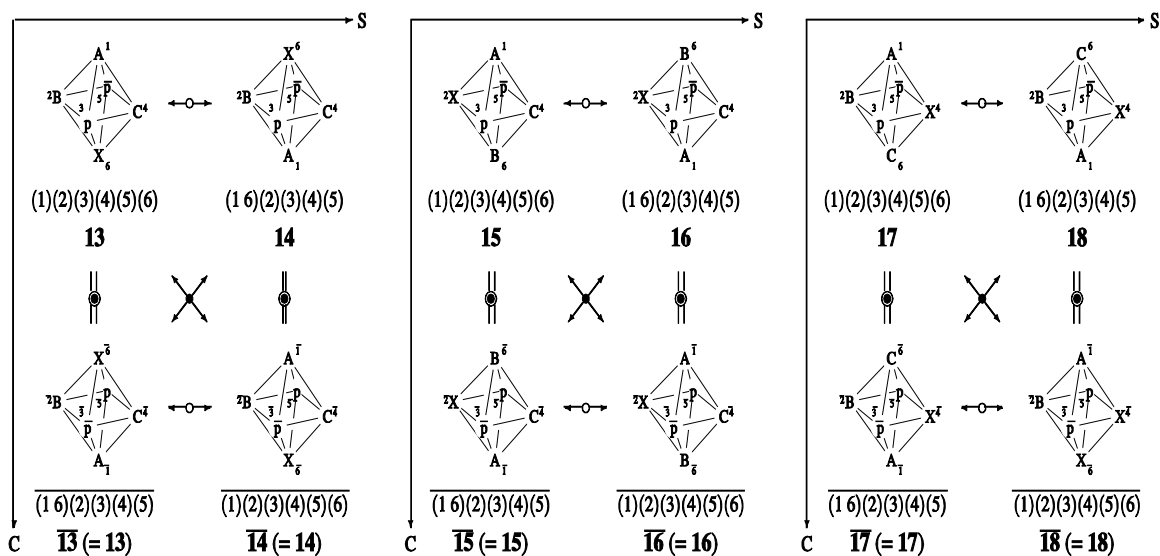


**Figure 5.** Type-V stereoisograms of promolecules with the composition  $ABCXp\bar{p}$ , which are evaluated by the PSI  $a_1^4c_2$ .

which leaves such necessary terms as  $p\bar{p}q\bar{q}r\bar{r}$ . The term  $3a_1^4c_2$  in Eq. 33 is concerned with the generation of such type-V promolecules as having the composition  $A^2BCp\bar{p}$  (9 and 10

in Figure 3). In addition, the term  $3a_1^4c_2$  corresponds to a type-V promolecules with the composition  $ABCXp\bar{p}$ , as depicted in Figure 5.

By the examination using the attached source code, the following equation is obtained as a net contribution of  $a_1^4c_2$  to type V:

$$V_2 = \frac{1}{48} (3(a_1^4c_2 - a_1^4c_2 + 2(a_4c_2 - a_2a_4) + 2(a_1^2a_2c_2 - a_1^2a_2^2) - 5(a_2^2c_2 - a_2^3) - 8(a_1a_3c_2 - a_1a_3a_2) + 8(a_4c_2 - a_2a_4))) \quad (35)$$

which leaves such necessary terms as  $A^2BCp\bar{p}$  (cf. Figure 3) and  $ABCXp\bar{p}$  (cf. Figure 5). Note that the last line of Eq. 35 is added to omit such terms as  $A^3Bp\bar{p}$ , which are shifted to contribute to the term  $6a_1^2c_2^2$ . As for octahedral stereoisomers with  $A^2BCp\bar{p}$ , Figure 13 of [42].

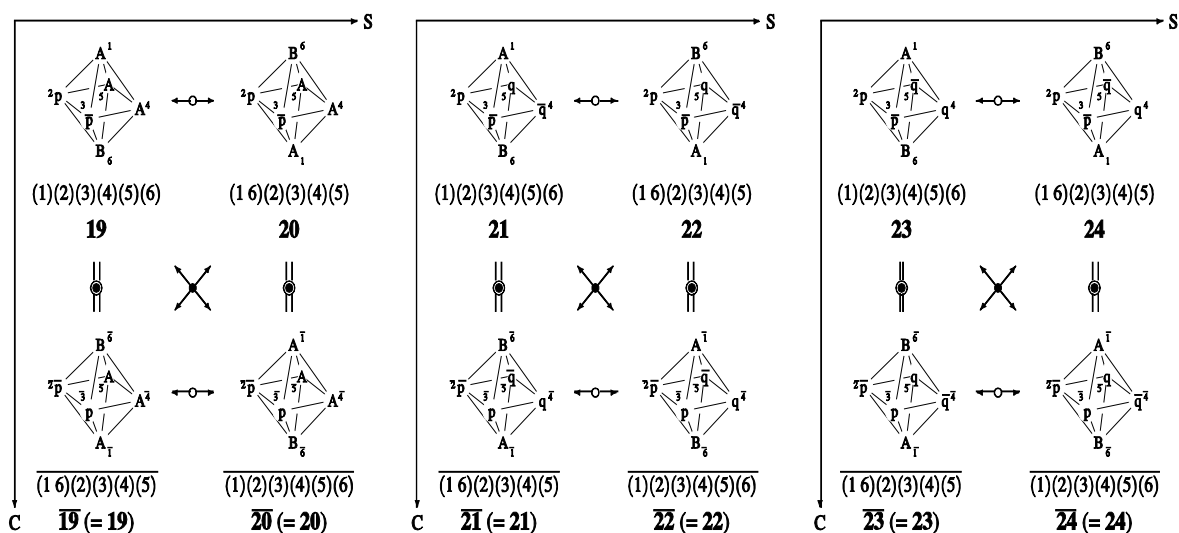


**Figure 6.** Type-V stereoisograms of promolecules with the compositions  $A^3Bp\bar{p}p$  and  $ABp\bar{p}q\bar{q}$ , which are evaluated by the PSI  $a_1^2c_2^2$ .

The term  $6a_1^2c_2^2$  in Eq. 33 is concerned with the generation of such type-V promolecules as having the composition  $A^3Bp\bar{p}$  (the first stereoisogram in Figure 6) and  $ABp\bar{p}q\bar{q}$  (the second and third stereoisograms in Figure 6)

By the examination using the attached source code, the following equation is obtained as a net contribution of  $a_1^2c_2^2$  to type V:

$$\begin{aligned}
V_3 = & \frac{1}{48} (6(a_1^2 c_2^2 - 2(a_1^2 c_4 - a_1^2 a_4)) - 2a_1^2 a_2 c_2 + a_1^2 a_2^2 \\
& - (a_2 c_2^2 - a_2^3) + 2(a_2 c_4 - a_2 a_4) + 2(a_2^2 c_2 - a_2^3) \\
& + 4(a_1 a_3 c_2 - a_1 a_3 a_2) - 4(a_4 c_2 - a_2 a_4)),
\end{aligned} \tag{36}$$

which leaves such necessary terms as  $A^3 B p \bar{p}$  and  $AB p \bar{p} q \bar{q}$  (Figure 6). Note that the last line of Eq. 36 is added to take account of such terms as  $A^3 B p \bar{p}$ . The last line of Eq. 36 is cancelled by the last line of Eq. 35, when Eq. 35 and Eq. 36 are summed up.

Among the terms appearing in the right-hand side of Eq. 33, the terms  $8c_6$  and  $6c_2 c_4$  do not contribute to the appearance of type-V stereoisograms. Hence, Eqs. 34, 35, and 36 are summed up to give the CI-CF for enumerating type-V stereoisograms:

$$\begin{aligned}
\text{CI-CF}^{[V]}(O_{h\tilde{i}\hat{i}}) &= V_1 + V_2 + V_3 \\
&= -\frac{1}{16} a_1^4 a_2 + \frac{1}{16} a_1^4 c_2 - \frac{1}{8} a_1^2 a_2 c_2 + \frac{1}{8} a_1^2 c_2^2 + \frac{1}{4} a_1^2 a_4 - \frac{1}{4} a_1^2 a_4 + \frac{1}{6} a_2^3 \\
&\quad - \frac{3}{16} a_2 c_2^2 + \frac{1}{48} c_2^3 - \frac{1}{2} a_2 a_4 + \frac{3}{8} a_2 c_4 + \frac{1}{4} a_4 c_2 - \frac{1}{8} c_2 c_4 - \frac{1}{6} a_6 + \frac{1}{6} c_6.
\end{aligned} \tag{37}$$

By introducing Eq. 37 into Eq. 33, the CI-CF for enumerating type-IV stereoisograms is obtained as follows:

$$\begin{aligned}
\text{CI-CF}^{[IV]}(O_{h\tilde{i}\hat{i}}) &= \frac{1}{8} a_1^4 a_2 + \frac{1}{4} a_1^2 a_2 c_2 - \frac{1}{2} a_1^2 a_4 + \frac{1}{2} a_1^2 c_4 - \frac{1}{3} a_2^3 \\
&\quad + \frac{3}{8} a_2 c_2^2 + a_2 a_4 - \frac{3}{4} a_2 c_4 - \frac{1}{2} a_4 c_2 + \frac{1}{2} c_2 c_4 + \frac{1}{3} a_6.
\end{aligned} \tag{38}$$

The modulated CI-CF is obtained by introducing Eq. 23 and Eq. 37 into Eq. 26:

$$\begin{aligned}
\text{CI-CF}''(O_h) &= \text{CI-CF}(O_h) - \text{CI-CF}^{[V]}(O_{h\tilde{i}\hat{i}}) \\
&= \frac{1}{48} b_1^6 + \frac{1}{16} a_1^4 a_2 + \frac{1}{16} b_1^2 b_2^2 + \frac{1}{8} a_1^2 a_2 c_2 \\
&\quad + \frac{1}{8} b_1^2 b_4 + \frac{1}{8} b_2^3 - \frac{1}{4} a_1^2 a_4 + \frac{1}{4} a_1^2 c_4 - \frac{1}{6} a_2^3 + \frac{3}{16} a_2 c_2^2 + \frac{1}{6} b_3^2 \\
&\quad + \frac{1}{2} a_2 a_4 - \frac{3}{8} a_2 c_4 - \frac{1}{4} a_4 c_2 + \frac{1}{4} c_2 c_4 + \frac{1}{6} a_6.
\end{aligned} \tag{39}$$

### 4.3. CI-CFs FOR ENUMERATING FIVE TYPES

Because the modulated CI-CF (Eq. 39 for CI-CF''(O<sub>h</sub>)) has been obtained to revise the effect of CI-CF(O<sub>h</sub>) (Eq. 9), it is used with the other CI-CFs, i.e., Eq. 17 for CI-CF(O), Eq. 18 for CI-CF(O<sub>7</sub>), Eq. 19 for CI-CF(O<sub>7</sub>), and Eq. 20 for CI-CF(O<sub>h $\tilde{7}$  $\tilde{i}$</sub> ). They are introduced into Eqs. 27–31. Thereby, we reach the following CI-CFs for enumerating stereoisograms of five types:

$$\begin{aligned} \text{CI-CF}^{\text{II}}(\text{O}_{h\tilde{7}\tilde{i}}) = & \frac{1}{48}a_1^6 - \frac{1}{16}a_1^4a_2 - \frac{1}{8}a_1^2a_2c_2 + \frac{1}{16}a_1^2c_2^2 + \frac{1}{4}a_1^2a_4 - \frac{1}{8}a_1^2c_4 + \frac{1}{6}a_2^3 \\ & - \frac{3}{16}a_2c_2^2 + \frac{1}{8}c_2^3 - \frac{1}{2}a_2a_4 + \frac{3}{8}a_2c_4 + \frac{1}{6}a_3^2 + \frac{1}{4}a_4c_2 - \frac{1}{4}c_2c_4 - \frac{1}{6}a_6 \end{aligned} \quad (40)$$

$$\begin{aligned} \text{CI-CF}^{\text{III}}(\text{O}_{h\tilde{7}\tilde{i}}) = & \frac{1}{16}b_1^4b_2 - \frac{1}{16}a_1^4a_2 + \frac{1}{8}b_1^2b_2^2 - \frac{1}{8}a_1^2a_2c_2 + \frac{1}{48}b_2^3 + \frac{1}{4}a_1^2a_4 - \frac{1}{4}a_1^2c_4 + \frac{1}{6}a_2^3 \\ & - \frac{3}{16}a_2c_2^2 + \frac{1}{8}b_2b_4 - \frac{1}{2}a_2a_4 + \frac{3}{8}a_2c_4 + \frac{1}{4}a_4c_2 - \frac{1}{4}c_2c_4 + \frac{1}{6}b_6 - \frac{1}{6}a_6 \end{aligned} \quad (41)$$

$$\begin{aligned} \text{CI-CF}^{\text{III}}(\text{O}_{h\tilde{7}\tilde{i}}) = & \frac{1}{96}b_1^6 - \frac{1}{96}a_1^6 - \frac{1}{32}b_1^4b_2 + \frac{1}{16}a_1^4a_2 - \frac{1}{32}a_1^4c_2 - \frac{1}{32}b_1^2b_2^2 \\ & + \frac{1}{8}a_1^2a_2c_2 - \frac{3}{32}a_1^2c_2^2 + \frac{1}{16}b_1^2b_4 + \frac{5}{96}b_2^3 - \frac{1}{4}a_1^2a_4 + \frac{3}{16}a_1^2c_4 - \frac{1}{6}a_2^3 \\ & + \frac{3}{16}a_2c_2^2 - \frac{7}{96}c_2^3 - \frac{1}{16}b_2b_4 + \frac{1}{12}b_3^2 + \frac{1}{2}a_2a_4 - \frac{3}{8}a_2c_4 - \frac{1}{12}a_3^2 \\ & - \frac{1}{4}a_4c_2 + \frac{3}{16}c_2c_4 - \frac{1}{12}b_6 + \frac{1}{6}a_6 - \frac{1}{12}c_6 \end{aligned} \quad (42)$$

$$\begin{aligned} \text{CI-CF}^{\text{IV}}(\text{O}_{h\tilde{7}\tilde{i}}) = & \frac{1}{8}a_1^4a_2 + \frac{1}{4}a_1^2a_2c_2 - \frac{1}{2}a_1^2a_4 + \frac{1}{2}a_1^2c_4 - \frac{1}{3}a_2^3 \\ & + \frac{3}{8}a_2c_2^2 + a_2a_4 - \frac{3}{4}a_2c_4 - \frac{1}{2}a_4c_2 + \frac{1}{2}c_2c_4 + \frac{1}{3}a_6 \end{aligned} \quad (43)$$

$$\begin{aligned} \text{CI-CF}^{\text{IV}}(\text{O}_{h\tilde{7}\tilde{i}}) = & -\frac{1}{16}a_1^4a_2 + \frac{1}{16}a_1^4c_2 - \frac{1}{8}a_1^2a_2c_2 + \frac{1}{8}a_1^2c_2^2 + \frac{1}{4}a_1^2a_4 - \frac{1}{4}a_1^2c_4 + \frac{1}{6}a_2^3 \\ & - \frac{3}{16}a_2c_2^2 + \frac{1}{48}c_2^3 - \frac{1}{2}a_2a_4 + \frac{3}{8}a_2c_4 + \frac{1}{4}a_4c_2 - \frac{1}{8}c_2c_4 - \frac{1}{6}a_6 + \frac{1}{6}c_6. \end{aligned} \quad (44)$$

The consistency of the modulated CI-CF (Eq. 39) is confirmed by the fact that Eq. 43 is identical with Eq. 38 and that Eq. 44 is identical with Eq. 37.

In order to conduct type-itemized enumeration of octahedral complexes, the ligand-inventory functions represented by Eqs. 11–13 are introduced into the type-itemized CIFs represented by Eqs. 40–44. The resulting equation of each type is expanded to give a generating function. In a similar way to the attached source code based on the GAP system, the full forms of Eqs. 11–13 are used in the type-itemized enumeration of this article. The number of inequivalent quadruplets of *RS*-stereoisomers (i.e., inequivalent stereoisograms) appears in the generating function as the coefficient of the term  $A^a B^b C^c X^x Y^y Z^z p^p q^q r^r \bar{r} \bar{s} \bar{s} u^u \bar{u} v^v \bar{v}$ , which is represented by the partition  $[\theta]$  (Eq. 14).

**Table 1.** Type-Itemized Enumeration of Octahedral Complexes with Achiral Proligands.

partition for the composition $A^a B^b C^c X^x Y^y Z^z p^p q^q r^r \bar{r} \bar{s} \bar{s} u^u \bar{u} v^v \bar{v}$	gross enum. $O_h$	enum. $O_{h\bar{i}}$	type-itemized enum.				
			I	II	III	IV	V
$[\theta]_1=[6,0,0,0,0,0,0,0,0,0,0,0,0,0,0,0]$	1	1	0	0	0	1	0
$[\theta]_2=[5,1,0,0,0,0,0,0,0,0,0,0,0,0,0,0]$	1	1	0	0	0	1	0
$[\theta]_3=[4,2,0,0,0,0,0,0,0,0,0,0,0,0,0,0]$	2	2	0	0	0	2	0
$[\theta]_4=[4,1,1,0,0,0,0,0,0,0,0,0,0,0,0,0]$	2	2	0	0	0	2	0
$[\theta]_5=[3,3,0,0,0,0,0,0,0,0,0,0,0,0,0,0]$	2	2	0	0	0	2	0
$[\theta]_6=[3,2,1,0,0,0,0,0,0,0,0,0,0,0,0,0]$	3	3	0	0	0	3	0
$[\theta]_7=[3,1,1,1,0,0,0,0,0,0,0,0,0,0,0,0]$	4	4	1	0	0	3	0
$[\theta]_8=[2,2,2,0,0,0,0,0,0,0,0,0,0,0,0,0]$	5	5	1	0	0	4	0
$[\theta]_9=[2,2,1,1,0,0,0,0,0,0,0,0,0,0,0,0]$	6	6	2	0	0	4	0
$[\theta]_{10}=[2,1,1,1,1,0,0,0,0,0,0,0,0,0,0,0]$	9	9	6	0	0	3	0
$[\theta]_{11}=[1,1,1,1,1,1,0,0,0,0,0,0,0,0,0,0]$	15	15	15	0	0	0	0

## 5. ENUMERATION RESULTS

### 5.1. OCTAHEDRAL COMPLEXES WITH ACHIRAL PROLIGANDS ONLY

Table 1 collects type-itemized enumeration of octahedral complexes with achiral prolignands only. The columns of gross enumeration indicate the numbers of octahedral complexes counted under the point group  $O_h$  and under the *RS*-stereoisomeric group  $O_{h\bar{i}}$ . Note that a pair of (self)-enantiomers is counted once under the point group  $O_h$ , while a quadruplet of

*RS*-stereoisomers is counted once under the *RS*-stereoisomeric group  $O_{h\tilde{i}\hat{i}}$ . The columns of type-itemized enumeration (type I to type V) indicate the numbers of octahedral complexes of five types. The values of the gross enumeration under the point group  $O_h$  satisfy Eq. 23. The values of the gross enumeration under the *RS*-stereoisomeric group  $O_{h\tilde{i}\hat{i}}$  satisfy Eq. 21.

Because Table 1 is concerned with achiral proligands only, there appear type-I or type-IV quadruplets. For example, the  $[\theta]_7$ -row of Table 1 indicates the presence of one type-I quadruplet and three type-IV quadruplets.

One type-I quadruplet with the composition  $A^3BCX$  ( $[\theta]_7$ ) has been depicted in the type-I frame of Figure 3, which contains a pair of enantiomers  $3/\bar{3}$ . Note that a type-I quadruplet is generally characterized by the presence of diagonal equality symbols, so that it is chiral, *RS*-stereogenic, and ascleral (type index  $[-,-,a]$ ).

The configuration of  $3$  (or  $\bar{3}$ ) is specified by a configuration index *OC*-6-43 according to the IUPAC rule IR-9.3.3.4 [43], where the priority sequence  $A > B > C > X$  is presumed. According to the IUPAC rule IR-9.3.4.8 [43], the absolute configuration of  $3$  is specified to be *OC*-6-23-*A*, while that of its *RS*-diastereomer  $4$  ( $=\bar{3}$ ) is specified to be *OC*-6-43-*C*. Note that a pair of *C/A*-descriptors is assigned to a pair of *RS*-diastereomers (not to a pair of enantiomers) [33], strictly speaking, although a pair of *RS*-diastereomers is coincident with a pair of enantiomers in case of type-I stereoisograms.

Among the three type-IV quadruplets with the composition  $A^3BCX$  ( $[\theta]_7$ ), one quadruplet has been depicted in the type-IV frame of Figure 3, which contains an achiral octahedral complex  $8$  having a *trans*-pair of proligands *A*-*X*. The remaining two type-IV quadruplets can be drawn by replacing the proligand *X* located at the *trans*-position of *A* by the proligand *B* or *C* so as to generate a *trans*-pair *A*-*B* or *A*-*C*. Note that a type-IV quadruplet is generally characterized by the presence of equality symbols in all directions, so that it is achiral, *RS*-astereogenic, and ascleral (type index  $[a,a,a]$ ).

The three type-IV quadruplets are differentiated by configuration indices according to the IUPAC rule IR-9.3.3.4 [43]. The configuration index of  $8$  is determined to be *OC*-6-41, while the other two quadruplets are determined to be *OC*-6-21 and *OC*-6-31, respectively.

## 5.2. OCTAHEDRAL COMPLEXES WITH ACHIRAL AND CHIRAL PROLIGANDS

Table 2 collects type-itemized numbers of inequivalent quadruplets of *RS*-stereoisomers with achiral and chiral proligands. Each quadruplet of chiral promolecules is counted as a fractional value, as designated by an asterisk. For example, the value  $1/2$  at the intersection between the  $[\theta]_{12}$ -row (with an asterisk) and the type-II-column in Table 2 corresponds to such a term as  $1 \times \frac{1}{2} (A^5p+ A^5\bar{p})$ , which indicates the presence of one type-II quadruplet



of *RS*-stereoisomers. Note that the composition  $A^5p$  is converted into the composition  $A^5\bar{p}$  vice versa under the action of a reflection. A type-II quadruplet is generally characterized by the presence of horizontal equality symbols, so that it is chiral, *RS*-astereogenic, and scleral (type index  $[-, a, -]$ ).

The value 1 at the intersection between the  $[\theta]_{13}$ -row (with an asterisk) and the type-II column in Table 2 should be interpreted to correspond to such a term as  $2 \times 1/2 (A^4p^2 + A^4\bar{p}^2)$ , which indicates the presence of two type-II quadruplets of *RS*-stereoisomers. Note that the composition  $A^4p^2$  is converted into the composition  $A^4\bar{p}^2$  vice versa under the action of a reflection. These type-II quadruplets are depicted in Figure 7. Each type-II quadruplet in Figure 7 contains a pair of enantiomers  $25/2\bar{5}$  or  $26/2\bar{6}$ .

According to the IUPAC rule IR-9.3.3.4 [43], a configuration index *OC*-6-11 is assigned to 25 and  $2\bar{5}$ , where the priority sequence  $A > p$  or  $A > \bar{p}$  is presumed. In a similar way, a configuration index *OC*-6-22 is assigned to 26 and  $2\bar{6}$ . The absolute configuration for each pair of such enantiomers as belonging to type II is not specified by *C/A*-descriptors due to IUPAC rule IR-9.3.4.8, because of *RS*-astereogenicity (not because of achirality). For detailed discussions, see [33].

On the other hand, the value 2 at the intersection between the  $[\theta]_{15}$ -row (without an asterisk) and the type-IV-column in Table 2 should be interpreted to correspond to such a term as  $2 \times A^4p\bar{p}$ , which indicates the presence of two type-IV quadruplets of *RS*-stereoisomers. Note that the composition  $A^4p\bar{p}$  remains unchanged under the action of a reflection. These type-IV quadruplets are depicted in Figure 8.

The configurations of 27 and 28 can be differentiated by configuration indices according to the IUPAC rule IR-9.3.3.4 [43]. Thus, a configuration index *OC*-6-11 is assigned to 27, while a configuration index *OC*-6-32 is assigned to 28, where the priority sequence  $A > p > \bar{p}$  is presumed.

The value 1 at the intersection between the  $[\theta]_{19}$ -row (without an asterisk) and the type-V column in Table 2 indicates the presence of one type-V quadruplet of *RS*-stereoisomers, which has the composition  $A^3Bp\bar{p}$ . The type-V quadruplet containing 19 and 20 has been drawn in Figure 6. According to the IUPAC rules IR-9.3.3.4 and IR-9.3.4.8 [43], 19 is determined to be *OC*-6-43-*a*, while 20 is determined to be *OC*-6-43-*c*, where the priority sequence  $A > B > p > \bar{p}$  is presumed. Note that a pair of *C/A*-descriptors is assigned to a pair of *RS*-diastereomers 19/20, which is contained in a type-V stereoisogram shown in Figure 6. The chirality-unfaithful feature [11] is emphasized by the lowercase labels '*c/a*' used in place of the uppercase labels '*C/A*' [33].

The value 2 at the intersection between the  $[\theta]_{29}$ -row (with an asterisk) and the type-II column in Table 2 should be interpreted to correspond to such a term as  $4 \times 1/2 (A^2BCp^2 + A^2BC\bar{p}^2)$ , which indicates the presence of four type-II quadruplets of *RS*-stereoisomers.

One type-II quadruplet containing  $5/\bar{5}$  is drawn in Figure 3. The remaining three type-II quadruplets containing  $29/\bar{29}$ ,  $30/\bar{30}$ , and  $31/\bar{31}$  are depicted in Figure 9.

According to the IUPAC rule IR-9.3.3.4 [43], a configuration index  $OC-6-32$  is assigned to  $5$  and  $\bar{5}$ , where the priority sequence  $A > B > C > p$  or  $A > B > C > \bar{p}$  is presumed. In a similar way, a configuration index  $OC-6-14$  is assigned to  $29$  and  $\bar{29}$ ; a configuration index  $OC-6-13$  is assigned to  $30$  and  $\bar{30}$ ; and a configuration index  $OC-6-44$  is assigned to  $31$  and  $\bar{31}$ . The absolute configuration for each pair of such enantiomers as belonging to type II is not specified by  $C/A$ -descriptors due to IUPAC rule IR-9.3.4.8, because of  $RS$ -astereogenicity (not because of achirality) [33].

**Table 2.** Type-Itemized Enumeration of Octahedral Complexes with Achiral and Chiral Proligands (Part 1).

partition for the composition $A^a B^b C^c X^x Y^y Z^z p^p q^q r^r \bar{r} \bar{s} \bar{s} u^u \bar{u} \bar{v} \bar{v}$	gross enum. $O_h$	gross enum. $O_{h\tilde{i}\hat{i}}$	type-itemized enum.				
			I	II	III	IV	V
$[\theta]_{12}^* = [5, 0, 0, 0, 0, 0, 1, 0, 0, 0, 0, 0, 0, 0, 0, 0, 0]$	1/2	1/2	0	1/2	0	0	0
$[\theta]_{13}^* = [4, 0, 0, 0, 0, 0, 2, 0, 0, 0, 0, 0, 0, 0, 0, 0, 0]$	1	1	0	1	0	0	0
$[\theta]_{14}^* = [4, 1, 0, 0, 0, 0, 1, 0, 0, 0, 0, 0, 0, 0, 0, 0, 0]$	1	1	0	1	0	0	0
$[\theta]_{15}^* = [4, 0, 0, 0, 0, 0, 1, 1, 0, 0, 0, 0, 0, 0, 0, 0, 0]$	2	2	0	0	0	2	0
$[\theta]_{16}^* = [3, 2, 0, 0, 0, 0, 1, 0, 0, 0, 0, 0, 0, 0, 0, 0, 0]$	3/2	3/2	0	3/2	0	0	0
$[\theta]_{17}^* = [3, 1, 1, 0, 0, 0, 1, 0, 0, 0, 0, 0, 0, 0, 0, 0, 0]$	5/2	2	0	3/2	1/2	0	0
$[\theta]_{18}^* = [3, 1, 0, 0, 0, 0, 2, 0, 0, 0, 0, 0, 0, 0, 0, 0, 0]$	3/2	3/2	0	3/2	0	0	0
$[\theta]_{19}^* = [3, 1, 0, 0, 0, 0, 1, 1, 0, 0, 0, 0, 0, 0, 0, 0, 0]$	4	3	0	2	1	0	0
$[\theta]_{20}^* = [3, 1, 0, 0, 0, 0, 1, 0, 1, 0, 0, 0, 0, 0, 0, 0, 0]$	5/2	2	0	3/2	1/2	0	0
$[\theta]_{21}^* = [3, 0, 0, 0, 0, 0, 3, 0, 0, 0, 0, 0, 0, 0, 0, 0, 0]$	1	1	0	1	0	0	0
$[\theta]_{22}^* = [3, 0, 0, 0, 0, 0, 2, 1, 0, 0, 0, 0, 0, 0, 0, 0, 0]$	3/2	3/2	0	3/2	0	0	0
$[\theta]_{23}^* = [3, 0, 0, 0, 0, 0, 2, 0, 1, 0, 0, 0, 0, 0, 0, 0, 0]$	3/2	3/2	0	3/2	0	0	0
$[\theta]_{24}^* = [3, 0, 0, 0, 0, 0, 1, 1, 1, 0, 0, 0, 0, 0, 0, 0, 0]$	5/2	2	0	3/2	1/2	0	0
$[\theta]_{25}^* = [3, 0, 0, 0, 0, 0, 1, 0, 1, 0, 1, 0, 0, 0, 0, 0, 0]$	5/2	2	0	3/2	1/2	0	0
$[\theta]_{26}^* = [2, 2, 0, 0, 0, 0, 2, 0, 0, 0, 0, 0, 0, 0, 0, 0, 0]$	3	5/2	0	2	1/2	0	0
$[\theta]_{27}^* = [2, 2, 0, 0, 0, 0, 1, 1, 0, 0, 0, 0, 0, 0, 0, 0, 0]$	6	5	0	0	1	4	0

$[\theta]_{28}^* = [2, 2, 0, 0, 0, 0, 1, 0, 1, 0, 0, 0, 0, 0, 0, 0, 0, 0]$	4	3	0	2	1	0	0
$[\theta]_{29}^* = [2, 1, 1, 0, 0, 0, 2, 0, 0, 0, 0, 0, 0, 0, 0, 0, 0, 0]$	4	3	0	2	1	0	0
$[\theta]_{30}^* = [2, 1, 1, 0, 0, 0, 1, 1, 0, 0, 0, 0, 0, 0, 0, 0, 0, 0]$	10	6	0	1	2	1	2
$[\theta]_{31}^* = [2, 1, 1, 0, 0, 0, 1, 0, 1, 0, 0, 0, 0, 0, 0, 0, 0, 0]$	15/2	9/2	0	3/2	3	0	0
$[\theta]_{32}^* = [2, 1, 0, 0, 0, 0, 3, 0, 0, 0, 0, 0, 0, 0, 0, 0, 0, 0]$	3/2	3/2	0	3/2	0	0	0
$[\theta]_{33}^* = [2, 1, 0, 0, 0, 0, 2, 1, 0, 0, 0, 0, 0, 0, 0, 0, 0, 0]$	4	3	0	2	1	0	0
$[\theta]_{34}^* = [2, 1, 0, 0, 0, 0, 2, 0, 1, 0, 0, 0, 0, 0, 0, 0, 0, 0]$	4	3	0	2	1	0	0
$[\theta]_{35}^* = [2, 1, 0, 0, 0, 0, 1, 1, 1, 0, 0, 0, 0, 0, 0, 0, 0, 0]$	15/2	9/2	0	3/2	3	0	0
$[\theta]_{36}^* = [2, 1, 0, 0, 0, 0, 1, 0, 1, 0, 1, 0, 0, 0, 0, 0, 0, 0]$	15/2	9/2	0	3/2	3	0	0
$[\theta]_{37}^* = [2, 0, 0, 0, 0, 0, 4, 0, 0, 0, 0, 0, 0, 0, 0, 0, 0, 0]$	1	1	0	1	0	0	0
$[\theta]_{38}^* = [2, 0, 0, 0, 0, 0, 3, 1, 0, 0, 0, 0, 0, 0, 0, 0, 0, 0]$	3/2	3/2	0	3/2	0	0	0
$[\theta]_{39}^* = [2, 0, 0, 0, 0, 0, 3, 0, 1, 0, 0, 0, 0, 0, 0, 0, 0, 0]$	3/2	3/2	0	3/2	0	0	0
$[\theta]_{40}^* = [2, 0, 0, 0, 0, 0, 2, 2, 0, 0, 0, 0, 0, 0, 0, 0, 0, 0]$	4	4	1	1	0	2	0
$[\theta]_{41}^* = [2, 0, 0, 0, 0, 0, 2, 0, 2, 0, 0, 0, 0, 0, 0, 0, 0, 0]$	3	5/2	0	2	1/2	0	0
$[\theta]_{42}^* = [2, 0, 0, 0, 0, 0, 2, 1, 1, 0, 0, 0, 0, 0, 0, 0, 0, 0]$	4	3	0	2	1	0	0
$[\theta]_{43}^* = [2, 0, 0, 0, 0, 0, 2, 0, 1, 1, 0, 0, 0, 0, 0, 0, 0, 0]$	4	3	0	2	1	0	0
$[\theta]_{44}^* = [2, 0, 0, 0, 0, 0, 2, 0, 1, 0, 1, 0, 0, 0, 0, 0, 0, 0]$	4	3	0	2	1	0	0
$[\theta]_{45}^* = [2, 0, 0, 0, 0, 0, 1, 1, 1, 1, 0, 0, 0, 0, 0, 0, 0, 0]$	9	7	2	0	2	3	0
$[\theta]_{46}^* = [2, 0, 0, 0, 0, 0, 1, 1, 1, 0, 1, 0, 0, 0, 0, 0, 0, 0]$	15/2	9/2	0	3/2	3	0	0
$[\theta]_{47}^* = [2, 0, 0, 0, 0, 0, 1, 0, 1, 0, 1, 0, 1, 0, 0, 0, 0, 0]$	15/2	9/2	0	3/2	3	0	0

The value 1 at the intersection between The  $[\theta]_{29}$ -row (with an asterisk) and the type-III column in Table 2 should be interpreted to correspond to such a term as  $2 \times 1/2$  ( $A^2BCp^2 + A^2BC\bar{p}^2$ ), which indicates the presence of two type-III quadruplets of *RS*-stereoisomers. They are depicted in Figure 10. A type-III quadruplet is generally characterized by the absence of equality symbols in all directions, so that it is chiral, *RS*-stereogenic, and scleral (type index  $[-, -, -]$ ).

The  $[\theta]_{30}$ -row (without an asterisk) in Table 2 indicates the presence of one type-II, two type-III, one type-IV, and two type-V stereoisograms.

One type-II quadruplet of *RS*-stereoisomers  $36/\overline{36}$  with the composition  $A^2BCp\bar{p}$  is depicted in the upperleft part of Figure 11. According to the IUPAC rule IR-9.3.3.4 [43], a

configuration index *OC*-6-15 is assigned to 36, while *OC*-6-14 is assigned to 36, where the priority sequence  $A > B > C > p > \bar{p}$  is presumed. The absolute configuration for each pair of such enantiomers as belonging to type II is not specified by *C/A*-descriptors due to IUPAC rule IR-9.3.4.8, because of *RS*-astereogenicity (not because of achirality) [33].

Among the two type-III quadruplets with  $A^2BCp\bar{p}$  ( $[\theta]_{30}$ ), one has been already depicted in the type-III frame of Figure 3 ( $6/\bar{6}/7/\bar{7}$ ). The other is depicted in the upperright part of Figure 11 ( $37/\bar{37}/38/\bar{38}$ ). As for the type-III frame of Figure 3, *OC*-6-52-*C* assigned to 6 is paired with *OC*-6-52-*A* assigned to 7, while *OC*-6-42-*A* assigned to 6 is paired with *OC*-6-42-*C* assigned to 7. As for the upperright part of Figure 11, *OC*-6-53-*C* assigned to 37 is paired with *OC*-6-53-*A* assigned to 38, while *OC*-6-43-*A* assigned to 37 is paired with *OC*-6-43-*C* assigned to  $\bar{38}$ . It should be noted that *OC*-6-52-*C* assigned to 6, for example, is not paired with *OC*-6-42-*A* assigned to  $\bar{6}$ , because the configuration-index parts are different from each other, even though the *C/A*-labels are paired. It follows that a pair of *C/A*-descriptors is assigned to a pair of *RS*-diastereomers, not to a pair of enantiomers.

One type-IV quadruplet, which consists of an achiral promolecule 39 with the composition  $A^2BCp\bar{p}$ , is depicted in the lower left part of Figure 11.

Among the two type-V quadruplets with the composition  $A^2BCp\bar{p}$ , one has been depicted in the type-V frame of Figure 3 (9/10). The other is depicted in the lowerright part of Figure 11 (40/41). The pair of 9/10 (or the pair of 40/41) is in an *RS*-diastereomeric relationship, which is specified by *C/A*-descriptors due to IUPAC rule IR-9.3.4.8. When the priority sequence  $A > B > C > p > \bar{p}$  is presumed, *OC*-6-32-*a* assigned to 9 is paired with *OC*-6-32-*c* assigned to 10; and *OC*-6-54-*a* assigned to 40 is paired with *OC*-6-54-*c* assigned to 41. The lowercase labels *c/a* are used to emphasize the chirality-unfaithful features of type-V quadruplets.

Table 3 is the list of additional type-itemized numbers of inequivalent quadruplets of *RS*-stereoisomers with achiral and chiral proligands.

The  $[\theta]_{49}$ -row (without an asterisk) in Table 3 indicates the presence of six type-III and three type-V stereoisograms. The three type-V quadruplets with the composition  $ABCXp\bar{p}$  have been already depicted in Figure 5, where each type-V quadruplet is characterized to be achiral, *RS*-stereogenic, and scleral (type index  $[a,-,-]$ ). The pair of 13/14 (or 15/16 or 17/18) exhibits an *RS*-diastereomeric relationship, which corresponds to the term ‘pseudoasymmetry’ in the conventional terminology of stereochemistry. When the priority sequence  $A > B > C > X > p > \bar{p}$  is presumed, *OC*-6-43-*a* assigned to 13 is paired with *OC*-6-43-*c* assigned to 14; *OC*-6-24-*c* assigned to 15 is paired with *OC*-6-24-*a* assigned to 16; and *OC*-6-34-*a* assigned to 17 is paired with *OC*-6-34-*c* assigned to 18.

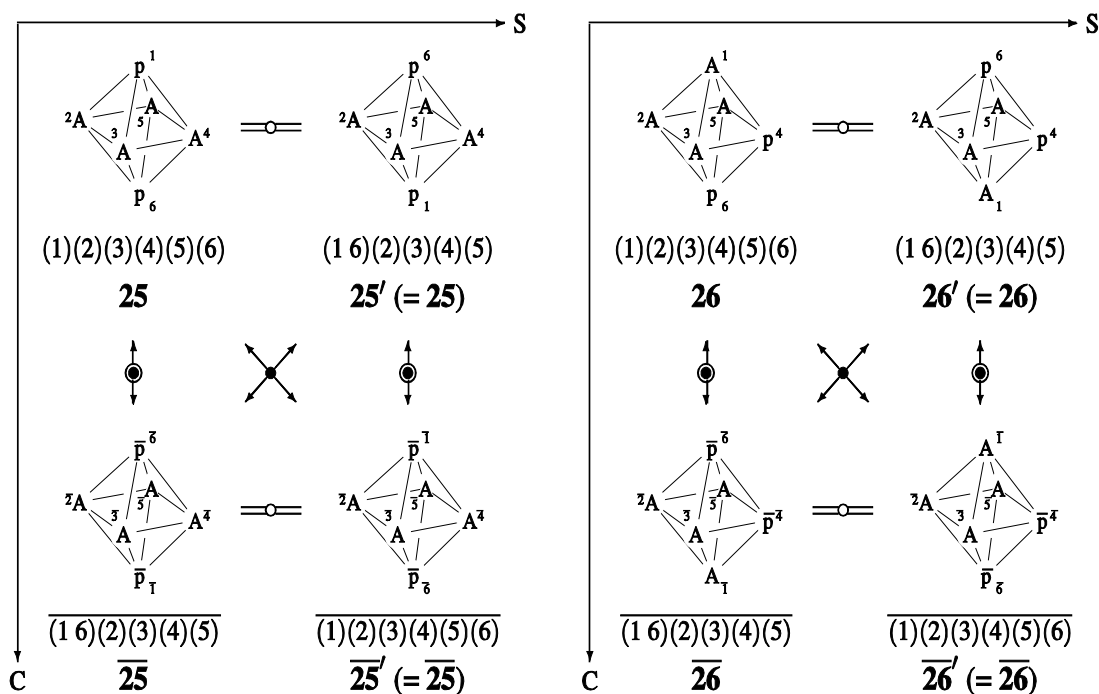


**Figure 7.** Type-II stereoisograms of promolecules with the composition  $1/2 (A^4 p^2 + A^4 \bar{p}^2)$ , which corresponds to the  $[\theta]_{13}$ -row of Table 2.

The  $[\theta]_{62}$ -row (without an asterisk) in Table 3 indicates the presence of one type-I, six type-III, and two type-V stereoisograms. The two type-V quadruplets with the composition  $ABp\bar{p}q\bar{q}$  ( $[\theta]_{62}$ ) have been already depicted in Figure 6, where each type-V quadruplet is characterized to be achiral, *RS*-stereogenic, and scleral (type index  $[a, -, -]$ ). The pair of 21/22 (or 23/24) exhibits an *RS*-diastereomeric relationship, which corresponds to the term 'pseudoasymmetry' in the conventional terminology of stereochemistry. When the priority sequence  $A > B > p > \bar{p} > q > \bar{q}$  is presumed, *OC*-6-26-*a* assigned to 21 is paired with *OC*-6-26-*c* assigned to 22; and *OC*-6-25-*a* assigned to 23 is paired with *OC*-6-25-*c* assigned to 24.

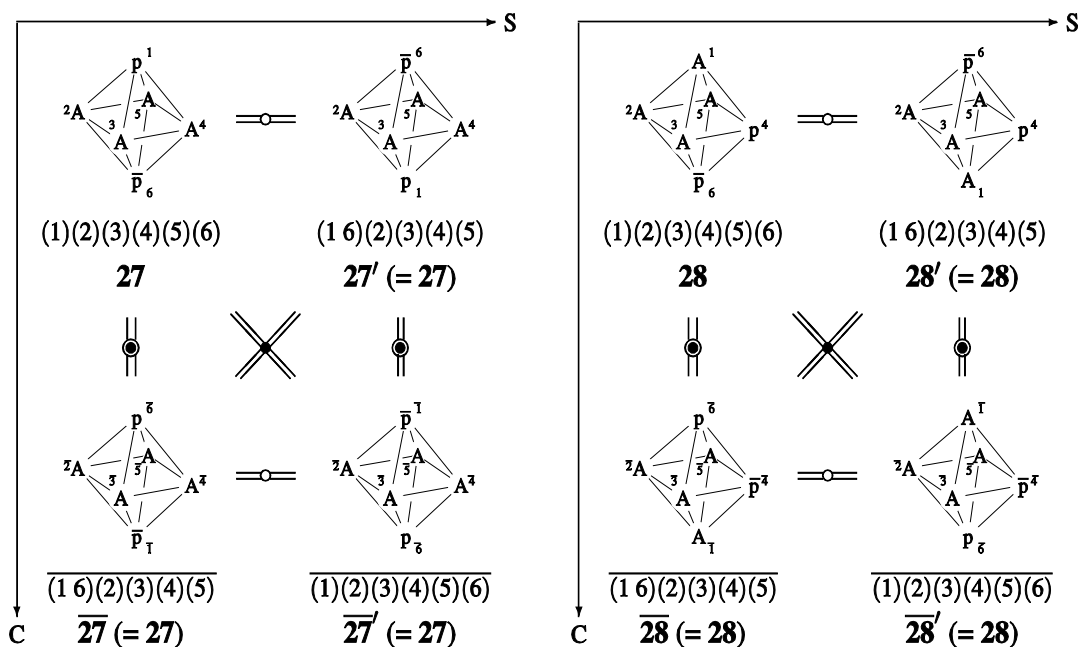


**Figure 8.** Type-IV stereoisograms of promolecules with the composition  $A^4p\bar{p}$ , which corresponds to the  $[\theta]_{15}$ -row of Table 2.

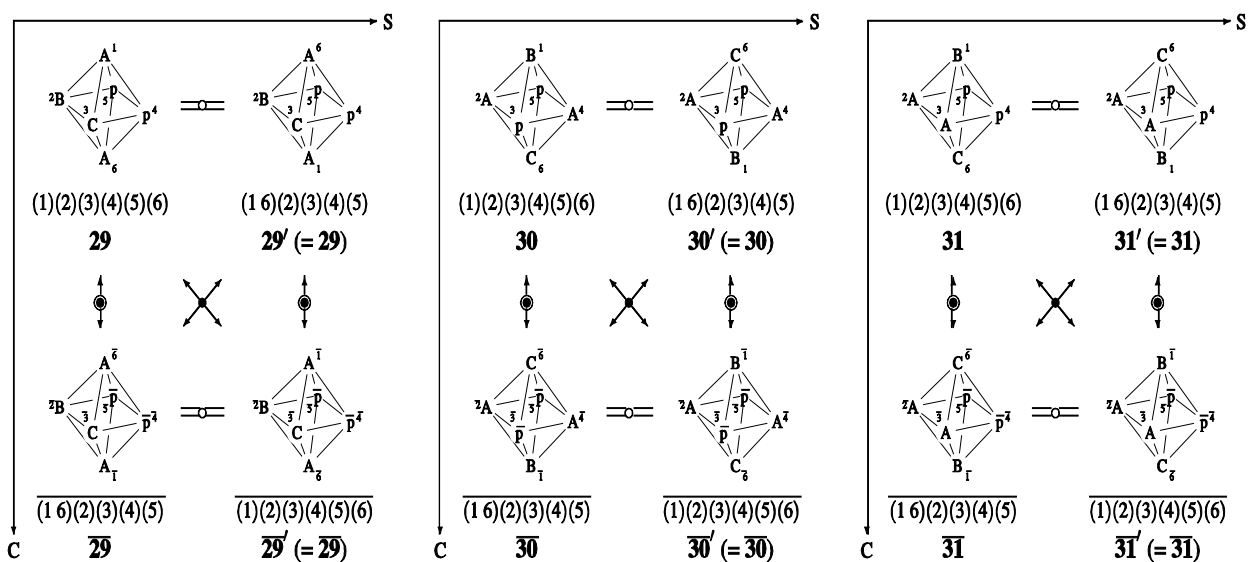


**Figure 9.** Type-II stereoisograms of promolecules with the composition  $1/2(A^2BCp^2 + A^2BC\bar{p}^2)$ , which corresponds to the  $[\theta]_{29}$ -row of Table 2. One more type-II stereoisogram ( $5/\bar{5}$ ) is drawn in Figure 3.

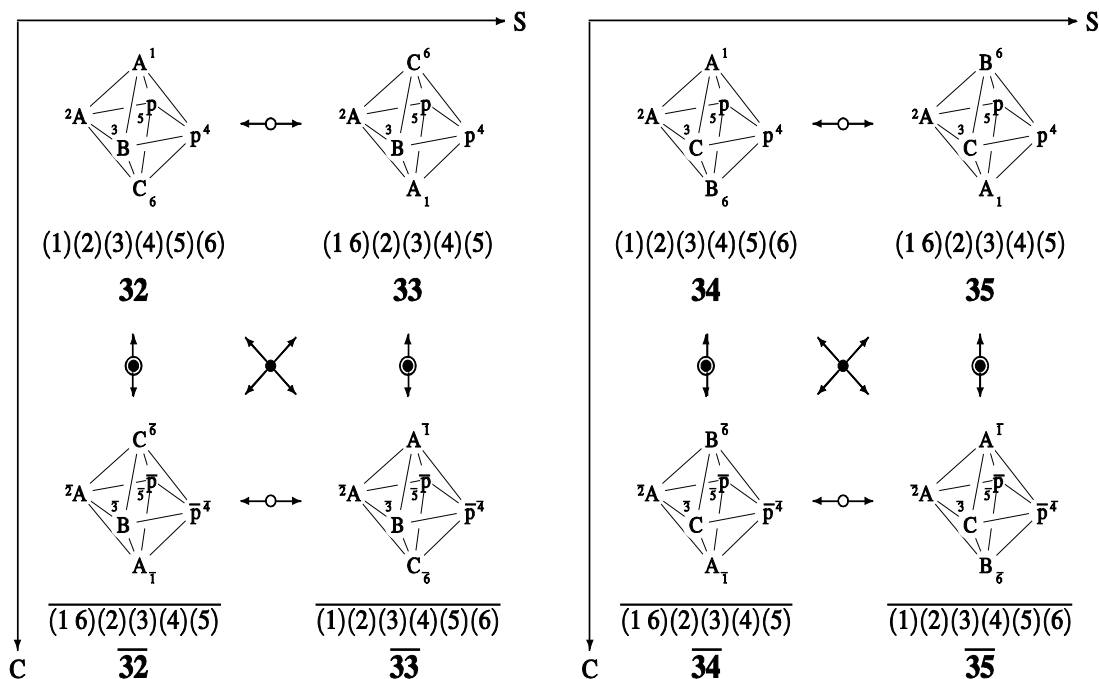


**Figure 10.** Type-III stereoisograms of promolecules with the composition  $1/2 (A^2BCp^2 + A^2BC\bar{p}^2)$ , which corresponds to the  $[\theta]_{29}$ -row of Table 2.

The type-I quadruplet with the composition  $ABp\bar{p}q\bar{q}$  ( $[\theta]_{62}$ ) is depicted in Figure 12. The chiral, *RS*-stereogenic, and ascleral behavior of Figure 12 (type index  $[-, -, a]$ ) is characterized by the presence of equality symbols in the diagonal directions, so that the *RS*-diastereomeric relationship between 42 and 43 ( $= \bar{4}2$ ) is coincident with the enantiomeric relationship between 42 and  $\bar{4}2$ . When the priority sequence  $A > B > p > \bar{p} > q > \bar{q}$  is presumed, *OC*-6-24-*A* assigned to 42 is paired with *OC*-6-24-*C* assigned to 43. The pair of the labels assigned originally to a pair of *RS*-diastereomers 42/43 can be interpreted to be assigned to a pair of enantiomers 42/ $\bar{4}2$  ( $= 43$ ) in a chirality-faithful fashion [11].

### 5.3. OCTAHEDRAL COMPLEXES WITH CHIRAL PROLIGANDS ONLY

Table 4 collects type-itemized numbers of inequivalent quadruplets of *RS*-stereoisomers with chiral proligands only.

The value of 1 at the intersection between the  $[\theta]_{111}$ -row and the type-V-column in Table 4 indicates the presence of one type-V stereoisogram with the composition  $p\bar{p}q\bar{q}r\bar{r}$ . The type-V stereoisogram has been depicted in Figure 4, in which a pair of 11 and 12 is

determined to be *RS*-diastereomeric. When the priority sequence  $p > \bar{p} > q > \bar{q} > r > \bar{r}$  is presumed, *OC*-6-24-*a* assigned to 11 is paired with *OC*-6-24-*c* assigned to 12.

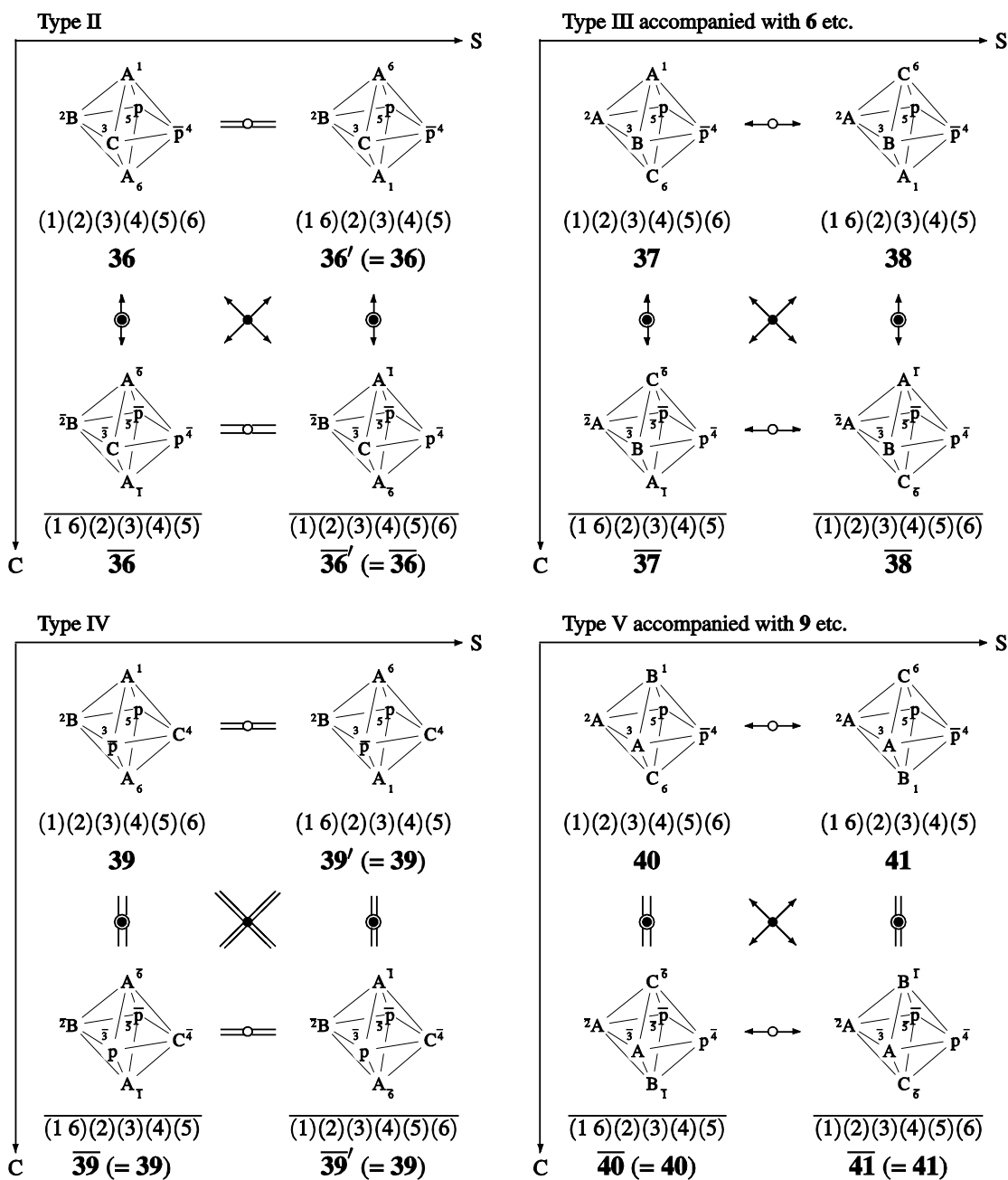


**Figure 11.** Several stereoisograms of promolecules with the composition  $A^2BCp\bar{p}$ , which corresponds to the  $[\theta]_{30}$ -row of Table 2.



## 6. CONCLUSION

Fujita's proligand method [28] is extended to treat type-itemized enumeration of quadruplets of octahedral complexes under the action of the corresponding *RS*-stereoisomeric group. A modulated CI-CF is evaluated from the CI-CF of the point group  $O_h$  by trial-and error calculation of type-V quadruplets contained in stereoisograms. Then, the modulated CI-CF is combined with a CI-CF of the maximum chiral point group (O), a CI-CF of the maximum *RS*-permutation group, a CI-CF of the maximum ligand-reflection group, and a CI-CF of the *RS*-stereoisomeric group so as to generate CI-CFs for evaluating type-I to type-V quadruplets. By introducing ligand-inventory functions into the CI-CFs, the numbers of quadruplets of octahedral complexes are obtained and shown in tabular forms. Several stereoisograms for typical complexes are depicted. Their configuration indices due to IUPAC rule IR-9.3.3.4 [43] as well as *C/A* descriptors due to IUPAC rule IR-9.3.4.8 are discussed on the basis of Fujita's stereoisogram approach [34].

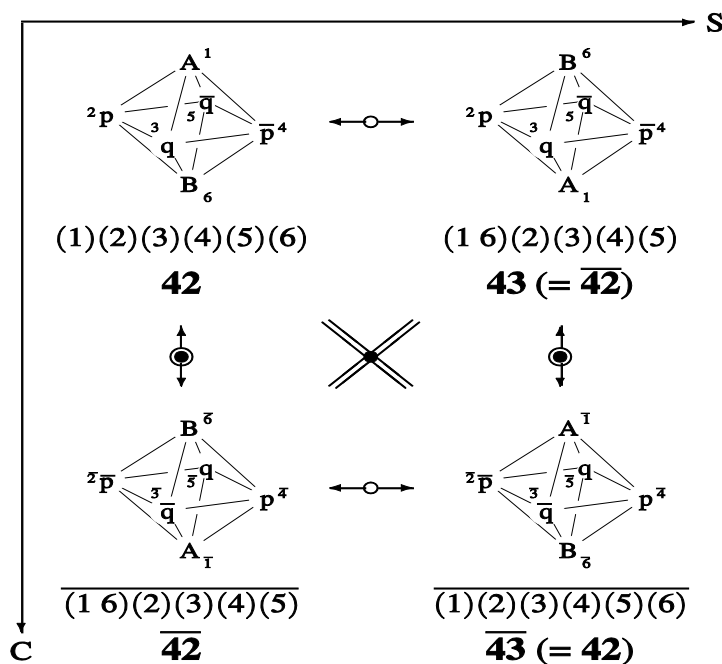


**Figure 12.** Type-I stereoisogram of promolecules with the composition  $ABp \bar{p}q \bar{q}$ , which corresponds to the  $[\theta]_{62}$ -row of Table 3.

## APPENDIX

The following source code for evaluation of the modulated CI-CF is based on the GAP system [44]. The file named test\_V.gap containing this code is stored in a directory shown in the command Read. This Read sentence is copied and pasted on a command line of the

GAP system. The execution result is stored in the log file named test\_Vlog.txt, which is specified by the command LogTo. The type-itemized enumeration can be done by using the CI-CFs of the respective types (Eqs. 40–44) in place of V\_1 etc.

```
#Read("c:/fujita0/fujita2015/ligancy6/calcGAP/test_V.gap");
LogTo("c:/fujita0/fujita2015/ligancy6/calcGAP/test_Vlog.txt");
#####
# Setting variables #
#####
A := Indeterminate(Rationals, "A"); B := Indeterminate(Rationals, "B");
C := Indeterminate(Rationals, "C"); x := Indeterminate(Rationals, "x");
y := Indeterminate(Rationals, "y"); z := Indeterminate(Rationals, "z");
p := Indeterminate(Rationals, "p"); P := Indeterminate(Rationals, "P");
q := Indeterminate(Rationals, "q"); Q := Indeterminate(Rationals, "Q");
r := Indeterminate(Rationals, "r"); R := Indeterminate(Rationals, "R");
s := Indeterminate(Rationals, "s"); S := Indeterminate(Rationals, "S");
u := Indeterminate(Rationals, "u"); U := Indeterminate(Rationals, "U");
v := Indeterminate(Rationals, "v"); V := Indeterminate(Rationals, "V");
b_1 := Indeterminate(Rationals, "b_1"); b_2 := Indeterminate(Rationals, "b_2");
b_3 := Indeterminate(Rationals, "b_3"); b_4 := Indeterminate(Rationals, "b_4");
b_5 := Indeterminate(Rationals, "b_5"); b_6 := Indeterminate(Rationals, "b_6");
a_1 := Indeterminate(Rationals, "a_1"); a_2 := Indeterminate(Rationals, "a_2");
a_3 := Indeterminate(Rationals, "a_3"); a_4 := Indeterminate(Rationals, "a_4");
a_5 := Indeterminate(Rationals, "a_5"); a_6 := Indeterminate(Rationals, "a_6");
c_2 := Indeterminate(Rationals, "c_2"); c_4 := Indeterminate(Rationals, "c_4");
c_6 := Indeterminate(Rationals, "c_6");
#####
#type IV + 2 type V#
#####
CICF_VI_V := (1/24)*(c_2^3 + 3*a_1^4*c_2 + 8*c_6 + 6*a_1^2*c_2^2 + 6*c_2*c_4);
#####
#Evaluation of the term c_2^3#
#####
V1 := (1/48)*(c_2^3 - 3*(a_2*c_2^2 - a_2^2*c_2) - 6*(c_2*c_4 - a_2*c_4 - a_4*c_2
+ a_2*a_4) + 8*(c_6 - a_6) - a_2^3);
#####
#Evaluation of the term a_1^4*c_2#
#####
V2 := (1/48)*(3*(a_1^4*c_2 - a_1^4*a_2 + 2*(a_4*c_2 - a_2*a_4)
```

```

+ 2*(a_1^2*a_2*c_2 - a_1^2*a_2^2) - 5*(a_2^2*c_2 - a_2^3)
- 8*(a_1*a_3*c_2 - a_1*a_3*a_2) + 8*(a_4*c_2 - a_2*a_4));
#####
#Evaluation of the term a_1^2*c_2^2#
#####
V3 := (1/48)*(6*(a_1^2*c_2^2 - 2*(a_1^2*c_4 - a_1^2*a_4) - 2*a_1^2*a_2*c_2
+ a_1^2*a_2^2 - (a_2*c_2^2 - a_2^3) + 2*(a_2*c_4 - a_2*a_4) + 2*(a_2^2*c_2 - a_2^3)
+ 4*(a_1*a_3*c_2 - a_1*a_3*a_2) - 4*(a_4*c_2 - a_2*a_4));
#####
# CI-CF of type V#
#####
CICF_V := V1 + V2 + V3;
#####
# CI-CF of type IV#
#####
CICF_IV := CICF_VI_V - 2*CICF_V;
#####
#Ligand-inventory functions#
#####
aa_1 := A + B + C + x;
aa_2 := A^2 + B^2 + C^2 + x^2;
aa_3 := A^3 + B^3 + C^3 + x^3;
aa_4 := A^4 + B^4 + C^4 + x^4;
aa_6 := A^6 + B^6 + C^6 + x^6;
bb_3 := A^3 + B^3 + C^3 + x^3 + p^3 + P^3 + q^3 + Q^3 + r^3 + R^3;
bb_4 := A^4 + B^4 + C^4 + x^4 + p^4 + P^4 + q^4 + Q^4 + r^4 + R^4;
bb_6 := A^6 + B^6 + C^6 + x^6 + p^6 + P^6 + q^6 + Q^6 + r^6 + R^6;
cc_2 := A^2 + B^2 + C^2 + x^2 + 2*p*P + 2*q*Q + 2*r*R;
cc_4 := A^4 + B^4 + C^4 + x^4 + 2*p^2*P^2 + 2*q^2*Q^2 + 2*r^2*R^2;
cc_6 := A^6 + B^6 + C^6 + x^6 + 2*p^3*P^3 + 2*q^3*Q^3 + 2*r^3*R^3;
#####
#Generating functions#
#####
Display("##### CICF_VI_V, f_CICF_VI_V --- type IV + 2 type V #####");
Print("CICF_VI_V := ", CICF_VI_V, "\n");
f_CICF_VI_V := Value(CICF_VI_V,
[a_1, a_2, a_3, a_4, a_6, b_1, b_2, b_3, b_4, b_6, c_2, c_4, c_6],
[aa_1, aa_2, aa_3, aa_4, aa_6, bb_1, bb_2, bb_3, bb_4, bb_6, cc_2, cc_4, cc_6]);
Print("f_CICF_VI_V := ", f_CICF_VI_V, "\n");

```

```

Display("##### V1, f_V1 --- term c_2^3 #####");
Print("V1 := ", V1, "\n");
f_V1:= Value(V1,
[a_1, a_2, a_3, a_4, a_6, b_1, b_2, b_3, b_4, b_6, c_2, c_4, c_6],
[aa_1, aa_2, aa_3, aa_4, aa_6, bb_1, bb_2, bb_3, bb_4, bb_6, cc_2, cc_4, cc_6]);
Print("f_V1 := ", f_V1, "\n");
Display("##### V2, f_V2 --- term a_1^4*c_2 #####");
Print("V2 := ", V2, "\n");
f_V2:= Value(V2,
[a_1, a_2, a_3, a_4, a_6, b_1, b_2, b_3, b_4, b_6, c_2, c_4, c_6],
[aa_1, aa_2, aa_3, aa_4, aa_6, bb_1, bb_2, bb_3, bb_4, bb_6, cc_2, cc_4, cc_6]);
Print("f_V2 := ", f_V2, "\n");
Display("##### V3, f_V3 --- term a_1^2*c_2^2 #####");
Print("V3 := ", V3, "\n");
f_V3:= Value(V3,
[a_1, a_2, a_3, a_4, a_6, b_1, b_2, b_3, b_4, b_6, c_2, c_4, c_6],
[aa_1, aa_2, aa_3, aa_4, aa_6, bb_1, bb_2, bb_3, bb_4, bb_6, cc_2, cc_4, cc_6]);
Print("f_V3 := ", f_V3, "\n");
Display("##### CICF_V, f_CICF_V --- type V #####");
Print("CICF_V := ", CICF_V, "\n");
f_CICF_V:= Value(CICF_V,
[a_1, a_2, a_3, a_4, a_6, b_1, b_2, b_3, b_4, b_6, c_2, c_4, c_6],
[aa_1, aa_2, aa_3, aa_4, aa_6, bb_1, bb_2, bb_3, bb_4, bb_6, cc_2, cc_4, cc_6]);
Print("f_CICF_V := ", f_CICF_V, "\n");
Display("##### CICF_IV, f_CICF_IV --- type IV #####");
Print("CICF_IV := ", CICF_IV, "\n");
f_CICF_IV:= Value(CICF_IV,
[a_1, a_2, a_3, a_4, a_6, b_1, b_2, b_3, b_4, b_6, c_2, c_4, c_6],
[aa_1, aa_2, aa_3, aa_4, aa_6, bb_1, bb_2, bb_3, bb_4, bb_6, cc_2, cc_4, cc_6]);
Print("f_CICF_IV := ", f_CICF_IV, "\n");
LogTo();

```

**Table 3.** Type-Itemized Enumeration of Octahedral Complexes with Achiral and Chiral Proligands (Part 2).

partition for the composition $A^a B^b C^c X^x Y^y Z^z p^p q^q r^r \bar{r} \bar{r} s^s \bar{s} \bar{s} u^u \bar{u} \bar{u} v \bar{v} \bar{v}$	gross enum. $O_h$	$O_{h\bar{i}\hat{i}}$	type-itemized enum.				
			I	II	III	IV	V
$[\theta]_{48}^* = [1, 1, 1, 1, 1, 0, 1, 0, 0, 0, 0, 0, 0, 0, 0, 0, 0]$	15	15/2	0	0	15/2	0	0
$[\theta]_{49}^* = [1, 1, 1, 1, 0, 0, 1, 1, 0, 0, 0, 0, 0, 0, 0, 0, 0]$	18	9	0	0	6	0	3
$[\theta]_{50}^* = [1, 1, 1, 1, 0, 0, 1, 0, 1, 0, 0, 0, 0, 0, 0, 0, 0]$	15	15/2	0	0	15/2	0	0
$[\theta]_{51}^* = [1, 1, 1, 0, 0, 0, 3, 0, 0, 0, 0, 0, 0, 0, 0, 0, 0]$	5/2	2	0	3/2	1/2	0	0
$[\theta]_{52}^* = [1, 1, 1, 0, 0, 0, 2, 1, 0, 0, 0, 0, 0, 0, 0, 0, 0]$	15/2	9/2	0	3/2	3	0	0
$[\theta]_{53}^* = [1, 1, 1, 0, 0, 0, 2, 0, 1, 0, 0, 0, 0, 0, 0, 0, 0]$	15/2	9/2	0	3/2	3	0	0
$[\theta]_{54}^* = [1, 1, 1, 0, 0, 0, 1, 1, 1, 0, 0, 0, 0, 0, 0, 0, 0]$	15	15/2	0	0	15/2	0	0
$[\theta]_{55}^* = [1, 1, 0, 0, 0, 0, 4, 0, 0, 0, 0, 0, 0, 0, 0, 0, 0]$	1	1	0	1	0	0	0
$[\theta]_{56}^* = [1, 1, 0, 0, 0, 0, 3, 1, 0, 0, 0, 0, 0, 0, 0, 0, 0]$	5/2	2	0	3/2	1/2	0	0
$[\theta]_{57}^* = [1, 1, 0, 0, 0, 0, 3, 0, 1, 0, 0, 0, 0, 0, 0, 0, 0]$	5/2	2	0	3/2	1/2	0	0
$[\theta]_{58}^* = [1, 1, 0, 0, 0, 0, 2, 2, 0, 0, 0, 0, 0, 0, 0, 0, 0]$	5	4	0	1	1	2	0
$[\theta]_{59}^* = [1, 1, 0, 0, 0, 0, 2, 1, 1, 0, 0, 0, 0, 0, 0, 0, 0]$	15/2	9/2	0	3/2	3	0	0
$[\theta]_{60}^* = [1, 1, 0, 0, 0, 0, 2, 0, 1, 1, 0, 0, 0, 0, 0, 0, 0]$	15/2	9/2	0	3/2	3	0	0
$[\theta]_{61}^* = [1, 1, 0, 0, 0, 0, 2, 0, 1, 0, 1, 0, 0, 0, 0, 0, 0]$	15/2	9/2	0	3/2	3	0	0
$[\theta]_{62}^* = [1, 1, 0, 0, 0, 0, 1, 1, 1, 1, 0, 0, 0, 0, 0, 0, 0]$	17	9	1	0	6	0	2
$[\theta]_{63}^* = [1, 1, 0, 0, 0, 0, 1, 1, 1, 0, 1, 0, 0, 0, 0, 0, 0]$	15	15/2	0	0	15/2	0	0
$[\theta]_{64}^* = [1, 1, 0, 0, 0, 0, 1, 0, 1, 0, 1, 0, 1, 0, 0, 0, 0]$	15	15/2	0	0	15/2	0	0
$[\theta]_{65}^* = [1, 0, 0, 0, 0, 0, 5, 0, 0, 0, 0, 0, 0, 0, 0, 0, 0]$	1/2	1/2	0	1/2	0	0	0
$[\theta]_{66}^* = [1, 0, 0, 0, 0, 0, 4, 1, 0, 0, 0, 0, 0, 0, 0, 0, 0]$	1	1	0	1	0	0	0
$[\theta]_{67}^* = [1, 0, 0, 0, 0, 0, 4, 0, 1, 0, 0, 0, 0, 0, 0, 0, 0]$	1	1	0	1	0	0	0
$[\theta]_{68}^* = [1, 0, 0, 0, 0, 0, 3, 2, 0, 0, 0, 0, 0, 0, 0, 0, 0]$	3/2	3/2	0	3/2	0	0	0
$[\theta]_{69}^* = [1, 0, 0, 0, 0, 0, 3, 0, 2, 0, 0, 0, 0, 0, 0, 0, 0]$	3/2	3/2	0	3/2	0	0	0
$[\theta]_{70}^* = [1, 0, 0, 0, 0, 0, 3, 1, 1, 0, 0, 0, 0, 0, 0, 0, 0]$	5/2	2	0	3/2	1/2	0	0
$[\theta]_{71}^* = [1, 0, 0, 0, 0, 0, 3, 0, 1, 1, 0, 0, 0, 0, 0, 0, 0]$	5/2	2	0	3/2	1/2	0	0

$[\theta]_{72}^* = [1, 0, 0, 0, 0, 0, 3, 0, 1, 0, 1, 0, 0, 0, 0, 0, 0, 0]$	5/2	2	0	3/2	1/2	0	0
$[\theta]_{73}^* = [1, 0, 0, 0, 0, 0, 2, 2, 1, 0, 0, 0, 0, 0, 0, 0, 0, 0]$	4	3	0	2	1	0	0
$[\theta]_{74}^* = [1, 0, 0, 0, 0, 0, 2, 1, 2, 0, 0, 0, 0, 0, 0, 0, 0, 0]$	4	3	0	2	1	0	0
$[\theta]_{75}^* = [1, 0, 0, 0, 0, 0, 2, 1, 1, 1, 0, 0, 0, 0, 0, 0, 0, 0]$	15/2	9/2	0	3/2	3	0	0
$[\theta]_{76}^* = [1, 0, 0, 0, 0, 0, 2, 1, 1, 0, 1, 0, 0, 0, 0, 0, 0, 0]$	15/2	9/2	0	3/2	3	0	0
$[\theta]_{77}^* = [1, 0, 0, 0, 0, 0, 2, 0, 1, 1, 1, 0, 0, 0, 0, 0, 0, 0]$	15/2	9/2	0	3/2	3	0	0
$[\theta]_{78}^* = [1, 0, 0, 0, 0, 0, 2, 0, 1, 0, 1, 0, 1, 0, 0, 0, 0, 0]$	15/2	9/2	0	3/2	3	0	0
$[\theta]_{79}^* = [1, 0, 0, 0, 0, 0, 1, 1, 1, 1, 1, 0, 0, 0, 0, 0, 0, 0]$	15	15/2	0	0	15/2	0	0
$[\theta]_{80}^* = [1, 0, 0, 0, 0, 0, 1, 1, 1, 0, 1, 0, 1, 0, 0, 0, 0, 0]$	15	15/2	0	0	15/2	0	0
$[\theta]_{81}^* = [1, 0, 0, 0, 0, 0, 1, 0, 1, 0, 1, 0, 1, 0, 1, 0, 0, 0]$	15	15/2	0	0	15/2	0	0

**Table 4.** Type-Itemized Enumeration of Octahedral Complexes with Chiral Proligands.

partition for the composition $A^a B^b C^c X^x Y^y Z^z p^p p^p q^q r^r \bar{r} \bar{r} s^s \bar{s} \bar{s} u^u \bar{u} \bar{u} v \bar{v} \bar{v}$	gross $O_h$	enum. $O_{h\tilde{i}}$	type-itemized enum.				
			I	II	III	IV	V
$[\theta]_{82}^* = [0, 0, 0, 0, 0, 0, 6, 0, 0, 0, 0, 0, 0, 0, 0, 0, 0, 0]$	1/2	1/2	0	1/2	0	0	0
$[\theta]_{83}^* = [0, 0, 0, 0, 0, 0, 5, 1, 0, 0, 0, 0, 0, 0, 0, 0, 0, 0]$	1/2	1/2	0	1/2	0	0	0
$[\theta]_{84}^* = [0, 0, 0, 0, 0, 0, 5, 0, 1, 0, 0, 0, 0, 0, 0, 0, 0, 0]$	1/2	1/2	0	1/2	0	0	0
$[\theta]_{85}^* = [0, 0, 0, 0, 0, 0, 4, 2, 0, 0, 0, 0, 0, 0, 0, 0, 0, 0]$	1	1	0	1	0	0	0
$[\theta]_{86}^* = [0, 0, 0, 0, 0, 0, 4, 0, 2, 0, 0, 0, 0, 0, 0, 0, 0, 0]$	1	1	0	1	0	0	0
$[\theta]_{87}^* = [0, 0, 0, 0, 0, 0, 4, 1, 1, 0, 0, 0, 0, 0, 0, 0, 0, 0]$	1	1	0	1	0	0	0
$[\theta]_{88}^* = [0, 0, 0, 0, 0, 0, 4, 0, 1, 1, 0, 0, 0, 0, 0, 0, 0, 0]$	1	1	0	1	0	0	0
$[\theta]_{89}^* = [0, 0, 0, 0, 0, 0, 4, 0, 1, 0, 1, 0, 0, 0, 0, 0, 0, 0]$	1	1	0	1	0	0	0
$[\theta]_{90}^* = [0, 0, 0, 0, 0, 0, 3, 3, 0, 0, 0, 0, 0, 0, 0, 0, 0, 0]$	2	2	0	0	0	2	0
$[\theta]_{91}^* = [0, 0, 0, 0, 0, 0, 3, 0, 3, 0, 0, 0, 0, 0, 0, 0, 0, 0]$	1	1	0	1	0	0	0
$[\theta]_{92}^* = [0, 0, 0, 0, 0, 0, 3, 2, 1, 0, 0, 0, 0, 0, 0, 0, 0, 0]$	3/2	3/2	0	3/2	0	0	0
$[\theta]_{93}^* = [0, 0, 0, 0, 0, 0, 3, 1, 2, 0, 0, 0, 0, 0, 0, 0, 0, 0]$	3/2	3/2	0	3/2	0	0	0
$[\theta]_{94}^* = [0, 0, 0, 0, 0, 0, 3, 1, 1, 1, 0, 0, 0, 0, 0, 0, 0, 0]$	5/2	2	0	3/2	1/2	0	0
$[\theta]_{95}^* = [0, 0, 0, 0, 0, 0, 3, 1, 1, 0, 1, 0, 0, 0, 0, 0, 0, 0]$	5/2	2	0	3/2	1/2	0	0

$[\theta]_{96}^* = [0,0,0,0,0,0,3,0,2,1,0,0,0,0,0,0,0]$	3/2	3/2	0	3/2	0	0	0
$[\theta]_{97}^* = [0,0,0,0,0,0,3,0,2,0,1,0,0,0,0,0,0]$	3/2	3/2	0	3/2	0	0	0
$[\theta]_{98}^* = [0,0,0,0,0,0,3,0,1,1,1,0,0,0,0,0,0]$	5/2	2	0	3/2	1/2	0	0
$[\theta]_{99}^* = [0,0,0,0,0,0,3,0,1,0,1,0,1,0,0,0,0]$	5/2	2	0	3/2	1/2	0	0
$[\theta]_{100}^* = [0,0,0,0,0,0,2,2,2,0,0,0,0,0,0,0,0]$	3	5/2	0	2	1/2	0	0
$[\theta]_{101}^* = [0,0,0,0,0,0,2,2,1,1,0,0,0,0,0,0,0]$	5	5	2	1	0	2	0
$[\theta]_{102}^* = [0,0,0,0,0,0,2,2,1,0,1,0,0,0,0,0,0]$	4	3	0	2	1	0	0
$[\theta]_{103}^* = [0,0,0,0,0,0,2,1,2,1,0,0,0,0,0,0,0]$	4	3	0	2	1	0	0
$[\theta]_{104}^* = [0,0,0,0,0,0,2,1,2,0,1,0,0,0,0,0,0]$	4	3	0	2	1	0	0
$[\theta]_{105}^* = [0,0,0,0,0,0,2,1,1,1,1,0,0,0,0,0,0]$	15/2	9/2	0	3/2	3	0	0
$[\theta]_{106}^* = [0,0,0,0,0,0,2,1,1,0,1,0,1,0,0,0,0]$	15/2	9/2	0	3/2	3	0	0
$[\theta]_{107}^* = [0,0,0,0,0,0,2,0,2,0,2,0,0,0,0,0,0]$	3	5/2	0	2	1/2	0	0
$[\theta]_{108}^* = [0,0,0,0,0,0,2,0,2,0,1,1,0,0,0,0,0]$	4	3	0	2	1	0	0
$[\theta]_{109}^* = [0,0,0,0,0,0,2,0,1,1,1,1,0,0,0,0,0]$	15/2	9/2	0	3/2	3	0	0
$[\theta]_{110}^* = [0,0,0,0,0,0,2,0,1,1,1,0,1,0,0,0,0]$	15/2	9/2	0	3/2	3	0	0
$[\theta]_{111}^* = [0,0,0,0,0,0,1,1,1,1,1,1,0,0,0,0,0]$	16	11	6	0	4	0	1
$[\theta]_{112}^* = [0,0,0,0,0,0,1,1,1,1,1,0,1,0,0,0,0]$	15	15/2	0	0	15/2	0	0
$[\theta]_{113}^* = [0,0,0,0,0,0,1,1,1,0,1,0,1,0,1,0,0]$	15	15/2	0	0	15/2	0	0
$[\theta]_{114}^* = [0,0,0,0,0,0,1,0,1,0,1,0,1,0,1,0,1]$	15	15/2	0	0	15/2	0	0

## REFERENCES

1. S. Fujita, Integrated discussion on stereogenicity and chirality for restructuring stereochemistry, *J. Math. Chem.* **35** (2004) 265–287.
2. S. Fujita, A proof for the existence of five stereogenicity types on the basis of the existence of five types of subgroups of RS-stereoisomeric groups. Hierarchy of groups for restructuring stereochemistry (Part 3), *MATCH Commun. Math. Comput. Chem.* **54** (2005) 39–52.

3. S. Fujita, Stereogenicity revisited. Proposal of holantimers for comprehending the relationship between stereogenicity and chirality, *J. Org. Chem.* **69** (2004) 3158–3165.
4. S. Fujita, Pseudoasymmetry, stereogenicity, and the *RS*-nomenclature comprehended by the concepts of holantimers and stereoisograms, *Tetrahedron* **60** (2004) 11629–11638.
5. S. Fujita, Stereoisograms for discussing chirality and stereogenicity of allene derivatives, *Memoirs of the Faculty of Engineering and Design, Kyoto Institute of Technology* **53** (2005) 19–38.
6. J. A. Le Bel, Sur les relations qui existent entre les formules atomiques des corps organique et le pouvoir rotatoire de leurs dissolutions, *Bull. Soc. Chim. Fr. (2)* **22** (1874) 337–347.
7. J. A. Le Bel, On the Relations Which Exist Between the Atomic Formulas of Organic Compounds and the Rotatory Power of Their Solutions, In *Classics in the Theory of Chemical Combination (Classics of Science, Vol. I)*; O. T. Benfey, Ed., Dover: New York, 1963; pp 161–171.
8. J. H. van't Hoff, Voorstel tot Uitbreiding der tegenwoordig in de scheikunde gebruikte Structure-Formules in de ruimte; benevens een daarmee samenhangende opmerking omtrent het verband tusschen optisch Vermogen en Chemische Constitutie van Organische Verbindingen, *Archives Néerlandaises des Sciences exactes et naturelles* **9** (1874) 445–454.
9. J. H. van't Hoff, A Suggestion Looking to the Extension into Space of the Structural Formulas at Present Used in Chemistry. And a Note Upon the Relation Between the Optical Activity and the Chemical Constitution of Organic Compounds, In *Foundations of Stereochemistry, Memoirs of Pasteur, van't Hoff, Le Bel and Wislicenus*; G. M. Richardson, Ed., American Book Co.: New York, 1901; pp 35–46.
10. S. Fujita, Stereoisograms for specifying chirality and *RS*-stereogenicity. A versatile tool for avoiding the apparent inconsistency between geometrical features and *RS*-nomenclature in stereochemistry, *MATCH Commun. Math. Comput. Chem.* **61** (2009) 11–38.
11. S. Fujita, *RS*-Stereodescriptors determined by *RS*-stereogenicity and their chiralityfaithfulness, *J. Comput. Aided Chem.* **10** (2009) 16–29.
12. S. Fujita, Complete settlement of long-standing confusion on the term “prochirality” in stereochemistry. Proposal of pro-*RS*-stereogenicity and integrated treatment with prochirality, *Tetrahedron* **62** (2006) 691–705.
13. S. Fujita, Substitution criteria based on stereoisograms to determine prochirality and pro-*RS*-stereogenicity, *MATCH Commun. Math. Comput. Chem.* **61** (2009) 39–70.



14. S. Fujita, *Pro-R/pro-S-Descriptors* specified by *RS*-diastereotopic relationships, not by stereoheterotopic relationships, *J. Comput. Aided Chem.* **10** (2009) 76–95.
15. S. Fujita, Stereoisograms for reorganizing the theoretical foundations of stereochemistry and stereoisomerism: I. Diagrammatic representations of *RS*-stereoisomeric groups for integrating point groups and *RS*-permutation groups, *Tetrahedron: Asymmetry* **25** (2014) 1153–1168.
16. S. Fujita, Stereoisograms for reorganizing the theoretical foundations of stereochemistry and stereoisomerism: II. Rational avoidance of misleading standpoints for *R/S*stereodescriptors of the Cahn-Ingold-Prelog system, *Tetrahedron: Asymmetry* **25** (2014) 1169–1189.
17. S. Fujita, Stereoisograms for reorganizing the theoretical foundations of stereochemistry and stereoisomerism: III. Rational avoidance of misleading standpoints for *Pro-R/Pro-S*descriptors, *Tetrahedron: Asymmetry* **25** (2014) 1190–1204.
18. S. Fujita, The stereoisogram approach for remedying discontents of stereochemical terminology, *Tetrahedron: Asymmetry* **25** (2014) 1612–1623.
19. S. Fujita, *Symmetry and Combinatorial Enumeration in Chemistry*, Springer-Verlag, Berlin-Heidelberg, 1991.
20. S. Fujita, *Diagrammatical Approach to Molecular Symmetry and Enumeration of Stereoisomers*, University of Kragujevac, Faculty of Science, Kragujevac, 2007.
21. S. Fujita, Symmetry-itemized enumeration of quadruplets of *RS*-stereoisomers: I — The fixed-point matrix method of the USCI approach combined with the stereoisogram approach, *J. Math. Chem.* **52** (2014) 508–542.
22. S. Fujita, Symmetry-itemized enumeration of quadruplets of *RS*-stereoisomers: II — The partial-cycle-index method of the USCI approach combined with the stereoisogram approach, *J. Math. Chem.* **52** (2014) 543–574.
23. S. Fujita, Symmetry-itemized enumeration of *RS*-stereoisomers of allenes. I. The fixedpoint matrix method of the USCI approach combined with the stereoisogram approach, *J. Math. Chem.* **52** (2014) 1717–1750.
24. S. Fujita, Symmetry-itemized enumeration of *RS*-stereoisomers of allenes. II. The partialcycle- index method of the USCI approach combined with the stereoisogram approach, *J. Math. Chem.* **52** (2014) 1751–1793.
25. S. Fujita, Stereoisograms for three-membered heterocycles: I. Symmetry-itemized enumeration of oxiranes under an *RS*-stereoisomeric group, *J. Math. Chem.* **53** (2015) 260–304.
26. S. Fujita, Stereoisograms for three-membered heterocycles: II. Chirality, *RS*-stereogenicity, and ortho-stereogenicity on the basis of the proligand-promolecule model, *J. Math. Chem.* **53** (2015) 305–352.

27. S. Fujita, Stereoisograms for three-membered heterocycles: III. *R/S*-stereodescriptors for characterizing the *RS*-stereogenic aspect of absolute configuration, *J. Math. Chem.* **53** (2015) 353–373.
28. S. Fujita, *Combinatorial Enumeration of Graphs, Three-Dimensional Structures, and Chemical Compounds*, University of Kragujevac, Faculty of Science, Kragujevac, 2013.
29. S. Fujita, Combinatorial enumeration of *RS*-stereoisomers itemized by chirality, *RS*-stereogenicity, and sclerality, *MATCH Commun. Math. Comput. Chem.* **58** (2007) 611–634.
30. S. Fujita, Itemized enumeration of quadruplets of *RS*-stereoisomers under the action of *RS*-stereoisomeric groups, *MATCH Commun. Math. Comput. Chem.* **61** (2009) 71–115.
31. S. Fujita, Type-itemized enumeration of quadruplets of *RS*-stereoisomers. I. Cycle indices with chirality fittingness modulated by type-IV quadruplets, *J. Math. Chem.* (2015); DOI 10.1007/s10910-015-0561-z.
32. S. Fujita, Type-itemized enumeration of quadruplets of *RS*-stereoisomers: II. Cycle indices with chirality fittingness modulated by type-V quadruplets, *J. Math. Chem.* (2015); DOI 10.1007/s10910-015-0562-y.
33. S. Fujita, Stereoisograms of octahedral complexes. I. Chirality and *RS*-stereogenicity, *MATCH Commun. Math. Comput. Chem.* **71** (2014) 511–536.
34. S. Fujita, *Mathematical Stereochemistry*, De Gruyter, Berlin, 2015.
35. S. Fujita, Promolecules with a subsymmetry of  $O_h$ . Combinatorial enumeration and stereochemical properties, *Polyhedron* **12** (1993) 95–110.
36. S. Fujita, Symmetry-itemized enumeration of cubane derivatives as three-dimensional entities by the fixed-point matrix method of the USCI approach, *Bull. Chem. Soc. Jpn.* **84** (2011) 1192–1207.
37. S. Fujita, Generalization of partial cycle indices and modified bisected mark tables for combinatorial enumeration, *Bull. Chem. Soc. Jpn.* **73** (2000) 329–339.
38. S. Fujita, Graphs to chemical structures 1. Sphericity indices of cycles for stereochemical extension of Pólya's theorem, *Theor. Chem. Acc.* **113** (2005) 73–79.
39. S. Fujita, Graphs to chemical structures 2. Extended sphericity indices of cycles for stereochemical extension of Pólya's coronas, *Theor. Chem. Acc.* **113** (2005) 80–86.
40. S. Fujita, Graphs to chemical structures 3. General theorems with the use of different sets of sphericity indices for combinatorial enumeration of nonrigid stereoisomers, *Theor. Chem. Acc.* **115** (2006) 37–53.
41. S. Fujita, Stereochemistry and stereoisomerism characterized by the sphericity concept, *Bull. Chem. Soc. Jpn.* **74** (2001) 1585–1603.

42. S. Fujita, Stereoisograms of octahedral complexes. II. *RS*-Stereogenicity vs. stereogenicity as well as *RS*-stereoisomerism vs. stereoisomerism, *MATCH Commun. Math. Comput. Chem.* **71** (2014) 537–574.
43. N. G. Connelly, T. Damhus, R. M. Hartshorn, A. T. Hutton, and IUPAC, *Nomenclature of Inorganic Chemistry, IUPAC Recommendations 2005*, RSC Publishing, Cambridge, 2005.
44. The GAP Team, GAP – Groups, Algorithms and Programming, version 4.4.10, 2010, <http://www.gap-system.org>.



# ***Half-Century Journey from Synthetic Organic Chemistry to Mathematical Stereochemistry through Chemoinformatics***

**SHINSAKU FUJITA**

Shonan Institute of Chemoinformatics and Mathematical Chemistry, Kaneko 479-7 Ooimachi, Ashigara-Kami-Gun, Kanagawa-Ken, 258-0019 Japan

Correspondence should be addressed to shinsaku\_fujita@nifty.com

Received 10 October 2015; Accepted 12 October 2015

ACADEMIC EDITOR: ALI REZA ASHRAFI

**ABSTRACT** My half-century journey started from synthetic organic chemistry. During the first stage of my journey, my interest in stereochemistry was initiated through the investigation on the participation of steric effects in reactive intermediates, cyclophanes, strained heterocycles, and organic compounds for photography. In chemoinformatics as the next stage of the journey, I proposed the concept of imaginary transition structures (ITSs) as computer-oriented representation of organic reactions. My interest was stimulated to attack combinatorial enumeration through the investigation on enumeration of subgraphs of ITSs. Stereochemistry and combinatorial enumeration was combined in my interest, so that I reached mathematical stereochemistry as the final stage of my journey. Fujita's unit-subduced-cycle-index (USCI) approach, Fujita's proligand method, and Fujita's stereoisogram approach were developed, so as to integrate van't Hoff's way (asymmetry, stereogenicity) and Le Bel's way (dissymmetry, chirality), which caused continuous confusion in the history of stereochemistry.

**KEYWORDS** sphericity, combinatorial enumeration, stereoisogram, stereochemistry.

## **1. INTRODUCTION**

I started my research career as a synthetic organic chemist in 1965 (a half century ago), when I joined the research group of Prof. Hitosi Nozaki, Kyoto University. I conducted experimental works on regioselective reactions of nitrenes [1] under the guidance of late Prof. Hidemasa Takaya (Kyoto University; at that time, a doctor-course student) and Prof. Ryoji Noyori (Nagoya University, the Nobel laureate in chemistry, 2001; at that time, a research instructor). In the same laboratory room, I had a fortunate opportunity to see the initial event of homogeneous asymmetric synthesis [2], by which Prof. Noyori was later

awarded the Nobel prize for chemistry, 2001 [3]. The event strongly impressed me with the importance of stereochemistry in the R&D on synthetic organic chemistry.

During a half century, I changed my positions three times: Kyoto University (1968–1972), Fuji Photo Film Co. Ltd. (1972–1997), and Kyoto Institute of Technology (1997–2007). In 2007, I have started Shonan Institute of Chemoinformatics and Mathematical Chemistry as a private laboratory. Although my research interests have shifted among synthetic organic chemistry, chemoinformatics, and mathematical stereochemistry, the first impression concerning the importance of stereochemistry remains unchanged through the half century.

The conventional stereochemistry for supporting synthetic organic chemistry was restricted to a qualitative phase, which had no sufficient mathematical formulations. My studies on synthetic organic chemistry demonstrated the participation of steric effects in reactive intermediates (such as nitrenes), cyclophanes, strained heterocycles, and organic compounds for photography. For example, steric hindrance avoids undesirable side reactions so as to enhance dye-releasing efficiency in instant color photography, as described in my book [4]. However, discussions on such steric effects were restricted to a qualitative phase.

The stereochemistry for supporting chemoinformatics had both qualitative and quantitative phases, which required theoretical foundations with mathematical formulations. In particular, enumeration and classification of organic compounds as three-dimensional (3D) entities inevitably required quantitative treatments with mathematical formulations. The struggle in chemoinformatics resulted in the concept of *imaginary transition structures* (ITSs), as summarized in my book [5]. However, this concept was still restricted to two-dimensional (2D) structures (graphs) and to the scope of the conventional stereochemistry without mathematical formulations.

It follows that my efforts focused on the development of new mathematical formulations, which enabled us to extend the conventional stereochemistry, to treat 3D structures effectively, and thereby to develop a new version of ITSs with 3D information. The first accomplishment was *the unit-subduced-cycle-index (USCI) approach*, which provided us with powerful methods of enumerating organic compounds in a symmetry-itemized fashion. The concept of *sphericities of orbits* was a key to treat 3D structures, as described in my book [6]. Fujita's USCI approach was further exploited to develop the concept of *mandalas*, which meets requirements of both chemists and mathematicians, as described in my book [7].

In comparison with symmetry-itemized enumeration, gross enumeration is convenient to get brief information on enumeration. Within the scope of 2D structures (graphs), Pólya's theorem has been adopted widely [8]. To accomplish gross enumeration of 3D structures, in contrast, I have developed *the proligand method*, as summarized in my







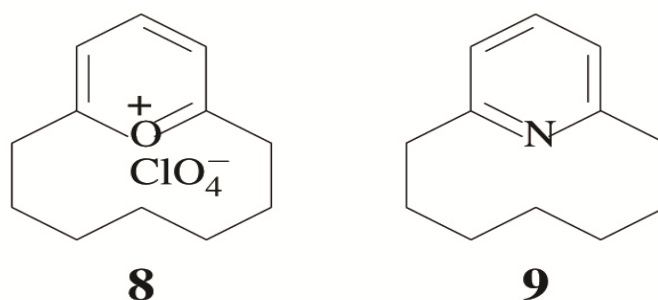


**Figure 4.** [7](2,6)pyrylophanium perchlorate and [7](2,6)Pyridinophane

As carbon analogs of [7](2,6)pyridinophanes (9 etc.), the nitrogen atom was replaced by a carbon atom to synthesize [7]metacyclophanes [32]. The heptamethylene chains of them were replaced by hexamethylene chains to produce [6]metacyclophanes [33, 34], where the steric effects of the hexamethylene chain on the steric strain of a benzene ring were compared with those of heptamethylene chain by means of nuclear-magnetic-resonance (NMR) technique.

### 2.3. ORGANIC CHEMISTRY OF PHOTOGRAPHY

In 1972, I moved to Ashigara Research Laboratories, Fuji Photo Film Co., Ltd., where I was first engaged in the R&D of organic compounds for instant color photography during about 15 years [35, 36].

Instant color photography adopted by Fuji is based on dye releasers, each of which is nondiffusible but releases a dye moiety in an unexposed area, as shown in Figure 5. From a viewpoint of patentability, we selected *o*-sulphonamidophenol as a dye-releasing moiety. Thus, a dye releaser **13**, which is initially immobile because of the presence of B (a ballast group), is oxidized by the action of an oxidized electron transfer agent **12** (ETAox) in an unexposed area. The resulting quinone monoimide **15** is hydrolyzed so as to release a diffusible dye **17**.

To adjust the redox potential of the *o*-sulphonamidophenol moiety of the dye releaser **13**, the substitution of an alkoxy substituent (as a ballast group) was found to be necessary in addition to an alkyl group. However, the mechanistic investigation of the hydrolysis process of **15** revealed that the substitution of an alkoxy substituent causes an undesirable side reaction [37, 38]. To avoid the undesirable side reaction, a sterically bulky group (e.g., a *tert*-butyl group) was introduced at the position adjacent to the alkoxy substituent.

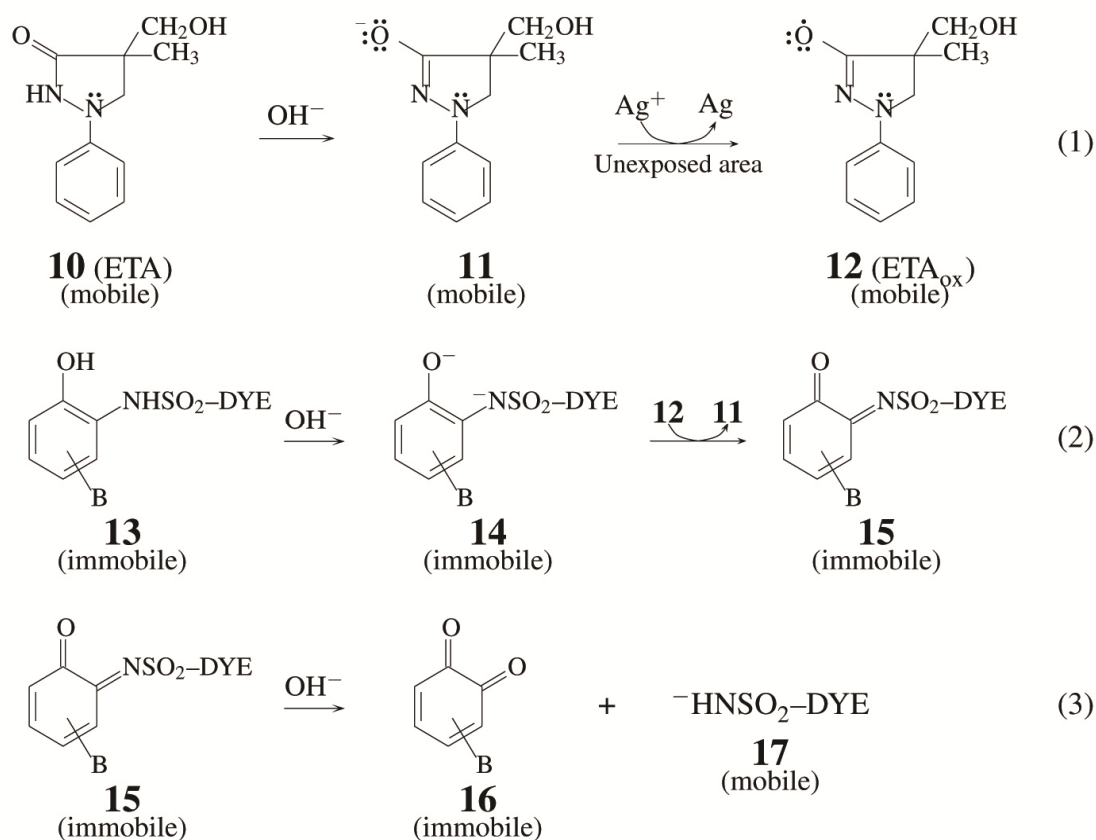


**Figure 5.** Mechanism of dye releasing in an unexposed area of instant color film (reversal type). The symbol B represents a ballast group for giving undiffusibility to the dye releaser. The symbol DYE is a dye moiety, so that DYE-SO<sub>2</sub>NH<sup>-</sup> represents a diffusible dye.

Finally, we selected an effective dye-releasing moiety shown in a shadowed box of Figure 6 [39], where the steric hindrance due to a *tert*-butyl group inhibits the undesired side reaction during the hydrolysis step. Moreover, a methoxyethoxy group in another shadowed box brought about the higher efficiency of dye releasing process [40]. The enhanced efficiency due to a methoxyethoxy group has been ascribed to the protonation of an imido nitrogen which would be assisted by a neighboring chelation of two oxygens [41, 42].

An instant color system requires three dye releasers according to the subtractive color reproduction, e.g., a cyan dye-releaser **18** [39], a magenta dye-releaser **19** [43], and a yellow dye-releaser **20** [39], as shown in Figure 6.

The R&D described above resulted in the FI-10 film, which was put on the market in 1981 under the system name “FOTORAMA” from Fuji Photo Film. Thereby, I (with Koichi Koyama and Shigetoshi Ono) was awarded Synthetic Organic Chemistry Award, Japan (1982). Our accomplishment was summarized as account articles [44, 45]. Later, I

published a book entitled “Organic Chemistry of Photography” [4], Chapters 15–20 of which dealt with the R&D of organic compounds for instant color photography.

### 3. JOURNEY IN CHEMOINFORMATICS

#### 3.1. MOTIVATION GIVEN IN THE EDITORIAL COMMITTEE OF A JOURNAL

At the final stage of the project of developing dye releasers for instant color photography, I served as a member of the editorial committee of *Yuki Gosei Kagaku Kyokai-Shi (Journal of Synthetic Organic Chemistry, Japan)* during 1979–1982.

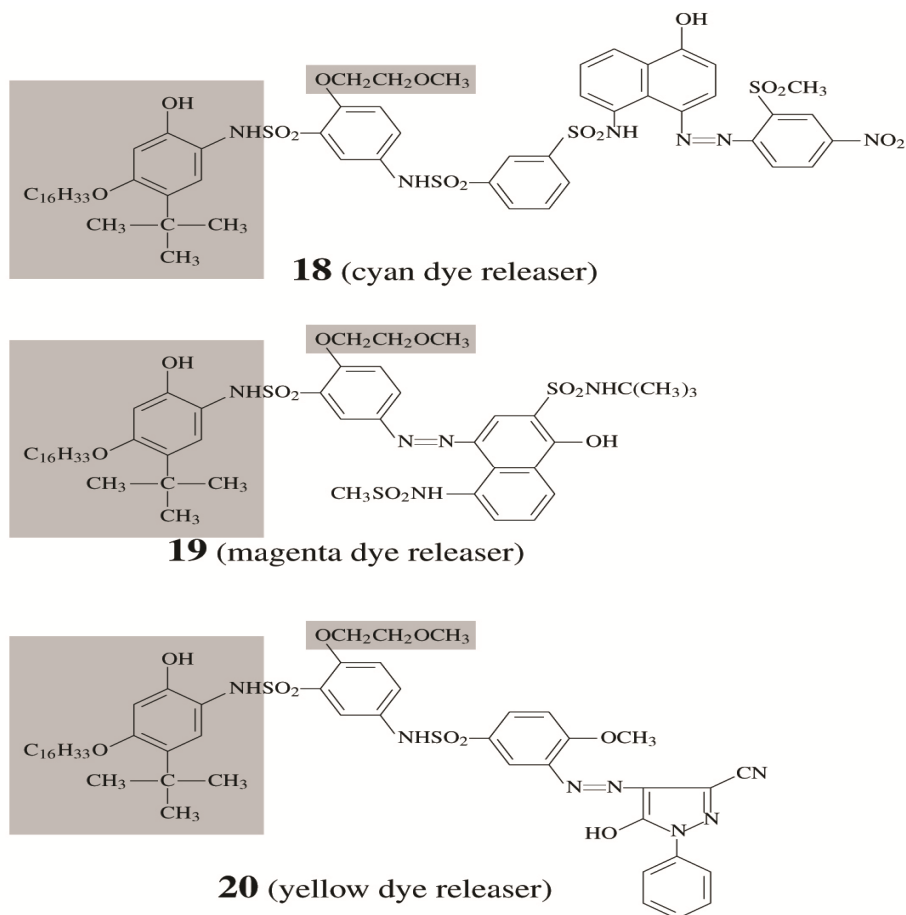


**Figure 6.** Dye releasers for instant color photography. The shadowed box indicates a common dye-releasing moiety.

The journal had a long-term series named “New Syntheses”, which appears in every issue even now. Because syntheses abstracted in the series had not been classified into types of reactions at that time, the editorial committee decided to attach keywords of reaction types for the sake of easy retrieval. Then, the selection of keywords was assigned to me as a member of the committee. After a list of selected keywords was adopted by the committee, the application was started from the issue 8 of volume 38 (1980). Compare the previous format of the issue 7 with the renewed format of the issue 8 of the same volume, if your library stores *Yuki Gosei Kagaku Kyokai-Shi*. The renewed format of “New Syntheses” is still active even in the recent issues of volume 73 (2015).

During the process of selection, I became aware that such keywords of reaction types were not linked with moieties to be attacked. For example, a keyword ‘cyclization’ attached to an abstracted item ‘formation of oxazoles’ was silent about how a cyclic moiety (oxazole) was formed from starting compounds. Thereby, I was motivated to develop a new system for specifying both reaction types and attacked moieties in an integrated fashion.

### 3.2. PROPOSAL OF IMAGINARY TRANSITION STRUCTURES (ITSS)

After trials and errors during several years, I reached the concept of *imaginary transition structures* (ITSS). The construction of an ITS is illustrated in Figure 7, which represents an acid-catalyzed hydrolysis of ethyl acetate.

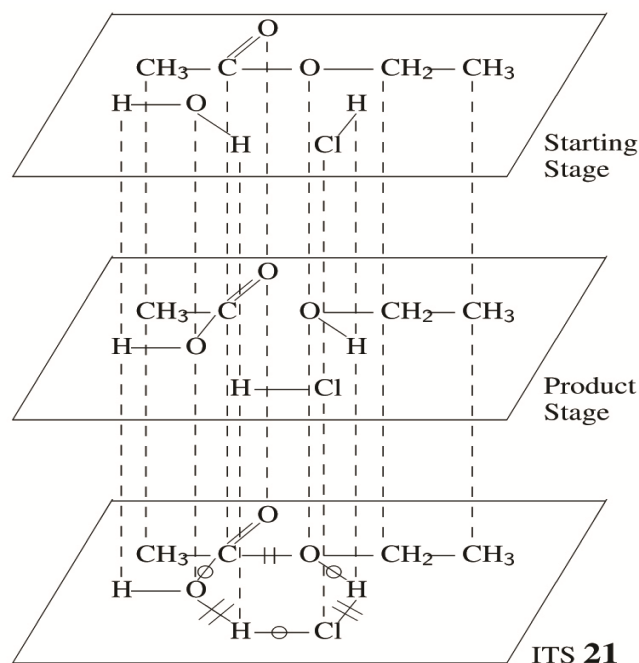


**Figure 7.** Construction of an imaginary transition structure (ITS) for representing an acid-catalyzed hydrolysis of ethyl acetate.



contain usual structural formulas for representing organic compounds as a subcategory. In other words, an ITS is an extended structural formula having three kinds of bonds (in-bonds, out-bonds, and par-bonds), whereas usual structural formulas have par-bonds only.

**Table 1.** Fifteen imaginary bonds and complex bond numbers (CBNs)  
Enrollment in local colleges, 2005.

$b =$	-3	-2	-1	0	+1	+2	+3
			$\parallel$	—	$\ominus$		
			(1-1)	(1+0)	(0+1)		
		$\#$	$\parallel$	—	$\ominus$	$\oplus$	
		(2-2)	(2-1)	(2+0)	(1+1)	(0+2)	
	$\#$	$\#$	$\parallel$	—	$\ominus$	$\oplus$	$\oplus$
	(3-3)	(3-2)	(3-1)	(3+0)	(2+1)	(1+2)	(0+3)

By using complex bond numbers, the data of an ITS is stored in the form of an *ITS connection table* [46], which is an extension of a connection table of a usual organic compound. For example, the data of the ITS **21** give an ITS connection table shown in Figure 9, where lines 8–19 store the information on the nodes of **21** and lines 20–31 store the information on the complex bond numbers of the respective bonds of **21**. For the numbering of nodes, see the ITS **21** shown in Figure 8.

Because ITSs put focus on covalent bonds, the original formulation of ITSs is not capable of treating formal charges appearing in nitro groups, sulfonic acids, and so on. For avoid this type of apparent difficulties, the concept of a *charge space* has been developed, where a three dimensional ITS with charges is recognized to be a synthesis space attached by a charge space [47].

The hydrolysis shown in Figure 7 has a multi-step mechanism from the starting stage to the product stage, if the participation of a proton dissociated from a hydrochloric acid is taken into consideration. To harmonize such a multi-step mechanism with the ITS **21**, the calculation of CBNs has been formulated. Thereby, a multi-step reaction (or a multi-step synthesis) can be treated within the scope of the ITS approach [48].

### 3.4. SUBSTRUCTURES (SUBGRAPHS) OF ITSs

Because ITSs for representing organic reactions can be regarded as an extension of structural formulas for representing organic compounds, there is much correspondence

between them. Most remarkable correspondence is concerned with their substructures (subgraphs). Just as substructures (subgraphs) of a structural formula provide information on compound types, substructures (subgraphs) of an ITS provide information on reaction types [49, 50].

00000380. iup											
I No 98640001-991022-01											
hydroxy-de-ethoxy lation											
hydroxy-de-alkoxy lation											
hydroxy-de-ethoxy -substitution											
hydroxy-de-alkoxy -substitution											
The hydrolysis of ethyl acetate											
11	0	IUPAC									
1	c	CH <sub>3</sub>	10	20	0	0	0	0	0	0	0
2	c	C	35	20	0	0	0	0	0	0	0
3	0	0	60	20	0	0	0	0	0	0	0
4	c	CH <sub>2</sub>	85	20	0	0	0	0	0	0	0
5	c	CH <sub>3</sub>	110	20	0	0	0	0	0	0	0
6	0	0	35	45	0	0	0	0	0	0	0
7	0	0	25	10	0	0	0	0	0	0	0
8	H	H	35	0	0	0	0	0	0	0	0
9	H	H	10	10	0	0	0	0	0	0	0
10	H	H	70	10	0	0	0	0	0	0	0
11	c <sub>1</sub>	c <sub>1</sub>	60	0	0	0					
1	2	1	0	0	1	0	0	0	0		
2	3	1	-1	0	1	0	0	0	0		
2	6	2	0	0	1	0	0	0	0		
2	7	0	+1	0	1	0	0	0	0		
3	4	1	0	0	1	0	0	0	0		
3	10	0	+1	0	1	0	0	0	0		
4	5	1	0	0	1	0	0	0	0		
7	8	1	-1	0	1	0	0	0	0		
7	9	1	0	0	1	0	0	0	0		
8	11	0	+1	0	1	0	0	0	0		
10	11	1	-1	0	1	0	0	0	0		
999	0	0	0	0	0	0	0	0	0		

Figure 9. Connection table of ITS 21.

### 3.4.1. REACTION-CENTER GRAPHS, REACTION GRAPHS, AND BASIC REACTION GRAPHS

By extracting bonds with  $b \neq 0$  of  $(a\ b)$  (CBN) from an ITS, we obtain a substructure for representing a net reaction. To refer to the resulting substructure, the term *reaction-center graph* (RCG) has been coined [49, 50]. For example, the ITS 22, which represents a Diels-Alder reaction between cyclopentadiene and maleic anhydride, contains an RCG 26 (Figure 10). The other ITS 23 representing another Diels-Alder reaction gives an RCG 27. The RCGs 26 and 27 are graphic expressions of Diels-Alder reactions, which maintain the information on nodes (participant atoms).

By omitting the information on nodes from the RCG 26 (or 27), we obtain a subgraph 30 called a *reaction graph* (RG), in which each node is represented by a bullet symbol ( $\bullet$ ) in an abstract fashion. The RG 30 is a more general expression of Diels-Alder reactions. As found in Figure 10, the RCG 28 (or 29) extracted from the ITS 24 (or 25) gives the corresponding RG 31, which represents a Claisen rearrangement in a more general fashion.

By omitting the information on par-bonds from the RG 30, we obtain a subgraph 32 called a *basic reaction graph* (BRG). The BRG 32 represents a net migration of electrons. As found in Figure 10, the BR 31 for representing Claisen rearrangements contains the same BRG 32. Moreover, the ITS 21 shown in Figure 8 contains the same BRG 32. It should be emphasized that the classification of organic reactions is replaced by graphic treatments of ITSs, which are illustrated from the ITS-column (left) to the BRG-column (right) of Figure 10.

### 3.4.2. REACTION STRINGS

As found in each of the ITSs, RCGs, RGs, and BRG collected in Figure 10, there appears a string in which in-bonds and out-bonds are linked alternately. Such a string is called a *reaction string*, which represents a shift of an electron pair. The number of reaction strings appearing in an ITS is a clue for classifying the ITS. Thereby, ITSs are classified into one-string reactions, two-string reactions, and so on.

In particular, two-string reactions in which the two reaction strings exhibit a spiro junction have been discussed as a remarkable category of reactions [51]. In addition, two-string reactions in which the two reaction strings exhibit a fused junction have been discussed as another remarkable category of reactions [52].



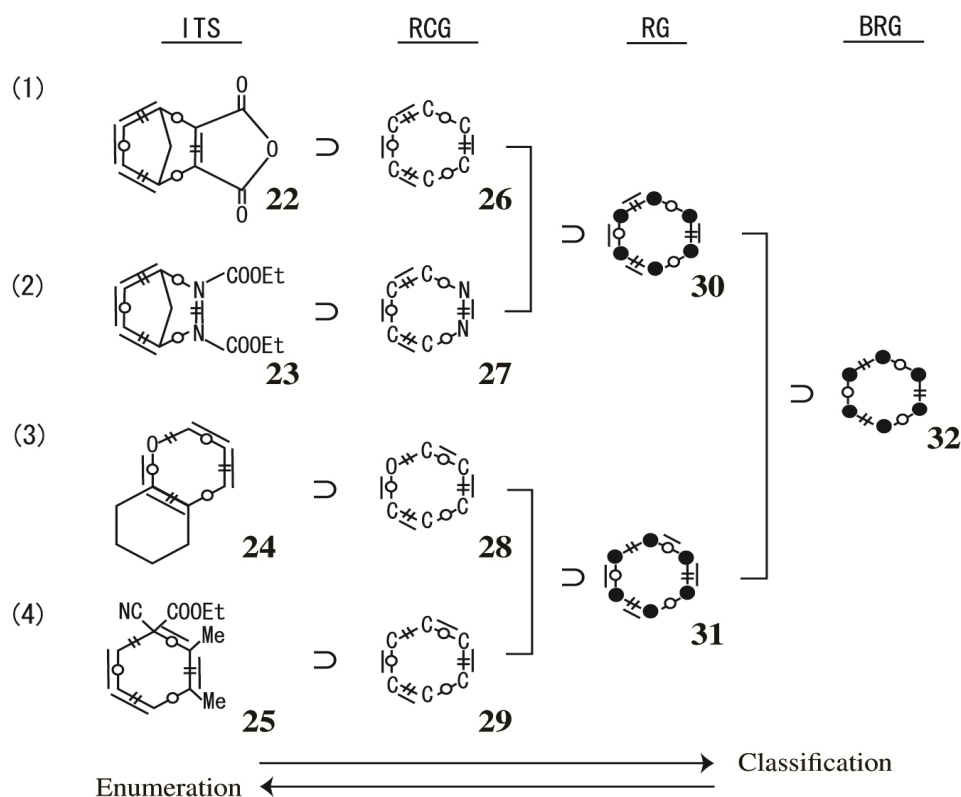


**Figure 10.** Six-membered imaginary transition structures (ITSs), reaction-center graphs (RCGs), and reaction graphs (RGs), which are related to a basic reaction graph (BRG).

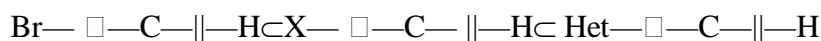
### 3.4.3. THREE-NODAL SUBGRAPHS AND FOUR-NODAL SUBGRAPHS

To retrieve substitution reactions, a *three-nodal subgraph* is defined as a substructure which consists of a reaction-center atom and adjacent atoms through an in-bond or an out-bond [53]. For example, the three-nodal subgraph  $\text{O}-\square-\text{C}-\parallel-\text{O}$  is extracted from the ITS **21** (Figure 8) to show a substitution reaction. A more definite subgraph can be extracted from **21** by attaching additional information, e.g.,  $(\text{H})\text{O}-\square-\text{C}(=\text{O})-\parallel-\text{O}(\text{C})$  for the purpose of representing a hydrolysis of an ester.

In a similar way, a *four-nodal subgraph* is defined for the purpose of retrieving C—C bond formations, C—C bond cleavages, additions, and eliminations [53]. For example, the four-nodal subgraph  $\text{Br}-\parallel-\text{C}-\square-\text{C}-\parallel-\text{Br}$  represents a C—C bond formation with debromination, while the four-nodal subgraph  $\text{O}-\square-\text{C}-\parallel-\text{C}-\square-\text{O}$  represents a C—C bond cleavage.

A hierarchical classification can be accomplished by considering the classification of atoms which are contained in a three-nodal or four-nodal subgraph [54]. For example,

the hierarchy ‘bromine ⊂ halogen ⊂ electron-attracting atom’ (Br ⊂ X ⊂ Het) provides the following hierarchy of three-nodal subgraphs:



This result expresses the hierarchy ‘bromination ⊂ halogenation ⊂ oxidation’ graphically.

#### 3.4.4. RING STRUCTURES IN ITSS

Among ring structures appearing in ITSs, *bridges of ring closure* (BC<sub>*n*</sub>), *bridges of ring opening* (BO<sub>*n*</sub>), and *bridges of rearrangement* (BR) are defined to retrieve ring closures, ring openings, and rearrangements, respectively [46].

The subscript *n* of BC<sub>*n*</sub> (or BO<sub>*n*</sub>) represents the number of bond formed (or cleaved) during the ring closure (or ring opening). For example, The ITS **22** (or **23**), the RCG **26** (or **27**), and the RG **30** are recognized to contain BC<sub>2</sub>'s at the respective levels of categorization. A pair of BC<sub>*n*</sub> and BO<sub>*n*</sub> is called a *reaction pair*, which corresponds to a pair of forward and reverse reactions.

A bridge of rearrangement (BR) is a key of single-access perception of rearrangement reactions [55]. For example, the ITS **24** (or **25**), the RCG **28** (or **29**), and the RG **31** are recognized to contain BRs at the respective levels of categorization. These BRs indicate Claisen rearrangements.

Among all of the ring structures contained in an ITS, a minimum set of ring structures for specifying reactions is defined as *an essential set of essential rings* (ESER) [56]. An algorithm developed for the detection of an ESER in an ITS has been effective to the logical perception of ring-opening, ring-closure, and rearrangement reactions. The algorithm has been applied to the detection of an ESER in a usual structural formula [57].

#### 3.4.5. CANONICAL NAMES OF ITSS

An algorithm for giving a canonical number and a canonical code to an ITS has been developed [58], where Morgan's algorithm for giving a canonical numbering to a structural formula has been extended to meet the presence of three kinds of bonds.

An algorithm for giving a canonical number and a canonical code to an RCG extracted from an ITS has been developed [59], where there has appeared a novel approach to the linear coding of reaction types.

### 3.5. ENUMERATION OF REACTION GRAPHS AND REACTION-CENTER GRAPHS

The classification shown in Figure 10 has been accomplished by examining from the left to the right in the following order: ITS (e.g., **22**) → RCG (e.g., **26**) → RG (e.g., **30**) → BRG (e.g., **32**). Let us examine the reverse order (right to left) in Figure 10. Then, the placement of four par-bonds on the edges of the BRG **32** generates an RG **30**; and the placement of

carbons on the nodes of the RG **30** generates an RCG **26**. As a result, the reverse order corresponds to the systematic method for enumerating RGs and RCGs.

Let us first enumerate RGs by starting from the BRG **32**, which belongs to a permutation group  $\mathbf{D}_3$ . By applying Pólya's theorem [8] to the six edges of the BRG **32**, we obtain the following cycle index (CI):

$$Z(\mathbf{D}_3; s_d) = (1/6)(s_1^6 + 3s_1^2s_2^2 + 2s_3^2). \quad (4)$$

Suppose that  $m$  double par-bonds and  $n$  single par-bonds are placed on the six edges of **32**. The dummy variables  $x$  and  $y$  are used to count double par-bonds and single par-bonds, respectively. Thereby, the following ligand-inventory function is obtained:

$$s_d = 1 + x^d + y^d \quad (5)$$

where the top term 1 in the right-hand side represents no edge substitution. After Eq. 5 is introduced into Eq. 4, the resulting equation is expanded to give the following generating function:

$$\begin{aligned} G(x,y) &= Z(\mathbf{D}_3; 1+x^d+y^d) \\ &= (1/6)\{(1+x+y)^6 + 3(1+x+y)^2(1+x^2+x^2) + 2(1+x^3+x^3)^2\} \\ &= 1 + 2x + 2y + 4x^2 + 6xy + 4y^2 + 6x^3 + 12x^2y + 12xy^2 + 6y^3 + \\ &\quad 4x^4 + 12x^3y + x^6 + 2x^5y + 4x^4y^2 + 6x^3y^3 + 4x^2y^4 + 2xy^5 + y^6. \end{aligned} \quad (6)$$

where the coefficient of the term  $x^m y^n$  represents the number of RGs with  $m$  double par-bonds and  $n$  single par-bonds. Six-membered reaction graphs with single parbonds ( $m = 0, n = 0-6$ ) are depicted in Table 2, where the no.-of-RGs column collects the coefficients appearing in Eq. 6. The no.-of-RPs column of Table 2 collects the number of reaction pairs, where a pair of  $\text{BC}_n$  and  $\text{BO}_n$  (as well as an BR) is counted once in another calculation according to Pólya's theorem [60, 8].

This method is effective to accomplish systematic enumeration of organic reactions, e.g., even-membered RGs [49], odd-membered RGs [50], two-string RGs with spiro junction [51], and two-string RGs with fused junction [52].

Let us next enumerate RCGs by starting from an RG (**30** or **31**), where the six vertices accommodate a set of six atoms selected from carbon, nitrogen, and oxygen. In this case, the valence of each atom should be taken into consideration [61]. This type of enumeration with considering *obligatory minimum valences* (OMVs) has been conducted by using different ligand-inventory functions [62]. For OMVs of compound enumeration, see Chapter 14 of my book [6].

### 3.6. COMPUTER-RETRIEVAL SYSTEM BASED ON ITSS

#### 3.6.1. APART FROM THE 'STRUCTURE—REACTION-TYPE' PARADIGM

The conventional description of organic reactions is a scheme in which the starting stage and the product stage are combined with an arrow, or a verbal description of the starting stage attached by a reaction type, e.g., 'the hydrolysis of ethyl acetate' [63]. This means that the conventional description suffers from the 'structure—reaction-type' paradigm, which is not necessarily suitable to computer manipulation [64]. As discussed in the preceding subsections, the concept of imaginary transition structures (ITSs) is capable of overcoming this paradigm. The total features of ITSs as a new computer-oriented representation has been discussed in review articles [65, 66].

#### 3.6.2. DEVELOPMENT OF AN IN-HOUSE SYSTEM FORTUNITS

During 1986–1995, I was engaged in the development of an in-house system for retrieving organic reactions named FORTUNITS (Fuji Organic Reaction Treating Unity based on Imaginary Transition Structures). The FORTUNITS system was an integrated system composed of a subsystem of ITS registration, a subsystem of descriptive data, and a subsystem of retrieval system (running as a time-sharing system), as well as a subsystem of analyzing ITSs and a subsystem of analyzing compound structures (running as a batch system) [67, 68]. Several illustrations of computer displays have appeared in my review article [65], where in-bonds and out-bonds in ITSs are differentiated in the form of colored bonds.

### 3.7. PERSPECTIVES BROUGHT ABOUT BY THE CONCEPT OF ITSS

The ITS approach developed by Fujita stems from a principle that each organic reaction is represented by an ITS as a diagrammatic expression, which is recognized as a kind of structural formula. As a result, reaction types are ascribed to various substructures (subgraphs) contained in each ITS.

By applying the scheme [ITS  $\rightarrow$  RCG  $\rightarrow$  RG  $\rightarrow$  BRG] according to Fujita's ITS approach, more abstract substructures (subgraphs) as hierarchical descriptors of organic reactions are successively extracted from each ITS (cf. Figure 10). The reverse scheme [ITS  $\leftarrow$  RCG  $\leftarrow$  RG  $\leftarrow$  BRG], when combined with Pólya's theorem, gives a powerful methodology for enumerating organic reactions.

Moreover, the concept of ITSs provides a novel approach to the taxonomy of organic reactions. In other words, organic reactions are described systematically according to Fujita's ITS approach in a different way from classical descriptions in textbooks on

organic chemistry. The merits of ITSs have been summarized in my book on computer-oriented representation of organic reactions [5].

**Table 2.** Six-membered reaction graphs ( $m = 0, n = 0 - 6$ ).

m	n	no. of		reaction graphs (RGs)
		RGs	RPs	
0	0	1	1	
0	1	2	1	
0	2	4	3	
0	3	6	3	
0	4	4	3	
0	5	2	1	
0	6	1	1	

### 3.8. EXCURSIVE JOURNEY TO $X^Y$ MT<sub>E</sub>X, $X^Y$ M NOTATION, AND $X^Y$ MML

To continue my journey, I needed a writing tool for supporting both structural formulas and mathematical equations. Although the T<sub>E</sub>X/L<sup>A</sup>T<sub>E</sub>X system had already provided us with a satisfactory utility for writing mathematical equations, it lacked a utility for drawing structural formulas. So I decided to develop a utility for drawing structural formulas. The first version of  $X^Y$ MT<sub>E</sub>X was released in 1993 [69, 70]. Several improvements were added to enhance the feasibilities of  $X^Y$ MT<sub>E</sub>X [71, 72]. A book for introducing the  $X^Y$ MT<sub>E</sub>X system was published in 1997 [73]. The present version (Version 5.01) is available from

my homepage (<http://xymtex.com/>) with an on-line manual of 780 pages [74]. All of the structural formulas contained in this account article (except ITSs) have been drawn by X<sup>Y</sup>MT<sub>E</sub>X Version 5.01. For example, see Figures 5 and 6.

The codes of the X<sup>Y</sup>MT<sub>E</sub>X system can be regarded as a linear notation, which was brushed up into X<sup>Y</sup>M notations for electronic communication of structural formulas [75]. The X<sup>Y</sup>MML (X<sup>Y</sup>M Markup Language) was developed as a more advanced format (a markup language) [76, 77]. The X<sup>Y</sup>MJava system [78] and the X<sup>Y</sup>MML system [79] were developed as a WWW (World Wide Web) communication tool for publishing of structural formulas. The X<sup>Y</sup>MT<sub>E</sub>X system was discussed comprehensively as a versatile tool for writing, submission, publication, and internet communication in chemistry [80] as well as for publishing interdisciplinary chemistry/mathematics books [81].

## 4. JOURNEY IN MATHEMATICAL STEREOCHEMISTRY

### 4.1. MOTIVATION GIVEN THROUGH THE DEVELOPMENT OF FUJITA'S ITS APPROACH IN CHEMOINFORMATICS

In Fujita's ITS approach, stereochemical data of organic reactions have been treated in the form of three-dimensional imaginary transition structures (3D ITSs) with charges [47]. However, during the investigation on enumeration of organic reactions according to the reverse scheme [ITS ← RCG ← RG ← BRG] (Figure 10), I became aware that Pólya's theorem [60, 8] is concerned with graphs (under the action of permutation groups), not with 3D structures (under the action of point groups). This feature of Pólya's theorem means insufficient applicability to 3D structures, which are essential to discuss stereochemistry.

The traditional foundations of modern stereochemistry, on the other hand, lack mathematical formulations of 3D structures. Although 3D structures are discussed by using point groups from a viewpoint of quantum chemistry [82], the discussions on 3D structures from a stereochemical viewpoint are restricted to qualitative phase [83]. For example, the conventional terms 'enantiotopic' [84] and 'stereoheterotopic' [85] cannot be applied to quantitative purposes such as combinatorial enumeration of 3D structures under the action of point groups.

As found in the preceding paragraphs, mathematical formulations of 3D structures require new items which provide the linkage between mathematics and stereochemistry, i.e., *mathematical stereochemistry* as an interdisciplinary field. This section is devoted to the introduction of Fujita's USCI approach [6, 7], Fujita's proligand method [9], Fujita's

stereoisogram approach [18], and related topics, as state-of-the-art embodiments of mathematical stereochemistry.

#### 4.2. FUJITA'S UNIT-SUBDUCED-CYCLE-INDEX (USCI) APPROACH

Fujita's USCI (unit-subduced-cycle-index) approach puts stress on equivalence relationships and equivalence classes (frequently called *orbits*) [86, 87]. Each orbit is governed by a coset representation and by a sphericity index, so that a set of suborbitals derived from the orbit is characterized by a product of such sphericity indices, which is called a *unit subduced cycle index with chirality fittingness* (USCI-CF) [6]. This exhibits a sharp contrast to the traditional foundations of stereochemistry, which make light of equivalence relationships and equivalence classes.

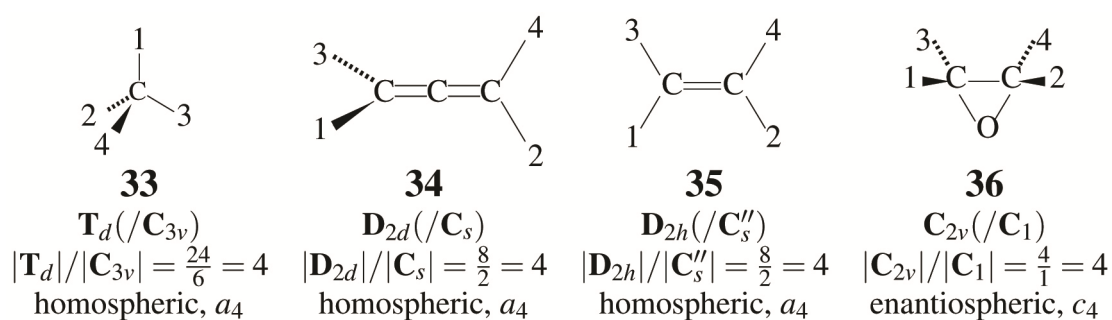


**Figure 11.** Representative stereoskeletons of ligancy 4. The four positions of each skeleton (numbered from 1 to 4) are equivalent to give a four-membered orbit governed by the cosetrepresentation shown below.

##### 4.2.1. EQUIVALENCE CLASSES (ORBITS) AND COSET REPRESENTATIONS

In Fujita's USCI approach, an equivalence relationship is selected as a set of operations contained in a point group. The *proligand-promolecule model* is adopted for the purpose of avoiding effects of conformations [88]. A *proligand* is defined as an abstract ligand (group or substituent) which is characterized by chirality/achirality. A *promolecule* is defined as an abstract molecule which is derived by putting proligands on the substitution positions of a rigid *stereoskeleton* (or shortly, skeleton).

Such a rigid stereoskeleton is selected in accord with the purpose of our discussions. Representative stereoskeletons of ligancy 4 are shown in Figure 11: a tetrahedral skeleton 33 of the point group  $T_d$  (order,  $|T_d| = 24$ ), an allene skeleton 34 of  $D_{2d}$  (order,  $|D_{2d}| = 8$ ), an ethylene skeleton 35 of  $D_{2h}$  (order,  $|D_{2h}| = 8$ ), and an oxirane skeleton 36 of  $C_{2v}$  (order,  $|C_{2v}| = 4$ ).

The four positions of each stereoskeleton are equivalent under the action of the corresponding point group, so that they construct an equivalence class (orbit). Each orbit is

governed by a *coset representation* (CR) of the point group of a stereoskeleton at issue. For example, the four positions of a tetrahedral skeleton **33** construct an orbit governed by the CR, which is generated algebraically by considering a coset decomposition of a point group  $\mathbf{T}_d$  by its subgroup  $\mathbf{C}_{3v}$ , as shown in Table 3. The CR is a transitive permutation representation of degree 4 ( $= |\mathbf{T}_d|/|\mathbf{C}_{3v}| = 24/6$ ). The symbol  $\mathbf{T}_d/\mathbf{C}_{3v}$  has been coined to denote the CR by Fujita [6], where it specifies the global symmetry  $\mathbf{T}_d$  of the skeleton **33** as well as the local symmetry  $\mathbf{C}_{3v}$  of each of the four positions. The resulting set of products of cycles for representing  $\mathbf{T}_d/\mathbf{C}_{3v}$  is isomorphic to the symmetric group of degree 4 ( $\mathbf{S}^{[4]}$ ) [6, 89].

In a similar way, the other stereoskeletons collected in Fig. 11 are characterized by the following coset representations (CRs): the CR  $\mathbf{D}_{2d}/\mathbf{C}_s$  for an allene skeleton **34** [88], the  $\mathbf{CRD}_{2h}/\mathbf{C}_s''$  for an ethylene skeleton **35** [90], and the CR  $\mathbf{C}_{2v}/\mathbf{C}_1$  for an oxirane skeleton **36** [91]. These CRs are isomorphic to the subgroups of the symmetric group of degree 4 ( $\mathbf{S}^{[4]}$ ).

#### 4.2.2. SPHERICITIES AND CHIRALITY FITTINGNESS

Each orbit is categorized into either one of three kinds by examining the global symmetry  $\mathbf{G}$  and the local symmetry  $\mathbf{G}_i$  of the corresponding CR  $\mathbf{G}/\mathbf{G}_i$  [6]. As summarized in Table 4, there appear *enantiospheric*, *homospheric*, and *hemispheric* orbits according to the terms defined by Fujita [89]. These orbits are characterized by sphericity indices for orbits, i.e.,  $a_d$  for  $d$ -membered homospheric orbits,  $c_d$  for  $d$ -membered enantiospheric orbits, and  $b_d$  for  $d$ -membered hemispheric orbits, where the subscript  $d$  represents the degree of the CR, which is calculated to be  $d = |\mathbf{G}|/|\mathbf{G}_i|$ .

The three kinds of sphericities control the modes of substitution on the positions of the respective orbits. The mode of substitution is called *chirality fittingness*, as illustrated in Figure 12 [6]. For example, the  $\mathbf{T}_d/\mathbf{C}_{3v}$ -orbit of the tetrahedral skeleton **33** is determined to be homospheric (Table 4), because both the global symmetry  $\mathbf{T}_d$  and the local symmetry  $\mathbf{C}_{3v}$  are achiral. Hence, the four positions of **33** accommodate four achiral proligands of the same kind (e.g., A) according to the chirality fittingness shown in Figure 12(a), where the global symmetry  $\mathbf{T}_d$  maintains during this mode of substitution. This means that the resulting orbit of A's in the tetrahedral derivative  $\text{CA}_4$  is governed by the CR  $\mathbf{T}_d/\mathbf{C}_{3v}$ . This mode of substitution is represented by the sphericity index  $a_4$  assigned to  $\mathbf{T}_d/\mathbf{C}_{3v}$ , where the subscript 4 of  $a_4$  is calculated to be  $|\mathbf{T}_d|/|\mathbf{C}_{3v}| = 24/6 = 4$ . The same discussions are effective to the homospheric orbits of the allene skeleton **34** and the ethylene skeleton **35**.

On the other hand, the  $\mathbf{C}_{2v}/\mathbf{C}_1$ -orbit of the oxirane skeleton **36** is determined to be enantiospheric (Table 4), because the global symmetry  $\mathbf{C}_{2v}$  is achiral, while the local symmetry  $\mathbf{C}_1$  is chiral. Hence, the four positions of **36** exhibit three modes of substitution to maintain the global symmetry  $\mathbf{C}_{2v}$ , as shown in Figure 12(b). One mode is the accommodation of four achiral proligands of the same kind (e.g., A) according to the



chirality fittingness shown in the first diagram of Figure 12(b). The other mode is a compensated accommodation of two chiral proligands  $p$ 's (on the positions 1 and 4) and two chiral proligands  $\bar{p}$ 's (on the positions 2 and 3) according to the second diagram of Figure 12(b) (the third diagram degenerates onto the second diagram in this example), where a pair of  $p$  and  $\bar{p}$  is an enantiomeric pair in isolation. Note that one half of the  $C_{2v}/C_1$ -orbit of the oxirane skeleton **36** (the positions 1 and 4) and the other half (positions 2 and 3) are separated to give two  $C_2/C_1$ -orbits under an appropriate chiral condition, while they are compensated under an achiral condition so as to maintain the global achirality  $C_{2v}$ .

#### 4.2.3. SUBDUCTION OF COSET REPRESENTATIONS AND USCI-CFS

The generation of derivatives from a given skeleton is treated by applying the concept of *subduction of coset representations* in Fujita's USCI approach [6]. The CR  $G/(G_i)$  of a given skeleton is restricted to give a permutation representation of a subgroup  $G_j$ , where this process is called *a subduction of a coset representation* and denoted by the symbol  $G/(G_i) \downarrow G_j$ , as proposed by Fujita [92]. The permutation representation  $G/(G_i) \downarrow G_j$  may be transitive or intransitive under the subgroup  $G_j$ , so that it can be treated algebraically to give a sum of coset representations, as discussed in Chapter 9 of [6]. Several results of subductions of coset representations have appeared in Appendix C of [6]. For example,  $T_d/(C_{3v}) \downarrow C_{3v}$  gives the following result:

$$T_d/(C_{3v}) \downarrow C_{3v} = C_{3v}/(C_s) + C_{3v}/(C_{3v}), \quad (7)$$

which is calculated algebraically by using the mark table of  $T_d$  (Appendix A of [6]) and the inverse mark table of  $C_{3v}$  (Appendix B of [6]) according to the procedure described in Chapter 9 of [6].

The data of subduction of  $T_d/(C_{3v})$  and related data (Table 5) are cited from a more recent report [93], which has discussed differences between point groups (e.g.,  $T_d$ ) and permutation groups (e.g.,  $S^{[4]}$ , the symmetric group of degree 4). The subduction of Eq. 7 appears in the  $C_{3v}$ -row of Table 5.

**Table 3.** Coset representation  $T_d(/C_{3v})$ .

Symmetry operation		CR $T_d(/C_{3v})$ as product of cycles	PSI(product sphericity indices)	Product of dummy variables	
T	$I$	$\sim$	(1)(2)(3)(4)	$b_1^4$	$s_1^4$
	$C_{2(1)}$	$\sim$	(1 2)(3 4)	$b_2^2$	$s_2^2$
	$C_{2(2)}$	$\sim$	(1 4)(2 3)	$b_2^2$	$s_2^2$
	$C_{2(3)}$	$\sim$	(1 3)(2 4)	$b_2^2$	$s_2^2$
	$C_{3(1)}$	$\sim$	(1)(2 3 4)	$b_1 b_3$	$s_1 s_3$
	$C_{3(2)}$	$\sim$	(1 2 4)(3)	$b_1 b_3$	$s_1 s_3$
	$C_{3(3)}$	$\sim$	(1 4 3)(2)	$b_1 b_3$	$s_1 s_3$
	$C_{3(4)}$	$\sim$	(1 3 2)(4)	$b_1 b_3$	$s_1 s_3$
	$C_{3(1)}^2$	$\sim$	(1)(2 4 3)	$b_1 b_3$	$s_1 s_3$
	$C_{3(4)}^2$	$\sim$	(1 2 3)(4)	$b_1 b_3$	$s_1 s_3$
	$C_{3(3)}^2$	$\sim$	(1 4 2)(3)	$b_1 b_3$	$s_1 s_3$
	$C_{3(2)}^2$	$\sim$	(1 3 4)(2)	$b_1 b_3$	$s_1 s_3$

Symmetry operation	CR $T_d$ ( $/C_{3v}$ ) as product of cycles	PSI(product sphericity indices)	Product of dummy variables
$T\sigma_{d(1)}$	$\sigma_{d(1)} \sim \overline{(1)(2\ 4)(3)}$	$a_1^2 c_2$	$s_1^2 s_2$
	$\sigma_{d(6)} \sim \overline{(1\ 3)(2)(4)}$	$a_1^2 c_2$	$s_1^2 s_2$
	$\sigma_{d(2)} \sim \overline{(1)(2)(3\ 4)}$	$a_1^2 c_2$	$s_1^2 s_2$
	$\sigma_{d(4)} \sim \overline{(1\ 2)(3)(4)}$	$a_1^2 c_2$	$s_1^2 s_2$
	$\sigma_{d(3)} \sim \overline{(1)(2\ 3)(4)}$	$a_1^2 c_2$	$s_1^2 s_2$
	$\sigma_{d(5)} \sim \overline{(1\ 4)(2)(3)}$	$a_1^2 c_2$	$s_1^2 s_2$
	$S_{4(3)} \sim \overline{(1\ 2\ 3\ 4)}$	$c_4$	$s_4$
	$S_{4(3)}^3 \sim \overline{(1\ 4\ 3\ 2)}$	$c_4$	$s_4$
	$S_{4(1)} \sim \overline{(1\ 4\ 2\ 3)}$	$c_4$	$s_4$
	$S_{4(1)}^3 \sim \overline{(1\ 3\ 2\ 4)}$	$c_4$	$s_4$
	$S_{4(2)}^3 \sim \overline{(1\ 2\ 4\ 3)}$	$c_4$	$s_4$
	$S_{4(2)} \sim \overline{(1\ 3\ 4\ 2)}$	$c_4$	$s_4$

**Table 4.** Sphericities of Orbits [89].

G	G <sub>i</sub>	Sphericity of G/G <sub>i</sub> )	Chirality fittingness (object allowed)	Sphericity index <i>d</i>	Dummy variable <i>d</i>
achiral	achiral	homospheric	achiral	<i>a<sub>d</sub></i>	<i>S<sub>d</sub></i>
achiral	chiral	enantiospheric	achiral, <sup>a</sup> chiral <sup>b</sup>	<i>c<sub>d</sub></i>	<i>S<sub>d</sub></i>
chiral	chiral	hemispheric	achiral, <sup>c</sup> chiral	<i>b<sub>d</sub></i>	<i>S<sub>d</sub></i>

<sup>a</sup>An achiral object is restricted to be chiral. One half and the other half of the orbit are superimposable by a rotoreflection operator of G.

<sup>b</sup>The orbit accommodates the half number ( $|G|/2|G_i|$ ) of chiral objects and the half number of chiral objects of opposite chirality so as to accomplish compensated chiral packing

<sup>c</sup> An achiral object is restricted to be chiral.

<sup>d</sup>  $d = |G|/|G_i|$  where  $|G|$  and  $|G_i|$  represent the respective orders.

The resulting orbits  $C_{3v}/(C_s)$  and  $C_{3v}/(C_{3v})$  are both homospheric, so that they are characterized by the sphericity indices  $a_3$  and  $a_1$ , because the sizes of these orbits are calculated to be  $|C_{3v}|/|C_s| = 6/2 = 3$  and  $|C_{3v}|/|C_{3v}| = 6/6 = 1$ . Then, the total subduction (Eq. 7) is represented by the product  $a_1a_3$ , which is called a *unit subduced cycle index with chirality fittingness* (USCICF). This term has been coined by keeping in mind the following scheme of derivation for combinatorial enumeration: a *unit subduced cycle index with chirality fittingness* (USCI-CF) → a *subduced cycle index with chirality fittingness* (SCI-CF) → a *cycle index with chirality fittingness* (CI-CF).

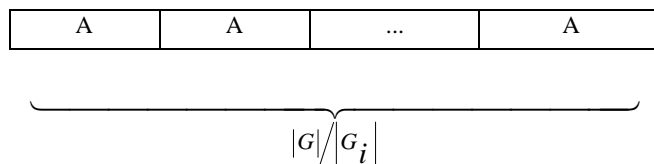
The procedure of subduction is repeated to cover all of the subgroups to give USCICFs as collected in the USCICF-column of Table 5. Note that  $T_d$  has the following non-redundant set of subgroups (SSG):

$$\text{SSG}_{T_d} = \{C_1, C_2, C_s, C_3, S_4, D_2, C_{2v}, C_{3v}, D_{2d}, T, T_d\}, \quad (8)$$

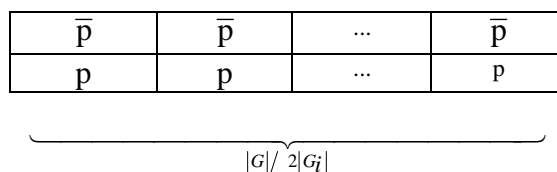
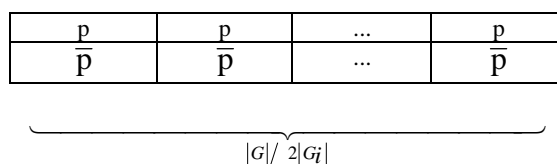
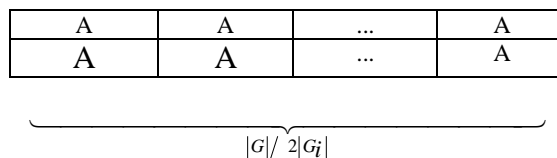
where the subgroups are aligned in the ascending order of their orders after an appropriate representative is selected from each set of conjugate subgroups.

The data of subduction of  $T_d/(C_{3v})$  collected in Table 5 can be applied in a qualitative fashion. The sphericity of each CR collected in the sphericity-column of Table 5 governs the mode of substitution according to the chirality fittingness shown in Figure 12. Thereby, a set of proligands is selected in accord with the chirality fittingness of each CR of a subgroup. For example, a  $C_{3v}$ -molecule **39** shown in Figure 13 is generated by placing three achiral proligands A's on the homospheric  $C_{3v}/(C_s)$ -orbit and one achiral proligand B on the homospheric  $C_{3v}/(C_{3v})$ -orbit in accord with Eq. 7 (or the  $C_{3v}$ -column of Table 5).

(a) Chirality fittingness of a homospheric orbit (sphericity index:  $a_d$ )



(b) Chirality fittingness of an enantiospheric orbit (sphericity index:  $c_d$ )



(c) Chirality fittingness of a hemispheric orbit (sphericity index:  $b_d$ )

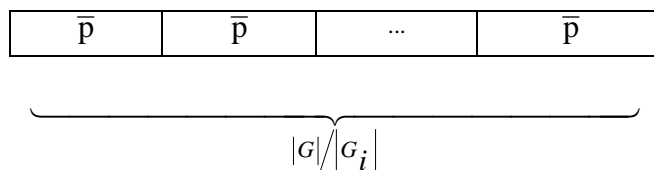
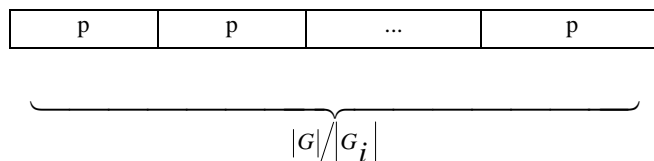
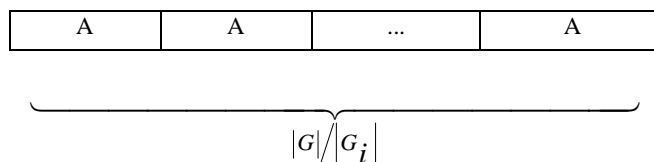


**Figure 12.** Chirality fittingness of orbits with three kinds of sphericities. The subscript  $d$  of each sphericity index is calculated to be  $d = |G|/|G_i|$  [6, 89].

In a similar way, the data of the respective subductions collected in Table 5 can be used to generate the derivatives collected in Figure 13 by referring to the chirality

fittingness shown in Figure 12. A pair of derivatives linked with an underbrace is a pair of *RS*-diastereomers according to Fujita's stereoisogram approach [18].

From a qualitative point of view, Fujita's USCI approach enables us to rationalize various stereochemical phenomena in a systematic fashion [6, 7].

1. The first category of qualitative applications involves the methodology of molecular design: systematic derivation from methane and adamantane skeletons of *Td*-symmetry [94], systematic design of molecules of high symmetry [95], systematic design of chiral molecules of high symmetry [96], desymmetrization of achiral skeletons by monosubstitution [97], as well as chirality and stereogenicity for square-planar complexes [98].
2. The second category of qualitative applications is concerned with the proposal of the *SCR* (*subduction-of-coset-representation*) notation, which aims at systematic classification of molecular symmetries [91, 99].
3. The third category of qualitative applications is concerned with theoretical foundations, e.g., the proposal of the *proligand-promolecule model* and the formulation of *matched and mismatched molecules* [88], *chirogenic sites* in an enantiospheric orbit [100], characterization of prochirality and classification of meso-compounds [101], general treatments of local chirality and prochirality [89], as well as systematic characterization of prochirality, prostereogenicity, and stereogenicity by means of the sphericity concept [102].
4. The fourth category of qualitative applications is concerned with the merits of Fujita's USCI approach as compared with the conventional terminology of stereochemistry: stereochemistry and stereoisomerism characterized by the sphericity concept [93], an approach to topic relationships [103], approaches for restructuring stereochemistry by novel terminology [90, 104], and sphericity beyond topicity [86, 87]. Introductory discussions on importance of orbits and sphericity indices and on importance of local symmetries in subductions of coset representations have appeared in an internet journal [105, 106].

#### 4.2.4. SYMMETRY-ITEMIZED ENUMERATION

Fujita's USCI approach supports four methods of symmetry-itemized enumeration of chemical compounds [6], i.e., the fixed-point-matrix (FPM) method [92, 107], the partial-cycle-index (PCI) method [108], the elementary-superposition (ES) method [109, 110], and the partial-superposition (PS) method [110].

The enumeration based on the tetrahedral skeleton **33** has been conducted by using the FPM method and the results have been reported in a tabular form (Table 1 of Ref. [88] and Table 21.1 of a book [6]). The PCI method is applied to the enumeration based on the tetrahedral skeleton **33** [93]. The results have been obtained in the form of generating

functions, where the coefficients of respective terms have been reported in a tabular form (Table 1 of Ref. [93]). Here, the PCI method applied to 33 [93] is described to show a representative embodiment of Fujita's USCI approach.

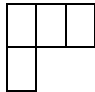
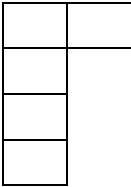
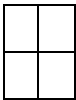

The USCI-CFs listed in Table 5 is aligned in accord with the SSG shown in Eq. 8:

$$\text{USCI-CF}_{T_d}(C_{3v}) = (b_1^4, b_2^2, a_1^2 c_2, b_1 b_3, c_4, b_4, a_2^2, a_1 a_3, a_4, b_4, a_4), \quad (9)$$

**Table 5.** Subduction of a  $T_d(C_{3v})$ -Orbit [93].

Subgroup of $T_d$	Young's tableau	Cycle structure	Subduction of $T_d(C_{3v})$	Sphericity	USCI-CF
$T_d$		$4^1$	$T_d(C_{3v})$	homospheric	$a_4$
$T$		$4^1$	$T(C_3)$	hemispheric	$b_4$
$D_{2d}$		$4^1$	$D_{2d}(C_s)$	homospheric	$a_4$
$C_{3v}$		$3^1 1^1$	$C_{3v}(C_s)$ $C_{3v}(C_{3v})$	homospheric homospheric	$a_1 a_3$
$C_{2v}$		$2^2$	$C_{2v}(C_s)$ $C_{2v}(C'_s)$	homospheric homospheric	$a_2^2$
$D_2$		$4^1$	$D_2(C_1)$	hemispheric	$b_4$
$S_4$		$4^1$	$S_4(C_1)$	enantiospheric	$c_4$

---

$C_3$		$3^1 1^1$	$C_3(/C_1)$ $C_3(/C_3)$	hemispheric hemispheric	$b_1 b_3$
$C_s$		$2^1 1^2$	$C_s(/C_1)$ $C_s(/C_s)$ $C_s(/C_s)$	enantiospheric homospheric homospheric	$a_1^2 c_2$
$C_2$		$2^2$	$C_2(/C_1)$ $C_2(/C_1)$	hemispheric hemispheric	$b_2^2$
$C_1$		$1^4$	$C_1(/C_1)$ $C_1(/C_1)$ $C_1(/C_1)$ $C_1(/C_1)$	hemispheric hemispheric hemispheric hemispheric	$b_1^4$

---

which is regarded as a formal row vector. Because of the subduction of a single CR, this formal row vector of USCI-CFs is considered to be a row vector of *subduced cycle indices with chirality fittingness* (SCI-CFs) according to Def. 19.3 of [6]. The formal vector (Eq. 9) is multiplied by the inverse mark table  $M_{-1} T_d$  (Table B.10 shown in Appendix B of a book [6]) to give a formal vector:



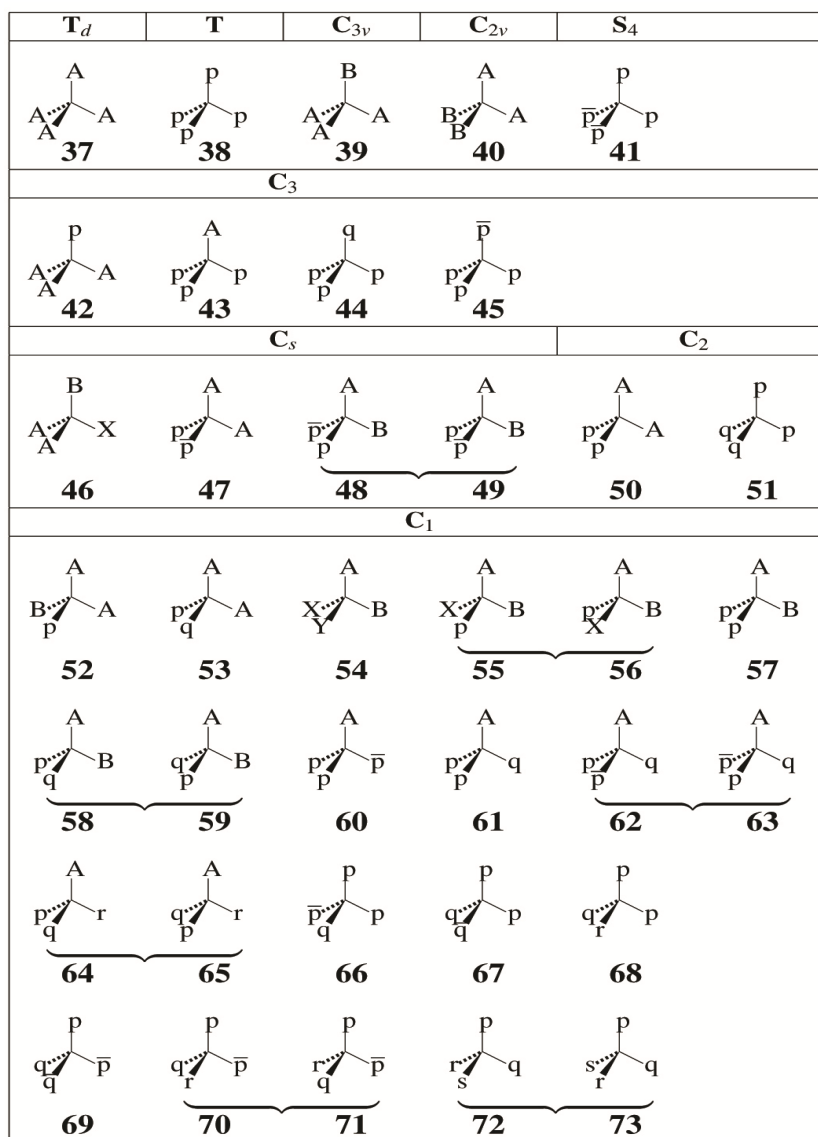


**Figure 13.** Promolecules from a tetrahedral skeleton [88].

$$(\dots, \text{PCI-CF}(\mathbf{G}_j), \dots) = \text{USCI-CF}_{T_d} (\text{C}_{3v}) \times M_{T_d}^{-1}, \quad (10)$$

where the element  $\text{PCI-CF}(\mathbf{G}_j)$  is the PCI-CF for each subgroup  $\mathbf{G}_j$  ( $\mathbf{G}_j \in \text{SSG}_{T_d}$ ). See Def.19.6 of [6]. Thereby, PCI-CFs for every subgroups of  $\text{SSG}_{T_d}$  (Eq. 8) are obtained as follows:

$$\text{PCI-CF}(\mathbf{C}_1) = \frac{1}{24}b_1^4 - \frac{1}{8}b_2^2 - \frac{1}{4}a_1^2c_2 - \frac{1}{6}b_1b_3 + \frac{1}{4}b_4$$

$$+\frac{1}{4}a_2^2 + \frac{1}{2}a_1a_3 - \frac{1}{2}a_4 \quad (11)$$

$$\text{PCI-CF}(\mathbf{C}_2) = \frac{1}{4}b_2^2 - \frac{1}{4}c_4 - \frac{1}{4}b_4 - \frac{1}{4}a_2^2 + \frac{1}{2}a_4 \quad (12)$$

$$\text{PCI-CF}(\mathbf{C}_s) = \frac{1}{2}a_1^2c_2 - \frac{1}{2}a_2^2 - a_1a_3 + a_4; \quad (13)$$

$$\text{PCI-CF}(\mathbf{C}_3) = \frac{1}{2}b_1b_3 - \frac{1}{2}a_1a_3 - \frac{1}{2}b_4 + \frac{1}{2}a_4 \quad (14)$$

$$\text{PCI-CF}(\mathbf{S}_4) = \frac{1}{2}c_4 - \frac{1}{2}a_4 \quad (15)$$

$$\text{PCI-CF}(\mathbf{D}_2) = 0 \quad (16)$$

$$\text{PCI-CF}(\mathbf{C}_{2v}) = \frac{1}{2}a_2^2 - \frac{1}{2}a_4 \quad (17)$$

$$\text{PCI-CF}(\mathbf{C}_{3v}) = a_1a_3 - a_4 \quad (18)$$

$$\text{PCI-CF}(\mathbf{D}_{2d}) = 0 \quad (19)$$

$$\text{PCI-CF}(\mathbf{T}) = \frac{1}{2}b_4 - \frac{1}{2}a_4 \quad (20)$$

$$\text{PCI-CF}(\mathbf{T}_d) = a_4 \quad (21)$$

These PCI-CFs have been first noted in the articles by Fujita [86, 93].

Suppose that the four positions of **33** accommodate a set of proligands selected from the following proligand inventory:

$$\mathbf{L} = \{ \text{A, B, X, Y ; } p, \bar{p}, q, \bar{q}, r, \bar{r}, s, \bar{s} \}, \quad (22)$$

where the uppercase symbols, A, B, X, and Y, denote achiral proligands, while the paired lowercase symbols, p and  $\bar{p}$  etc., denote chiral proligands having opposite chirality senses. The chirality or achirality of each proligand is decided in isolation (when detached). Theorem 19.6 (or Theorem 9.7) of a book [6] permits us to adopt the following set of ligand-inventory functions:

$$a_d = \text{A}^d + \text{B}^d + \text{X}^d + \text{Y}^d \quad (23)$$

$$c_d = \text{A}^d + \text{B}^d + \text{X}^d + \text{Y}^d + 2p^{d/2}\bar{p}^{d/2} + 2q^{d/2}\bar{q}^{d/2} + 2r^{d/2}\bar{r}^{d/2} + 2s^{d/2}\bar{s}^{d/2} \quad (24)$$

$$b_d = \text{A}^d + \text{B}^d + \text{X}^d + \text{Y}^d + p^d + q^d + r^d + s^d + \bar{p}^d + \bar{q}^d + \bar{r}^d + \bar{s}^d. \quad (25)$$

It should be noted that the power  $d/2$  appearing in Eq. 24 is an integer because the subscript  $d$  of  $c_d$  is always even in the light of the enantiosphericity of the corresponding orbit. See Table 4 and Figure 12 for the chirality fittingness of orbits.

The ligand-inventory functions (Eqs. 23–25) are introduced into the PCI-CFs (Eqs. 11–21). After expansion, we obtain the following generating functions [86, 93]:

$$\begin{aligned}
 f_{C_1} = & \{(ABXp + ABX\bar{p}) + \dots\} + \{(ABpq + AB\bar{p}q) + \dots\} \\
 & + \{(Ap\bar{p}q + App\bar{q}) + \dots\} + \{(Apqr + Ap\bar{q}r) + \dots\} \\
 & + \{(pqrs + \overline{pqrs}) + \dots\} + \{(p\bar{p}qr + ppqr) + \dots\} \\
 & + \left\{\frac{1}{2}(A^2Bp + A^2B\bar{p}) + \dots\right\} + \left\{\frac{1}{2}(ABp^2 + AB\bar{p}^2) + \dots\right\} \\
 & + \left\{\frac{1}{2}(A^2pq + A\overline{pq}) + \dots\right\} + \left\{\frac{1}{2}(Ap^2\bar{p} + App^2) + \dots\right\} \\
 & + \left\{\frac{1}{2}(Ap^2q + A\bar{p}^2\bar{q}) + \dots\right\} + \left\{\frac{1}{2}(p^2\bar{p}q + p\bar{p}^2\bar{q}) + \dots\right\} \\
 & + \left\{\frac{1}{2}(p^2q\bar{q} + \bar{p}^2q\bar{q}) + \dots\right\} + \left\{\frac{1}{2}(p^2qr + \bar{p}^2\bar{q}r) + \dots\right\} \\
 & + \{p\bar{p}q\bar{q} + p\bar{p}r\bar{r} + \dots\} \\
 & + \{ABXY\}
 \end{aligned} \tag{26}$$

$$f_{C_2} = \left\{\frac{1}{2}(A^2p^2 + A^2\bar{p}^2) + \dots\right\} + \left\{\frac{1}{2}(p^2q^2 + \bar{p}^2\bar{q}^2) + \dots\right\} \tag{27}$$

$$\begin{aligned}
 f_{C_s} = & \{2ABp\bar{p} + 2ABq\bar{q} + \dots\} + \{A^2p\bar{p} + \dots\} \\
 & + \{A^2BX + A^2BY + \dots\}
 \end{aligned} \tag{28}$$

$$\begin{aligned}
 f'_{C_3} = & \left\{\frac{1}{2}(A^3p + A^3\bar{p}) + \dots\right\} + \left\{\frac{1}{2}(Ap^3 + A\bar{p}^3) + \dots\right\} \\
 & + \left\{\frac{1}{2}(p^3q + \bar{p}^3\bar{q}) + \dots\right\} + \left\{\frac{1}{2}(p^3\bar{p} + p\bar{p}^3) + \dots\right\}
 \end{aligned} \tag{29}$$

$$f_{S_4} = \{p^2\bar{p}^2 + q^2\bar{q}^2 + r^2\bar{r}^2 + s^2\bar{s}^2\} \tag{30}$$

$$f_{C_{2v}} = \{A^2B^2 + A^2X^2 + A^2Y^2 + \dots\} \tag{31}$$

$$f_{C_{3v}} = \{A^3B + A^3X + A^3Y + \dots\} \tag{32}$$

$$f_T = \left\{\frac{1}{2}(p^4 + \bar{p}^4) + \dots\right\} \tag{33}$$

$$f_{Td} = \{A^4 + B^4 + X^4 + Y^4\}. \tag{34}$$

In these generating functions, the coefficient of the term  $A^a B^b X^x Y^y p^p \bar{p}^{\bar{p}} q^q \bar{q}^{\bar{q}} r^r \bar{r}^{\bar{r}} s^s \bar{s}^{\bar{s}}$  indicates the number of inequivalent (self-)enantiomeric pairs to be counted. Note that such a term as  $1/2(\text{ABX}_p + \text{ABX}_{\bar{p}})$  indicates the presence of one enantiomeric pair of promolecules under the point-group symmetry. It follows that the term  $(\text{ABX}_p + \text{ABX}_{\bar{p}})$  in the generating function  $f_{C_1}$  (Eq. 26) is interpreted to be  $2 \times 1/2(\text{ABX}_p + \text{ABX}_{\bar{p}})$ , which indicates the presence of two pairs of enantiomeric promolecules. The enumeration results represented by the generating functions (Eqs. 26–34) are consistent with the data listed in Tables 4 and 5 of Ref. [93] as tabular forms.

The promolecules enumerated by Eqs. 26–34 are depicted in Figure 13. Each pair of braces appearing in Eqs. 26–34 contains terms of the same pattern of substitution, e.g.,  $A^4$ ,  $B^4$ ,  $X^4$ , and  $Y^4$  in  $f_{T_d}$  (Eq. 34), so that an appropriate representative (e.g.,  $A^4$ ) is depicted in Figure 13. Hence, 30 pairs of braces in Eqs. 26–34 corresponds to the 30 promolecules depicted in Figure 13, where a pair of promolecules linked with an underbrace (e.g., **48** and **49**) corresponds to the coefficient 2 of each term in a pair of braces (e.g.,  $2\text{ABp}\bar{p}$  in  $f_{C_s}$  of Eq. 28). Because a pair of (self-)enantiomers is counted once in Eqs. 26–34, an appropriate promolecule selected from a pair of enantiomers is depicted in Figure 13. A pair of promolecules linked with an underbrace in Figure 13 represents a pair of *RS*-diastereomers according to Fujita's stereoisogram approach, as will be discussed later.

The four methods supported by Fujita's USCI approach have been applied to symmetry-itemized enumerations starting from various skeletons, e.g., cage-shaped skeletons [111], adamantane isomers [112], non-rigid tetrahedral molecules [113],  $D_{3h}$ -skeletons [114],  $D_{2d}$ -skeletons [109], a dodecahedrane skeleton of  $I_h$ -symmetry [115], a fullerene skeleton of  $I_h$ -symmetry [108], imaginary transition structures for counting organic reactions [61], flexible six-membered skeletons [116], a benzene skeleton of  $D_{6h}$ -symmetry [117], ferrocene derivatives [118], a dumbbell skeleton of  $D_{\infty h}$ -symmetry [119], an octahedral skeleton of  $O_h$ -symmetry [120, 121], and a cubane skeleton of  $O_h$ -symmetry [122, 123].

#### 4.2.5. THE CONCEPT OF MANDALAS

The concept of *mandalas* has been proposed to give a diagrammatic introduction to Fujita's USCI approach in a series of articles [124, 125, 126]. Just as there appears an orbit of positions in a molecule (an intramolecular orbit), there appears an orbit of promolecules as an intermolecular orbit, which can be formulated by starting from the concept of mandalas. Group-theoretical foundations for the concept of mandalas have been discussed to bring about diagrammatic expressions for characterizing symmetries of 3D structures [127]. The

concept of mandalas has been applied to the diagrammatic formulation of Fujita's proligand method [128].

#### 4.2.6. RESTRICTED ENUMERATIONS

The symmetry-itemized enumeration described above presumes that two or more orbits of vertices in a given skeleton accommodate proligands independently. In contrast, this presumption should be modified in symmetry-itemized enumeration of Kekulé structures, in which double bonds are not adjacent to each other. This type of restricted enumerations should take account of interaction between vertex substitution and edge substitution. For this purpose, the concept of *restricted subduced cycle indices* (RSCIs) has been proposed by Fujita [129].

The *restricted-subduced-cycle-index (RSCI) method* has been applied to symmetry-itemized enumeration of Kekulé structures of fullerene C<sub>60</sub> [129]. Fujita's RSCI method has been applied to counting matchings of graphs, so that it has been applied to Z-counting polynomials and the Hosoya index as well as to matching polynomials [130]. Fujita's RSCI method has been applied to enumeration of Kekulé structures in general and perfect matchings of graphs [131].

The FPM method of Fujita's USCI approach is modified to meet restricted conditions, so that *the restricted-fixed-point-matrix (RFPM) method* has been proposed on the basis of RSCIs [132]. The RFPM method has been applied to enumeration of three-dimensional structures derived from a dodecahedrane skeleton. The PCI method of Fujita's USCI approach is modified to meet restricted conditions, so that *the restricted-partial-cycle-index (RPCI) method* has been proposed on the basis of RSCIs [133]. The RPCI method has been applied to enumeration of three-dimensional structures derived from a dodecahedrane skeleton. A series of articles discussing general methods for treating interaction between two or more orbits has appeared [134, 135, 136].

### 4.3. FUJITA'S PROLIGAND METHOD AND RELATED METHODS

Although Fujita's USCI approach enables us to accomplish symmetry-itemized enumeration, gross enumeration without such symmetry-itemization is desirable if a brief perspective is necessary. The proligand method and related methods developed by Fujita are powerful to accomplish gross enumeration [9].

#### 4.3.1. SPHERICITY OF CYCLES

Because each operation of a point group is a generator of a cyclic subgroup, the corresponding product of cycles can be correlated to the cyclic subgroup. Thereby, the concept of *sphericities of cycles* has been developed by Fujita [137], where it is correlated

to the concept of sphericities of orbits *for cyclic subgroups*. An odd- or even-cycle in a product of cycles for each operation of a point group is classified into three kinds as follows:

1. A  $d$ -cycle in a product of cycles for a (roto)reflection is classified to be a homospheric cycle, if  $d$  is odd. A sphericity index  $a_d$  is assigned to the homospheric  $d$ -cycle.
2. A  $d$ -cycle in a product of cycles for a (roto)reflection is classified to be an enantiospheric cycle, if  $d$  is even. A sphericity index  $c_d$  is assigned to the enantiospheric  $d$ -cycle.
3. A  $d$ -cycle in a product of cycles for a rotation is classified to be a hemispheric cycle, even if  $d$  is odd or even. A sphericity index  $b_d$  is assigned to the hemispheric  $d$ -cycle.

Then, the product of cycles for a (roto)reflection or a rotation is characterized by a *product of sphericity indices* (PSIs), which is calculated from the assigned sphericity indices for cycles. Table 3 collects such products of cycles for the respective operations of the CR  $\mathbf{T}_d(\mathbf{C}_{3v})$ , where the operations of subgroup  $\mathbf{T}$  represent rotations, while those of the coset  $\mathbf{T}\sigma_{d(1)}$  represent (roto)reflections. For example, the rotation  $\mathbf{C}_{3(1)}$  (a three-fold rotation) is denoted by the PSI  $b_1b_3$ , because the 1-cycle (1) and the 3-cycle (2 3 4) are both hemispheric. On the other hand, the reflection  $\sigma_{d(1)}$  (a dihedral reflection) is denoted by the PSI  $a_1^2c_2$ , because the 1-cycles (1) and (3) are homospheric as well as the 2-cycle (2 4) is enantiospheric.

It should be noted that the PSIs for cycles (cf. Table 3) are closely related to the USCI-CFs for orbits (cf. Table 5), where they are mediated through cyclic subgroups.

#### 4.3.2. FUJITA'S PROLIGAND METHOD FOR GROSS ENUMERATION

Fujita's proligand method has been developed by using the PSIs defined above [137, 138, 139], so that we are able to accomplish gross enumeration of 3D structures under point groups.

According to Fujita's proligand method, a *cycle index with chirality fittingness* (CI-CF) is defined as the sum of PSIs for all of the operations of a given group, where the sum is divided by the order of the group [137]. For example, the PSIs listed in Table 3 are summed up and divided by the order of  $\mathbf{T}_d$  ( $|\mathbf{T}_d| = 24$ ), so as to give the following CI-CF for the point group  $\mathbf{T}_d$ :

$$\text{CI-CF}(\mathbf{T}_d(/C_{3v})) = \frac{1}{24}(b_1^4 + 3b_2^2 + 8b_1b_3 + 6a_1^2c_2 + 6c_4). \quad (35)$$

Note that the CI-CF (Eq. 35) can be alternatively obtained by summing up the PCI-CFs (Eqs. 11–21).

After ligand-inventory functions (e.g., Eqs. 23–25) for a ligand inventory (e.g.,  $\mathbf{L}$  represented by Eq. 22) are introduced into the CI-CF (e.g., Eq. 35), the resulting equation is expanded to give a generating function, in which the coefficient of each term represents the number of promolecules with the corresponding composition [137]. For example, the introduction of Eqs. 23–25 into Eq. 35 and the subsequent expansion provide a generating function for gross enumeration of promolecules on the basis of a tetrahedral skeleton **33**. Although the generating function is omitted here, it is equal to the sum of the symmetry-itemized generating functions represented by Eqs. 26–34.

#### 4.3.3. FUJITA'S PROLIGAND METHOD VS. PÓLYA'S THEOREM

Pólya's theorem has been widely used to accomplish gross enumeration of chemical compounds as graphs [8, 60], where the action of permutation groups such as the symmetric group of degree 4 ( $\mathbf{S}^{[4]}$ ) is presumed to control the behavior of graphs. As found by the terms 'graphs' and 'permutation groups', Pólya's theorem is incapable of enumerating *3D structures* (not 'graphs'), because it lacks the concept of *sphericities of cycles* under the action of *point groups* (not 'permutation groups') such as  $\mathbf{T}_d$  [140].

For example, Pólya's theorem uses a set of products of dummy variables collected in Table 3, which stems from the symmetric group of degree 4 ( $\mathbf{S}^{[4]}$ ). Hence, the cycle index  $\text{CI}(\mathbf{S}^{[4]})$  is calculated as follows:

$$\text{CI}(\mathbf{S}^{[4]}) = \frac{1}{24}(s_1^4 + 3s_2^2 + 8s_1s_3 + 6s_1^2s_2 + 6s_4). \quad (36)$$

The CI (Eq. 36) lacks sphericities of cycles in comparison with Eq. 35, which is obtained by using a set of products of sphericity indices (PSIs) on the basis of Fujita's proligand method. In other words, the three kinds of SIs ( $a_d$ ,  $c_d$ , and  $b_d$ ) in Eq. 35 (Fujita's proligand method) degenerate into one kind of dummy variables ( $s_d$ ) in Eq. 36 (Pólya's theorem), so that 3D structures are projected into graphs.

A book concerning Fujita's proligand method and related enumeration tools has been published under the title "Combinatorial Enumeration of Graphs, Three-Dimensional Structures, and Chemical Compounds" [9]. The expression 'Graphs, Three-Dimensional Structures' in this title connotes a sharp contrast to the expression 'Graphs' in the title of Pólya's book "Combinatorial Enumeration of Groups, Graphs, and Chemical Compounds" [8].

#### 4.3.4. RECURSIVE ENUMERATION OF MONOSUBSTITUTED ALKANES AND ALKANES

Fujita's proligand method has been applied to the recursive enumeration of mono-substituted alkanes [141, 142] and alkanes [143, 144]. The results are shown in Table 6 [145], which also contains the results based on Pólya's theorem for the sake of comparison. Note that a pair of (self-)enantiomers is counted once by Fujita's proligand method, while a constitution (graph) is counted once by Pólya's theorem.

Further recursive enumerations of monosubstituted alkanes and alkanes have been investigated by paying attention to various effects: structural effects [146], modes of categorization [145, 147], effects of asymmetric and pseudoasymmetric centers [148, 149], and effects of internal branching [150, 151]. Systematic comparison between 3D structures and graphs has been described [152, 153]. These results have been summarized to give a solution to a long-standing interdisciplinary problem over 130 years [154].

#### 4.3.5. RELATED METHODS FOR GROSS ENUMERATION

The concept of sphericities of orbits in Fujita's USCI approach is closely related to the concept of sphericities of cycles in Fujita's proligand method. The close relationship between these concepts can be demonstrated by several derivations of CI-CFs from USCI-CFs on the basis of the properties of inverse mark tables, which can be effectively restricted to cyclic subgroups. According to the procedures of such reduction, several methods of gross enumeration has been developed by Fujita [9], i.e., the markaracter method [155, 156], the characteristic-monomial (CM) method [157, 158, 159, 160, 161, 162], the extended-superposition (ExS) method [163], and the double-coset-representation (DCR) method [164]. Because these methods are based on the USCI approach, each of them requires a set of fundamental data (mark tables, inverse mark tables, subduction of coset representations, USCIs, and USCI-CFs), which are generally difficult to prepare in case of large groups. Hence, Fujita's proligand method would be selected for the purpose of practical enumeration. It should be noted, however, that these related methods based on the USCI approach assure the Fujita's proligand method and symmetry-itemized enumeration based on Fujita's USCI approach.



**Table 6.** Enumeration of Alkanes  $C_nH_{2n+2}$ [145].

$n$	Constitutional isomers by Pólya's theorem	3D structural isomers by Fujita's proligand method
1	1	1
2	1	1
3	1	1
4	2	2
5	3	3
6	5	5
7	9	9
8	18	19
9	35	38
10	75	88
11	159	203
12	355	509
13	802	1299
14	1858	3459
15	4347	9347
16	10359	25890
17	24894	72505
18	60523	205877
19	148284	589612
20	366319	1703575
21	910726	4954686
22	2278658	14502108
23	5731580	42671509
24	14490245	126180490
25	36797588	374749447
26	93839412	1117505952
27	240215803	3344714436
28	617105614	10045148539
29	1590507121	30264120901
30	4111846763	91449677878
31	10660307791	277096805630
32	27711253769	841783833517
33	72214088660	2563418291362
34	188626236139	7823943663908
35	493782952902	23931052067297

36	1295297588128	73345833181110
37	3404490780161	225226025743122
38	8964747474595	692862470624367
39	23647478933969	2135109239262173
40	62481801147341	6590223616010654
41	165351455535782	20372876580255143
42	438242894769226	63073132550694742
43	1163169707886427	195544793394384827
44	3091461011836856	607057684131345479
45	8227162372221203	1886989279103128211
46	21921834086683418	5872733742149957594
47	58481806621987010	18298681742426380229
48	156192366474590639	57080340544235225497
49	417612400765382272	178246302614039769705
50	1117743651746953270	557189473902522080578

By selecting cubane derivatives as probes of gross enumeration, Fujita's proligand method [165] has been compared with the markaracter method [166], the CM method [167], the ExS method [163], and the DCR method [164]. For the symmetry-itemized enumeration of cubane derivatives, see [122, 123].

#### 4.4. FUJITA'S STEREOISOGRAM APPROACH

A given skeleton has been treated on the basis of a permutation group in the conventional methodology of stereochemistry, as Mislow and Siegel [168] pointed out that stereoisomers are recognized as prototypes of permutation isomers proposed by Ugi et al. [169]. On the other hand, a given skeleton has been treated on the basis of a point group in Fujita's USCI approach [6]. Even if the same skeleton is selected as a probe, the action of a permutation group is different from the action of a point group. For example, the action of the symmetric group of degree 4 ( $S^{[4]}$ ) onto a tetrahedral skeleton **33** has been detailedly examined, so as to be different from the action of the point group  $T_d$  onto **33** [93]. Fujita's stereoisogram approach [10] has brought about *Aufheben*, in which point groups and permutation groups are integrated to create *RS*-stereoisomeric groups as a new category of groups.

##### 4.4.1. DIFFERENCES BETWEEN POINT GROUPS AND PERMUTATION GROUPS

Figure 14 illustrates a set of stereoisomers of 2,3,4-trihydroxyglutaric acids (**74**,  $\overline{\mathbf{74}}$ , **75**, and **76**), which exhibits different behaviors towards the point group  $T_d$  and towards the symmetric group of degree 4 ( $S^{[4]}$ ). Let us examine these stereoisomers according to Ref.

[93], after they are converted into the corresponding promolecules (**57**,  $\overline{\mathbf{57}}$ , **48**, and **49**) according to the proligand-promolecule model.

The symmetry-itemized enumeration under the action of the point group  $T_d$  [93] indicates the presence of one pair of enantiomers with the composition  $ABp_2$  or  $AB\overline{p}_2$  (**57** and  $\overline{\mathbf{57}}$ , cf. the term  $\frac{1}{2}(ABp^2+AB\overline{p}^2)$  in  $f_{C_i}$  (Eq. 26)) and two achiral promolecules with the composition  $ABp\overline{p}$  (**48** and **49**, cf. the term  $2ABp\overline{p}$  in  $f_{C_s}$  (Eq. 28)). See Figure 14(a).

In contrast, the symmetry-itemized enumeration under the action of the permutation group  $S^{[4]}$  [93] indicates the presence of one promolecule with the composition  $ABp^2$  (**57**), one promolecule with the composition  $AB\overline{p}^2$  ( $\overline{\mathbf{57}}$ ), and one pair of **48** and **49**. See Figure 14(b). Because the conventional terminology of stereochemistry depends upon a pair of terms ‘chirality/ achirality’ even under the action of  $S^{[4]}$ , the pairing of **48** (achiral) and **49** (achiral) cannot be rationalized, so that it is regarded as an exceptional case named ‘pseudoasymmetry’. Moreover, **57** with  $ABp^2$  and  $\overline{\mathbf{57}}$  with  $AB\overline{p}^2$  are separately counted under  $S^{[4]}$ , where they are not recognized to give a pair of enantiomers.

In order to comprehend stereochemistry and stereoisomerism, I have proposed the stereoisogram approach [10], where the enumeration results of Figure 14(b) are harmonized with those of Figure 14(a). Thereby, **48** and **49** are recognized to be *RS*-stereogenic, so that they are pairwise counted once as a pair of *RS*-diastereomers under the action of an *RS*-permutation group which is isomorphic to the permutation group  $S^{[4]}$ . Moreover, **57** is *RS*-astereogenic and is not paired with  $\overline{\mathbf{57}}$  (also *RS*-astereogenic) under the *RS*-permutation group.

#### 4.4.2. RS-STEREoisomeric Groups

According to Fujita’s stereoisogram approach [10, 11], a given point group can be extended to generate the corresponding *RS*-stereoisomeric group, which is characterized by a stereoisogram as a diagrammatic expression. As a typical example, let us examine the point group  $T_d$  (order 24), which can be extended to generate the corresponding *RS*-stereoisomeric group  $T_{d\overline{\sigma}i}$  (order 48).

The point group  $T_d$  for the tetrahedral skeleton **33** is decomposed as follows:

$$\mathbf{T}_d = \mathbf{T} + \mathbf{T}\sigma, \quad (37)$$

where the symbol  $\sigma$  is a representative selected from the 12 (roto)reflection operations of  $T_d$  (the  $\mathbf{T}\sigma_{d(1)}$  part of Table 3). The coset decomposition shown by Eq. 37 characterizes an enantiomeric relationship between **33** (and its homomers; A) and  $\mathbf{T}\sigma_{d(1)}\mathbf{33}$  (and its homomers; B), as shown in the vertical direction of Figure 15.

An *RS-permutation* denoted by the symbol  $\tilde{\sigma}$  is defined as an operation which has the same permutation as  $\sigma$  but no alternation of chirality. Then, the *RS-permutation group*  $\mathbf{T}_{\tilde{\sigma}}$  is defined as follows:

$$\mathbf{T}_{\tilde{\sigma}} = \mathbf{T} + \mathbf{T}\tilde{\sigma}, \quad (38)$$

which has been noted previously (Eq. 44 of [170]). The *RS-permutation group*  $\mathbf{T}_{\tilde{\sigma}}$  is isomorphic to the symmetric group of degree 4 ( $\mathbf{S}^{[4]}$ ), so that  $\mathbf{T}_{\tilde{\sigma}}$  and  $\mathbf{S}^{[4]}$  can be equalized for practical purposes of enumerating tetrahedral promolecules. The coset decomposition shown by Eq. 38 characterizes an *RS-diastereomeric relationship* between **33** (and its homomers; A) and **77** (and its homomers; C), as shown in the horizontal direction of Figure 15.

A ligand reflection is defined as an operation which has the same permutation as a rotation ( $\in \mathbf{T}$ ) but alternation of chirality. Let the symbol  $\hat{I}$  represent an operation which has the same permutation as  $I$  but alternation of chirality. Thereby, the *ligand-reflection group*  $\mathbf{T}_{\hat{I}}$  is defined as follows:

$$\mathbf{T}_{\hat{I}} = \mathbf{T} + \mathbf{T}\hat{I}, \quad (39)$$

which has been noted previously (Eq. 57 of [170]). Then, there appear 12 ligand reflections contained the coset  $\mathbf{T}\hat{I}$ . The coset decomposition shown by Eq. 39 characterizes a *holantimeric relationship* between **33** (and its homomers; A) and  $\overline{\mathbf{77}}$  (and its homomers; D), as shown in the diagonal direction of Figure 15.

Because the group  $\mathbf{T}$  contained in Eqs. 37–39 as a common subgroup, the *RS-stereoisomeric group*  $\mathbf{T}_{d\tilde{\sigma}\hat{I}}$  can be formulated as follows:

$$\mathbf{T}_{d\tilde{\sigma}\hat{I}} = \mathbf{T} + \mathbf{T}\sigma + \mathbf{T}\tilde{\sigma} + \mathbf{T}\hat{I}, \quad (40)$$

where the group  $\mathbf{T}$  is a normal subgroup of  $\mathbf{T}_{d\tilde{\sigma}\hat{I}}$ . This coset decomposition has been noted previously (Eq. 8 of [170]).

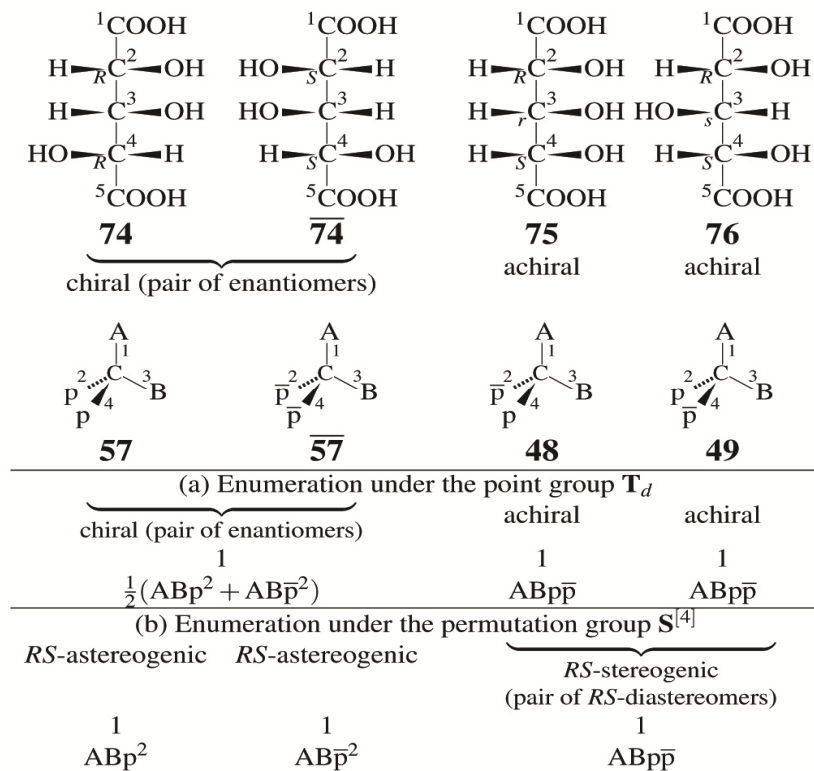


**Figure 14.** 2,3,4-Trihydroxyglutaric acids and the corresponding promolecules: (a) the itemized numbers under the point group  $T_d$  and (b) the itemized numbers under the permutation group  $S^{[4]}$ . The two achiral derivatives (**75** and **76**) or the corresponding promolecules (**48** and **49**) exhibit a pseudoasymmetric feature.

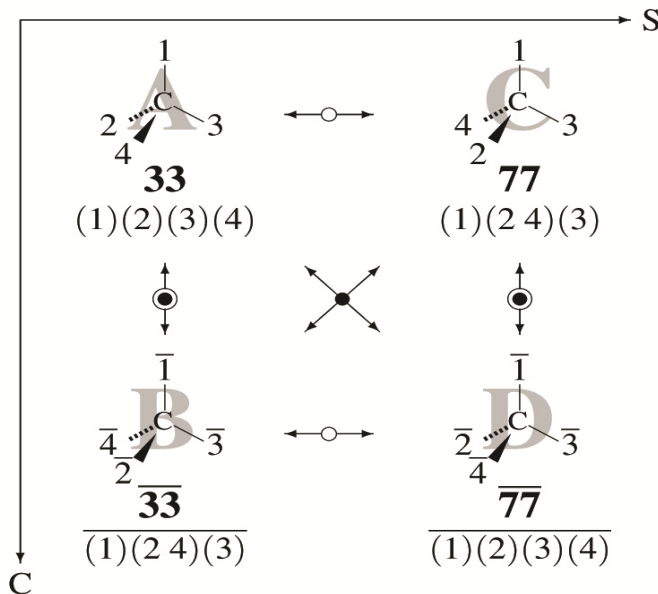


**Figure 15.** Elementary stereoisogram of numbered tetrahedral skeletons. The other modes of sequential numbering are permitted without losing generality [13].

The respective cosets of Eq. 40 correspond to the skeletons depicted in Figure 15, i.e.,  $\mathbf{T}$  to  $33$  (and its homomers; A),  $\mathbf{T}\sigma$  to  $\overline{33}$  (and its homomers; B),  $\mathbf{T}\tilde{\sigma}$  to  $77$  (and its homomers; C), and  $\mathbf{T}\hat{\Gamma}$  to  $\overline{77}$  (and its homomers; D). These skeletons are referred to as being *RS*-stereoisomeric to one another under the action of the *RS*-stereoisomeric group  $\mathbf{T}_{d\tilde{\sigma}\hat{\Gamma}}$  (Eq. 40). The resulting diagram (Figure 15) is called *an elementary stereoisogram of numbered tetrahedral skeletons* [13]. Thus, a quadruplet of numbered tetrahedral skeletons is controlled by the *RS*-stereoisomeric group  $\mathbf{T}_{d\tilde{\sigma}\hat{\Gamma}}$  (Eq. 40).

#### 4.4.3. FIVE TYPES OF STEREOISOGRAMS

Because the subgroup  $\mathbf{T}$  is a normal subgroup of the *RS*-stereoisomeric group  $\mathbf{T}_{d\tilde{\sigma}\hat{\Gamma}}$ , the coset decomposition represented by Eq. 40 provides the following factor group [171]:

$$\mathbf{T}_{d\tilde{\sigma}\hat{\Gamma}}/\mathbf{T} = \{\mathbf{T}, \mathbf{T}\sigma, \mathbf{T}\tilde{\sigma}, \mathbf{T}\hat{\Gamma}\}, \quad (41)$$

which is isomorphic to Klein's four-group or the point group  $\mathbf{C}_{2v}$ . Because the numbered tetrahedral skeletons of the elementary stereoisogram (Figure 15) correspond to the respective cosets appearing in Eq. 41, a quadruplet of the numbered tetrahedral skeletons is found to be controlled by the factor group  $\mathbf{T}_{d\tilde{\sigma}\hat{\Gamma}}/\mathbf{T}$  (Eq. 41).

Just as Klein's four-group has five subgroups, the factor group  $\mathbf{T}_{d\tilde{\sigma}\hat{\Gamma}}/\mathbf{T}$  (Eq. 41) has the following five subgroups:

$$\text{Type I: } \mathbf{T}_i/\mathbf{T} \text{ (cf. Eq. 39)} \quad (42)$$

$$\text{Type II: } \mathbf{T}_{\bar{\sigma}}/\mathbf{T} \text{ (cf. Eq. 38)} \quad (43)$$

$$\text{Type III: } \mathbf{T}/\mathbf{T} \quad (44)$$

$$\text{Type IV: } \mathbf{T}_{d\bar{\sigma}i}/\mathbf{T} \text{ (cf. Eq. 40)} \quad (45)$$

$$\text{Type V: } \mathbf{T}_d/\mathbf{T} \text{ (cf. Eq. 37),} \quad (46)$$

which correspond to  $\mathbf{T}_{d\bar{\sigma}i}/\mathbf{T}$  (Eq. 40) itself and its maximum subgroups (Eqs. 37–39) as well as the common normal subgroup  $\mathbf{T}$ .

By placing a set of proligands to the four-positions of each tetrahedral skeleton of the elementary stereoisogram (Figure 15), there appear a *stereoisogram* containing a quadruplet of promolecules, where an equality symbol is placed in vertical, horizontal, or diagonal directions if two promolecules in each direction are identical with each other. Meanwhile, the global symmetry  $\mathbf{T}_{d\bar{\sigma}i}/\mathbf{T}$  (Eq. 41) is restricted to one of the five subgroups (Eqs. 42–46), which is assigned to the generated stereoisogram.

A set of proligands  $\text{ABp}^2$  is placed on the four positions of the skeleton **33** (Figure 15), so as to generate the promolecule **57** (Figure 14) as a reference promolecule. Thereby, there appears a stereoisogram shown in Figure 16. The stereoisogram belongs to type II, which is characterized by the presence of horizontal equality symbols. Such a type-II stereoisogram is determined to be chiral, *RS*-astereogenic, and scleral, so as to be denoted by the type index  $[-, a, -]$ . It should be noted that the quadruplet of promolecules (**57**,  $\overline{\mathbf{57}}$ ,  $\mathbf{57}'$  ( $= \mathbf{57}$ ), and  $\overline{\mathbf{57}'}$  ( $= \overline{\mathbf{57}}$ )) is regarded as one equivalence class of *RS*-stereoisomers, which is interpreted to be a pair of enantiomers (**57** and  $\overline{\mathbf{57}}$ ).

By placing a set of proligands  $\text{ABp}\bar{\text{p}}$  on the four positions of the skeleton **33** (Figure 15), the promolecule **48** (Figure 17) is generated as a reference promolecule. Thereby, there appears a stereoisogram shown in Figure 17. The stereoisogram belongs to type V, which is characterized by the presence of vertical equality symbols. Such a type-V stereoisogram is determined to be achiral, *RS*-stereogenic, and scleral, so as to be denoted by the type index  $[a, -, -]$ . It should be noted that the quadruplet of promolecules (**48**,  $\overline{\mathbf{48}}$  ( $= \mathbf{48}$ ), **49**, and  $\overline{\mathbf{49}}$  ( $= \mathbf{49}$ )) is regarded as one equivalence class of *RS*-stereoisomers, which is interpreted to be one pair of *RS*-diastereomers **48** and **49**. The achirality of **48** or **49** is assured by the vertical equality symbol, which indicates that **48** (or **49**) is self-enantiomeric.

A set of proligands  $\text{ABXY}$  is placed on the four positions of the skeleton **33** (Figure 15) so as to generate the promolecule **54** (Figure 18) as a reference promolecule. Thereby, there appears a stereoisogram shown in Figure 18. The stereoisogram belongs to type I, which is characterized by the presence of diagonal equality symbols. Such a type-I stereoisogram is determined to be chiral, *RS*-stereogenic, and ascleral, so as to be denoted by the type index  $[-, -, a]$ . It should be noted that the quadruplet of promolecules (**54**,  $\overline{\mathbf{54}}$ ,

$54'$  (=  $54$ ), and  $\overline{54}'$  (=  $54$ )) is regarded as one equivalence class of *RS*-stereoisomers, which is interpreted to be one pair of enantiomers  $54$  and  $\overline{54}$

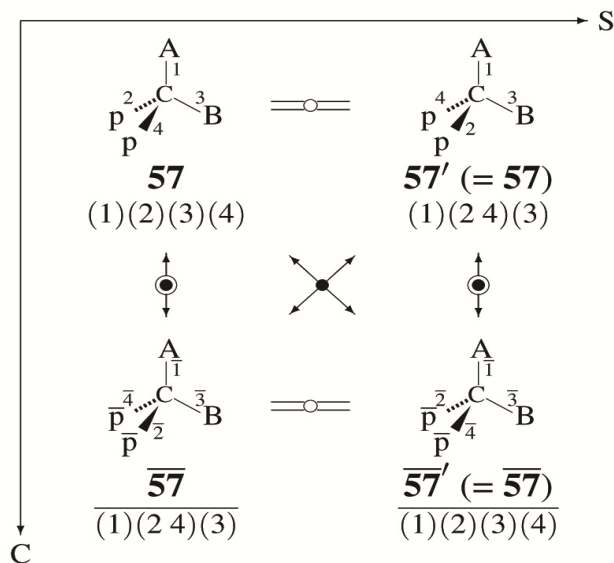


**Figure 16.** Stereoisogram of type II for characterizing a quadruplet of *RS*-stereoisomers with the composition  $ABp^2$  or  $AB\bar{p}^2$  on the basis of a tetrahedral skeleton. This stereoisogram contains one pair of enantiomers [172].

In addition, there appear type-III and type-IV stereoisograms as two extreme types of stereoisograms. A type-III stereoisogram characterized by the absence of equality symbols in all the directions, while a type-IV stereoisogram characterized by the presence of equality symbols in all the directions.

Figure 19 collects stereoisograms of five types, each of which represents a quadruplet of

*RS*-stereoisomers, where the symbols  $A$  and  $\bar{A}$  (or  $B$  and  $\bar{B}$ ) represent a pair of enantiomeric promolecules [12]. A type-III stereoisogram exhibits an extreme feature, in which the four *RS*-stereoisomers (i.e.,  $A, \bar{A}, B$  and  $\bar{B}$ ) are different from one another. A type-IV stereoisogram exhibits another extreme feature, in which the appears a degenerate *RS*-stereoisomer (i.e.,  $A$ )[10, 12].

The merits of stereoisograms have been discussed from a viewpoint of a new scheme for investigating geometric and stereoisomeric features [173]. Fujita's stereoisogram approach has been applied to allene derivatives [174], trigonal bipyramidal compounds [175, 176], prismane derivatives [177, 178], octahedral complexes [179, 180], and cubane derivatives [181].



To discuss local symmetries, the concept of *correlation diagrams of stereoisograms* has been proposed by Fujita [182, 183, 184]. Theory of organic stereoisomerism in harmony with molecular symmetry has been demonstrated [185].

It is worthwhile to mention discrimination between *RS*-stereoisomeric groups and stereoisomeric groups in assigning *E/Z*-descriptors to ethylene derivatives [186]. Such stereoisomeric groups are concerned with *extended stereoisogram sets* for characterizing *E/Z*-descriptors and *cis,trans*-isomerizations, the latter of which have been represented by a *radical space* in Fujita's ITS approach [58].

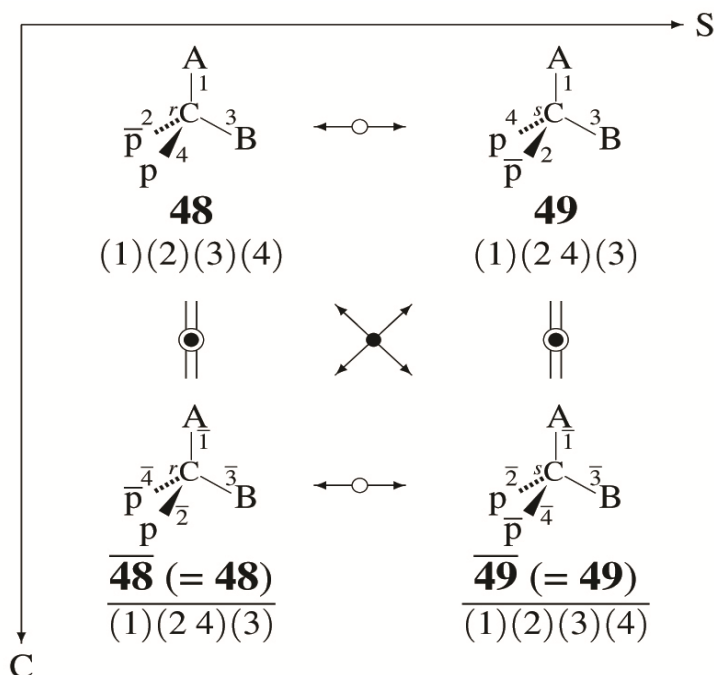


**Figure 17.** Stereoisogram of type V for characterizing a quadruplet of *RS*-stereoisomers with the composition  $ABp\bar{p}$  on the basis of a tetrahedral skeleton. This stereoisogram contains two achiral promolecules [172].

#### 4.4.4. NEW THEORETICAL FOUNDATIONS FOR R/S-DESCRIPTORS

A pair of *R/S*-descriptors of the Cahn-Ingold-Prelog (CIP) system [16, 17] has been used to specify a pair of enantiomers (e.g., a pair of **54** and  $\overline{\mathbf{54}}$ ; an asymmetric case) and a pair of diastereomers (**48** and **49**; a pseudoasymmetric case). The term ‘chirality’ has been originally used to rationalize the CIP system [16], so that the pairing of diastereomers (e.g., **48** and **49**) has not been supported by a sufficient theoretical foundation. The term ‘stereogenicity’ in place of the term ‘chirality’ has been later used to rationalize these conflicting cases [17] after the discussions by Mislow and Siegel [168]. However, the term

‘stereogenicity’ also covers *Z/E*-descriptors for specifying a diastereomeric relationship [187]. This usage of ‘stereogenicity’ in modern stereochemistry is misleading because chirality and stereogenicity are not clearly differentiated from each other. In particular, a pair of chirality/achirality is solely taken into consideration, so that the interaction between chirality and stereogenicity is underestimated or disregarded in modern stereochemistry.

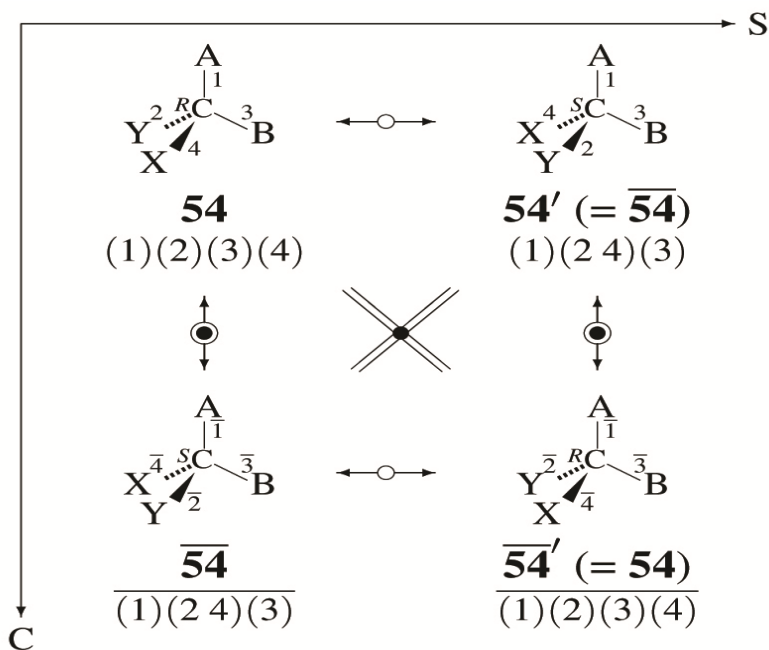
According to Fujita’s stereoisogram approach [10, 11, 12], in contrast, there appear three pairs of attributes (or three pairwise relationships): that is to say, a pair of chirality/achirality (enantiomeric and self-enantiomeric relationships in the vertical directions of a stereoisogram), a pair of *RS*-stereogenicity/*RS*-astereogenicity (*RS*-diastereomeric or self-*RS*-diastereomeric relationships in the horizontal direction), and a pair of sclerality/asclerality (holantimeric or selfholantimeric relationships in the diagonal direction).

An important conclusion of Fujita’s stereoisogram approach is that a pair of *R/S*-descriptors is originally assigned to a pair of *RS*-diastereomers, not to a pair of enantiomers, where an *RS*-diastereomeric relationship stems from *RS*-stereogenicity inherent in a stereoisogram of type I, type III, or type V (see Figure 19) [13, 188]. Three aspects of absolute configuration (the chiral aspect, the *RS*-stereogenic aspect, and the scleral aspect) have been pointed out on the basis of Fujita’s stereoisogram approach, so as to revise the conventional terminology based on a single chiral aspect of absolute configuration [189].

For example, a pair of *RS*-diastereomers **48** and **49** in the type-V stereoisogram (Figure 17) is specified by a pair of lowercase labels ‘*r*’ and ‘*s*’, where the priority sequence  $A > B > p > \bar{p}$  is presumed. This example clearly demonstrates that a pair of *R/S*-descriptors is assigned on the basis of the *RS*-stereogenic aspect, not on the basis of the chiral aspect of absolute configuration, because both **48** and **49** are achiral. Hence, the lowercase labels stems from the chirality-unfaithful nature [190].

Along the same line, a pair of *RS*-diastereomers **54** and **54'** ( $= \overline{\mathbf{54}}$ ) in the type-I stereoisogram (Figure 18) is specified by a pair of uppercase labels ‘*R*’ and ‘*S*’, where the priority sequence  $A > B > X > Y$  is presumed. Because the *RS*-diastereomeric relationship is coincident with the enantiomeric relationship in such a type-I stereoisogram, the pair of labels ‘*R*’ and ‘*S*’, which is originally assigned to the pair of *RS*-diastereomers **54** and **54'** (due to the *RS*-stereogenic aspect), is interpreted to be assigned to the pair of enantiomers **54** and  $\overline{\mathbf{54}}$  (due to the chiral aspect). Note that the uppercase labels stems from the chirality-faithful nature [190].

Misleading standpoints for *R/S*-descriptors of the CIP system have been rationally avoided by Fujita’s stereoisogram approach [14, 191]. Moreover, misleading classification of isomers and stereoisomers in organic chemistry has been discussed by emphasizing equivalence relationships and equivalence classes [192]. A recent book by Fujita [18] deals with the feasibility of Fujita’s stereoisogram approach in detail.

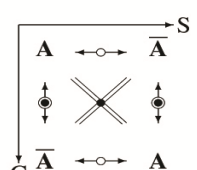
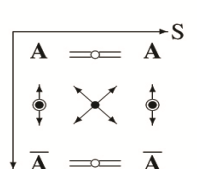
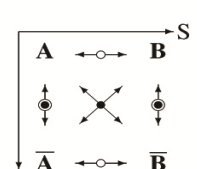
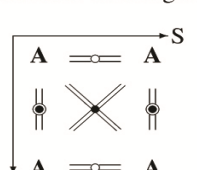
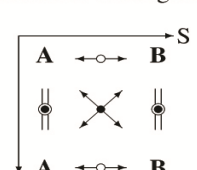


**Figure 18.** Stereoisogram of type I for characterizing a quadruplet of *RS*-stereoisomers with the composition ABXY on the basis of a tetrahedral skeleton. This stereoisogram contains one pair of enantiomers [172].

#### 4.4.5. PROCHIRALITY VS. PRO-*RS*-STEREOGENICITY

The formulation of Fujita's USCI approach teaches us that the term *prochirality* should be used in a purely geometrical fashion [89]. According to Fujita's stereoisogram approach, the concept of *pro-*RS*-stereogenicity* [193, 194] has been proposed to settle long-standing confusion on the term 'prochirality' of Hanson's definition [195].

As pointed out in recent articles [15, 196, 191], Hanson's definition of the term 'prochirality' for giving *pro-R/pro-S*-descriptors [195] should be abandoned. A pair of *pro-R/pro-S*-descriptors should be assigned on the basis of *pro-*RS*-stereogenicity* (not Hanson's 'prochirality'), just as a pair of *R/S*-descriptors should be assigned on the basis of *RS*-stereogenicity (not 'chirality' nor 'stereogenicity') [13, 14, 197].

		<i>RS</i> -astereogenic	<i>RS</i> -stereogenic
chiral			<p><b>Type I:</b> <math>[-, -, a]</math> chiral/<i>RS</i>-stereogenic/ascleral</p>  <p>two promolecules one pair of enantiomers one pair of <i>RS</i>-diastereomers two ascleral promolecules one quadruplet of <i>RS</i>-stereoisomers</p>
		<p><b>Type II:</b> <math>[-, a, -]</math> chiral/<i>RS</i>-astereogenic/scleral</p>  <p>two promolecules one pair of enantiomers two <i>RS</i>-astereogenic promolecules one pair of holantimers one quadruplet of <i>RS</i>-stereoisomers</p>	<p><b>Type III:</b> <math>[-, -, -]</math> chiral/<i>RS</i>-stereogenic/scleral</p>  <p>four promolecules two pairs of enantiomers two pairs of <i>RS</i>-diastereomers two pairs of holantimers one quadruplet of <i>RS</i>-stereoisomers</p>
achiral		<p><b>Type IV:</b> <math>[a, a, a]</math> achiral/<i>RS</i>-astereogenic/ascleral</p>  <p>one promolecule one achiral promolecule one <i>RS</i>-astereogenic promolecule one ascleral promolecule one quadruplet of <i>RS</i>-stereoisomers</p>	<p><b>Type V:</b> <math>[a, -, -]</math> achiral/<i>RS</i>-stereogenic/scleral</p>  <p>two promolecules two achiral promolecules one pair of <i>RS</i>-diastereomers one pair of holantimers one quadruplet of <i>RS</i>-stereoisomers</p>

**Figure 19.** Stereoisograms for representing *RS*-stereoisomers of five types [12]. The symbols **A** and  $\bar{\mathbf{A}}$  (or **B** and  $\bar{\mathbf{B}}$ ) represent a pair of enantiomers. Each stereoisogram consists of a quadruplet of *RS*-stereoisomers, which may coalesce with one another according to either one of the five *RS*-stereoisomeric types.

Substitution criteria based on stereoisograms have been proposed to determine prochirality and pro-*RS*-Stereogenicity [198]. The term *RS-diastereotopic relationship* has been coined to specify *pro-R/pro-S*-descriptors [199]. The term ‘stereoheterotopic relationship’ [200] should be abandoned because it connotes ‘enantiotopic’ (due to chirality) and ‘diastereotopic’ (due to stereogenicity) which are conceptually different.

The merits of Fujita’s stereoisogram approach in discussions on prochirality vs. pro-*RS*-stereogenicity have been demonstrated by recent articles [15, 201, 202].

#### 4.4.6. ENUMERATION OF INEQUIVALENT QUADRUPLETS OF *RS*-STEREISOMERS

The FPM method and the PCI method supported by Fujita’s USCI approach have been extended to meet the requirements of Fujita’s stereoisogram approach [203, 204].

The symmetry-itemized enumeration of quadruplets of *RS*-stereoisomers based on a tetrahedral skeleton **33** has been conducted by an extended FPM method [203] or by an extended PCI method [204] under the action of the *RS*-stereoisomeric group  $\mathbf{T}_{d\tilde{\sigma}\hat{i}}$ . This *RS*-stereoisomeric group has 33 subgroups up to conjugacy to provide a non-redundant set of subgroups (SSG):

$$\begin{aligned} \text{SSG}_{\mathbf{T}_{d\tilde{\sigma}\hat{i}}} = & \left\{ \begin{array}{cccccccccccc} 1 & 2 & 3 & 4 & 5 & 6 & 7 & 8 & 9 & 10 \\ \mathbf{C}_1, \mathbf{C}_2, \mathbf{C}_{\hat{\sigma}}, \mathbf{C}_{\tilde{\sigma}}, \mathbf{C}_S, \mathbf{C}_{\hat{i}}, \mathbf{C}_3, \mathbf{S}_{\tilde{4}}, \mathbf{S}_4, \mathbf{D}_2, \\ 11 & 12 & 13 & 14 & 15 & 16 & 17 & 18 \\ \mathbf{C}_{2\tilde{\sigma}}, \mathbf{C}_{2\hat{\sigma}}, \mathbf{C}_{2\nu}, \mathbf{C}_S\tilde{\sigma}\hat{\sigma}, \mathbf{C}_{2\hat{i}}, \mathbf{C}_S\tilde{\sigma}\hat{\sigma}, \mathbf{C}_{3\tilde{\sigma}}, \mathbf{C}_{3\nu}, \\ 19 & 20 & 21 & 22 & 23 & 24 & 25 & 26 \\ \mathbf{C}_{3\hat{i}}, \mathbf{D}_{2\tilde{\sigma}}, \mathbf{S}_{\tilde{4}\hat{\sigma}}, \mathbf{S}_{\tilde{4}\hat{i}}, \mathbf{D}_{2d}, \mathbf{S}_{4\tilde{\sigma}\hat{\sigma}}, \mathbf{D}_{2\hat{i}}, \mathbf{C}_{2\nu}\tilde{\sigma}\hat{i}, \\ 27 & 28 & 29 & 30 & 31 & 32 & 33 \\ \mathbf{T}, \mathbf{C}_{3d}\tilde{\sigma}\hat{i}, \mathbf{C}_{3\nu}\tilde{\sigma}\hat{i}, \mathbf{D}_{2d}\tilde{\sigma}\hat{i}, \mathbf{T}_{\tilde{\sigma}}, \mathbf{T}_{\hat{i}}, \mathbf{T}_d, \mathbf{T}_{d\tilde{\sigma}\hat{i}} \end{array} \right\} \end{aligned} \quad (47)$$

where the subgroups are aligned in the ascending order of their orders.

The four positions of **33** belongs to an orbit governed by the coset representation the  $\mathbf{T}_{d\tilde{\sigma}\hat{i}}(/C_{3\nu\tilde{\sigma}\hat{i}})$ , degree of which is calculated to be  $|\mathbf{T}_{d\tilde{\sigma}\hat{i}}|(|C_{3\nu\tilde{\sigma}\hat{i}}|)=48/12=4$ . The subduction of  $\mathbf{T}_{d\tilde{\sigma}\hat{i}}(/C_{3\nu\tilde{\sigma}\hat{i}})$ , can be conducted in an extended fashion, so as to generate USCI-CFs under the *RS*-stereoisomeric group  $\mathbf{T}_{d\tilde{\sigma}\hat{i}}$

The fixed-point matrix (FPM) method of the USCI approach is applied to the extended USCI-CFs. Thereby, the numbers of quadruplets are calculated in an itemized fashion with respect to the subgroups of  $\mathbf{T}_{d\tilde{\sigma}\hat{i}}$ , where they are given in a matrix (tabular) form [203]. In a parallel way, the PCI method of the USCI approach is applied to the extended USCI-CFs. Thereby, the numbers of quadruplets are calculated in an itemized

fashion with respect to the subgroups of  $\mathbf{T}_{d\bar{\sigma}\hat{i}}$ , where they are given in the form of generating functions [204]. Several generating functions are cited as follows (Eqs. 44–48 of Ref. [204]):

$$f_{C_1} \stackrel{\text{I}}{=} \left\{ \frac{1}{2} (\text{ABXp} + \text{ABX}\bar{\text{p}}) + \dots \right\} + \left\{ \frac{1}{2} (\text{ABpq} + \text{AB}\bar{\text{p}}\bar{\text{q}}) + \dots \right\} \\ + \left\{ \frac{1}{2} (\text{Ap}\bar{\text{p}}\text{q} + \text{App}\bar{\text{q}}) + \dots \right\} + \left\{ \frac{1}{2} (\text{Apqr} + \text{Ap}\bar{\text{q}}\bar{\text{r}}) + \dots \right\} \\ + \left\{ \frac{1}{2} (\text{pqrs} + \text{p}\bar{\text{q}}\bar{\text{r}}\bar{\text{s}}) + \dots \right\} + \left\{ \frac{1}{2} (\text{p}\bar{\text{p}}\text{qr} + \text{p}\bar{\text{p}}\bar{\text{q}}\bar{\text{r}}) + \dots \right\} \quad (48)$$

$$f_{C_{\bar{\sigma}}} \stackrel{\text{II}}{=} \left\{ \frac{1}{2} (\text{A}^2\text{Bp} + \text{A}^2\text{B}\bar{\text{p}}) + \dots \right\} + \left\{ \frac{1}{2} (\text{ABp}^2 + \text{AB}\bar{\text{p}}^2) + \dots \right\} \\ + \left\{ \frac{1}{2} (\text{A}^2\text{pq} + \text{A}^2\bar{\text{p}}\bar{\text{q}}) + \dots \right\} + \left\{ \frac{1}{2} (\text{Ap}^2\bar{\text{p}} + \text{Ap}\bar{\text{p}}^2) + \dots \right\} \\ + \left\{ \frac{1}{2} (\text{Ap}^2\text{q} + \text{A}\bar{\text{p}}^2\bar{\text{q}}) + \dots \right\} + \left\{ \frac{1}{2} (\text{p}^2\bar{\text{p}}\text{q} + \text{p}\bar{\text{p}}^2\bar{\text{q}}) + \dots \right\} \\ + \left\{ \frac{1}{2} (\text{p}^2\text{q}\bar{\text{q}} + \bar{\text{p}}^2\text{q}\bar{\text{q}}) + \dots \right\} + \left\{ \frac{1}{2} (\text{p}^2\text{qr} + \bar{\text{p}}^2\bar{\text{q}}\bar{\text{r}}) + \dots \right\} \quad (49)$$

$$f_{C_{\hat{\sigma}}} \stackrel{\text{III}}{=} \{ \text{p}\bar{\text{p}}\text{q}\bar{\text{q}} + \text{p}\bar{\text{p}}\text{r}\bar{\text{r}} + \dots \} \quad (50)$$

$$f_{C_s} \stackrel{\text{IV}}{=} \{ \text{ABp}\bar{\text{p}} + \text{ABq}\bar{\text{q}} + \dots \} \quad (51)$$

$$f_{C_{\hat{i}}} \stackrel{\text{V}}{=} \text{ABXY} \quad (52)$$

(omitted)

The term  $1/2(\text{ABp}^2 + \text{AB}\bar{\text{p}}^2)$  in  $f_{C_{\bar{\sigma}}}$  (Eq. 49) indicates that the quadruplet of *RS* stereoisomers shown in the type-II stereoisogram (Figure 16) is counted once under the *RS*-stereoisomeric group  $\mathbf{T}_{d\bar{\sigma}\hat{i}}$ . Note that this quadruplet contains one pair of enantiomers **57** and  $\bar{\mathbf{57}}$ . Compare this enumeration with the term  $1/2(\text{ABp}^2 + \text{AB}\bar{\text{p}}^2)$  in  $f_{C_s}$  (Eq. 26) obtained under the point group  $\mathbf{T}_d$ . See also the enumeration under the point group  $\mathbf{T}_d$  (Figure 14(a)) and the enumeration under the permutation group  $\mathbf{S}^{[4]}$  (Figure 14(b)).

The term  $\text{ABp}\bar{\text{p}}$  in  $f_{C_s}$  (Eq. 51) indicates that the quadruplet of *RS*-stereoisomers shown in the type-V stereoisogram (Figure 17) is counted once under the *RS*-stereoisomeric group  $\mathbf{T}_{d\bar{\sigma}\hat{i}}$ . Compare this enumeration with the term  $2\text{ABp}\bar{\text{p}}$  in  $f_{C_s}$  (Eq. 28) obtained

under the point group  $T_d$ . Note that the quadruplet of Figure 17 contains two achiral promolecules **48** and **49**. See also the enumeration under the permutation group  $S^{[4]}$  (Figure 14(b)), where **48** and **49** are recognized to be a pair of *RS*-diastereomers.

Symmetry-Itemized enumeration of inequivalent quadruplets of *RS*-stereoisomers have been applied to an allene skeleton [205, 206] and an oxirane skeleton [207, 208, 209].

Group hierarchy for stereoskeletons of ligancy 4 has been examined [172], where Fujita's stereoisogram approach is combined with Fujita's proligand method.

Because symmetry-itemized enumerations require mark tables and subduction tables which are not always available, simpler methods are desirable in order to grasp succinct features of *RS*-stereoisomers. As such simpler methods, type-itemized enumerations of quadruplets of *RS*-stereoisomers have been reported [170, 210]. More systematic methods which combine Fujita's proligand method with Fujita's stereoisogram approach have been recently reported as on-line first articles [211, 212].

## 5. CONCLUSIONS OF MY HALF-CENTURY JOURNEY

### 5.1. CREATION OF NEW CONCEPTS

My half-century journey has created several new concepts, which are linked with appropriate diagrammatic expressions: e.g., the concept of ITSs which supports Fujita's ITS approach for discussing organic reactions, the concept of sphericities of orbits which supports Fujita's USCI approach for discussing geometric features of stereochemistry, the concept of sphericities of cycles which supports Fujita's proligand method for discussing gross enumeration and recursive enumeration, and the concept of stereoisograms which supports Fujita's stereoisogram approach for discussing stereoisomeric features of stereochemistry.

As a milestone of my journey, these concepts have been demonstrated comprehensively in my recent book entitled "mathematical stereochemistry" [18], which will provide reliable mathematical foundations for further investigation of stereochemistry.

### 5.2. INTEGRATION OF VAN'T HOFF'S WAY AND LE BEL'S WAY

Modern stereochemistry suffers from conceptual faults and misleading terminology brought about by the lack of reliable mathematical formulations.

1. The conceptual faults stem from the different ways taken by van't Hoff (asymmetry, stereogenicity) [19, 20] and Le Bel (dissymmetry, chirality) [21, 22] at the beginning of stereochemistry and have been continuous sources of confusion over 140 years.

2. Modern stereochemistry lays stress on van't Hoff's way and treats inconsistent cases due to Le Bel's way as exceptions (e.g., pseudoasymmetry). This course of remedy without reliable mathematical formulations is rather ad hoc so as to bring about the misleading terminology to stereoisomerism, the Cahn-Ingold-Prelog system, the *pro-R/pro-S* system and so on.

Fujita's USCI approach emphasizes point groups for the purpose of investigating geometrical features of organic compounds, where point groups are definitely distinguished from permutation groups by developing the concept of sphericities. As found in the enumeration of Fujita's USCI approach, the concept of sphericities provides the distinction between Le Bel's way and van't Hoff's way, because the former is related to point groups (dissymmetry, chirality), while the latter is related to permutation groups (asymmetry, stereogenicity).

Fujita's stereoisogram approach integrates point groups and permutation groups to create *RS*-stereoisomeric groups, after permutation groups are restricted to *RS*-permutation groups and after ligand-reflection groups are created as a new category of groups. Stereoisograms have been developed as diagrammatic expressions of *RS*-stereoisomeric groups. A quadruplet of *RS*-stereoisomers in each stereoisogram is *an intermediate concept for mediating between enantiomers and stereoisomers*. Thereby, van't Hoff's way and Le Bel's way are integrated to reach Aufheben, where *the vertical direction of a stereoisogram is concerned with the chiral aspect for supporting Le Bel's way and the horizontal direction of a stereoisogram is concerned with the RS-stereogenic aspect for supporting van't Hoff's way*. The key for the Aufheben is the diagonal direction of a stereoisogram for characterizing the scleral aspect, which has been hidden behind the confusion over 140 years in modern stereochemistry. As a result, the concept of *RS*-stereoisomers based on stereoisograms provides us with rational theoretical foundations for remedying the conceptual faults and misleading terminology of modern stereochemistry.

### 5.3. PARADIGM SHIFT PROVIDED BY FUJITA'S STEREOISOGRAM APPROACH

The concept of *RS*-stereoisomers as an intermediate concept brings about a paradigm shift, so that modern stereochemistry will be restructured substantially on the basis of mathematical formulations. This fact is parallel to the historical event that Avogadro's theory has brought about a paradigm shift in chemistry by creating the intermediate concept of *molecule* (e.g., H<sub>2</sub>O), which mediates between atoms (e.g., hydrogen atoms and oxygen atoms) and substances (e.g., water). This means that classical descriptions of textbooks on organic chemistry and on stereochemistry should be thoroughly revised in conceptually deeper levels, but not in superficial verbal levels.



## REFERENCES

1. H. Nozaki, S. Fujita, H. Takaya, and R. Noyori, Photochemical reaction of ethyl azidoformate with cyclic ethers and acetals, *Tetrahedron* **23** (1967) 45–49.
2. H. Nozaki, H. Takaya, S. Moriuchi, and R. Noyori, Homogeneous catalysis in the decomposition of diazo compounds by copper chelates: Asymmetric carbenoid reactions, *Tetrahedron* **24** (1968) 3655–3669.
3. R. Noyori. Asymmetric catalysis: Science and opportunities (Nobel lecture, December 8, 2001); <http://www.nobelprize.org/nobelprizes/chemistry/laureates/2001/noyorilecture.html>.
4. S. Fujita, *Organic Chemistry of Photography*, Springer-Verlag, Berlin-Heidelberg, 2004.
5. S. Fujita, *Computer-Oriented Representation of Organic Reactions*, Yoshioka-Shoten, Kyoto, 2001.
6. S. Fujita, *Symmetry and Combinatorial Enumeration in Chemistry*, Springer-Verlag, Berlin-Heidelberg, 1991.
7. S. Fujita, *Diagrammatical Approach to Molecular Symmetry and Enumeration of Stereoisomers*, University of Kragujevac, Faculty of Science, Kragujevac, 2007.
8. G. Pólya and R. C. Read, *Combinatorial Enumeration of Groups, Graphs, and Chemical Compounds*, Springer-Verlag, New York, 1987.
9. S. Fujita, *Combinatorial Enumeration of Graphs, Three-Dimensional Structures, and Chemical Compounds*, University of Kragujevac, Faculty of Science, Kragujevac, 2013.
10. S. Fujita, Stereogenicity revisited. Proposal of holantimers for comprehending the relationship between stereogenicity and chirality, *J. Org. Chem.* **69** (2004) 3158–3165.
11. S. Fujita, Integrated discussion on stereogenicity and chirality for restructuring stereochemistry, *J. Math. Chem.* **35** (2004) 265–287.
12. S. Fujita, Pseudoasymmetry, stereogenicity, and the *RS*-nomenclature comprehended by the concepts of holantimers and stereoisograms, *Tetrahedron* **60** (2004) 11629–11638.
13. S. Fujita, Stereoisograms for reorganizing the theoretical foundations of stereochemistry and stereoisomerism: I. Diagrammatic representations of *RS*-stereoisomeric groups for integrating point groups and *RS*-permutation groups, *Tetrahedron: Asymmetry* **25** (2014) 1153–1168.
14. S. Fujita, Stereoisograms for reorganizing the theoretical foundations of stereochemistry and stereoisomerism: II. Rational avoidance of misleading

- standpoints for *R/S*-stereodescriptors of the Cahn-Ingold-Prelog system, *Tetrahedron: Asymmetry* **25** (2014) 1169–1189.
15. S. Fujita, Stereoisograms for reorganizing the theoretical foundations of stereochemistry and stereoisomerism: III. Rational avoidance of misleading standpoints for *Pro-R/Pro-S*-descriptors, *Tetrahedron: Asymmetry* **25** (2014) 1190–1204.
  16. R. S. Cahn, C. K. Ingold, and V. Prelog, Specification of molecular chirality, *Angew. Chem. Int. Ed. Eng.* **5** (1966) 385–415.
  17. V. Prelog and G. Helmchen, Basic principles of the CIP-system and proposal for a revision, *Angew. Chem. Int. Ed. Eng.* **21** (1982) 567–583.
  18. S. Fujita, *Mathematical Stereochemistry*, De Gruyter, Berlin, 2015.
  19. J. H. van't Hoff, *La Chimie Dans L'Espace*, P. M. Bazendijk, Rotterdam, 1875.
  20. J. H. van't Hoff, *Die Lagerung der Atome im Raume*, (German Translation by F. Herrmann), Friedrich Vieweg und Sohn, Braunschweig, 1877.
  21. J. A. Le Bel, Sur les relations qui existent entre les formules atomiques des corps organiques et le pouvoir rotatoire de leurs dissolutions, *Bull. Soc. Chim. Fr. (2)* **22** (1874) 337–347.
  22. J. A. Le Bel, On the Relations Which Exist Between the Atomic Formulas of Organic Compounds and the Rotatory Power of Their Solutions, In *Classics in the Theory of Chemical Combination (Classics of Science, Vol. I)*; O. T. Benfey, Ed., Dover: New York, 1963; pp 161–171.
  23. H. Nozaki, Y. Okuyama, and S. Fujita, Addition of carbethoxynitrene to *trans*- and *cis*-propenylbenzene, *Can. J. Chem.* **46** (1968) 3332–3336.
  24. S. Fujita and H. Nozaki, Reactions of nitrenes (in Japanese), In *Reactive Intermediates (I) (Hannosei Chukantai in Japanese)*; K. Ichikawa, T. Saegusa, H. Tsubomura, H. Nozaki, and I. Moria, Eds., Kagaku Dojin: Kyoto, 1971; Chapter 5, pp 107–136.
  25. S. Fujita, Nitrenes (in Japanese), In *Carbenes, Ylides, Nitrenes, and Benzynes*; T. Goto, Ed., Hirokawa: Tokyo, 1976; Chapter 3, pp 263–339.
  26. S. Fujita, T. Hiyama, and H. Nozaki, Steric course in oxidative ring opening of aziridine-1-carboxylates with dimethyl sulfoxide, *Tetrahedron Lett.* (1969) 1677–1678.
  27. S. Fujita, T. Hiyama, and H. Nozaki, Oxidative ring-opening of aziridine-1-carboxylates with sulfoxides, *Tetrahedron* **26** (1970) 4347–4352.
  28. S. Fujita, K. Imamura, and H. Nozaki, The absolute configuration of 2-phenylaziridine and its derivatives, *Bull. Chem. Soc. Jpn.* **44** (1971) 1975–1977.
  29. H. Nozaki, S. Fujita, and T. Mori, [7](2,6)Pyridinophane and [7](2,6)pyrylophanium perchlorate, *Bull. Chem. Soc. Jpn.* **42** (1969) 1163.

30. S. Fujita and H. Nozaki, Synthesis and conformational studies of [7](2,6)pyridinophanes, *Bull. Chem. Soc. Jpn.* **44** (1971) 2827–2833.
31. S. Fujita and H. Nozaki, Heterophanes. syntheses and structures (review), *Yuki Gosei Kagaku Kyokai-Shi/J. Synth. Org. Chem. Jpn.* **30** (1972) 679–693.
32. S. Fujita, S. Hirano, and H. Nozaki, [7]Metacyclophane and its 13-bromo derivative, *Tetrahedron Lett.* (1972) 403–406.
33. S. Hirano, T. Hiyama, S. Fujita, and H. Nozaki, [6]Metacyclophane and the related compounds, *Chem. Lett.* (1972) 707–708.
34. S. Hirano, H. Hara, T. Hiyama, S. Fujita, and H. Nozaki, Synthetic and structural studies of [6]-, [7]-, and [10]metacyclophanes, *Tetrahedron* **31** (1975) 2219–2227.
35. S. Fujita, Organic compounds for instant photography, *Yuki Gosei Kagaku Kyokai-Shi/J. Synth. Org. Chem. Jpn.* **39** (1981) 331–344.
36. S. Fujita, Image-providing compounds for instant color photography. Their syntheses and characteristics as functionalized dyes, *Yuki Gosei Kagaku Kyokai-Shi/J. Synth. Org. Chem. Jpn.* **40** (1982) 176–187.
37. S. Fujita, Regiospecific attack of methoxide ion on 4-alkoxy-o-quinone imines. a novel route to p-quinone monoacetals, *J. Chem. Soc., Chem. Commun.* (1981) 425–426.
38. S. Fujita, Synthesis and reactions of o-benzoquinone monosulfonimides, *J. Org. Chem.* **48** (1983) 177–183.
39. S. Fujita, K. Koyama, Y. Inagaki, and K. Waki, US Patent 4336322, 1982; Color Photographic Light-Sensitive Material.
40. S. Fujita, H. Hayashi, Y. Y. Shigetoshi Ono, and T. Harada, US Patent 4268625, 1981; Photographic Light-Sensitive Element for the Color Diffusion Transfer Process.
41. S. Fujita, K. Koyama, and S. Ono, Dye releasers for instant color photography. Molecular design and synthetic design, *Nippon Kagaku Kai-Shi* (1991) 1–22.
42. S. Fujita, K. Koyama, and S. Ono, Dye releasers for instant color photography, *Rev. Heteroatom Chem.* **7** (1992) 229–267.
43. S. Fujita, T. Harada, and Y. Yoshida, US Patent 4268624, 1981; Photographic Light-Sensitive Sheet for the Color Diffusion Transfer Process.
44. S. Fujita, K. Koyama, and S. Ono, R&D of dye releasers for Fuji instant color system (FOTORAMA), *Nikkakyo Geppo* (11) (1982) 29–39.
45. S. Fujita, R&D of dye releasers for instant color photography: Design, evaluation, and synthesis, In *Organic Synthesis in Japan, Past, Present, and Future*; R. Noyori, Ed., Tokyo Kagaku Dojin: Tokyo, 1992; pp 89–96.
46. S. Fujita, Description of organic reactions based on imaginary transition structures.  
1. Introduction of new concepts, *J. Chem. Inf. Comput. Sci.* **26** (1986) 205–212.

47. S. Fujita, Description of organic reactions based on imaginary transition structures. 8. Synthesis space attached by a charge space and three-dimensional imaginary transition structures with charges, *J. Chem. Inf. Comput. Sci.* **27** (1987) 111–115.
48. S. Fujita, Description of organic reactions based on imaginary transition structures. 5. Recombination of reaction strings in a synthesis space and its application to the description of synthetic pathways, *J. Chem. Inf. Comput. Sci.* **26** (1986) 238–242.
49. S. Fujita, Description of organic reactions based on imaginary transition structures. 2. Classification of one-string reactions having an even-membered cyclic reaction graph, *J. Chem. Inf. Comput. Sci.* **26** (1986) 212–223.
50. S. Fujita, Description of organic reactions based on imaginary transition structures. 3. Classification of one-string reactions having an odd-membered cyclic reaction graph, *J. Chem. Inf. Comput. Sci.* **26** (1986) 224–230.
51. S. Fujita, Description of organic reactions based on imaginary transition structures. 6. Classification and enumeration of two-string reactions with one common node, *J. Chem. Inf. Comput. Sci.* **27** (1987) 99–104.
52. S. Fujita, Description of organic reactions based on imaginary transition structures. 7. Classification and enumeration of two-string reactions with two or more common nodes, *J. Chem. Inf. Comput. Sci.* **27** (1987) 104–110.
53. S. Fujita, Description of organic reactions based on imaginary transition structures. 4. Three-nodal and four-nodal subgraphs for a systematic classification of reactions, *J. Chem. Inf. Comput. Sci.* **26** (1986) 231–237.
54. S. Fujita, A novel approach to systematic classification of organic reactions. Hierarchical subgraphs of imaginary transition structures, *J. Chem. Soc. Perkin II* (1988) 597–616.
55. S. Fujita, Description of organic reactions based on imaginary transition structures. 9. Single-access perception of rearrangement reactions, *J. Chem. Inf. Comput. Sci.* **27** (1987) 115–120.
56. S. Fujita, Logical perception of ring-opening, ring-closure, and rearrangement reactions based on imaginary transition structures. Selection of the essential set of essential rings (ESER), *J. Chem. Inf. Comput. Sci.* **28** (1988) 1–9.
57. S. Fujita, A new algorithm for selection of synthetically important rings. The essential set of essential set of essential rings (ESER) for organic structures, *J. Chem. Inf. Comput. Sci.* **28** (1988) 78–82.
58. S. Fujita, Canonical numbering and coding of imaginary transition structures. A novel approach to the linear coding of individual organic reactions, *J. Chem. Inf. Comput. Sci.* **28** (1988) 128–137.
59. S. Fujita, Canonical numbering and coding of reaction-center graphs and reduced reaction-center graphs abstracted from imaginary transition structures. A novel

- approach to the linear coding of reaction types, *J. Chem. Inf. Comput. Sci.* **28** (1988) 137–142.
60. G. Pólya, Kombinatorische Anzahlbestimmungen für Gruppen, Graphen und chemische Verbindungen, *Acta Math.* **68** (1937) 145–254.
  61. S. Fujita, Enumeration of organic reactions by counting substructures of imaginary transition structures. Importance of orbits governed by coset representations, *J. Math. Chem.* **7** (1991) 111–133.
  62. S. Fujita, A novel approach to the enumeration of reaction types by counting reactioncenter graphs which appear as the substructures of imaginary transition structures, *Bull. Chem. Soc. Jpn.* **61** (1988) 4189–4206.
  63. S. Fujita, The description of organic reactions, *Yuki Gosei Kagaku Kyokai-Shi/J. Synth. Org. Chem. Jpn.* **44** (1986) 354–364.
  64. S. Fujita, “Structure-reaction type” paradigm in the conventional methods of describing organic reactions and the concept of imaginary transition structures overcoming this paradigm, *J. Chem. Inf. Comput. Sci.* **27** (1987) 120–126.
  65. S. Fujita, Imaginary transition structures. A novel approach to computer-oriented representation of organic reactions, *Yuki Gosei Kagaku Kyokai-Shi/J. Synth. Org. Chem. Jpn.* **47** (1989) 396–412.
  66. S. Fujita, Graphic characterization and taxonomy of organic reactions, *J. Chem. Educ.* **67** (1990) 290–293.
  67. S. Fujita, S. Hanai, M. Miyakawa, M. Takeuchi, S. Nakayama, and T. Yasuda, The FORTUNITS system for retrieving organic reactions based on imaginary transition structures, In *Computer Aided Innovation of New Materials II, Part 2*; M. Doyama, K. J. M. Tanaka, and R. Yamamoto, Eds., Elsevier: Amsterdam, 1993; pp 967–972.
  68. S. Fujita, FORTUNITS—Development of reaction database based on imaginary transition structures, *CICSJ Bulletin* **12** (1994) 9–12.
  69. S. Fujita, Typesetting structural formulae with the text formatter TEX/LATEX, *Comput. Chem.* **18** (1994) 109–116.
  70. S. Fujita, XYMTEX for drawing chemical structural formulas, *TUGboat* **16** (1) (1995) 80–88.
  71. S. Fujita, Size reduction of chemical structural formulas in XYMTEX (version 3.00), *TUGboat* **22** (4) (2001) 285–289.
  72. S. Fujita, Development of XYMTEX2PS for PostScript typesetting of chemical documents containing structural formulas, *J. Comput. Chem. Jpn.* **4** (2005) 69–78.
  73. S. Fujita, *XYMTEX—Typesetting Chemical Structural Formulas*, Addison-Wesley Japan, Tokyo, 1997.
  74. S. Fujita, *XYMTEX: Reliable Tool for Drawing Chemical Structural Formulas*, On-line Manual, <http://xymtex.com/fujitas3/xymtex/xym501/manual/xymtex-manualPS.pdf>, 2013.

75. S. Fujita, N. Tanaka, XYM notations for electronic communication of organic chemical structures, *J. Chem. Inf. Comput. Sci.* **39** (1999) 903–914.
76. S. Fujita, N. Tanaka, XYM markup language (XYMML) for electronic communication of chemical documents containing structural formulas and reaction schemes, *J. Chem. Inf. Comput. Sci.* **39** (1999) 915–927.
77. S. Fujita, N. Tanaka, XYMTEX (version 2.00) as implementation of the XYM notation and XYM markup language, *TUGboat* **21** (1) (2000) 7–14.
78. N. Tanaka, S. Fujita, XYMJava system for world wide web communication of organic chemical structures, *J. Computer Aided Chem.* **3** (2002) 37–47.
79. N. Tanaka, T. Ishimaru, S. Fujita, WWW (world wide web) communication and publishing of structural formulas by XYMML (XYM markup language)", *J. Computer Aided Chem.* **3** (2002) 81–89.
80. S. Fujita, Articles, books, and internet documents with structural formulas drawn by XYMTEX — Writing, submission, publication, and internet communication in chemistry, *Asian J. TEX* **3** (2009) 89–108.
81. S. Fujita, The XYMTEX system for publishing interdisciplinary chemistry/mathematics books, *TUGboat* **34** (3) (2013) 325–328.
82. F. A. Cotton, *Chemical Applications of Group Theory*, Wiley-International, New York, 1971.
83. E. L. Eliel and S. H. Wilen, *Stereochemistry of Organic Compounds*, John Wiley & Sons, New York, 1994.
84. K. Mislow and M. Raban, Stereoisomeric relationships of groups in molecules, *Top. Stereochem.* **1** (1967) 1–38.
85. H. Hirschmann, Stereoheterotopism and prochirality, *Trans. N. Y. Acad. Sci. Ser. II* **41** (1983) 61–69.
86. S. Fujita, Sphericity governs both stereochemistry in a molecule and stereoisomerism among molecules, *Chem. Rec.* **2** (2002) 164–176.
87. S. Fujita, Sphericity beyond topicity in characterizing stereochemical phenomena. Novel concepts based on coset representations and their subductions, *Bull. Chem. Soc. Jpn.* **75** (2002) 1863–1883.
88. S. Fujita, Promolecules for characterizing stereochemical relationships in non-rigid molecules, *Tetrahedron* **47** (1991) 31–46.
89. S. Fujita, Chirality fittingness of an orbit governed by a coset representation. Integration of point-group and permutation-group theories to treat local chirality and prochirality, *J. Am. Chem. Soc.* **112** (1990) 3390–3397.
90. S. Fujita, Enantiomeric and diastereomeric relationships of ethylene derivatives. Restructuring stereochemistry by a group-theoretical and combinatorial approach, *J. Math. Chem.* **32** (2002) 1–17.

91. S. Fujita, Systematic classification of molecular symmetry by subductions of coset representations, *Bull. Chem. Soc. Jpn.* **63** (1990) 315–327.
92. S. Fujita, Subduction of coset representations. An application to enumeration of chemical structures, *Theor. Chim. Acta* **76** (1989) 247–268.
93. S. Fujita, Stereochemistry and stereoisomerism characterized by the sphericity concept, *Bull. Chem. Soc. Jpn.* **74** (2001) 1585–1603.
94. S. Fujita, Point groups based on methane and adamantane ( $T_d$ ) skeletons, *J. Chem. Educ.* **63** (1986) 744–746.
95. S. Fujita, Subductive and inductive derivation for designing molecules of high symmetry, *J. Chem. Inf. Comput. Sci.* **31** (1991) 540–546.
96. S. Fujita, Systematic design of chiral molecules of high symmetry. Achiral skeletons substituted with chiral ligands, *Bull. Chem. Soc. Jpn.* **73** (2000) 2679–2685.
97. S. Fujita, Desymmetrization of achiral skeletons by mono-substitution. Its characterization by subduction of coset representations, *Bull. Chem. Soc. Jpn.* **74** (2001) 1015–1020.
98. S. Fujita, Chirality and stereogenicity for square-planar complexes, *Helv. Chim. Acta* **85** (2002) 2440–2457.
99. S. Fujita, The SCR notation for systematic classification of molecular symmetries, *Memoirs of the Faculty of Engineering and Design, Kyoto Institute of Technology* **47** (1999) 111–126.
100. S. Fujita, Theoretical foundation of prochirality. Chirogenic sites in an enantiospheric orbit, *Bull. Chem. Soc. Jpn.* **64** (1991) 3313–3323.
101. S. Fujita, Characterization of prochirality and classification of meso-compounds by means of the concept of size-invariant subductions, *Bull. Chem. Soc. Jpn.* **73** (2000) 2009–2016.
102. S. Fujita, Systematic characterization of prochirality, prostereogenicity, and stereogenicity by means of the sphericity concept, *Tetrahedron* **56** (2000) 735–740.
103. S. Fujita, Chiral replacement criterion for characterizing holotopic and hemitopic relationships, *Bull. Chem. Soc. Jpn.* **73** (2000) 1979–1986.
104. S. Fujita, Prochirality revisited. An approach for restructuring stereochemistry by novel terminology, *J. Org. Chem.* **67** (2002) 6055–6063.
105. S. Fujita, A novel way for understanding the desymmetrization of the tetrahedron in introductory courses of organic stereochemistry (Part I). Importance of orbits and sphericity indices, *Chem. Educ. J.* **8** (2005) Registration No. 8–8.
106. S. Fujita, A novel way for understanding the desymmetrization of the tetrahedron in introductory courses of organic stereochemistry (Part II). Importance of local symmetries appearing in subductions of coset representations, *Chem. Educ. J.* **8** (2005) Registration No. 8–9.

107. S. Fujita, Systematic enumeration of high symmetry molecules by means of unit subduced cycle indices with and without chirality fittingness, *Bull. Chem. Soc. Jpn.* **63** (1990) 203–215.
108. S. Fujita, Soccerane derivatives of given symmetries. Systematic enumeration by means of unit subduced cycle indices, *Bull. Chem. Soc. Jpn.* **64** (1991) 3215–3223.
109. S. Fujita, Unit subduced cycle indices and the superposition theorem. Derivation of a new theorem and its application to enumeration of compounds based on a  $D_{2d}$  skeleton, *Bull. Chem. Soc. Jpn.* **63** (1990) 2770–2775.
110. S. Fujita, The USCI approach and elementary superposition for combinatorial enumeration, *Theor. Chim. Acta* **82** (1992) 473–498.
111. S. Fujita, Systematic enumerations of highly symmetric cage-shaped molecules by unit subduced cycle indices, *Bull. Chem. Soc. Jpn.* **62** (1989) 3771–3778.
112. S. Fujita, Adamantane isomers with given symmetries. Systematic enumeration by unit subduced cycle indices, *Tetrahedron* **46** (1990) 365–382.
113. S. Fujita, Enumeration of non-rigid molecules by means of unit subduced cycle indices, *Theor. Chim. Acta* **77** (1990) 307–321.
114. S. Fujita, Systematic enumerations of compounds derived from  $D_{3h}$  skeletons. An application of unit subduced cycle indices, *Bull. Chem. Soc. Jpn.* **63** (1990) 1876–1883.
115. S. Fujita, Unit subduced cycle indices with and without chirality fittingness for  $I_h$  group. An application to systematic enumeration of dodecahedrane derivatives, *Bull. Chem. Soc. Jpn.* **63** (1990) 2759–2769.
116. S. Fujita, Subsymmetry-itemized enumeration of flexible cyclohexane derivatives, *Bull. Chem. Soc. Jpn.* **67** (1994) 2935–2948.
117. S. Fujita, Benzene derivatives with achiral and chiral substituents and relevant derivatives derived from  $D_{6h}$ -skeletons. Symmetry-itemized enumeration and symmetry characterization by the unit-subduced-cycle-index approach, *J. Chem. Inf. Comput. Sci.* **39** (1999) 151–163.
118. S. Fujita, Systematic enumeration of ferrocene derivatives by unit-subduced-cycle-index method and characteristic-monomial method, *Bull. Chem. Soc. Jpn.* **72** (1999) 2409–2416.
119. S. Fujita, Combinatorial enumeration of non-rigid isomers with given ligand symmetries on the basis of promolecules with a symmetry of  $D_{\infty h}$ , *J. Chem. Inf. Comput. Sci.* **40** (2000) 426–437.
120. S. Fujita, Promolecules with a subsymmetry of  $O_h$ . Combinatorial enumeration and stereochemical properties, *Polyhedron* **12** (1993) 95–110.
121. S. Fujita and N. Matsubara, Edge configurations on a regular octahedron. Their exhaustive enumeration and examination with respect to edge numbers and point-



- group symmetries, *Internet Electronic Journal of Molecular Design* **2** (2003) 224–241.
122. S. Fujita, Symmetry-itemized enumeration of cubane derivatives as three-dimensional entities by the fixed-point matrix method of the USCI approach, *Bull. Chem. Soc. Jpn.* **84** (2011) 1192–1207.
123. S. Fujita, Symmetry-itemized enumeration of cubane derivatives as three-dimensional entities by the partial-cycle-index method of the USCI approach, *Bull. Chem. Soc. Jpn.* **85** (2012) 793–810.
124. S. Fujita, Orbits in a molecule. A novel way of stereochemistry through the concepts of coset representations and sphericities (Part 1), *MATCH Commun. Math. Comput. Chem.* **54** (2005) 251–300.
125. S. Fujita, Orbits among molecules. A novel way of stereochemistry through the concepts of coset representations and sphericities (Part 2), *MATCH Commun. Math. Comput. Chem.* **55** (2006) 5–38.
126. S. Fujita, Combinatorial enumeration of stereoisomers by linking orbits in molecules with orbits among molecules. A novel way of stereochemistry through the concepts of coset representations and sphericities (Part 3), *MATCH Commun. Math. Comput. Chem.* **55** (2006) 237–270.
127. S. Fujita, Group-theoretical foundations for the concept of mandalas as diagrammatical expressions for characterizing symmetries of stereoisomers, *J. Math. Chem.* **42** (2007) 481–534.
128. S. Fujita, Mandalas and Fujita's proligand method. A novel way of stereochemistry through the concepts of coset representations and sphericities (Part 4), *MATCH Commun. Math. Comput. Chem.* **57** (2007) 5–48.
129. S. Fujita, The restricted-subduced-cycle-index (RSCI) method for symmetry-itemized enumeration of Kekulé structures and its application to fullerene C<sub>60</sub>, *Bull. Chem. Soc. Jpn.* **85** (2012) 282–304.
130. S. Fujita, The restricted-subduced-cycle-index (RSCI) method for counting matchings of graphs and its application to Z-counting polynomials and the Hosoya index as well as to matching polynomials., *Bull. Chem. Soc. Jpn.* **85** (2012) 439–449.
131. S. Fujita, Restricted enumerations by the unit-subduced-cycle-index (USCI) approach. IV. The restricted-subduced-cycle-index (RSCI) method for enumeration of Kekulé structures and or perfect matchings of graphs, *MATCH Commun. Math. Comput. Chem.* **69** (2013) 333–354.
132. S. Fujita, Enumeration of three-dimensional structures derived from a dodecahedrane skeleton under a restriction condition. I. The restricted-fixed-point-matrix (RFPM) method based on restricted subduced cycle indices, *J. Comput. Chem. Jpn.* **11** (2012) 131–139.

133. S. Fujita, Enumeration of three-dimensional structures derived from a dodecahedrane skeleton under a restriction condition. II. The restricted-partial-cycle-index (RPCI) method based on restricted subduced cycle indices, *J. Comput. Chem. Jpn.* **11** (2012) 140–148.
134. S. Fujita, Restricted enumerations by the unit-subduced-cycle-index (USCI) approach. I. Factorization of subduced cycle indices, *MATCH Commun. Math. Comput. Chem.* **69** (2013) 263–290.
135. S. Fujita, Restricted enumerations by the unit-subduced-cycle-index (USCI) approach. II. Restricted subduced cycle indices for treating interaction between two or more orbits, *MATCH Commun. Math. Comput. Chem.* **69** (2013) 291–310.
136. S. Fujita, Restricted enumerations by the unit-subduced-cycle-index (USCI) approach. III. The restricted-partial-cycle-index (RPCI) method for treating interaction between two or more orbits, *MATCH Commun. Math. Comput. Chem.* **69** (2013) 311–332.
137. S. Fujita, Graphs to chemical structures 1. Sphericity indices of cycles for stereochemical extension of Pólya's theorem, *Theor. Chem. Acc.* **113** (2005) 73–79.
138. S. Fujita, Graphs to chemical structures 2. Extended sphericity indices of cycles for stereochemical extension of Pólya's coronas, *Theor. Chem. Acc.* **113** (2005) 80–86.
139. S. Fujita, Graphs to chemical structures 3. General theorems with the use of different sets of sphericity indices for combinatorial enumeration of nonrigid stereoisomers, *Theor. Chem. Acc.* **115** (2006) 37–53.
140. S. Fujita, Sphericities of cycles. What Pólya's theorem is deficient in for stereoisomer enumeration, *Croat. Chem. Acta* **79** (2006) 411–427.
141. S. Fujita, Graphs to chemical structures 4. Combinatorial enumeration of planted threedimensional trees as stereochemical models of monosubstituted alkanes, *Theor. Chem. Acc.* **117** (2007) 353–370.
142. S. Fujita, Numbers of monosubstituted alkanes as stereoisomers, *J. Comput. Chem. Jpn.* **6** (2007) 59–72.
143. S. Fujita, Graphs to chemical structures 5. Combinatorial enumeration of centroidal and bicentroidal three-dimensional trees as stereochemical models of alkanes, *Theor. Chem. Acc.* **117** (2007) 339–351.
144. S. Fujita, Enumeration of alkanes as stereoisomers, *MATCH Commun. Math. Comput. Chem.* **57** (2007) 265–298.
145. S. Fujita, Alkanes as stereoisomers. Enumeration by the combination of two dichotomies for three-dimensional trees, *MATCH Commun. Math. Comput. Chem.* **57** (2007) 299–340.
146. S. Fujita, Enumeration of primary, secondary, and tertiary monosubstituted alkanes as stereoisomers, *J. Comput. Chem. Jpn.* **6** (2007) 73–90.

147. S. Fujita, Combinatorial enumeration of three-dimensional trees as stereochemical models of alkanes. An approach based on Fujita's proligand method and dual recognition as uninuclear and binuclear promolecules., *J. Math. Chem.* **43** (2008) 141–201.
148. S. Fujita, Numbers of achiral and chiral monosubstituted alkanes having a given carbon content and given numbers of asymmetric and pseudoasymmetric centers, *Bull. Chem. Soc. Jpn.* **81** (2008) 193–219.
149. S. Fujita, Numbers of asymmetric and pseudoasymmetric centers in enumeration of achiral and chiral alkanes of given carbon contents, *MATCH Commun. Math. Comput. Chem.* **59** (2008) 509–554.
150. S. Fujita, Effect of internal branching on numbers of monosubstituted alkanes as three-dimensional structures and as graphs, *Bull. Chem. Soc. Jpn.* **81** (2008) 1078–1093.
151. S. Fujita, Categorization and enumeration of achiral and chiral alkanes of a given carbon content by considering internal branching, *Bull. Chem. Soc. Jpn.* **81** (2008) 1423–1453.
152. S. Fujita, Systematic comparison between three-dimensional structures and graphs (Part 1). The fate of asymmetry and pseudoasymmetry in the enumeration of monosubstituted alkanes, *MATCH Commun. Math. Comput. Chem.* **62** (2009) 23–64.
153. S. Fujita, Systematic comparison between three-dimensional structures and graphs (Part 2). The fate of asymmetry and pseudoasymmetry in the enumeration of alkanes, *MATCH Commun. Math. Comput. Chem.* **62** (2009) 65–104.
154. S. Fujita, Numbers of alkanes and monosubstituted alkanes. A long-standing interdisciplinary problem over 130 years, *Bull. Chem. Soc. Jpn.* **83** (2010) 1–18.
155. S. Fujita, Dominant representations and a markaracter table for a group of finite order, *Theor. Chim. Acta* **91** (1995) 291–314.
156. S. Fujita, Subduction of dominant representations for combinatorial enumeration, *Theor. Chim. Acta* **91** (1995) 315–332.
157. S. Fujita, Subduction of Q-conjugacy representations and characteristic monomials for combinatorial enumeration, *Theor. Chem. Acc.* **99** (1998) 224–230.
158. S. Fujita, Markaracter tables and Q-conjugacy character tables for cyclic subgroups. An application to combinatorial enumeration, *Bull. Chem. Soc. Jpn.* **71** (1998) 1587–1596.
159. S. Fujita, Direct subduction of Q-conjugacy representations to give characteristic monomials for combinatorial enumeration, *Theor. Chem. Acc.* **99** (1998) 404–410.
160. S. Fujita, Characteristic monomial tables for enumeration of achiral and chiral isomers, *Bull. Chem. Soc. Jpn.* **72** (1999) 13–20.

161. S. Fujita, Characteristic monomials with chirality fittingness for combinatorial enumeration of isomers with chiral and achiral ligands, *J. Chem. Inf. Comput. Sci.* **40** (2000) 1101–1112.
162. S. Fujita, The unit-subduced-cycle-index methods and the characteristic-monomial method. Their relationship as group-theoretical tools for chemical combinatorics, *J. Math. Chem.* **30** (2001) 249–270.
163. S. Fujita, Combinatorial enumeration of cubane derivatives as three-dimensional entities. IV. Gross enumeration by the extended superposition method, *MATCH Commun. Math. Comput. Chem.* **67** (2012) 669–686.
164. S. Fujita, Combinatorial enumeration of cubane derivatives as three-dimensional entities. V. Gross enumeration by the double coset representation method, *MATCH Commun. Math. Comput. Chem.* **67** (2012) 687–712.
165. S. Fujita, Combinatorial enumeration of cubane derivatives as three-dimensional entities. I. Gross enumeration by the proligand method, *MATCH Commun. Math. Comput. Chem.* **67** (2012) 5–24.
166. S. Fujita, Combinatorial enumeration of cubane derivatives as three-dimensional entities. II. Gross enumeration by the markaracter method, *MATCH Commun. Math. Comput. Chem.* **67** (2012) 25–54.
167. S. Fujita, Combinatorial enumeration of cubane derivatives as three-dimensional entities. III. Gross enumeration by the characteristic-monomial method *MATCH Commun. Math. Comput. Chem.* **67** (2012) 649–668.
168. K. Mislow and J. Siegel, Stereoisomerism and local chirality, *J. Am. Chem. Soc.* **106** (1984) 3319–3328.
169. I. Ugi, J. Dugundji, R. Kopp, and D. Marquarding, *Perspectives in Theoretical Stereochemistry*, Springer-Verlag, Berlin-Heidelberg, 1984.
170. S. Fujita, Itemized enumeration of quadruplets of *RS*-stereoisomers under the action of *RS*-stereoisomeric groups, *MATCH Commun. Math. Comput. Chem.* **61** (2009) 71–115.
171. S. Fujita, A proof for the existence of five stereogenicity types on the basis of the existence of five types of subgroups of *RS*-stereoisomeric groups. Hierarchy of groups for restructuring stereochemistry (Part 3), *MATCH Commun. Math. Comput. Chem.* **54** (2005) 39–52.
172. S. Fujita, Combinatorial approach to group hierarchy for stereoskeletons of ligancy 4, *J. Math. Chem.* **53** (2015) 1010–1053.
173. S. Fujita, A new scheme for investigating geometric and stereoisomeric features in stereochemistry, *Tetrahedron* **65** (2009) 1581–1592.
174. S. Fujita, Stereoisograms for discussing chirality and stereogenicity of allene derivatives, *Memoirs of the Faculty of Engineering and Design, Kyoto Institute of Technology* **53** (2005) 19–38.

175. S. Fujita, Stereoisograms of trigonal bipyramidal compounds: I. Chirality and *RS*-stereogenicity free from the conventional “chirality” and “stereogenicity”, *J. Math. Chem.* **50** (2012) 1791–1814.
176. S. Fujita, Stereoisograms of trigonal bipyramidal compounds: II. *RS* - Stereogenicity/*RS*-stereoisomerism versus stereogenicity/stereoisomerism, leading to a revised interpretation of Berry’s pseudorotation, *J. Math. Chem.* **50** (2012) 1815–1860.
177. S. Fujita, Importance of the proligand-promolecule model in stereochemistry. I. The unitsubduced-cycle-index (USCI) approach to geometric features of prismane derivatives, *J. Math. Chem.* **50** (2012) 2202–2222.
178. S. Fujita, Importance of the proligand-promolecule model in stereochemistry. II. The stereoisogram approach to stereoisomeric features of prismane derivatives, *J. Math. Chem.* **50** (2012) 2168–2201.
179. S. Fujita, Stereoisograms of octahedral complexes. I. Chirality and *RS*-stereogenicity, *MATCH Commun. Math. Comput. Chem.* **71** (2014) 511–536.
180. S. Fujita, Stereoisograms of octahedral complexes. II. *RS*-stereogenicity vs. stereogenicity as well as *RS*-stereoisomerism vs. stereoisomerism, *MATCH Commun. Math. Comput. Chem.* **71** (2014) 537–574.
181. S. Fujita, Stereoisograms of cubane derivatives, *Bull. Chem. Soc. Jpn.* **88** (2015) 1653–1679.
182. S. Fujita, Correlation diagrams of stereoisograms for characterizing stereoisomers as binuclear and uninuclear promolecules, *MATCH Commun. Math. Comput. Chem.* **63** (2010) 3–24.
183. S. Fujita, Correlation diagrams of stereoisograms for characterizing uninuclear promolecules. A remedy for over-simplified dichotomy in stereochemical terminology, *MATCH Commun. Math. Comput. Chem.* **63** (2010) 25–66.
184. S. Fujita, Correlation diagrams of stereoisograms for characterizing stereoisomers of cyclobutane derivatives, *J. Math. Chem.* **47** (2010) 145–166.
185. S. Fujita, Theory of organic stereoisomerism in harmony with molecular symmetry, *J. Math. Chem.* **49** (2011) 95–162.
186. S. Fujita, Group-theoretical discussion on the *E/Z*-nomenclature for ethylene derivatives. Discrimination between *RS*-stereoisomeric groups and stereoisomeric groups, *J. Chem. Inf. Comput. Sci.* **44** (2004) 1719–1726.
187. The Commission on the Nomenclature of Organic Chemistry of IUPAC, Rules for the nomenclature of organic chemistry. Section E: Stereochemistry (Recommendations 1974), *Pure and App. Chem.* **45** (1976) 11–30.
188. S. Fujita, Stereoisograms for specifying chirality and *RS*-stereogenicity. A versatile tool for avoiding the apparent inconsistency between geometrical features

- and *RS*-nomenclature in stereochemistry, *MATCH Commun. Math. Comput. Chem.* **61** (2009) 11–38.
189. S. Fujita, Three aspects of an absolute configuration on the basis of the stereoisogram approach and revised terminology on related stereochemical concepts, *J. Math. Chem.* **52** (2014) 1514–1534.
190. S. Fujita, *R/S*-Stereodescriptors determined by *RS*-stereogenicity and their chirality faithfulness, *J. Comput. Aided Chem.* **10** (2009) 16–29.
191. S. Fujita, The stereoisogram approach for remedying discontents of stereochemical terminology, *Tetrahedron: Asymmetry* **25** (2014) 1612–1623.
192. S. Fujita, Misleading classification of isomers and stereoisomers in organic chemistry, *Bull. Chem. Soc. Jpn.* **87** (2014) 1367–1378.
193. S. Fujita, Complete settlement of long-standing confusion on the term “prochirality” in stereochemistry. Proposal of pro-*RS*-stereogenicity and integrated treatment with prochirality, *Tetrahedron* **62** (2006) 691–705.
194. S. Fujita, Stereoisograms for reexamining the concept of prochirality, *Yuki Gosei Kagaku Kyokai-Shi/J. Synth. Org. Chem. Jpn.* **66** (2008) 995–1004.
195. K. R. Hanson, Applications of the sequence rule., *J. Am. Chem. Soc.* **88** (1966) 2731–2742.
196. S. Fujita, Prochirality and pro-*RS*-stereogenicity. Stereoisogram approach free from the conventional “prochirality” and “prostereogenicity”, In *Carbon Bonding and Structures. Advances in Physics and Chemistry*; M. V. Putz, Ed., Springer-Verlag: Dordrecht Heidelberg London, 2011; Vol. 5 of *Carbon Materials: Chemistry and Physics* Chapter 10, pp 227–271.
197. S. Fujita, Stereoisograms: A remedy against oversimplified dichotomy between enantiomers and diastereomers in stereochemistry, In *Chemical Information and Computational Challenge in the 21st Century*; M. V. Putz, Ed., Nova: New York, 2012; Chapter 9, pp 223–242.
198. S. Fujita, Substitution criteria based on stereoisograms to determine prochirality and pro-*RS*-stereogenicity, *MATCH Commun. Math. Comput. Chem.* **61** (2009) 39–70.
199. S. Fujita, *Pro-R/pro-S*-Descriptors specified by *RS*-diastereotopic relationships, not by stereoheterotopic relationships, *J. Comput. Aided Chem.* **10** (2009) 76–95.
200. H. Hirschmann and K. R. Hanson, The differentiation of stereoheterotopic groups, *Eur. J. Biochem.* **22** (1971) 301–309.
201. S. Fujita, Extended pseudoasymmetry and geometric prochirality clarifying the scope of the concepts of holantimers and stereoisograms, *Tetrahedron: Asymmetry* **23** (2012) 623–634.
202. S. Fujita, Stereoisograms of octahedral complexes. III. Prochirality, pro-*RS*-stereogenicity, and pro-ortho-stereogenicity free from the conventional

- “prochirality” and “prostereogenicity”, *MATCH Commun. Math. Comput. Chem.* **71** (2014) 575–608.
203. S. Fujita, Symmetry-itemized enumeration of quadruplets of *RS*-stereoisomers: I the fixed-point matrix method of the USCI approach combined with the stereoisogram approach, *J. Math. Chem.* **52** (2014) 508–542.
204. S. Fujita, Symmetry-itemized enumeration of quadruplets of *RS*-stereoisomers: II the partial-cycle-index method of the USCI approach combined with the stereoisogram approach, *J. Math. Chem.* **52** (2014) 543–574.
205. S. Fujita, Symmetry-itemized enumeration of *RS*-stereoisomers of allenes. I. The fixed point matrix method of the USCI approach combined with the stereoisogram approach, *J. Math. Chem.* **52** (2014) 1717–1750.
206. S. Fujita, Symmetry-itemized enumeration of *RS*-stereoisomers of allenes. II. the partialcycle-index method of the USCI approach combined with the stereoisogram approach, *J. Math. Chem.* **52** (2014) 1751–1793.
207. S. Fujita, Stereoisograms for three-membered heterocycles: I. Symmetry-itemized enumeration of oxiranes under an *RS*-stereoisomeric group, *J. Math. Chem.* **53** (2015) 260–304.
208. S. Fujita, Stereoisograms for three-membered heterocycles: II. Chirality, *RS*-stereogenicity, and ortho-stereogenicity on the basis of the proligand-promolecule model, *J. Math. Chem.* **53** (2015) 305–352.
209. S. Fujita, Stereoisograms for three-membered heterocycles: III. *R/S*-Stereodescriptors for characterizing the *RS*-stereogenic aspect of absolute configuration, *J. Math. Chem.* **53** (2015) 353–373.
210. S. Fujita, Combinatorial enumeration of *RS*-stereoisomers itemized by chirality, *RS*-stereogenicity, and sclerality, *MATCH Commun. Math. Comput. Chem.* **58** (2007) 611–634.
211. S. Fujita, Type-itemized enumeration of quadruplets of *RS*-stereoisomers. I. Cycle indices with chirality fittingness modulated by type-IV quadruplets, *J. Math. Chem.* (2015); DOI 10.1007/s10910-015-0561-z.
212. S. Fujita, Type-itemized enumeration of quadruplets of *RS*-stereoisomers: II. Cycle indices with chirality fittingness modulated by type-V quadruplets, *J. Math. Chem.* (2015); DOI 10.1007/s10910-015-0562-y.





## ***Enumeration of Conformers of Octahedral [M(ABC)<sub>6</sub>] Complex on the Basis of Computational Group Theory***

HIROSHI SAKIYAMA<sup>1</sup> AND KATSUSHI WAKI<sup>2</sup>

<sup>1</sup>Department of Material and Biological Chemistry, Faculty of Science, Yamagata University, Japan

<sup>2</sup>Department of Mathematical Sciences, Faculty of Science, Yamagata University, Japan

Correspondence should be addressed to Hiroshi Sakiyama (Email: saki@sci.kj.yamagata-u.ac.jp)

Received 18 February 2016; Accepted 7 March 2016

ACADEMIC EDITOR: HASSAN YOUSEFI AZARI NEJAD

**ABSTRACT** Conformers of [M(ABC)<sub>6</sub>] complex have been enumerated on the basis of computational group theory, where M is the central metal, and ABC is the ligand, bound to M through A. Based on the 16 conformers of the M(AB)<sub>6</sub> core unit, 7173 conformers have been found for the [M(ABC)<sub>6</sub>] complex, which are assigned to nine point groups, 1 D<sub>3d</sub>, 4 D<sub>3</sub>, 4 S<sub>6</sub>, 5 C<sub>2h</sub>, 7 C<sub>3</sub>, 182 C<sub>2</sub>, 15 C<sub>s</sub>, 23 C<sub>i</sub>, and 6932 C<sub>1</sub>.

**KEYWORDS** Enumeration • conformer • octahedral [M(ABC)<sub>6</sub>] complex • Computational Group Theory.

### **1. INTRODUCTION**

Group theory is useful in enumerating conformers of a molecule. In the liquid phase or in the gas phase, conformers may coexist in the equilibrium mixed state, and in such a case, it is important to know the structures and ratio of the conformers in order to understand the nature of the compound better. Enumeration by the group theory is mutually exclusive and collectively exhaustive. Therefore, we can efficiently examine the structures of the conformers in conformational analysis.

The conformers of an octahedral [M(AB)<sub>6</sub>] complex molecule (Figure 1a) have been enumerated [1,2] by the computational group theory (CGT) method [3], where M is the central metal of the molecule, and AB is the ligand including the donor atom, A. Here we say the molecule is “octahedral”, because the coordination geometry around the central metal ion, which corresponds to the central MA<sub>6</sub> unit, is octahedral. The MA<sub>6</sub> unit belongs

to  $O_h$  point group; however, when M-A-B is bent, the  $[M(AB)_6]$  complex molecule can take various structures belonging to  $D_{3d}$ ,  $D_3$ ,  $S_6$ ,  $C_{2h}$ ,  $C_3$ ,  $C_2$ ,  $C_s$ ,  $C_i$ , and  $C_1$  point groups [1], due to the orientation of the ligands. The enumerated conformers were found to be useful in studying actual structures of related metal complexes, e. g. hexakis(methylamine- $\kappa N$ ) nickel(II) dication ( $[\text{Ni}(\text{CH}_3\text{NH}_2)_6]^{2+}$ ) and hexakis(*N*-methylformamide- $\kappa O$ )nickel(II) dication ( $[\text{Ni}(\text{NMF})_6]^{2+}$ ) [1,2].

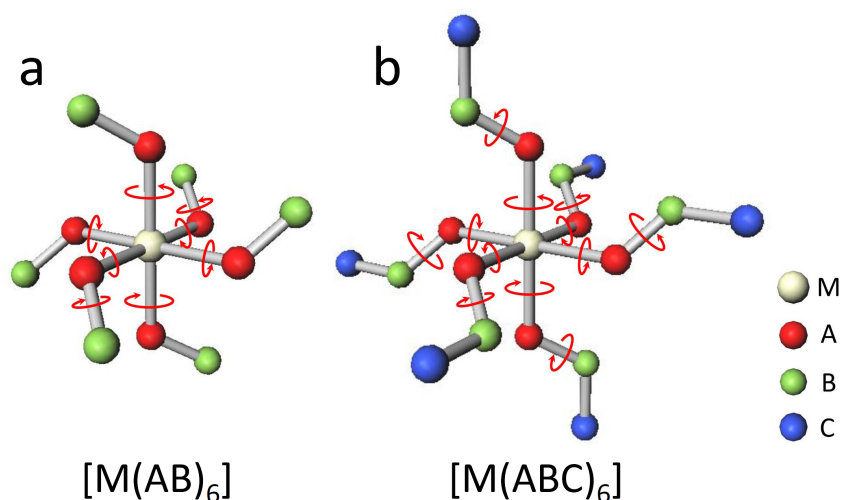


**Figure 1.** Structures of octahedral metal complexes,  $[M(AB)_6]$  (a) and  $[M(ABC)_6]$  (b).

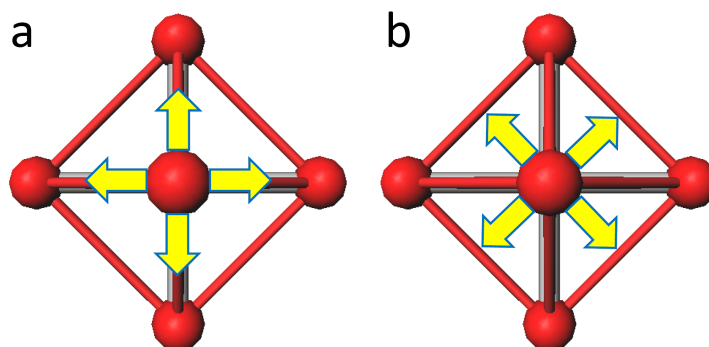


**Figure 2.** Edge directions (a) and bisected directions (b) from an apex of an octahedron.

Despite the success in enumerating the conformers of  $[M(AB)_6]$  complex, the enumeration for the extended  $[M(ABC)_6]$  complex (Figure 1b) has not been done. Therefore, in this study, enumeration of the conformers was conducted for  $[M(ABC)_6]$  complex by CGT method. The obtained result is expected to be useful in conformational analysis of related metal complexes. When extending the ligand from a donor atom, A, to a bound atom, B, there are two typical directions, edge directions and bisected directions

(Figure 2). In our previous study [2], the edge conformers (meridional conformers) was found to be related with the Fujita's edge configurations of  $m = 6$  [4]. In this study, since bisected structures are often seen in actual metal complexes [5,6], only bisected conformers were examined

## 2. METHODS

Conformers were obtained based on the computational group theory (CGT) method [3], which was performed using GAP program [7] on Intel Core i7-3770 (3.40GHz) computer. Three-dimensional models were drawn by Winmostar software [8], and the point groups were ascertained by the software.

## 3. RESULTS AND DISCUSSION

Conformers of  $[M(ABC)_6]$  complex were considered based on the previously enumerated conformers of  $[M(AB)_6]$  complex. Sixteen bisected conformers of  $[M(AB)_6]$  complex are listed in Table 1. Note that we describe, for example, a conformer shown in Figure 3 as  $[ [y+z], [x-z], [x-y], [-y-z], [-x+z], [-x+y] ]$ , indicating the orientations of six AB ligands as  $[y+z]$ ,  $[x-z]$ , etc. in the order of the numbering system  $[ x, y, z, -x, -y, -z ]$ . In this study, based on the  $M(AB)_6$  unit, each ligand, AB, was extended from atom B to atom C to consider the conformers of  $[M(ABC)_6]$  complex. For the extension of C, three directions were considered whose dihedral angles M-A-B-C were  $180^\circ$  (anti conformer),  $300^\circ$  (gauche conformer), and  $60^\circ$  (gauche conformer). This is thought to be sufficient for the purpose of conformational analysis.

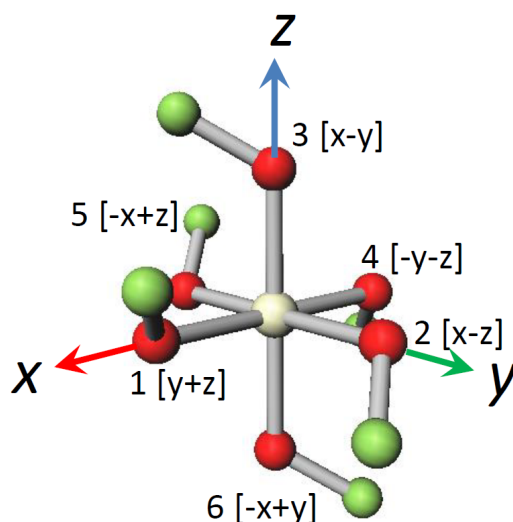


**Figure 3.** An example of a conformer with a numbering system.

**Table 1.** Bisected conformers of  $[M(AB)_6]$  [1].

No	Example	Point Group
B1	[ [y+z], [x-z], [x-y], [-y-z], [-x+z], [-x+y] ]	D3d
B2	[ [y+z], [-x-z], [x-y], [y+z], [-x-z], [x-y] ]	D3
B3	[ [y+z], [-x+z], [-x-y], [-y-z], [x-z], [x+y] ]	S6
B4	[ [y+z], [x-z], [-x+y], [-y-z], [-x+z], [x-y] ]	C2h
B5	[ [y+z], [-x+z], [x-y], [-y-z], [-x+z], [x-y] ]	C2
B6	[ [y+z], [-x+z], [x-y], [y-z], [-x+z], [-x-y] ]	C2
B7	[ [y+z], [x-z], [-x-y], [-y-z], [x+z], [-x+y] ]	C2
B8	[ [y+z], [-x+z], [-x-y], [-y-z], [x+z], [x-y] ]	C2
B9	[ [y+z], [-x+z], [x-y], [y-z], [-x-z], [x-y] ]	C2
B10	[ [y+z], [x-z], [-x+y], [-y-z], [-x+z], [-x+y] ]	Cs
B11	[ [y+z], [-x-z], [x-y], [-y-z], [-x+z], [x-y] ]	C1
B12	[ [y+z], [-x+z], [x-y], [y-z], [-x+z], [x-y] ]	C1
B13	[ [y+z], [-x-z], [-x+y], [-y+z], [-x-z], [x+y] ]	C1
B14	[ [y+z], [-x+z], [-x-y], [-y-z], [x+z], [-x+y] ]	C1
B15	[ [y+z], [-x-z], [-x+y], [-y-z], [-x+z], [x-y] ]	C1
B16	[ [y+z], [-x+z], [x-y], [-y+z], [-x-z], [x+y] ]	C1

As the result of CGT computation, for example, in the case of B1 conformer ( $D_{3d}$  point group) of the  $M(AB)_6$  unit, 74 conformers of  $[M(ABC)_6]$  complex, from B1-1 to B1-74, were derived as listed in Table 2. In the list, the conformers were described by dihedral angles ( $^\circ$ ) of six M-A-B-C units in the order of the numbering system [ x, y, z, -x, -y, -z ]. The 74 conformers include a  $D_{3d}$  structure, a  $D_3$  structure, a  $S_6$  structure, two  $C_{2h}$  structures, a  $C_3$  structure, 11  $C_2$  structures, three  $C_s$  structures, three  $C_i$  structures, and 51  $C_1$  structures, and some of the three-dimensional structures are shown in Figure 4. They have different structures; however, their  $M(AB)_6$  core units have the same structures, belonging to the  $D_{3d}$  point group.

**Table 2.** Bisected conformers of  $[M(ABC)_6]$  possessing  $M(AB)_6$  unit of  $D_{3d}$  symmetry<sup>a</sup>.

No	Dihedral angles (°) of M-A-B-C units	Point Group
B1-1	[ 180, 180, 180, 180, 180, 180 ]	$D_{3d}$
B1-2	[ 60, 60, 60, 60, 60, 60 ]	$D_3$
B1-3	[ 300, 60, 60, 60, 300, 300 ]	$S_6$
B1-4	[ 180, 300, 60, 180, 60, 300 ]	$C_{2h}$
B1-5	[ 180, 60, 300, 180, 300, 60 ]	$C_{2h}$
B1-6	[ 60, 180, 180, 180, 60, 60 ]	$C_3$
B1-7	[ 180, 60, 180, 180, 60, 180 ]	$C_2$
B1-8	[ 180, 60, 60, 180, 60, 60 ]	$C_2$
B1-9	[ 60, 180, 60, 180, 180, 180 ]	$C_2$
B1-10	[ 60, 300, 60, 180, 300, 180 ]	$C_2$
B1-11	[ 60, 300, 60, 60, 60, 300 ]	$C_2$
B1-12	[ 60, 60, 180, 180, 180, 180 ]	$C_2$
B1-13	[ 60, 60, 300, 180, 180, 300 ]	$C_2$
B1-14	[ 60, 60, 300, 60, 300, 60 ]	$C_2$
B1-15	[ 60, 60, 300, 60, 60, 300 ]	$C_2$
B1-16	[ 60, 60, 60, 180, 180, 60 ]	$C_2$
B1-17	[ 60, 60, 60, 180, 60, 180 ]	$C_2$
B1-18	[ 180, 60, 300, 180, 60, 300 ]	$C_s$
B1-19	[ 60, 180, 180, 180, 180, 300 ]	$C_s$
B1-20	[ 60, 180, 180, 180, 300, 180 ]	$C_s$
B1-21	[ 180, 300, 180, 180, 60, 180 ]	$C_i$
B1-22	[ 180, 300, 300, 180, 60, 60 ]	$C_i$
B1-23	[ 300, 300, 60, 60, 60, 300 ]	$C_i$
B1-24	[ 180, 60, 300, 180, 60, 60 ]	$C_1$
B1-25	[ 180, 60, 60, 180, 60, 300 ]	$C_1$
B1-26	[ 60, 180, 180, 180, 180, 180 ]	$C_1$
B1-27	[ 60, 180, 180, 180, 60, 180 ]	$C_1$
B1-28	[ 60, 180, 180, 180, 60, 300 ]	$C_1$
B1-29	[ 60, 180, 300, 180, 180, 180 ]	$C_1$
B1-30	[ 60, 180, 300, 180, 180, 300 ]	$C_1$
B1-31	[ 60, 180, 300, 180, 180, 60 ]	$C_1$
B1-32	[ 60, 180, 300, 180, 300, 300 ]	$C_1$
B1-33	[ 60, 180, 300, 180, 60, 180 ]	$C_1$
B1-34	[ 60, 180, 300, 180, 60, 300 ]	$C_1$
B1-35	[ 60, 180, 300, 180, 60, 60 ]	$C_1$
B1-36	[ 60, 180, 60, 180, 180, 300 ]	$C_1$

B1-37	[ 60, 180, 60, 180, 180, 60 ]	C <sub>1</sub>
B1-38	[ 60, 180, 60, 180, 300, 300 ]	C <sub>1</sub>
B1-39	[ 60, 180, 60, 180, 60, 180 ]	C <sub>1</sub>
B1-40	[ 60, 180, 60, 180, 60, 300 ]	C <sub>1</sub>
B1-41	[ 60, 300, 180, 180, 300, 180 ]	C <sub>1</sub>
B1-42	[ 60, 300, 180, 180, 60, 180 ]	C <sub>1</sub>
B1-43	[ 60, 300, 180, 180, 60, 300 ]	C <sub>1</sub>
B1-44	[ 60, 300, 300, 180, 300, 300 ]	C <sub>1</sub>
B1-45	[ 60, 300, 300, 180, 300, 60 ]	C <sub>1</sub>
B1-46	[ 60, 300, 300, 180, 60, 180 ]	C <sub>1</sub>
B1-47	[ 60, 300, 300, 180, 60, 300 ]	C <sub>1</sub>
B1-48	[ 60, 300, 300, 180, 60, 60 ]	C <sub>1</sub>
B1-49	[ 60, 300, 300, 60, 60, 300 ]	C <sub>1</sub>
B1-50	[ 60, 300, 300, 60, 60, 60 ]	C <sub>1</sub>
B1-51	[ 60, 300, 60, 180, 180, 180 ]	C <sub>1</sub>
B1-52	[ 60, 300, 60, 180, 180, 300 ]	C <sub>1</sub>
B1-53	[ 60, 300, 60, 180, 180, 60 ]	C <sub>1</sub>
B1-54	[ 60, 300, 60, 180, 300, 300 ]	C <sub>1</sub>
B1-55	[ 60, 300, 60, 180, 300, 60 ]	C <sub>1</sub>
B1-56	[ 60, 300, 60, 180, 60, 180 ]	C <sub>1</sub>
B1-57	[ 60, 300, 60, 180, 60, 300 ]	C <sub>1</sub>
B1-58	[ 60, 300, 60, 180, 60, 60 ]	C <sub>1</sub>
B1-59	[ 60, 60, 180, 180, 180, 300 ]	C <sub>1</sub>
B1-60	[ 60, 60, 180, 180, 300, 180 ]	C <sub>1</sub>
B1-61	[ 60, 60, 180, 180, 60, 180 ]	C <sub>1</sub>
B1-62	[ 60, 60, 180, 180, 60, 300 ]	C <sub>1</sub>
B1-63	[ 60, 60, 180, 180, 60, 60 ]	C <sub>1</sub>
B1-64	[ 60, 60, 300, 180, 300, 300 ]	C <sub>1</sub>
B1-65	[ 60, 60, 300, 180, 300, 60 ]	C <sub>1</sub>
B1-66	[ 60, 60, 300, 180, 60, 180 ]	C <sub>1</sub>
B1-67	[ 60, 60, 300, 180, 60, 300 ]	C <sub>1</sub>
B1-68	[ 60, 60, 300, 180, 60, 60 ]	C <sub>1</sub>
B1-69	[ 60, 60, 60, 180, 180, 300 ]	C <sub>1</sub>
B1-70	[ 60, 60, 60, 180, 300, 300 ]	C <sub>1</sub>
B1-71	[ 60, 60, 60, 180, 300, 60 ]	C <sub>1</sub>
B1-72	[ 60, 60, 60, 180, 60, 300 ]	C <sub>1</sub>
B1-73	[ 60, 60, 60, 180, 60, 60 ]	C <sub>1</sub>
B1-74	[ 60, 60, 60, 60, 60, 300 ]	C <sub>1</sub>

---

<sup>a</sup> The orientation is [ [y+z], [x-z], [x-y], [-y-z], [-x+z], [-x+y] ].

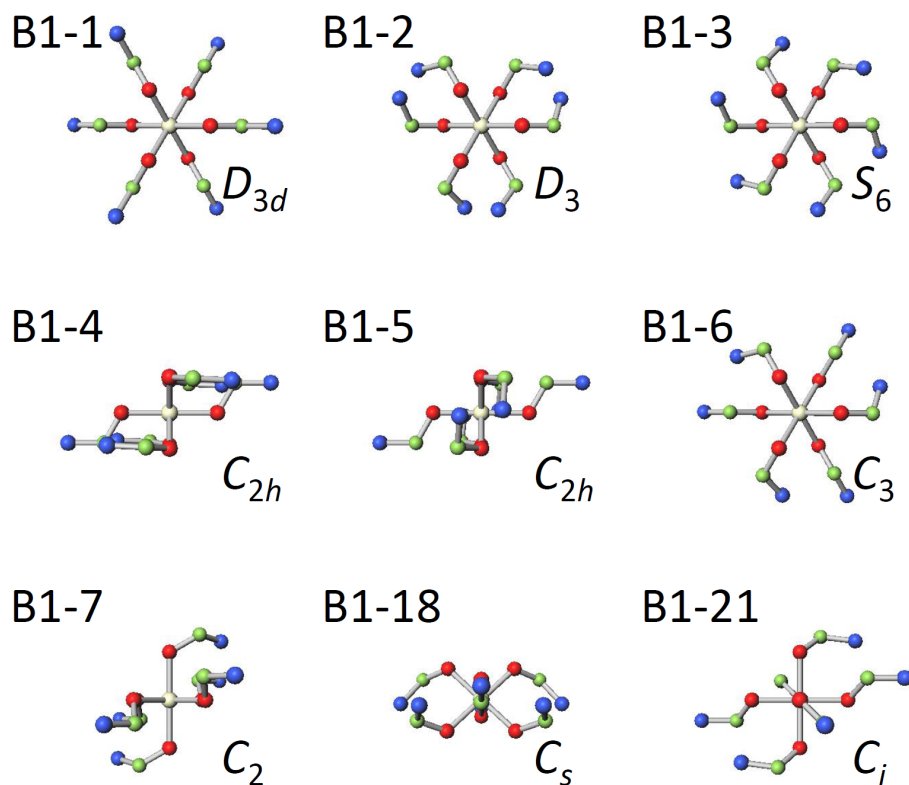


**Figure 4.** Examples of conformers for  $[M(ABC)_6]$  possessing  $M(AB)_6$  unit of  $D_{3d}$  symmetry.

In the same way, the rest of the conformers of the  $[M(ABC)_6]$  complex were considered based on the  $M(AB)_6$  core units from B2 to B16, and the point groups of the obtained conformers are summarized in Table 3. In total, 7173 conformers were found as the bisected conformers of  $[M(ABC)_6]$  complex. In Table 4, the 7173 conformers were re-categorized based on the resulting nine point groups,  $D_{3d}$ ,  $D_3$ ,  $S_6$ ,  $C_{2h}$ ,  $C_3$ ,  $C_2$ ,  $C_s$ ,  $C_i$ , and  $C_1$ . Except for the  $C_1$  symmetry, all of the other 241 bisected conformers of  $[M(ABC)_6]$  are tabled in Table S5 in supporting information. Some of the structures are depicted in Figure 5.

**Table 2.** Bisected conformers of  $[M(ABC)_6]$  possessing  $M(AB)_6$  unit of  $D_{3d}$  symmetry<sup>a</sup>.

No	Dihedral angles (°) of M-A-B-C units	Point Group
B1-1	[ 180, 180, 180, 180, 180, 180 ]	$D_{3d}$
B1-2	[ 60, 60, 60, 60, 60, 60 ]	$D_3$
B1-3	[ 300, 60, 60, 60, 300, 300 ]	$S_6$
B1-4	[ 180, 300, 60, 180, 60, 300 ]	$C_{2h}$
B1-5	[ 180, 60, 300, 180, 300, 60 ]	$C_{2h}$
B1-6	[ 60, 180, 180, 180, 60, 60 ]	$C_3$
B1-7	[ 180, 60, 180, 180, 60, 180 ]	$C_2$
B1-8	[ 180, 60, 60, 180, 60, 60 ]	$C_2$
B1-9	[ 60, 180, 60, 180, 180, 180 ]	$C_2$
B1-10	[ 60, 300, 60, 180, 300, 180 ]	$C_2$
B1-11	[ 60, 300, 60, 60, 60, 300 ]	$C_2$
B1-12	[ 60, 60, 180, 180, 180, 180 ]	$C_2$
B1-13	[ 60, 60, 300, 180, 180, 300 ]	$C_2$
B1-14	[ 60, 60, 300, 60, 300, 60 ]	$C_2$
B1-15	[ 60, 60, 300, 60, 60, 300 ]	$C_2$
B1-16	[ 60, 60, 60, 180, 180, 60 ]	$C_2$
B1-17	[ 60, 60, 60, 180, 60, 180 ]	$C_2$
B1-18	[ 180, 60, 300, 180, 60, 300 ]	$C_s$
B1-19	[ 60, 180, 180, 180, 180, 300 ]	$C_s$
B1-20	[ 60, 180, 180, 180, 300, 180 ]	$C_s$
B1-21	[ 180, 300, 180, 180, 60, 180 ]	$C_i$
B1-22	[ 180, 300, 300, 180, 60, 60 ]	$C_i$
B1-23	[ 300, 300, 60, 60, 60, 300 ]	$C_i$
B1-24	[ 180, 60, 300, 180, 60, 60 ]	$C_1$
B1-25	[ 180, 60, 60, 180, 60, 300 ]	$C_1$
B1-26	[ 60, 180, 180, 180, 180, 180 ]	$C_1$
B1-27	[ 60, 180, 180, 180, 60, 180 ]	$C_1$
B1-28	[ 60, 180, 180, 180, 60, 300 ]	$C_1$
B1-29	[ 60, 180, 300, 180, 180, 180 ]	$C_1$
B1-30	[ 60, 180, 300, 180, 180, 300 ]	$C_1$
B1-31	[ 60, 180, 300, 180, 180, 60 ]	$C_1$
B1-32	[ 60, 180, 300, 180, 300, 300 ]	$C_1$
B1-33	[ 60, 180, 300, 180, 60, 180 ]	$C_1$
B1-34	[ 60, 180, 300, 180, 60, 300 ]	$C_1$
B1-35	[ 60, 180, 300, 180, 60, 60 ]	$C_1$
B1-36	[ 60, 180, 60, 180, 180, 300 ]	$C_1$



B1-37	[ 60, 180, 60, 180, 180, 60 ]	$C_1$
B1-38	[ 60, 180, 60, 180, 300, 300 ]	$C_1$
B1-39	[ 60, 180, 60, 180, 60, 180 ]	$C_1$
B1-40	[ 60, 180, 60, 180, 60, 300 ]	$C_1$
B1-41	[ 60, 300, 180, 180, 300, 180 ]	$C_1$
B1-42	[ 60, 300, 180, 180, 60, 180 ]	$C_1$
B1-43	[ 60, 300, 180, 180, 60, 300 ]	$C_1$
B1-44	[ 60, 300, 300, 180, 300, 300 ]	$C_1$
B1-45	[ 60, 300, 300, 180, 300, 60 ]	$C_1$
B1-46	[ 60, 300, 300, 180, 60, 180 ]	$C_1$
B1-47	[ 60, 300, 300, 180, 60, 300 ]	$C_1$
B1-48	[ 60, 300, 300, 180, 60, 60 ]	$C_1$
B1-49	[ 60, 300, 300, 60, 60, 300 ]	$C_1$
B1-50	[ 60, 300, 300, 60, 60, 60 ]	$C_1$
B1-51	[ 60, 300, 60, 180, 180, 180 ]	$C_1$
B1-52	[ 60, 300, 60, 180, 180, 300 ]	$C_1$
B1-53	[ 60, 300, 60, 180, 180, 60 ]	$C_1$
B1-54	[ 60, 300, 60, 180, 300, 300 ]	$C_1$
B1-55	[ 60, 300, 60, 180, 300, 60 ]	$C_1$
B1-56	[ 60, 300, 60, 180, 60, 180 ]	$C_1$
B1-57	[ 60, 300, 60, 180, 60, 300 ]	$C_1$
B1-58	[ 60, 300, 60, 180, 60, 60 ]	$C_1$
B1-59	[ 60, 60, 180, 180, 180, 300 ]	$C_1$
B1-60	[ 60, 60, 180, 180, 300, 180 ]	$C_1$
B1-61	[ 60, 60, 180, 180, 60, 180 ]	$C_1$
B1-62	[ 60, 60, 180, 180, 60, 300 ]	$C_1$
B1-63	[ 60, 60, 180, 180, 60, 60 ]	$C_1$
B1-64	[ 60, 60, 300, 180, 300, 300 ]	$C_1$
B1-65	[ 60, 60, 300, 180, 300, 60 ]	$C_1$
B1-66	[ 60, 60, 300, 180, 60, 180 ]	$C_1$
B1-67	[ 60, 60, 300, 180, 60, 300 ]	$C_1$
B1-68	[ 60, 60, 300, 180, 60, 60 ]	$C_1$
B1-69	[ 60, 60, 60, 180, 180, 300 ]	$C_1$
B1-70	[ 60, 60, 60, 180, 300, 300 ]	$C_1$
B1-71	[ 60, 60, 60, 180, 300, 60 ]	$C_1$
B1-72	[ 60, 60, 60, 180, 60, 300 ]	$C_1$
B1-73	[ 60, 60, 60, 180, 60, 60 ]	$C_1$
B1-74	[ 60, 60, 60, 60, 60, 300 ]	$C_1$

---

<sup>a</sup> The orientation is [ [y+z], [x-z], [x-y], [-y-z], [-x+z], [-x+y] ].

**Table 3.** Conformers of  $[M(ABC)_6]$  derived from  $M(AB)_6$  core unit.

No	Point Group of $M(AB)_6$ Core Unit	Point Groups of $[M(ABC)_6]$ Conformer	Total
B1	$D_{3d}$	$D_{3d}, D_3, S_6, 2 C_{2h}, C_3, 11 C_2, 3 C_s, 3 C_i, 51 C_1$	74
B2	$D_3$	$3 D_3, 3 C_3, 24 C_2, 108 C_1$	138
B3	$S_6$	$3 S_6, 3 C_3, 8 C_i, 116 C_1$	130
B4	$C_{2h}$	$3 C_{2h}, 12 C_2, 3 C_s, 12 C_i, 168 C_1$	198
B5	$C_2$	$27 C_2, 351 C_1$	378
B6	$C_2$	$27 C_2, 351 C_1$	378
B7	$C_2$	$27 C_2, 351 C_1$	378
B8	$C_2$	$27 C_2, 351 C_1$	378
B9	$C_2$	$27 C_2, 351 C_1$	378
B10	$C_s$	$9 C_s, 360 C_1$	369
B11	$C_1$	$729 C_1$	729
B12	$C_1$	$729 C_1$	729
B13	$C_1$	$729 C_1$	729
B14	$C_1$	$729 C_1$	729
B15	$C_1$	$729 C_1$	729
B16	$C_1$	$729 C_1$	729
Total			7173

**Table 4.** Conformers of  $[M(ABC)_6]$ .

No	Point Group of $[M(ABC)_6]$ Conformer	Total
1	$D_{3d}$	1
2	$D_3$	4
3	$S_6$	4
4	$C_{2h}$	5
5	$C_3$	7
6	$C_2$	182
7	$C_s$	15
8	$C_i$	23
9	$C_1$	6932
Total		7173

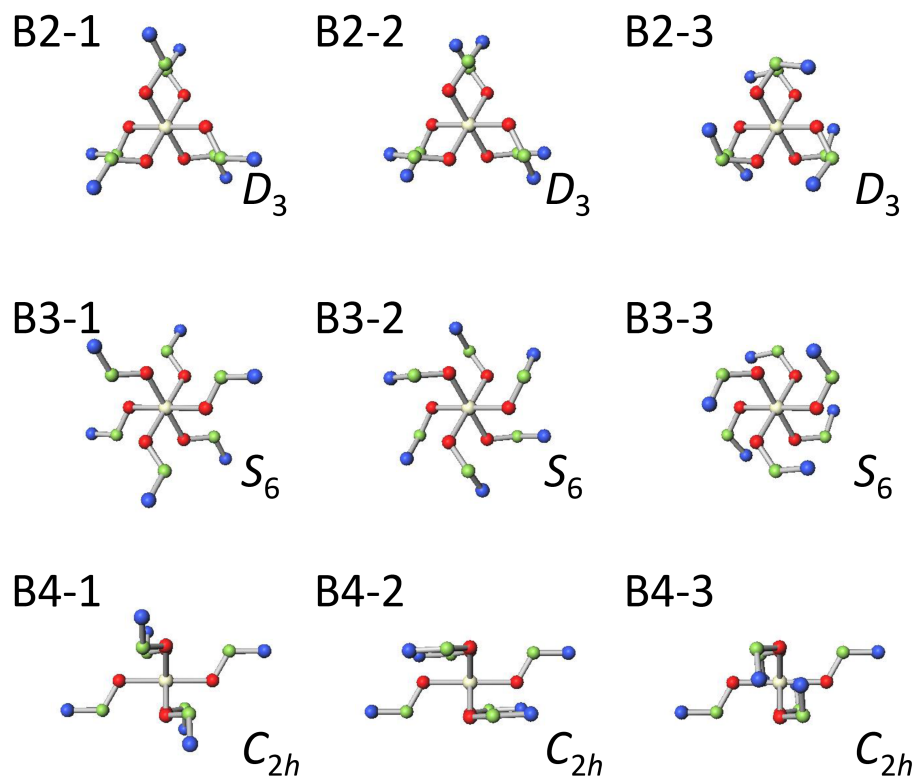


Figure 5. Examples of conformers for  $[M(ABC)_6]$ .

#### 4. CONCLUDING REMARKS

In this study, conformers of octahedral  $[M(ABC)_6]$  complex have been enumerated on the basis of computational group theory. Based on the 16 bisected conformers of the  $M(AB)_6$  core unit, 7173 conformers have been found for the  $[M(ABC)_6]$  complex, considering the anti and gauche conformations. The obtained structures were assigned to nine point groups, 1  $D_{3d}$ , 4  $D_3$ , 4  $S_6$ , 5  $C_{2h}$ , 7  $C_3$ , 182  $C_2$ , 15  $C_s$ , 23  $C_i$ , and 6932  $C_1$ . The results were summarized in tables, which is useful in conformational analysis of the related octahedral complexes.

#### ACKNOWLEDGMENT

This work was supported by JSPS KAKENHI Grant Number 15K05445. Financial support by Yamagata University is also acknowledged. The development of Winmoster software including point group analysis function by Mr. Norio Senda and Mr. Shinji Nagashiro is gratefully acknowledged.

**SUPPORTING INFORMATION:** Table S5.

## REFERENCES

1. H. Sakiyama, K. Waki, Conformational Analysis of Hexakis-Methylamine Nickel(II) Complex on the Basis of Computational Group Theory and Density Functional Theory, *J. Comput. Chem., Jpn.* **13** (2014) 223–228.
2. H. Sakiyama, K. Waki, Conformational Analysis of Hexakis-*N*-Methylformamide Nickel(II) Complex on the Basis of Computational Group Theory and Density Functional Theory, *J. Comput. Chem. Jpn. Int. Ed.* **1** (2015) 5–8.
3. D. F. Holt, Handbook of Computational Group Theory. In the series 'Discrete Mathematics and its Applications', Chapman & Hall/CRC 2005, xvi + 514 p.
4. S. Fujita, N. Matsubara, Edge Configurations on a Regular Octahedron. Their Exhaustive Enumeration and Examination With Respect to Edge Numbers and Point–Group Symmetries, *Internet Electronic Journal of Molecular Design* **2** (2003) 224–241.
5. R. Sudo, D. Yoshioka, M. Mikuriya, H. Sakiyama, Structural Feature of a Hexa-DMSO Cobalt(II) Complex: *Pseudo-S*<sub>6</sub> Symmetry and *Pseudo-C*<sub>2v</sub> Deformation, *X-ray Struct. Anal. Online* **28** (2012) 71–72.
6. R. Sudo, D. Yoshioka, M. Mikuriya, H. Sakiyama, Structural Features of Hexakis-DMSO Nickel(II) Complex Cations: *Pseudo-S*<sub>6</sub>- and *Pseudo-S*<sub>4</sub>-Propeller-Like Structures, *X-ray Struct. Anal. Online* **29** (2013) 17–18.
7. The GAP Group, GAP-Groups, Algorithms, and Programming, Version 4.7.9; 2015. (<http://www.gap-system.org>)
8. N. Senda, Winmostar Software, Version 6.005; 2016. (<http://winmostar.com>)

## ***QSPR modeling of heat capacity, thermal energy and entropy of aliphatic Aldehydes by using Topological Indices and MLR method***

**A. ALAGHEBANDI AND F. SHAFIEI**

Department of Chemistry, Science Faculty, Arak Branch, Islamic Azad University, Arak, Iran

Correspondence should be addressed to F. Shafiei (Email: f-shafiei@iau-arak.ac.ir)

Received 1 September 2015; Accepted 11 January 2016

ACADEMIC EDITOR: IVAN GUTMAN

**ABSTRACT** Quantitative Structure-Property Relationship (QSPR) models are useful in understanding how chemical structure relates to the physicochemical properties of natural and synthetic chemicals. In the present investigation the applicability of various topological indices are tested for the QSPR study on 24 aldehydes. The topological indices used for the QSPR analysis were Randić ( ${}^1\chi$ ) (the first order molecular connectivity), Balaban (J), Wiener (W) and Harary (H) indices. In this study, the relationship between the topological indices to the thermal energy (Eth), heat capacity ( $C_v$ ) and entropy(S) of 24 aldehydes are established. The thermodynamic properties are taken from HF level using the ab initio 6-31 G basis sets from the program package Gaussian 98. For obtaining appropriate QSPR model we have used multiple linear regression (MLR) techniques and followed Back ward regression analysis. The results have shown that combining the three descriptors (J, W,  ${}^1\chi$ ) could be used successfully for modeling and predicting the heat capacity ( $C_v$ ), two descriptors (J,  ${}^1\chi$ ) could be efficiently used for estimating the entropy (S) and one descriptors ( ${}^1\chi$ ) could be predict the thermal energy of compounds.

**KEYWORDS** Topological indices • Aldehydes • QSPR • MLR method.

### **1. INTRODUCTION**

Graph theory has been found to be a useful tool in Quantitative Structure- Activity Relationship (QSAR) and Quantitative Structure- Property Relationship (QSPR) [1–6]. A QSPR is a mathematical description of a property in terms of other properties (descriptors) that are of three broad classes hydrophobic, electronic, and steric. Numerous studies have been made related to the various fields by using what are called topological indices (TI) [7–12]. Topological indices are the digital value combined with chemical constitution purporting for correlation of chemical structures with various chemical and physical

properties that have constructed the effective and useful mathematical methods for finding good relationship between several data of the properties in these materials [13–16]. The use of the effective mathematical methods for making good correlations between several data properties of chemicals is important.

Recent years have seen the publication of a plethora of QSPR methods for the prediction of the normal boiling point, heat capacity, standard Gibbs energy of formation, vaporization enthalpy. Many of the studies deal with specific classes of compounds, especially alkanes [17,18], alcohols [19,20], aldehydes and ketones [21,22,23].

This method is useful when there is not any interaction between descriptors and their relation with linear defined activity. Heat capacity, thermal energy and entropy are applied in reactions for modification of reactants evaluation. In addition, they are useful for heat - energy balance design calculation. On the other hand, the tests for determining these properties are expensive and expense much more time. Therefore, we need the models to predict the heat capacity and other physico – chemical properties of molecules.

Ivanova and Gakh give a model for evaluation the heat capacity of alkanes by using artificial neural network (ANN) [23]. Yao proposed a general nonlinear model for evaluation of heat capacity that can be used for the prediction of liquid heat capacity of all organic compounds [24]. Lailong proposed model for predicting standard absolute entropy ( $S_{298}^{\circ}$ ) of inorganic compounds by using multivariate linear regression (MLR) and (ANN) methods [25].

In the present study, the multiple linear regression (MLR) techniques and back ward methods are used for modeling the thermal energy ( $E_{th}$ ), heat capacity ( $C_V$ ) and entropy ( $S$ ) of 24 aldehydes. The proposed QSPR models were based on molecular descriptors (topological indices) that can be calculated for any compound utilizing only the knowledge of its molecular structure (molecular graph).

The topological indices (Tis) used for the QSPR analysis were Wiener (W) [16], first order molecular connectivity ( $^1\chi$ ) [18], Balaban (J) [19] and Harary(H) [22] indices.

The aim of this study is to provide reliable QSPR models for predicting physicochemical properties of aldehydes.

## 2. MATERIALS AND METHODS

### 2.1. QUANTUM CHEMISTRY CALCULATIONS

The thermal energy ( $E_{th}$ ), heat capacity ( $C_V$ ), entropy ( $S$ ) and lumo energy ( $E_{lumo}$ ) of 24 aldehydes are taken from the quantum mechanics methodology with Hartree- Fock (HF) level using the ab initio 6-31G basis sets. The quantum chemistry data of the 24 congeners are listed in Table 1.

## 2.2. TOPOLOGICAL INDICES

All the used topological indices were calculated using all hydrogen suppressed graph by deleting all the carbon hydrogen from the structure of the aldehydes. The descriptors were calculated with chemicalize program [23]. Four topological indices tested in the present study are recorded in Table 2.

## 2.3. STATISTICAL ANALYSIS

Structure- Property models (MLR models) are generated using the multi linear regression procedure of SPSS version 16. The thermal energy ( $E_{th}$  kcal/mol), heat capacity ( $C_v$  cal/molK) and entropy ( $S$  cal/molK) are used as the dependent variable and  $^1\chi$ , J, H, and W indices as the independent variables. The models are assessed with R value (correlation coefficient), the  $R^2$  (coefficient of determination), the  $R^2$ - adjusted, the SD value (root of the mean square of errors), the F value (Fischer statistic), the D value (Durbin-Watson) and the Sig (significant).

## 3. RESULTS

Several linear QSPR models involving three-eight descriptors are established and strongest multivariable correlations are identified by the back ward method are significant at the 0.05 level and regression analysis of the SPSS program. In the first of this study we draw scattering plots of  $C_v$ ,  $S$  and  $E_{th}$  versus the four topological indices ( $^1\chi$ , J, W, H). Some of these plots are given in Fig. (1-3), respectively.

Distribution of the dependent variable against the independent variable for 41 chemicals employed in developing quantitative structure- Properties relationship. For obtaining appropriate QSPR model we have used maximum  $R^2$  method and followed Back ward regression analysis. The predictive ability of the model is discussed on the basis of predictive correlation coefficient.

### 3.1. QSPR MODELS FOR HEAT CAPACITY ( $C_v$ )

Initial regression analysis indicated that combination of seven topological indices and  $E_{lum0}$  plays a dominating role in modeling the heat capacity. In Table 3 are given the regression parameters and quality of correlation of the proposed models for heat capacity of 24 aldehydes.

It turns out that the heat capacity ( $C_v$ ) has a highly correlation with a combination of the three parameters, namely, Balaban (J), Randić ( $^1\chi$ ) and Wiener (W) indices. Fig 4 shows the linear correlation between the observed and the predicted heat capacity values obtained using Eq. (1).

### Model 3.1.1

$$C_v = 0.817 - 1.034J + 0.0001W + 9.182^1\chi$$

$$N=24 \quad R=1 \quad R^2=1 \quad R_{adj}^2=1 \quad SD=0.267 \quad F=1.083 \times 10^5 \quad Sig=0.000 \quad D=2.033(1)$$

### 3.2. QSPR MODELS FOR THERMAL ENERGY (ETH)

In Table 4 are given the regression parameters and quality of correlation of the proposed models for the thermal energy of 24 aldehydes.

Statistically significant models are obtained when one descriptors are used and that the quality of the model goes on improving with higher parameteric modeling (Table 4), the model (3) containing one descriptors ( $^1\chi$ ) is found as below:

### Model 3.2.3

$$E_{th} = -14.763 + 39.829^1\chi$$

$$N=24 \quad R=1 \quad R^2=1 \quad R_{adj}^2=1 \quad SD=2.609 \quad F=6.701 \times 10^4 \quad Sig=0.000 \quad D=2.129 \quad (2)$$

Figure 5 shows the linear correlation between the observed and the predicted thermal energy values obtained using Eq. (2).

### 3.3. QSPR MODELS FOR ENTROPY (S)

In Table 5 are given the regression parameters and quality of correlation of the proposed models for the entropy of 24 aldehydes.

It turns out that the entropy (S) has a good correlation with all descriptors as well as with a combination of the two parameters, namely, Balaban (J) and Randić ( $^1\chi$ ) indices. Fig 6 shows the linear correlation between the observed and the predicted entropy obtained using Eq. (3).



**Model 3.3.2**

$$S = 44.647 - 1.835J + 14.7811\chi$$

$$N = 24 \quad R = 1 \quad R^2 = 1 \quad R_{adj}^2 = 1 \quad SD = 0.236 \quad F = 5.517 \times 10^5 \quad D = 2.310 \quad \text{Sig} = 0.000(3)$$

**4. DISCUSSION**

We studied the relationship between topological indices to the thermal energy ( $E_{th}$ ), heat capacity ( $C_v$ ) and entropy ( $S$ ) of 24 aldehydes.

In this study, to find the best model for predict the properties mentioned, we will use the following sections.

**4.1. VERIFICATION AND VALIDITY OF MODELS**

In this section for verification and validity of the regression models, we will focus on the Durbin-Watson (D) statistic, unstandardized predicted and residual values.

**4.1.1. TEST FOR AUTOCORRELATION BY USING THE DURBIN-WATSON STATISTIC**

The Durbin-Watson statistic ranges in value from 0 to 4. A value near 2 indicates non-autocorrelation; a value toward 0 indicates positive autocorrelation; a value toward 4 indicates negative autocorrelation. Therefore the value of Durbin-Watson statistic is close to 2 if the errors are uncorrelated. In our all models, the value of Durbin-Watson statistic is close to 2 (See Eq. 1–3) and hence the errors are uncorrelated.

**4.2. REGULAR RESIDUALS**

The residual is difference between the observed value of the dependent variable ( $y$ ) and the predicted value ( $\hat{y}$ ). Plot the residuals, and use other diagnostic statistics, to determine whether our model is adequate and the assumptions of regression are met. The residuals can also identify how much a model explains the variation in the observed data. The residuals values of heat capacity, thermal energy and entropy expressed by Eqs. (1–3) are shown in Table 6. The residual plots, Figures 7–9, show a fairly random pattern. This random pattern indicates that a linear model provides a decent fit to the data.

**4.3. QSPR MODELS**

The QSPR model (3.1.1) reveals that the heat capacity of the aldehydes could be explained by three parameters. This model can explain about 100% of the experimental

variance of the dependent variable  $C_v$ . The combination of the three parameters (J,  ${}^1\chi$ , W) increases remarkably the predictive power of the QSPR model given by Eq. (1) ( $R^2 = 1$   $R_{adj}^2 = 1$   $SD=0.267$   $F=1.083 \times 10^5$   $Sig=0.000$   $D=2.033$ ).

The Back ward method values of the thermal energy shows that all of models (3.2.1-3.2.3) can explain about 100% of the variance of the thermal energy. The QSPR model given by Eq. (2) ( $R^2 = 1$   $R_{adj}^2 = 1$   $SD=2.609$   $F= 6.701 \times 10^4$   $Sig = 0.000$   $D=2.129$ ). As can be seen from the statistical parameters of the above equation, a considerable improvement is achieved by one descriptor ( ${}^1\chi$ ). This model has a minimum of independent variables and maximum of F, compared with another models.

Similarity, this method for the entropy shows that all of models (3.3.1, 3.3.2) can explain about 100% of the variance of the entropy and according to statistical parameters of the below equation, a considerable improvement is achieved by combining the two descriptors ( ${}^1\chi$ , J). The QSPR model given by Eq. (3) ( $R^2 = 1$   $R_{adj}^2 = 1$   $SD=0.236$   $F= 5.517 \times 10^5$   $D=2.310$   $Sig = 0.000$ ).

This model has a minimum of independent variables and maximum of F, compared with another model.

## 5. CONCLUSION

Graph theory has provided the chemist with a variety of very useful tools. This contains valuable structural information as evidenced by the success of their widespread applications in QSAR/QSPR. In this work, the relationship between topological indices (J, W, H,  ${}^1\chi$ ) and the heat capacity ( $C_v$ ), entropy (S), thermal energy ( $E_{th}$ ) of 24 aldehydes were studied.

The aforementioned results and discussion lead us to conclude that combining the three descriptors (J, W,  ${}^1\chi$ ) could be used successfully for modeling and predicting the heat capacity ( $C_v$ ), two descriptors (J,  ${}^1\chi$ ) could be efficiently used for estimating the entropy (S) and one descriptor ( ${}^1\chi$ ) could be used to predict the thermal energy of compounds. The training set models established by MLR method have good correlation of physicochemical properties, which means QSPR models could be used for prediction of the heat capacity ( $C_v$ ), entropy (S), thermal energy ( $E_{th}$ ) for a set of 24 aldehydes.

**Table 1.** Structural details and their thermal energy ( $E_{th}$ ), heat capacity ( $C_v$ ) and entropy ( $S$ ) for the aldehydes used in present study.

Compound	Formula	No.	$E_{th}$ kcal/mol	$C_v$ cal/molK	$S$ cal/molK
Ethanal	C <sub>2</sub> H <sub>4</sub> O	1	40.074	10.472	62.483
Propanal	C <sub>3</sub> H <sub>6</sub> O	2	60.162	14.719	69.255
Butanal	C <sub>4</sub> H <sub>8</sub> O	3	80.131	19.195	76.521
Pentanal	C <sub>5</sub> H <sub>10</sub> O	4	100.175	23.569	83.11
Hexanal	C <sub>6</sub> H <sub>12</sub> O	5	132.672	26.877	90.594
Heptanal	C <sub>7</sub> H <sub>14</sub> O	6	139.94	32.586	97.626
Octanal	C <sub>8</sub> H <sub>16</sub> O	7	159.879	37.083	104.813
Nonanal	C <sub>9</sub> H <sub>18</sub> O	8	179.812	41.597	112.474
Decanal	C <sub>10</sub> H <sub>20</sub> O	9	199.764	46.095	119.946
Undecanal	C <sub>11</sub> H <sub>22</sub> O	10	219.717	50.587	127.356
Dodecanal	C <sub>12</sub> H <sub>24</sub> O	11	239.673	55.061	134.061
Tridecanal	C <sub>13</sub> H <sub>26</sub> O	12	259.626	59.553	141.197
Tetradecanal	C <sub>14</sub> H <sub>28</sub> O	13	279.545	64.08	149.267
Pentadecanal	C <sub>15</sub> H <sub>30</sub> O	14	299.493	68.575	156.6
Hexadecanal	C <sub>16</sub> H <sub>32</sub> O	15	319.434	73.07	163.611
Heptadecanal	C <sub>17</sub> H <sub>34</sub> O	16	339.444	77.48	171.456
Octadecanal	C <sub>18</sub> H <sub>36</sub> O	17	360.034	81.825	178.205
Nonadecanal	C <sub>19</sub> H <sub>38</sub> O	18	380.088	86.245	185.815
Eicosanal	C <sub>20</sub> H <sub>40</sub> O	19	400.07	90.739	193.172
Heneicosanal	C <sub>21</sub> H <sub>42</sub> O	20	420.055	95.226	200.52
Docosanal	C <sub>22</sub> H <sub>44</sub> O	21	440.039	99.715	207.846
Tricosanal	C <sub>23</sub> H <sub>46</sub> O	22	460.024	104.206	215.418
Tetracosanal	C <sub>24</sub> H <sub>48</sub> O	23	480.006	108.692	222.462
Pentacosanal	C <sub>25</sub> H <sub>50</sub> O	24	499.992	113.185	230.223

**Table 2.** Topological indices values used in present study.

Comp.No	${}^1\chi$	J	H	W
1	1.41	1.63	2.5	4
2	1.91	1.97	4.33	10
3	2.41	2.19	6.42	20
4	2.91	2.34	8.7	35
5	3.41	2.45	11.15	56
6	3.91	2.53	13.74	84
7	4.41	2.6	16.46	120
8	4.91	2.65	19.26	165
9	5.41	2.69	22.22	220
10	5.91	2.73	25.24	286
11	6.41	2.76	28.34	364
12	6.91	2.78	31.52	455
13	7.41	2.81	34.77	560
14	7.91	2.83	38.09	680
15	8.41	2.85	41.47	816
16	8.91	2.86	44.91	969
17	9.41	2.88	48.41	1140
18	9.91	2.89	51.95	1330
19	10.41	2.9	55.55	1540
20	10.91	2.91	59.2	1771
21	11.41	2.92	62.89	2024
22	11.91	2.93	66.62	2300
23	12.41	2.94	70.4	2600
24	12.91	2.95	74.21	2925

**Table 3.** Regression parameters and quality of correlation of the proposed models for the heat capacity.

Model	independent variables	R	R <sup>2</sup>	R <sup>2</sup> <sub>adj</sub>	SD	F
1	J, ${}^1\chi$ , W	1	1	1	0.267	1.083×10 <sup>5</sup>

**Table 4.** Regression parameters and quality of correlation of the proposed models for the thermal energy.

Model	Independent variables	R	R <sup>2</sup>	R <sup>2</sup> <sub>adj</sub>	F	SD
1	J, W, <sup>1</sup> χ	1	1	1	2.232×10 <sup>4</sup>	2.610
2	W, <sup>1</sup> χ	1	1	1	3.256×10 <sup>4</sup>	2.647
3	<sup>1</sup> χ	1	1	1	6.701×10 <sup>4</sup>	2.609

**Table 5.** Regression parameters and quality of correlation of the proposed models for the entropy.

Model	Independent variables	R	R <sup>2</sup>	R <sup>2</sup> <sub>adj</sub>	SD	F	Sig
1	J, <sup>1</sup> χ, W	1	1	1	0.242	3.507×10 <sup>5</sup>	0.000
2	J, <sup>1</sup> χ	1	1	1	0.236	5.517×10 <sup>5</sup>	0.000

**Table 6.** Comparison between predicted and observed values of thermal energy, heat capacity and entropy of respect aldehydes.

Comp No	Observed (Cv)	Predicted (Cv)	Residual	Observed (Eth)	Predicted (Eth)	Residual	Observed (S)	Predicted (S)	Residual
1	10.472	10.442	0.030	40.074	39.731	0.343	62.483	61.826	0.657
2	14.719	14.678	0.041	60.162	61.152	-0.990	69.255	69.634	-0.379
3	19.195	19.036	0.159	80.131	81.808	-1.677	76.521	76.877	-0.356
4	23.569	23.463	0.106	100.175	102.028	-1.853	83.11	83.864	-0.754
5	26.877	27.928	-1.051	132.672	132.011	0.661	90.594	90.833	-0.239
6	32.586	32.421	0.165	139.945	141.827	-1.882	97.626	97.800	-0.174
7	37.083	36.919	0.164	159.879	161.609	-1.730	104.813	104.929	-0.116
8	41.597	41.432	0.165	179.812	181.295	-1.483	112.474	111.990	0.484
9	46.095	45.951	0.144	199.764	200.956	-1.192	119.946	119.271	0.675
10	50.587	50.463	0.124	219.717	220.659	-0.942	127.356	126.617	0.739
11	55.061	54.979	0.082	239.673	240.343	-0.670	134.061	133.970	0.091
12	59.553	59.497	0.056	259.626	260.013	-0.387	141.197	141.323	-0.126
13	64.08	63.998	0.082	279.545	279.802	-0.257	149.267	148.840	0.427
14	68.575	68.500	0.075	299.493	299.585	-0.092	156.6	156.317	0.283
15	73.07	72.993	0.077	319.434	319.429	0.005	163.611	163.820	-0.209
16	77.48	77.487	-0.007	339.444	339.274	0.170	171.456	171.242	0.214
17	81.825	81.960	-0.135	360.034	359.254	0.780	178.205	178.773	-0.568
18	86.245	86.433	-0.188	380.088	379.243	0.845	185.815	186.159	-0.344
19	90.739	90.895	-0.156	400.07	399.309	0.761	193.172	193.541	-0.369
20	95.226	95.344	-0.118	420.055	419.457	0.598	200.52	200.884	-0.364
21	99.715	99.781	-0.066	440.039	439.690	0.349	207.846	208.159	-0.313
22	104.206	104.206	0.000	460.024	460.012	0.012	215.418	215.356	0.062
23	108.692	108.616	0.076	480.006	480.427	-0.421	222.462	222.492	-0.030
24	113.185	113.013	0.172	499.992	500.940	-0.948	230.223	229.512	0.711

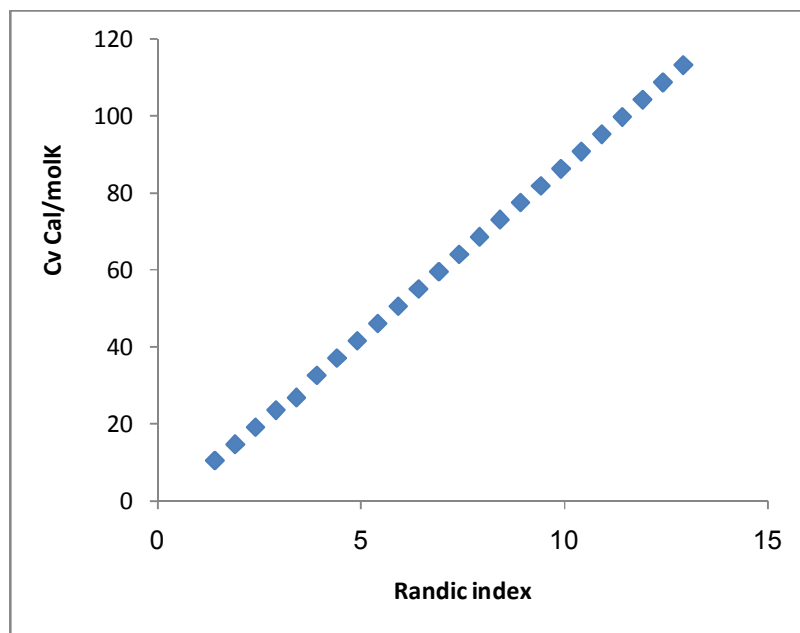


**Figure 1.** Plots of the Randić index ( $\chi^1$ ) versus heat capacity ( $C_v$ ) of 24 aldehydes.

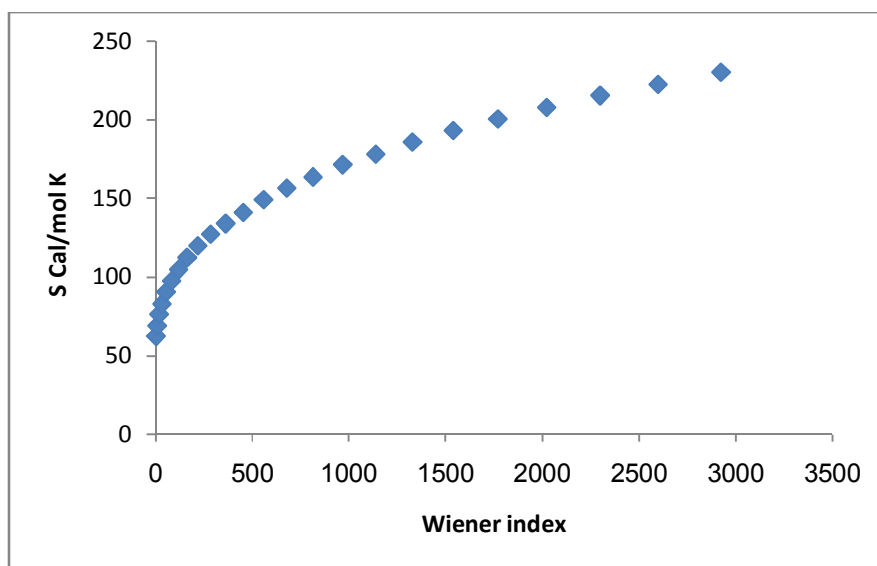


**Figure 2.** Plots of the Wiener index ( $W$ ) versus entropy ( $S$ ) of 24 aldehydes.

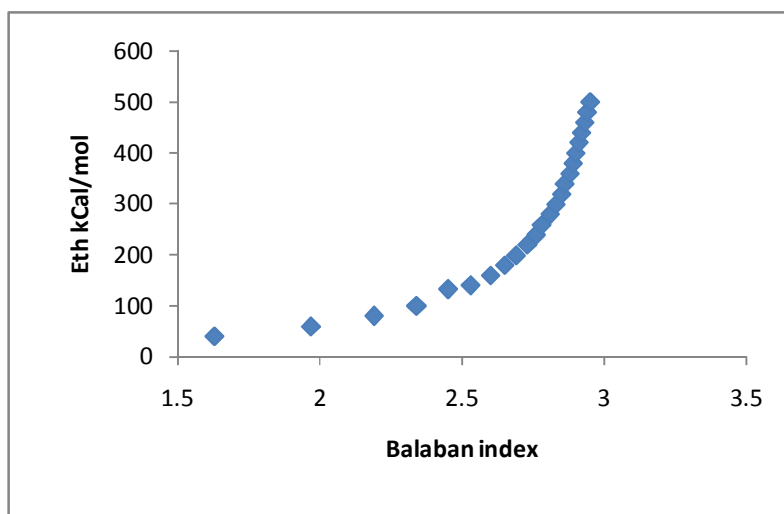


**Figure 3.** Plots of the Balaban index (J) versus thermal energy ( $E_{th}$ ) of 24 aldehydes.

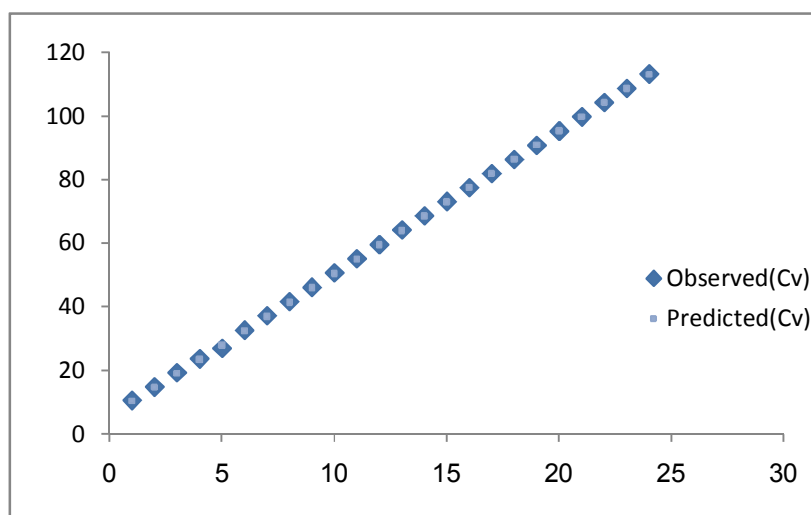


**Figure 4.** Comparison between the predicted and observed values of heat capacity by MLR.



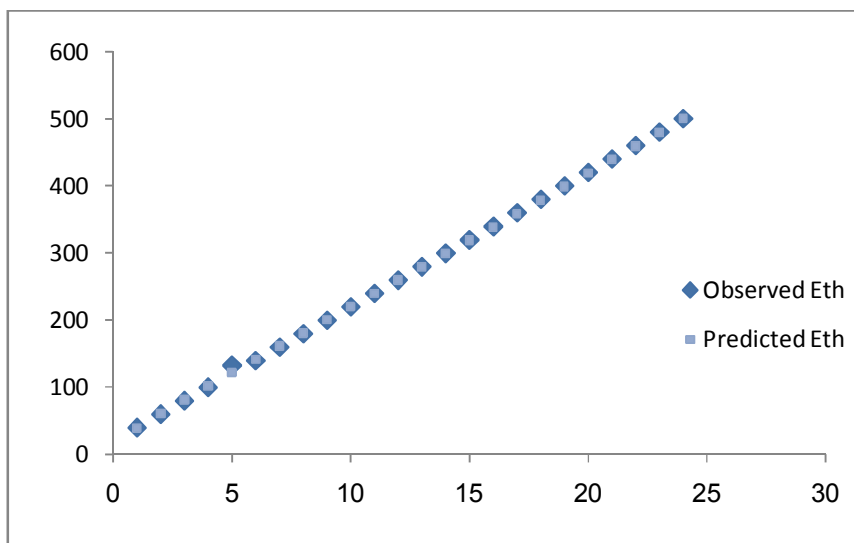


**Figure 5.** Comparison between the predicted and observed values of thermal energy by MLR.

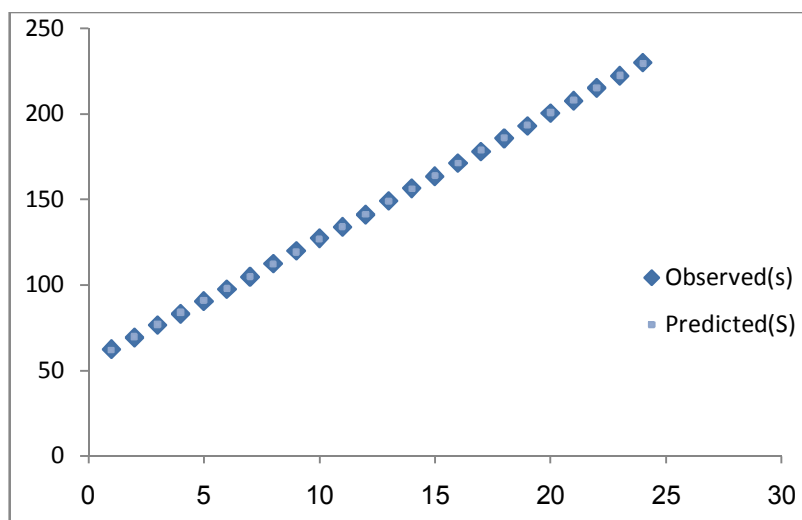


**Figure 6.** Comparison between the predicted and observed values of entropy(S) by MLR.

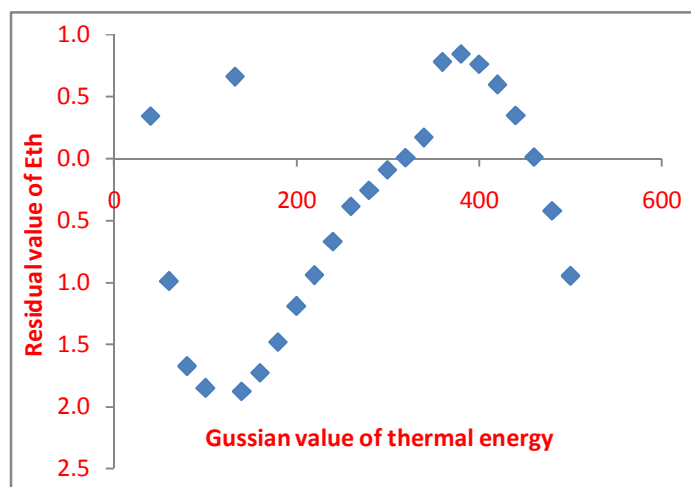


**Figure 7.** Plot of residuals against experimental value with Eq. (2) for the thermal energy of 24 aldehydes.



**Figure 8.** Plot of residuals against experimental value(Gaussian value) with Eq. (3) for the entropy of 24 aldehydes.

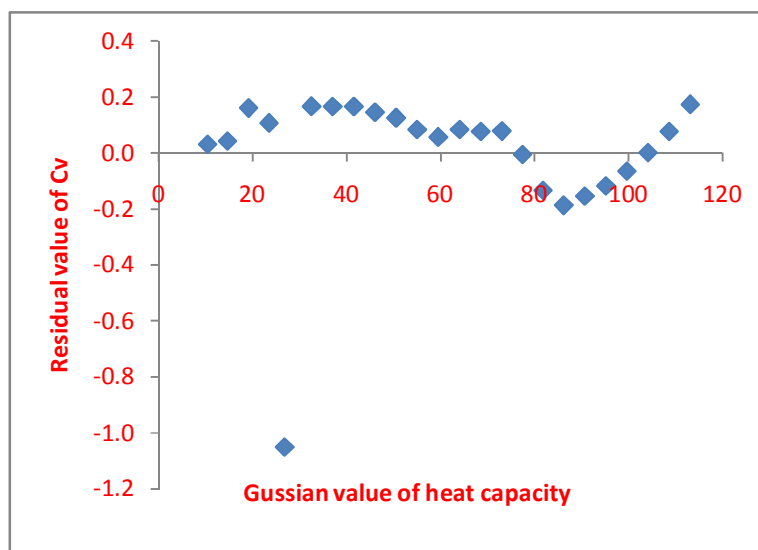


**Figure 9.** Plot of residuals against experimental value with Eq. (1) for the heat capacity of 24 aldehydes.

## REFERENCES

1. P. J. Hansen, P. C. Jurs, Chemical applications of graph theory .part I. fundamentals and topological indices, *J. Chem. Edu.* **65** (1988) 574–580.
2. H. Hosoya, Topological index: A newly proposed quantity characterizing the topological nature of structural isomers of saturated hydrocarbons, *Bull. Chem. Soc. Jpn.* **44** (1971) 2332–2339.
3. M. Randić, On characterization of molecular attributes, *Acta. Chim. Slov.* **45** (3) (1998) 239–252.
4. G. Rucker, C. Rucker, On topological indices, boiling points and cycloalkanes, *J. Chem. Inf. Comput. Sci.* **39** (1999) 788–802.
5. H. Wiener, Structural determination of paraffin boiling points, *J. Am. Chem. Soc.* **69** (1947) 17–20.

6. M. P. Gonzales, A. M. Helguera, M. A. Cabrera, Quantitative structure-activity relationship to predict toxicological properties of benzene derivative compounds, *Bioorganic & Medicinal Chemistry* **13** (2005) 1775–1781.
7. M. Randić, On characterization of molecular branches, *J. Am. Chem. Soc.* **97** (1975) 6609–6615.
8. Z. Slanina, M. C. Chao, S. L. Lee, I. Gutman, On applicability of the Wiener index to estimate relative stabilities of the higher-fullerene IPR isomers, *J. Serb. Chem. Soc.* **62** (3) (1997) 211–217.
9. D. Plavsic, S. Nikolić, N. Trinajstić, Z. Mihalić, On the Harary index for the characterization of chemical graphs, *J. Math. Chem.* **12** (1993) 235–250.
10. M. Randić, Quantitative structure – property relationship: boiling points of planar benzenoids. *New J. Chem.* **20** (1996) 1001–1009.
11. A. A. Taherpour, F. Shafiei, The structural relationship between Randić indices, adjacency matrices, distance matrices and maximum wave length of linear simple conjugated polyene compounds, *J. Mol. Struct. THEOCHEM* **726** (2005) 183–188.
12. A. A. Taherpour, Quantitative structural relationship study of electrochemical properties on the nano structures, *Fullerenes, Nanotubes Carbon Nanostructures* **16** (2) (2008) 142–153.
13. Y. P. Du, Y. Z. Liang, B.Y. Li, C. J. Xu, Orthogonalization of block variables by subspace–projection for quantitative structure property relationship (QSPR) data, *J. Chem. Inf. Comput. Sci.* **42** (2002) 1128–1138.
14. M. Randić, Characterization of molecular branching, *J. Am. Chem.* **97** (23) (1975) 6609–6615.
15. Z. Slanina, F. Uhlik, S. L. Lee, E. Osawa, Geometrical and thermodynamic approaches to the relatives stabilities of Fullerene isomers, *MATCH Commun. Math. Comput. Chem.* **44** (2001) 335–348.
16. B. Lučić, N. Trinajstić, New developments in QSPR/QSAR modeling based on topological index, *SAR QSAR Environ. Res.* **7** (1997) 45–62.
17. O. Ivanciuc, T. Ivanciuc, D. Cabrol-Bass, A. T. Balaban, Evaluation in quantitative structure–property relationship models of structural descriptors derived from information-theory operators, *J. Chem. Inf. Comput. Sci.* **40** (2000) 631–643.
18. D. Bonchev, Over all connectivities / topological complexities: A new powerful tool for QSPR/QSAR, *J. Chem. Inf. Comput. Sci.* **40** (2000) 934–941.
19. S. Liu, H. Liu, Z. Xia, C. Cao, Z. Li, Molecular distance edge vector (m): An extension from alkanes to alcohols, *J. Chem. Inf. Comput. Sci.* **39** (1999) 951–957.
20. V. Sharma, R. Goswami, A. K. Madan, A novel highly discriminating topological descriptor for structure–property and structure–activity studies, *J. Chem. Inf. Comput. Sci.* **37** (1997) 273–282.

21. Z. Lin, J. Xu, X. Zheng, Z. Li, Study on quantitative structure- property relationship of chain hydrocarbons, aldehydes and alkanones by molecular distance-edge vector, *Acta Phys. Chem. Sin.* **16** (2000) 153–161.
22. O. Ivanciuc, T. Ivanciuc, D. J. Klein, W. A. Seitz, A. T. Balaban, Wiener Index Extension by Counting Even/Odd Graph Distances, *J. Chem. Inf. Comput. Sci.* **41** (3) (2001) 536–549
23. A. A. Gakh, E. G. Gakh, B. G. Sumpter, D. W. Noid, Neural network graph theory approach to the prediction of the physical properties of organic compounds, *J. Chem. Inf. Comput. Sci.* **34** (4) (1994) 832–839.
24. X. J. Yao, B. Fan, J. P. Doucet, A. Panaye, M. Liu, R. Zhang, X. Zhang, Z. Hu, Quantitative structure property relationship models for the prediction of liquid heat capacity, *QSAR Comb. Sci.* **22** (1) (2003) 29–48.
25. L. Mu, C. Feng, Quantitative structure property relations (QSPRs) for predicting standard absolute entropy,  $S_{298}^{\circ}$  of inorganic compounds, *MATCH Commun. Math. Comput. Chem.* **57** (2007) 111–134.
26. H. Wiener, Structural determination of paraffin boiling points, *J. Am. Chem. Soc.* **69** (1947) 17–20.
27. M. Randić, On characterization of molecular branches, *J. Am. Chem. Soc.* **97** (1975) 6609–6615.
28. A. T. Balaban, Highly discriminating distance based topological indices, *Chem. Phys. Lett.* **89** (1982) 399–404.
29. C. K. Das, B. Zhou, N. Trinajstić, Bounds on Harary index, *J. Math. Chem.* **46** (4) (2009) 1369–1376.
30. WWW.Chemicalize.Org.



## On the Mark and Markaracter Tables of Finite Groups

MODJTABA GHORBANI

Department of Mathematics, Faculty of Science, Shahid Rajae Teacher Training University, Tehran, 16785–136, I. R. Iran

Correspondence should be addressed to M. GHORBANI (Email: [mghorbani@srttu.edu](mailto:mghorbani@srttu.edu))

Received 22 April 2016; Accepted 26 May 2016

ACADEMIC EDITOR: ALI REZA ASHRAFI

**ABSTRACT.** Let  $G$  be a finite group and  $C(G)$  be the family of representative conjugacy classes of subgroups of  $G$ . The matrix whose  $H, K$ -entry is the number of fixed points of the set  $G/K$  under the action of  $H$  is called the table of marks of  $G$  where  $H, K$  run through all elements in  $C(G)$ . Shinsaku Fujita for the first time introduced the term “markaracter” to discuss marks for permutation representations and characters for linear representations in a common basis. In this paper, we compute these tables for some classes of finite groups.

**KEYWORDS** group action • automorphism group • mark table • markaracter table

### 1. INTRODUCTION

A **graph** is a collection of points and lines connecting them. Let us to call these points and lines by vertices and edges, respectively. Two vertices  $x$  and  $y$  are adjacent, if  $e = uv$  be an edge of graph. A graph whose all pairs of vertices are connected by a path is called a connected graph. A simple graph is a graph without loop and parallel edges. The vertex and edge-sets of graph  $G$  are represented by  $V(G)$  and  $E(G)$ , respectively.

A **molecular graph** or a chemical graph is a labeled simple graph whose vertices and edges correspond to the atoms and chemical bonds, respectively. Its vertices are labeled with the kinds of the corresponding atoms and edges are labeled with the types of bonds. In a molecular graph, it is convenient to omit hydrogen atoms. A molecular graph is a representation of the structural formula of a chemical compound in terms of graph theory, see Figure 1. For given graph  $\Gamma$ , it is called a molecular graph if the maximum degree of every vertex reaches to four. Molecular graphs are significantly important in showing the mathematical applications in chemistry.

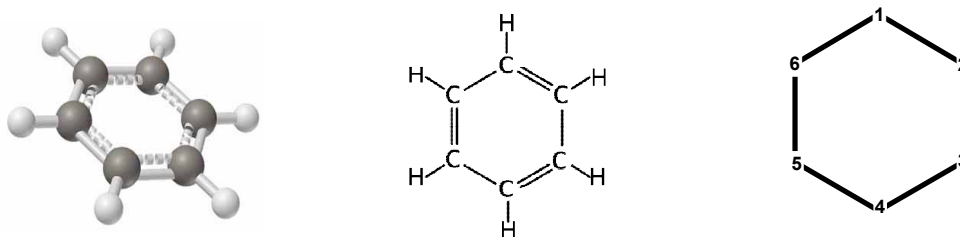


**Figure 1.** The molecular graph of benzene.

The *symmetry* of a molecule has a significant role in the analysis of the molecular structures and spectroscopy of molecules. This means that most often chemists like to classify the molecules according to their symmetry. The elements of symmetry are points, lines, planes and the collection of symmetry elements always form a group called *point group*. A geometrical figure is said to be symmetrical if there exists permutations which permute its parts while leaving the object as a whole unchanged. An isometry of this kind is called a symmetry.

Groups are often used to describe symmetries of objects. One goal of **Group Theory** is how the symmetry of a molecule is related to its physical properties and provides a method to determine the relevant physical information of the molecule. In other words, the symmetry of a molecule provides many important physical aspects and this is what makes group theory so powerful.

In general, a *group*  $\langle G, * \rangle$  is a set of elements with a binary operation "\*" which satisfy in three following properties:

1. Associative law, that is for every three elements  $a, b, c \in G$ , we have  $a*(b*c) = (a*b)*c$ .
2. There is an identity element,  $e$ , so that  $a*e = e*a = a$  for any  $a$  belonging to the group.
3. Every element has its inverse as the member of the group *i.e.*, if  $a \in G$ , then  $a^{-1} \in G$ .

If  $a*b = e$  it means that  $a$  is the inverse of  $b$  and vice versa. For the sake of simplicity, we usually omit the operation "\*" and we use  $ab$  instead of  $a*b$ . The order of a group is defined as the number of members of elements present in the group. The symmetries of a given object form a group called the symmetry group of the object. Obviously, every symmetry group is a subgroup of the group of all isometries.

The group  $G$  is cyclic if it can be generated by a single element. In this case we say that  $G$  has one generator. In other words, if  $G$  be a cyclic group, then there is an element  $g$  in  $G$ , where  $G = \{g, g^2, \dots, g^n = e\}$ . The order of this group is  $n$ . A group can be divided in several classes also called *conjugacy classes*. The importance of classes will be clear in our later studies. Choose any element, perform the so called similarity transformation *i.e.* compute  $xax^{-1}$ , where  $x$  and  $a$  belong to the group. For each  $a$ , perform this computation



with  $x$  being all members of the group. Hence, for every element  $x \in G$ , the conjugacy class  $x^G$  is as follows:

$$x^G = \{gxg^{-1} : g \in G\}.$$

**Example 1.** Consider the molecular graph of benzene in Figure 1. Here, we compute its symmetry group. This molecule has the structure of a hexagon with a carbon atom at each corner. Evidently, the simplest symmetry of this molecule is a clock-wise rotation  $\rho$  through the angle  $\pi/3 = 60^\circ$ . A six-fold repetition of this rotation brings each vertex back to its original position so  $\rho$  satisfies the operator equation  $\rho^6 = e$ . This relation implies that the set  $\{\rho, \dots, \rho^6 = e\}$  compose a group called the rotational symmetry group of a hexagon, or a cyclic group of order 6 and commonly denoted by  $Z_6$ . The order of a finite group is the number of elements it contains. The element  $\rho$  is said to be a generator of  $Z_6$ , because the entire group can be generated from  $\rho$  by the group operation. The group  $Z_6$  is completely determined by the condition  $\rho^6 = e$  and any such condition on the generators of a group is called a relation of the group. A set of relations which completely determine a group is called a presentation of the group. For  $Z_6$  the presentation consists of the single relation  $\rho^6 = e$ . The symmetry group of benzene has also another generator  $\delta$  that is a rotation by  $\pi$  radians about an axis passing through the center of a regular hexagon and vertices 1, 4. Hence, one can easily see that all elements of symmetry group of benzene are as follows:

$$\{\rho, \rho^2, \rho^3, \rho^4, \rho^5, \rho^6 = 1, \delta\rho, \delta\rho^2, \delta\rho^3, \delta\rho^4, \delta\rho^5, \delta\}.$$

Let  $X = \{1, 2, \dots, n\}$ , a permutation group on  $X$  is a group  $G$  whose elements are permutations of  $X$ , e.g. bijective functions from  $X$  to  $X$  and whose group operation is the composition of permutations in  $G$ . The group of all permutations of  $X$  is the symmetric group of  $X$  denoted by  $S_X$  or  $S_n$ , where  $X$  is finite. By this notation, a finite permutation group is a subgroup of the symmetric group  $S_n$ .

Consider the molecular graph  $H_2O$  of water molecule as depicted in Figure 2, the function

$$f = \begin{pmatrix} 1 & 2 & 3 \\ 2 & 1 & 3 \end{pmatrix} = (1, 2)$$

is a symmetry element of this graph.

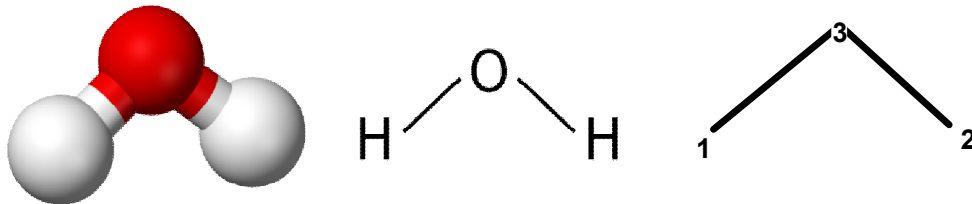


**Figure 2.** 2-D and 3-D graph of water molecule.

Let  $G$  be a group and  $X$  a non-empty set. An action of  $G$  on  $X$  is denoted by  $(G|X)$  and  $X$  is called a  $G$ -set. It induces a group homomorphism  $\varphi$  from  $G$  into the symmetric group  $SX$  on  $X$ , where  $\varphi(g)x = gx$  for all  $x \in X$ . The orbit of  $x$  will be denoted by  $Gx$  and defines as the set of all  $\varphi(g)x$ ,  $g \in G$ . The set of all  $G$ -orbits will be denoted by  $G \backslash X = \{Gx | x \in X\}$ . In the current study, we compute some properties of mark and markaracter tables. In the second and the third sections of the article, we present some elementary properties of these tables and we compute the markaracter tables of product groups in terms of Kronecker product. In the fourth section, we propose a formula for computing the full automorphism group of a graph via the mark table of its symmetry group. In section four, we also compute the symmetry group of some well-known molecular graphs.

## 2. MAIN RESULTS AND DISCUSSION

The concept of the table of marks of a finite group was introduced by one of the pioneers of finite groups, William Burnside in the second edition of his classical book [1]. This table describes a characterization of the permutation representations of a group  $G$  by certain numbers of fixed points and in some detail the partially ordered set of all conjugacy classes of subgroups of  $G$ . Hence it provides a very compact description of the subgroup lattice of  $G$ , see [2] for details. Suppose the set of fixed points of the subgroup  $U$  in the action of  $G$  on  $X$  is

$$\text{Fix}_X(U) = \{x \in X : x.u = x; \forall u \in U\}.$$

Then the  $ij^{\text{th}}$  entry of mark table of  $G$  is as follows:

$$M_{ij}(G) = |\text{Fix}_{G/G_j}(G_i)|.$$

Let also  $U$  and  $V$  be subgroups of  $G$  and  $v_G(V, U) = |\{U^g : g \in G, U^g \leq V\}|$ , thus we have:

**Lemma 1.** [2]  $|\text{Fix}_{G/U}(U)| = [G:U]v_G(V, U)/v_G(G, U)$ .

**Theorem 2.** Let  $G$  be a finite group and  $G_1, G_2, \dots, G_s$  be all non-conjugated subgroups of  $G$  in which  $|G_1| \leq |G_2| \leq \dots \leq |G_s|$ . Then the matrix  $M(G)$  is a lower triangular matrix and for all  $1 \leq i, j \leq s$ ,  $M_{ij} | M_{1j}$ .

**Proof.** By using definition of the markaracter table the first claim can be proved and for the second claim, use Lemma 1.

**Lemma 3.** Let  $G$  be a finite group and  $G_i \leq G$  be a subgroup. Then

$$M_{ii} = [N_G(G_i) : G_i].$$

In particular, if  $G_j$  be a normal subgroup of  $G$  ( $1 \leq j \leq s$ ), then

$$M_{ij} = \begin{cases} |G|/|G_j| & G_i \subseteq G_j \\ 0 & \text{otherwise} \end{cases}.$$

**Proof.** By using definition of the mark table, we have:

$$\begin{aligned} M_{ii} &= |\{gG_i : \forall x \in G_i, x.gG_i = gG_i\}| \\ &= |\{gG_i : \forall x \in G_i, g^{-1}xgG_i = G_i\}| \\ &= |\{gG_i : \forall x \in G_i, x \in gG_i g^{-1}\}| \\ &= |\{gG_i : G_i = gG_i g^{-1}\}|. \end{aligned}$$

On the other hand, similar to the proof of Lemma 1, one can see that

$$M_{ij} = |\{gG_j : G_i \subseteq g^{-1}G_j g\}|.$$

Since  $G_j$  is normal then,  $g^{-1}G_j g = G_j$ . This completes the proof.

Let the finite group  $G$  act on a finite set  $X = \{x_1, x_2, \dots, x_k\}$ . The permutation representation  $\mathfrak{R}(G)$  is a set of permutations  $\eta_g$  on  $X$ , each of which is associated with an element  $g \in G$  so that  $\mathfrak{R}(G)$  and  $G$  are homomorphic and  $\eta_g \eta_{g'} = \eta_{gg'}$  for any  $g, g' \in G$ . Let  $H$  be a subgroup of  $G$ . It is a well-known fact that the set of cosets of  $H$  in  $G$  provides a partition of  $G$  as  $G = Hg_1 + Hg_2 + \dots + Hg_m$ , where  $g_1 = I$ , the identity element of  $G$  and  $g_i \in G$ . The set of  $\{g_1, g_2, \dots, g_m\}$  is called a transversal. Consider the set of cosets  $\{Hg_1, Hg_2, \dots, Hg_m\}$ . Following **Shinsaku Fujita** [3], for any  $g \in G$ , the set of permutations,

$$\bar{\eta}_g = \begin{pmatrix} Hg_1 & Hg_2 & \dots & Hg_m \\ Hg_1 g & Hg_2 g & \dots & Hg_m g \end{pmatrix},$$

constructs a permutation representation of  $G$ , which is called a **coset representation** of  $G$  by  $H$  and notified as  $\mathfrak{R}(G/H)$ . The degree of  $\mathfrak{R}(G/H)$  is  $m = [G:H]$ , where  $|G|$  is the number of elements in  $G$ . Obviously, the coset representation  $\mathfrak{R}(G/H)$  is transitive, *i.e.* has one orbit.

The **Burnside's theorem** states that any permutation representation  $\mathfrak{R}(G)$  of a finite group  $G$  acting on  $X$  can be reduced into transitive CRs in accord with equation  $\mathfrak{R}(G) = \sum_{i=1}^s \alpha_i \mathfrak{R}(G/G_i)$ , wherein the multiplicity  $\alpha_i$  is a non-negative integer obtained by solving equations

$$\mu_j = \sum_{i=1}^s \alpha_i M_{ij}, \quad (1 \leq j \leq s). \tag{1}$$

Here  $\mu_j$  is the number of fixed points of  $G_j$  in  $\mathfrak{R}(G)$  named mark of  $G_j$ , and the symbol  $M_{ij}$  denotes the mark of  $G_j$  in  $\mathfrak{R}(G/G_i)$ . Following Burnside, the matrix  $M(G) = [M_{ij}]$  is called the **table of mark** or **mark table** of  $G$ . The matrix  $MC(G)$  obtained from  $M(G)$  in which we select rows and columns corresponding to the cyclic subgroups of  $G$  is called the **markaracter table** of  $G$ . Shinsaku Fujita in some of his leading papers [4-14], introduced the term markaracter to discuss marks for permutation representations and characters for linear representations in a common basis.

Throughout this paper our notation is standard and taken mainly from [15, 16]. We encourage the reader to consult papers by Balasubramanian [16,17], Kerber [18] and Pfeiffer [2] and references therein for background material as well as basic computational techniques, see also [19–21].

### 3. COMPUTING MARKARACTER TABLE OF SOME GROUPS

In this section we obtain some results about markaracter tables. Let  $p$  be a prime number and  $q$  be a positive integer such that  $q|p-1$ . Define the group  $F_{p,q}$  to be presented by

$$F_{p,q} = \langle a, b, a^p = b^q = 1, b^{-1}ab = a^u \rangle$$

where  $u$  is an element of order  $q$  in multiplicative group  $Z_p^*$ . It is easy to see that  $F_{p,q}$  is a non-abelian group of order  $pq$ .

**Theorem 4. (Lagrange's Theorem)** For any finite group  $G$ , the order of every subgroup  $H$  of  $G$  divides the order of  $G$ .

Let  $G$  be a group with mark table  $M(G)$  with non-conjugate subgroups  $G_1, G_2, \dots, G_n$ . Since  $M(G)$  is a lower triangular matrix, it is non-singular and so  $\det(M(G)) \neq 0$ . On the other hand, according to Lemma 3, one can see that

$$\det(M(G)) = \prod_{i=1}^n M_{ii} = \prod_{i=1}^n [N_G(G_i) : G_i].$$

If  $\det(M(G)) = p$ , then one can prove that  $G$  is isomorphic with cyclic group  $Z_p$ . Let  $G$  be a group of order  $n$ , if  $G$  has only one subgroup  $H$  (up to isomorphism), then regarding  $[G:H] = n/m$ ,  $H$  is normal subgroup of  $G$  of order  $m$ . Hence,  $M_{22} = n/m$  and so  $\det(M(G)) = n^2/m$ . If  $m$  is not prime, then according to Lagrange's Theorem,  $H$  and so  $G$  has a subgroup of order a prime  $p$  that divides  $|H|$ , a contradiction. Hence, both  $m$  and  $n/m$  are primes and so  $|G| = pq$ , where  $p, q$  are prime numbers. Again by Lagrange's Theorem, we can prove easily that  $p=q$  and so  $|G| = p^2$ . Because  $H$  is normal subgroup of order  $p$ ,  $G$  is isomorphic with cyclic group  $Z_{p^2}$  and so  $\det(M(G)) = p^3$ . Thus, we proved the following theorem.

**Theorem 5.** Let  $G$  be a finite group and  $p, q$  be two distinct prime numbers. Then

- i)  $\det(M(G)) = p$  if and only if  $G \cong Z_p$ .

- ii) There is no group with  $\det(M(G)) = pq$ .
- iii)  $\det(M(G)) = p^3$  if and only if  $G \cong Z_{p^2}$ .
- iv) There is no group with  $\det(M(G)) = p^4$ .

**Theorem 6.** The table of marks of group  $F_{p,q}$  is as reported in Table 1. Moreover,  $\det(M(G)) = pq^2$  if and only if  $G \cong F_{p,q}$  and  $\det(M(G)) = p^2q^2$  if and only if  $G \cong Z_{p^2}$ .

**Proof.** It is easy to see that all non-conjugate subgroups of  $G = F_{p,q}$  are  $G_1 = ()$ ,  $G_2 = Q$ ,  $G_3 = P$  and  $G_4 = G$ , in which  $|Q| = q$  and  $|P| = p$ . By Sylow theorem one can see that  $P \triangleleft G$ . So, by using Lemma 3, we have  $M_{12} = p$ ,  $M_{22} = 1$  and  $M_{32} = M_{42} = 0$ . On the other hand,  $Q \ntriangleleft G$ , because  $G$  is non-abelian, hence  $M_{23} = M_{43} = 0$  and  $M_{13} = M_{33} = 0$ .

$M(F_{p,q})$	$G_1$	$G_2$	$G_3$	$G_4$
$G/G_1$	$pq$	0	0	0
$G/G_2$	$p$	1	0	0
$G/G_3$	$q$	0	$q$	0
$G/G_4$	1	1	1	1

$M(Z_{p^2})$	$G_1$	$G_2$	$G_3$	$G_4$
$G/G_1$	$pq$	0	0	0
$G/G_2$	$p$	$p$	0	0
$G/G_3$	$q$	0	$q$	0
$G/G_4$	1	1	1	1

**Table 1.(a)** The table of marks of group  $F_{p,q}$  and **(b)** The table of marks of group  $Z_{p^2}$ .

Fujita in some of his papers computed the markaracter table of cyclic groups. Here, we demonstrate how to compute the markaracter table of some abelian groups.

**Theorem 7.** Let  $G$  and  $H$  be groups acting on sets  $X$  and  $Y$ , respectively. Then

$$|\text{Fix}_{X \times Y}(U \times V)| = |\text{Fix}_X(U)| \times |\text{Fix}_Y(V)|,$$

where  $U \leq G$ ,  $V \leq H$  and  $\text{Fix}_X(U) = \{x \in X \mid xg = x, \forall g \in U\}$ .

**Proof.** We have:

$$\begin{aligned} |\text{Fix}_{X \times Y}(U \times V)| &= |\{(x,y) \mid (x,y)(g,h) = (x,y); \forall (g,h) \in U \times V\}| \\ &= |\{(x,y) \mid (xg,yh) = (x,y); \forall (g,h) \in U \times V\}| \\ &= |\{(x,y) \mid xg = x \& yh = y; \forall g \in U \& \forall h \in V\}| \\ &= |\{(x,y) \mid x \in \text{Fix}_X(U) \& y \in \text{Fix}_Y(V)\}| \\ &= |\text{Fix}_X(U)| \times |\text{Fix}_Y(V)|. \end{aligned}$$

**Corollary 8 [22].** Let  $G$  and  $H$  be groups of co-prime orders acting on sets  $X$  and  $Y$ , respectively. If  $MC(G) = [a_{ij}]$  and  $MC(H) = [b_{ij}]$ , then  $MC(G \times H) = [c_{rs}]$ , where  $c_{rs} = a_{i_r i_s} b_{j_r j_s}$  and  $G_{i_r} \times H_{j_r}$  ( $G_{i_s} \times H_{j_s}$ ) are the  $r$ th column and  $s$ th row of  $MC(G \times H)$ , respectively.

For any two arbitrary matrices  $A$  and  $B$ , we have the **direct product** or **Kronecker product**  $A \otimes B$  defined as

$$\begin{bmatrix} a_{11}B & a_{12}B & \cdots & a_{1n}B \\ \vdots & \vdots & \ddots & \vdots \\ a_{m1}B & a_{m2}B & \cdots & a_{mn}B \end{bmatrix}.$$

Note that if  $A$  is  $m$ -by- $n$  and  $B$  is  $p$ -by- $r$  then  $A \otimes B$  is an  $mp$ -by- $nr$  matrix. This multiplication is not usually commutative. It is an easy task to show that in Corollary 8,  $M(G \times H)$  is the Kronecker product  $M(G) \otimes M(H)$ . We now apply Lemma 3 to find another method for computing this table. To simplify our argument, in the following example, we only compute the mark table of a cyclic group of order  $p^n q^m$ .

**Example 2.** Let  $G$  be a cyclic group of order  $p^n q^m$ . It is a well-known fact that  $G$  is isomorphic to  $H \times K$  in which  $H$  and  $K$  are subgroups of  $G$  of order  $p^n$  and  $q^m$ , respectively. Suppose  $H_1, H_2, \dots, H_{n+1}$  and  $K_1, K_2, \dots, K_{m+1}$  are all subgroups of  $H$  and  $K$ , respectively. One can see that  $MC(H) = [a_{ij}]$  and  $MC(K) = [b_{ij}]$ , where

$$a_{ij} = \begin{cases} p^{n-j+1} & j \leq i \\ 0 & \text{otherwise} \end{cases} \text{ and } b_{ij} = \begin{cases} q^{m-j+1} & j \leq i \\ 0 & \text{otherwise} \end{cases}.$$

Then  $MC(H \times K) = [c_{rs}]$ , in which

$$c_{rs} = \begin{cases} p^{n-j_r+1} q^{m-j_s+1} & j_r \leq i_r, j_s \leq i_s \\ 0 & \text{otherwise} \end{cases}.$$

The dihedral group  $D_{2n}$  is the symmetry group of an  $n$ -sided regular polygon for  $n > 1$ . These groups are one of the most important classes of finite groups currently applicable in chemistry. For example  $D_6, D_8, D_5$  and  $D_{12}$  point groups are dihedral groups. One group presentation for  $D_{2n}$  is  $\langle x, y \mid x^2 = y^n = 1, (xy)^n = 1 \rangle$ .

**Theorem 9 [22].** Suppose  $G = D_{2n}$  is the dihedral group of order  $2n$ . Then

$$\begin{aligned} 1 = G_1, \langle b \rangle = G_2, \langle ab \rangle = G_3, \langle a^{n/2} \rangle = G_4, \langle a^{v_5} \rangle = G_5, \langle a^{v_6} \rangle = G_6, \\ \dots, \langle a^{v_{t+1}} \rangle = \langle a \rangle = G_{t+2} \end{aligned}$$

are all cyclic non-conjugate subgroups of  $D_n$  such that  $v_i$  divides  $n$  and  $t$  is the number of divisors of  $n$ . Moreover the markaracter table of  $G$  is as reported in Table 2.

**Proof.** Suppose  $MC(G) = [a_{ij}]$  is markaracter table of  $D_{2n}$ . We first assume  $n$  is even. Then the conjugacy classes of  $D_{2n}$  are

$$\{1\}, \{a^{n/2}\}, \{a^r, a^{-r}\} \ (1 \leq r \leq n/2), \{a^s b \mid 0 \leq s \leq n-1 \ \& \ 2 \mid s\}, \{a^s b \mid 0 \leq s \leq n-1 \ \& \ 2 \nmid s\}.$$

Hence up to conjugacy there are three subgroups of order 2,  $G_2 = \langle b \rangle$ ,  $G_3 = \langle ab \rangle$ ,  $G_4 = \langle a^{n/2} \rangle$  and  $t = d(n)$  cyclic subgroups whose orders divide  $n$ , say  $G_5, \dots, G_{t+2} = \langle a \rangle$ . By using Lemma 3,  $a_{ij} = |\{G_i g \mid G_j \subseteq g^{-1} G_i g\}|$  and so  $a_{ii} = |N_G(G_i)| / |G_i|$ . Clearly,  $N_G(\langle b \rangle) = \{1, b, a^{n/2}, a^{n/2} b\}$ ,  $N_G(\langle a^{n/2} \rangle) = G$  and  $N_G(\langle ab \rangle) = \{1, ab, a^{n/2}, a^{1+n/2} b\}$ . So  $a_{22} = a_{33} = 2$  and  $a_{44} = n$ . Suppose  $j \mid n$ . By an elementary fact in finite groups  $o(a^j) = n/j$ . Since every subgroup of  $\langle a \rangle$  is normal in  $G$ ,  $a_{ij} = 2n/(n/j) = 2j$ . If  $v_j \mid v_i$  then  $G_j \subseteq G_i$  and so  $a_{ij} = 2j$ , as desired. We now assume that  $n$  is odd. Then the conjugacy classes of  $D_{2n}$  are  $\{1\}$ ,  $\{a^r, a^{-r}\}$  ( $1 \leq r \leq (n-1)/2$ ),  $\{a^s b \mid 0 \leq s \leq n-1\}$  and up to conjugacy there is one only subgroup of order 2 and  $d(n)$  cyclic subgroups whose orders divide  $n$ . Now a similar argument as above, complete the proof.

$M(D_{2n})$	$G_1$	$G_2$	$G_3$	$G_4$	$G_i = \langle a^{v_i} \rangle \ (5 \leq i \leq t+2)$
$G/\langle \rangle$	$2n$	0	0	0	0
$G/G_2$	$N$	2	0	0	0
$G/G_3$	$N$	0	2	0	0
$G/G_4$	$N$	0	0	$n$	0
$G/G_i \ (5 \leq i \leq t+2)$	$2j$	0	0	$\alpha$	$\gamma$

**Table 2(a).** The markaracter table of  $D_{2n}$ , where  $n$  is even.

$M(D_{2n})$	$G_1$	$G_2$	$G_j = \langle x^j \rangle \ (3 \leq j \leq t+2)$
$G/\langle \rangle$	$2n$	0	0
$G/G_2$	$n$	1	0
$G/G_j \ (3 \leq j \leq t+2)$	$2j$	0	$\alpha$

**Table 2(b).** The markaracter table of  $D_{2n}$ , where  $n$  is odd.

$$\text{where } \alpha = \begin{cases} 2j & v_j \mid \frac{n}{2} \\ 0 & \text{Otherwise} \end{cases} \quad \text{and } \gamma = \begin{cases} 2j & v_j \mid v_i \\ 0 & \text{Otherwise} \end{cases}.$$

#### 4. APPLICATION IN CHEMISTRY

A bijection  $\sigma$  on vertices set of graph  $\Gamma$  is named an automorphism of graph, if it preserves the edge set. In other words,  $\sigma$  is an automorphism if  $e = uv$  is an edge, then  $\sigma(e) = \sigma(u)\sigma(v)$  is an edge of  $E$ . Let  $Aut(\Gamma) = \{\alpha: V \rightarrow V, \alpha \text{ is bijection}\}$ , then  $Aut(\Gamma)$  under the composition of mappings forms a group.

The adjacency matrix  $A(\Gamma)$  of graph  $\Gamma$  with vertex set  $V(\Gamma) = \{v_1, v_2, \dots, v_n\}$  is the  $n \times n$  symmetric matrix  $[a_{ij}]$  such that  $a_{ij} = 1$  if  $v_i$  and  $v_j$  are adjacent and 0, otherwise. The **Euclidean matrix** of a chemical graph to find its symmetry. Here the Euclidean matrix of a molecular graph  $\Gamma$  is a matrix  $D(\Gamma) = [d_{ij}]$ , where for  $i \neq j$ ,  $d_{ij}$  is the Euclidean distance between the nuclei  $i$  and  $j$ . In this matrix  $d_{ii}$  can be taken as zero if all the nuclei are equivalent. Otherwise, one may introduce different weights for different nuclei. Suppose  $\sigma$  is a permutation on  $n$  atoms of the molecule under consideration. Then the permutation matrix  $P_\sigma$  is defined as  $P_\sigma = [x_{ij}]$ , where  $x_{ij} = 1$  if  $i = \sigma(j)$  and 0 otherwise. It is easy to see that  $P_\sigma P_\tau = P_{\sigma\tau}$ , for any two permutations  $\sigma$  and  $\tau$  on  $n$  objects, and so the set of all  $n \times n$  permutation matrices is a group isomorphic to the symmetric group  $S_n$  on  $n$  symbols. For computing the symmetry of a molecule, it is sufficient to solve the matrix equation  $P^t E P = E$ , where  $E$  is the Euclidean matrix of the molecule under consideration and  $P$  varies on the set of all permutation matrices with the same dimension as  $E$ .

By having the mark character table of symmetry group of a graph, we can compute the full automorphism group of underlying graph by an algebraic way. Consider the following example. The full automorphism group of a graph is one of the most important problem in graph theory and this is the first attempt to solve this problem by using the mark table.

**Example 3.** Consider the skeleton of naphthalene, Figure 3. The generators of its symmetry group are  $\lambda$  and  $\omega$ , where  $\lambda = (1, 9)(2, 10)(3, 7)(4, 8)$  and  $\omega = (1, 2)(3, 4)(5, 6)(7, 8)(9, 10)$ . The subgroups of  $G$  are  $G_1 = \langle () \rangle$ ,  $G_2 = \langle \lambda \rangle$ ,  $G_3 = \langle \omega \rangle$ ,  $G_4 = \langle \lambda \omega \rangle$  and  $G_5 = G$ . This group is isomorphic with  $Z_2 \times Z_2$ , where  $Z_2$  is a group of order 2. Since every group of order 4 is abelian and then  $Z_2 \times Z_2$ , by using Corollary 4, for any subgroup  $G_i$  of  $Z_2 \times Z_2$ ,  $M_{ij} = 0$  or  $|Z_2 \times Z_2|/|G_i|$ . But for the pure subgroup  $H$  of  $Z_2 \times Z_2$ ,  $|H| = 2$ . This implies the entries of mark table are 1, 2 and 4. By Theorem 2,  $M_{11} = 4$  and  $M_{i1} = 0$  for  $2 \leq i \leq 4$ . Also  $M_{4j} = 1$  for  $1 \leq j \leq 4$ . Since all subgroups in Abelian group are normal, by using Corollary 4, we have



$M_{12} = M_{22} = 2$  and  $M_{32} = M_{42} = 0$ . Using again Corollary 4, it is easy to see that  $M_{13} = M_{33} = 2$  and  $M_{23} = M_{43} = 0$ . In Tables 1 and 2, the mark table and markaracter table of this group are computed. On the other hand, the number of  $(\mu_j)$  of fixed points are obtained by a geometrical examination of Eq.(1):

$$(10,2,0,0,0) = (\alpha_{G_1}, \alpha_{G_2}, \alpha_{G_3}, \alpha_{G_4}, \alpha_{G_5}) \times \begin{pmatrix} 4 & 0 & 0 & 0 & 0 \\ 2 & 2 & 0 & 0 & 0 \\ 2 & 0 & 2 & 0 & 0 \\ 2 & 0 & 0 & 2 & 0 \\ 1 & 1 & 1 & 1 & 1 \end{pmatrix}.$$

So, by solving these equations we have  $\alpha_{G_5} = \alpha_{G_4} = \alpha_{G_3} = 0$ ,  $\alpha_{G_1} = 2$ ,  $\alpha_{G_2} = 1$  and  $P_G = 2G(/G_1) + G(/G_2)$ . This implies sub-orbits of  $X$  are  $X_{11} = \{1, 2, 9, 10\}$ ,  $X_{21} = \{5, 6\}$ ,  $X_{12} = \{3, 4, 7, 8\}$ .

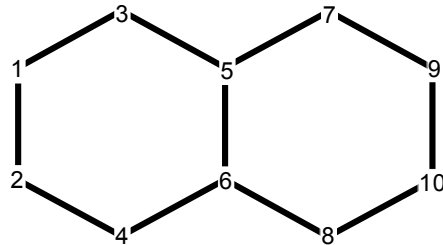


Figure 3. The skeleton of naphthalene.

$M(Z_2 \times Z_2)$	$G_1$	$G_2$	$G_3$	$G_4$	$G_5$
$G(/G_1)$	4	0	0	0	0
$G(/G_2)$	2	2	0	0	0
$G(/G_3)$	2	0	2	0	0
$G(/G_4)$	2	0	0	2	0
$G(/G_5)$	1	1	1	1	1

Table 3. Mark table of the point group  $Z_2 \times Z_2$ .

$MC(Z_2 \times Z_2)$	$G_1$	$G_2$	$G_3$	$G_4$
$G/G_1$	4	0	0	0
$G/G_2$	2	2	0	0
$G/G_3$	2	0	2	0
$G/G_4$	2	0	0	2

**Table 4.** Markaracter table of the point group  $Z_2 \times Z_2$ .

Using a similar discussion, the generators of the point group of antheracene skeleton (Figure 4) are  $\delta$  and  $\gamma$ , where

$$\gamma = (1, 13)(2, 14)(3, 11)(4, 12)(5, 9)(6, 10),$$

$$\eta = (1, 2)(3, 4)(5, 6)(7, 8)(9, 10)(11, 12)(13, 14).$$

The subgroups of  $G$  are  $G_1 = \langle () \rangle$ ,  $G_2 = \langle \gamma \rangle$ ,  $G_3 = \langle \eta \rangle$ ,  $G_4 = \langle \gamma\eta \rangle$  and  $G_5 = G$ . Also, the mark table and markaracter table of this group are the same of naphthalene. Similarly, one can see that the sub-orbits of  $X$  are  $X_{11} = \{1, 2, 13, 14\}$ ,  $X_{21} = \{7, 8\}$ ,  $X_{22} = \{5, 6, 9, 10\}$  and  $X_{12} = \{3, 4, 11, 12\}$ .

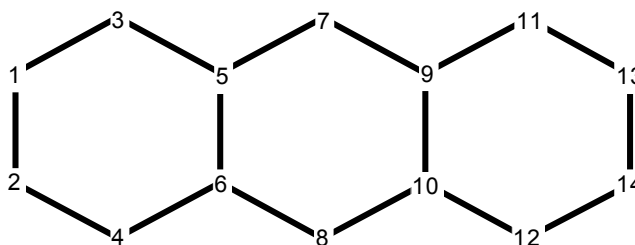


**Figure 4.** The skeleton of antheracene.

In generally, consider the graph of benzenoid chain with exactly  $n$  hexagons, Figure 5. Its point group is isomorphic with group  $Z_2 \times Z_2$  generated by  $\alpha$  and  $\beta$  where

$$\alpha = (1, 3)(2, 4) \cdots (4n - 4, 4n - 2)(4n - 3, 4n - 1),$$

$$\beta = (1, 2)(3, 4) \cdots (4n - 1, 4n)(4n + 1, 4n + 2).$$

This implies the mark table and markaracter table of a benzenoid chain with exactly  $n$  hexagons are similar to antheracene and naphthalene.

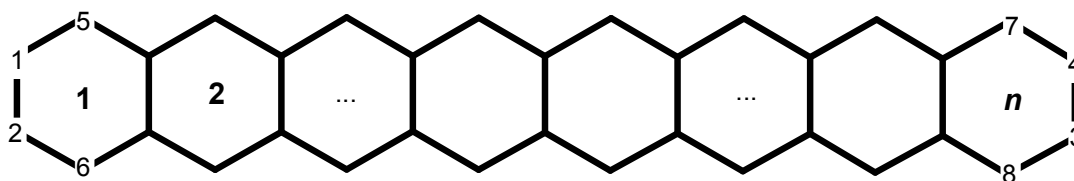


**Figure 5.** The skeleton of a benzenoid chain with  $n$  hexagons.

## REFERENCES

1. W. Burnside, *Theory of Groups of Finite Order*, The University Press, Cambridge, 1897.
2. G. Pfeiffer, The subgroups of  $M_{24}$ , or how to compute the table of marks of a finite group, *Exp. Math.* 6 (3) (1997) 247–270.
3. S. Fujita, Markaracter tables and Q-conjugacy character tables for cyclic groups. An application to combinatorial enumeration, *Bull. Chem. Soc. Jpn.* 71 (1998) 1587–1596.
4. S. Fujita, Maturity of finite groups. An application to combinatorial enumeration of isomers, *Bull. Chem. Soc. Jpn.* 71 (1998) 2071–2080.
5. S. Fujita, Inherent automorphism and Q-conjugacy character tables of finite groups, An application to combinatorial enumeration of isomers, *Bull. Chem. Soc. Jpn.* 71 (1998) 2309–2321.
6. S. Fujita, *Combinatorial enumeration of graphs, three-dimensional structures, and chemical compounds*, Mathematical Chemistry Monographs: MCM 15, Kragujevac, 2013.
7. S. Fujita, Subduction of Q-conjugacy representations and characteristic monomials for combinatorial enumeration, *Theor. Chem. Acc.* 99 (1998) 224–230.
8. S. Fujita, Systematic enumeration of ferrocene derivatives by unit-subduced-cycle-index method and characteristic-monomial method, *Bull. Chem. Soc. Jpn.* 72 (1999) 2409–2416.
9. S. Fujita, A simple method for enumeration of non-rigid isomers. An application of characteristic monomials, *Bull. Chem. Soc. Jpn.* 72 (1999) 2403–2407.
10. S. Fujita, Möbius function and characteristic monomials for combinatorial enumeration, *Theor. Chem. Acc.* 101 (1999) 409–420.
11. S. Fujita, Characteristic monomials with chirality fittingness for combinatorial enumeration of isomers with chiral and achiral ligands, *J. Chem. Inf. Comput. Sci.* 4 (2000) 1101–1112.

12. S. Fujita, The unit-subduced-cycle-index methods and the characteristic-monomial method. Their relationship as group-theoretical tools for chemical combinatorics, *J. Math. Chem.* 30(3) (2001) 249–270.
13. S. Fujita, *Symmetry and Combinatorial Enumeration in Chemistry*, Springer-Verlag, Berlin-Heidelberg, 1991.
14. S. Fujita, *Diagrammatical Approach to Molecular Symmetry and Enumeration of Stereoisomers*, *Mathematical Chemistry Monographs: MCM 4*, Kragujevac, 2007.
15. N. Trinajstić, *Chemical Graph Theory*, CRC Press, Boca Raton, FL., 1992.
16. K. Balasubramanian, “Combinatorics and Spectroscopy” in *Chemical Group Theory. Techniques and Applications*, Gordon and Breach Publications, Amsterdam, 1995.
17. K. Balasubramanian, Recent applications of group theory to chemical physics in conceptual quantum chemistry: Models and applications, *Croat. Chim. Acta* 57 (1984) 1465–1492.
18. A. Kerber, Enumeration under finite group action, basic tools, results and methods, *MATCH Commun. Math. Comput. Chem.* 46 (2002) 151–198.
19. S. El-Basil, Prolegomenon on Theory and Applications of Tables of Marks, *MATCH Commun. Math. Comput. Chem.* 46 (2002) 7–23.
20. M. Ghorbani, Enumeration of hetero fullerenes: a survey, *MATCH Commun. Math. Comput. Chem.* 68 (2012) 381–414.
21. M. Ghorbani, Remarks on markcharacter table of fullerene graphs, *J. Comput. Theor. Nanosci.* 11 (2014) 363–379.
22. A. R. Ashrafi and M. Ghorbani, A note on markcharacter tables of finite groups, *MATCH Commun. Math. Comput. Chem.* 59 (2008) 595–603.

## ***Weak Algebraic Hyperstructures as a Model for Interpretation of Chemical Reactions***

**B. DAVVAZ**

Department of Mathematics, Yazd University, Yazd, Iran

Correspondence should be addressed to B. Davvaz (Email: davvaz@yazd.ac.ir)

Received 22 November 2014; Accepted 7 January 2016

ACADEMIC EDITOR: ALI REZA ASHRAFI

**ABSTRACT** The concept of weak algebraic hyperstructures or  $H_v$ -structures constitute a generalization of the well-known algebraic hyperstructures (semihypergroup, hypergroup and so on). The overall aim of this paper is to present an introduction to some of the results, methods and ideas about chemical examples of weak algebraic hyperstructures. In this paper after an introduction of basic definitions and results about weak algebraic hyperstructures, we review:

- (1) Weak algebraic hyperstructures associated with chain reactions.
- (2) Weak algebraic hyperstructures associated with dismutation reactions.
- (3) Weak algebraic hyperstructures associated with redox reactions.

**KEYWORDS** Weak algebraic hyperstructure • hypergroup •  $H_v$ -group • chain reaction • dismutation reaction • redox reaction.

### **1. INTRODUCTION**

The hyperstructure notion was introduced in 1934 by the French mathematicians Marty, at the 8th Congress of Scandinavian Mathematicians. The motivating example was the quotient of a group by any, not necessary normal, subgroup. Algebraic hyperstructures in the sense of Marty are a suitable generalization of classical algebraic structures. In a classical algebraic structure, the composition of two elements is an element, while in an algebraic hyperstructure, the composition of two elements is a set. Many papers and several books have been written till now on hyperstructures [2, 3, 4, 14, 32]. Many of them are dedicated to the applications of hyperstructures in other disciplines. In 1996, Santilli and Vougiouklis [24] point out that in physics the most interesting hyperstructures are the one called  $e$ -hyperstructures. The  $e$ -hyperstructures are special kind of hyperstructures and they can be interpreted as a generalization of two important concepts for physics: Isotopies and

Genotopies. In [15], Davvaz, Santilli and Vougiouklis studied multi-valued hyperstructures following the apparent existence in nature of a realization of two-valued hyperstructures with hyperunits characterized by matter-antimatter systems and their extensions, where matter is represented with conventional mathematics and antimatter is represented with isodual mathematics, also see [16]. In [17], the authors presented Ying's twin universes, Santilli's isodual theory of antimatter, and Davvaz–Santilli–Vougiouklis two-valued hyperstructures representing matter and antimatter in two distinct but co-existing space times. They identified a seemingly new map for both matter and antimatter providing a mathematical prediction of Ying's twin universes, and introduced a four-fold hyperstructure representing matter-antimatter as well as Ying's twin universes, all co-existing in distinct space times. Another motivation for the study of hyperstructures comes from physical phenomenon as the nuclear fission. This motivation and the results were presented by Hošková, Chvalina and Račková (see [20, 21]). In [11], the authors provided, for the first time, a physical example of hyperstructures associated with the elementary particle physics, Leptons. They have considered this important group of the elementary particles and shown that this set along with the interactions between its members can be described by the algebraic hyperstructures.

Mendel, the father of genetics took the first steps in defining “contrasting characters, genotypes in  $F1$  and  $F2$  . . . and setting different laws”. The genotypes of  $F2$  is dependent on the type of its parents genotype and it follows certain roles. In [18], Ghadiri et al. analyzed the second generation genotypes of monohybrid and a dihybrid with a mathematical structure. They used the concept of  $H_v$ -semigroup structure in the  $F2$ -genotypes with cross operation and proved that this is an  $H_v$ -semigroup. They determined the kinds of number of the  $H_v$ -subsemigroups of  $F2$ -genotypes. In [10], inheritance issue based on genetic information is looked at carefully via a new hyperalgebraic approach. Several examples are provided from different biology points of view, and it is shown that the theory of hyperstructures exactly fits the inheritance issue.

Another motivation for the study of hyperstructures comes from chemical reactions. In [6], Davvaz and Dehghan-Nezhad provided examples of hyperstructures associated with chain reactions. In [7], Davvaz et al. introduced examples of weak hyperstructures associated with dismutation reactions. In [12], Davvaz et al. investigated the examples of hyperstructures and weak hyperstructures associated with redox reactions, see [1, 8, 9, 13].

## 2. WEAK ALGEBRAIC HYPERSTRUCTURES

Weak hyperstructures or  $H_v$ -structures were introduced by Vougiouklis at the Fourth AHA congress (1990) [28]. The concept of an  $H_v$ -structure constitutes a generalization of the well-known algebraic hyperstructures (smihypergroup, hypergroup, hyperring and so on). Actually some axioms concerning the above hyperstructures such as the associative law,

the distributive law and so on are replaced by their corresponding weak axioms. Since then the study of  $H_v$ -structure theory has been pursued in many directions by Vougiouklis, Davvaz, Spartalis, Dramalidis, Hořková, and others. In this section, we present some definitions and basic facts about weak hyperstructures [5, 29, 31].

Let  $H$  be a non-empty set and  $\cdot : H \times H \rightarrow \rho^*(H)$  be a hyperoperation. The “ $\cdot$ ” in  $H$  is called *weak associative* if

$$x \cdot (y \cdot z) \cap (x \cdot y) \cdot z \neq \emptyset, \text{ for all } x, y, z \in H.$$

The “ $\cdot$ ” is called *weak commutative* if

$$x \cdot y \cap y \cdot x \neq \emptyset, \text{ for all } x, y \in H.$$

The “ $\cdot$ ” is called *strongly commutative* if

$$x \cdot y = y \cdot x, \text{ for all } x, y \in H.$$

The hyperstructure  $(H, \cdot)$  is called an  $H_v$ -semigroup if “ $\cdot$ ” is weak associative. An  $H_v$ -semigroup is called an  $H_v$ -group if

$$a \cdot H = H \cdot a = H, \text{ for all } a \in H.$$

In an obvious way, the  $H_v$ -subgroup of an  $H_v$ -group is defined.

Consider  $H = \{e, a, b, c\}$  and define  $*$  on  $H$  with the help of the following table:

*	$e$	$a$	$b$	$c$
$e$	$e$	$a$	$b$	$c$
$a$	$a$	$e, a$	$c$	$b$
$b$	$b$	$c$	$e, b$	$a$
$c$	$c$	$b$	$a$	$e, c$

Then  $(H, *)$  is an  $H_v$ -group which is not a hypergroup. Indeed, we have

$$(a * b) * c = c * c = \{e, c\}, \quad a * (b * c) = a * a = \{e, a\}.$$

Therefore,  $*$  is not associative.

A first motivation to study the weak hyperstructures is the following example.

Let  $(G, \cdot)$  be a group and  $R$  be an equivalence relation on  $G$ . In  $G/R$  consider the hyperoperation  $\odot$  defined by  $x \odot y = \{z \mid z \in x \cdot y\}$ , where  $x$  denotes the equivalence class of the element  $x$ . Then,  $(G, \odot)$  is an  $H_v$ -group which is not always a hypergroup.

All the weak properties for hyperstructures can be applied for subsets. For example, if  $(H, \cdot)$  is a weak commutative  $H_v$ -group, then for all non-empty subsets  $A, B, C$  of  $H$ , we have  $(A \cdot B) \cap (B \cdot A) \neq \emptyset$  and  $A \cdot (B \cdot C) \cap (A \cdot B) \cdot C \neq \emptyset$ . To prove this, one has simply to take one element of each set.

Let  $(H_1, \cdot), (H_2, *)$  be two  $H_v$ -groups. A map  $f : H_1 \rightarrow H_2$  is called an  $H_v$ -homomorphism or a *weak homomorphism* if

$$f(x \cdot y) \cap f(x) * f(y) \neq \emptyset, \text{ for all } x, y \in H_1.$$

$f$  is called an *inclusion homomorphism* if

$$f(x \cdot y) \subseteq f(x) * f(y), \text{ for all } x, y \in H_1.$$

Finally,  $f$  is called a *strong homomorphism* or a *good homomorphism* if

$$f(x \cdot y) = f(x) * f(y), \text{ for all } x, y \in H_1.$$

If  $f$  is onto, one to one and strong homomorphism, then it is called an *isomorphism*.

Moreover, if the domain and the range of  $f$  are the same  $H_v$ -group, then the isomorphism is called an *automorphism*. We can easily verify that the set of all automorphisms of  $H$ , defined by  $\text{Aut } H$ , is a group.

Several  $H_v$ -structures can be defined on a set  $H$ . A partial order on these hyperstructures can be introduced, as follows.

Let  $(H, \cdot)$  and  $(H, *)$  be two  $H_v$ -groups defined on the same set  $H$ . We say that “ $\cdot$ ” less than or equal to “ $*$ ” and we write  $\cdot \leq *$ , if there is  $f \in \text{Aut}(H, *)$  such that  $x \cdot y \subseteq f(x * y)$ , for all  $x, y \in H$ . If a hyperoperation is weak associative, then every greater hyperoperation, defined on the same set is also weak associative. In [30], the set of all  $Hv$ -groups with a scalar unit defined on a set with three elements is determined using this property.

Greater hyperoperation from the one of a given  $Hv$ -group defines an  $H_v$ -group. The weak commutativity is also valid for every greater hyperoperation. We remark that this statement is not true for hypergroups.

Let  $(H, \cdot)$  be an  $H_v$ -group. The relation  $\beta^*$  is the smallest equivalence relation on  $H$  such that the quotient  $H/\beta^*$  is a group.  $\beta^*$  is called the *fundamental equivalence relation* on  $H$ . If  $U$  denotes the set of all finite products of elements of  $H$ , then a relation  $\beta$  can be defined on  $H$  whose transitive closure is the fundamental relation  $\beta^*$ . The relation  $\beta$  is defined as follows: for  $x$  and  $y$  in  $H$  we write  $x\beta y$  if and only if  $\{x, y\} \subseteq u$  for some  $u \in U$ . We can rewrite the definition of  $\beta^*$  on  $H$  as follows:  $a\beta^*b$  if and only if there exist  $z_1, \dots, z_{n+1} \in H$  with  $z_1 = a, z_{n+1} = b$  and  $u_1, \dots, u_n \in U$  such that  $\{z_i, z_{i+1}\} \subseteq u_i$  ( $i = 1, \dots, n$ ). Suppose that  $\beta^*(a)$  is the equivalence class containing  $a \in H$ . Then, the product  $\odot$  on  $H/\beta^*$  is defined as follows:

$$\beta^*(a) \odot \beta^*(b) = \{\beta^*(c) \mid c \in \beta^*(a) \cdot \beta^*(b)\} \text{ for all } a, b \in H.$$

It is not difficult to see that  $\beta^*(a) \odot \beta^*(b)$  is the singleton  $\{\beta^*(c)\}$  for all  $c \in \beta^*(a) \cdot \beta^*(b)$ . In this way  $H/\beta^*$  becomes a group.

Let  $(H, \cdot)$  be an  $H_v$ -group. An element  $x \in H$  is called *single* if its fundamental class is singleton, i.e.,  $\beta^*(x) = \{x\}$ . Denote by  $SH$  the set of all single elements of  $H$ . Let  $(H, \cdot)$  be an  $H_v$ -group and  $x \in SH$ . Let  $a \in H$  and take any element  $v \in H$  such that  $x \in a \cdot v$ . Then,

$$\beta^*(a) = \{h \in H \mid h \cdot v = x\}.$$

Suppose that  $(H, \cdot)$  is an  $H_v$ -group such that  $SH$  is non-empty. Then, the only greater hyperoperations  $\cdot < *$  for which the  $H_v$ -groups  $(H, *)$  contain single elements are the ones with the same fundamental group, since the fundamental classes are determined from the products of a single element with the elements of the group. On the other hand, a less



hyperoperation  $\circ$  can have the same set  $SH$  if only in the products of non-single elements the  $\circ$  is less than  $\cdot$ . Finally, if  $\rho$  and  $\sigma$  are equivalence relations with  $\rho < \sigma$  such that  $H/\rho$  and  $H/\sigma$  are non-equal groups, then they can not have both single elements.

Let  $(H, \cdot)$  be an  $H_V$ -group with (left, right) identity elements. Then,  $H$  is called (*left, right*) *reversible* in itself when any relation  $c \in a \cdot b$  implies the existence of a left inverse  $a'$  of  $a$  and a right inverse  $b'$  of  $b$  such that  $b \in a' \cdot c$  and  $a \in c \cdot b'$ . The  $H_V$ -group  $(H, \cdot)$  is called *feebly quasi-canonical* if it is regular, reversible and satisfies the following conditions:

For each  $a \in H$ , if  $a', a''$  are inverses of  $a$ , then for each  $x \in H$ , we have:

$$a' \cdot x = a'' \cdot x \text{ and } x \cdot a' = x \cdot a''.$$

A feebly quasi-canonical  $H_V$ -group  $H$  is called *feebly canonical* if it is strongly commutative.

### 3. CHEMICAL REACTIONS

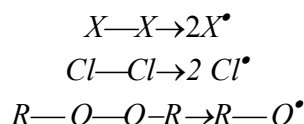
Chemistry is the study of matter and of the changes matter undergoes. A chemical equation describes the products of a reaction that from the starting molecules or atoms. Chemistry seeks to predict the products that result from the reaction of specific quantities of atoms or molecules. Chemists accomplish this task by writing and balancing chemical equations. Symmetry is very important in chemistry researches and group theory is the tool that is used to determine symmetry. Classical algebraic structures (group theory) is a mathematical method by which aspects of a molecule's symmetry can be determined. Algebraic hyperstructures are generalizations of classical algebraic structures. In a classical algebraic structure, the composition of two elements is a set. A motivation for the study of hyperstructures comes from chemical reactions. In [6], Davvaz and Dehghan-Nezhad provided examples of hyperstructures associated with chain reactions. In [7], Davvaz et al. introduced examples of weak hyperstructures associated with dismutation reactions. In [12], Davvaz et al. investigated the examples of hyperstructures and weak hyperstructures associated with redox reactions. In this section we review these examples. For more details we refer to [6, 7, 12].

#### 3.1 CHAIN REACTIONS

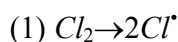
Chain reaction, in chemistry and physics, process yielding products that initiate further processes of the same kind, a self-sustaining sequence. Examples from chemistry are burning a fuel gas, the development of rancidity in fats, "knock" in internal combustion engines, and the polymerization of ethylene to polyethylene. The best known examples in physics are nuclear fissions brought about by neutrons. Chain reactions are in general very rapid but are also highly sensitive to reaction

conditions, probably because the substances that sustain the reaction are easily affected by substances other than the reactants themselves. An atom or group of atoms possessing an odd (unpaired) electron is called radical. Radical species can be electrically neutral, in which case they are sometimes referred to as free radicals. Pairs of electrically neutral "free" radicals are formed via homolytic bond breakage. This can be achieved by heating in non-polar solvents or the vapor phase. At elevated temperature or under the influence of ultraviolet light at room temperature, all molecular species will dissociate into radicals. Homolysis or homolytic bond fragmentation occurs when (in the language of Lewis theory) a two electron covalent bond breaks and one electron goes to each of the partner species.

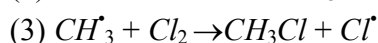
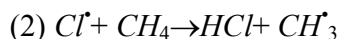
For example, chlorine,  $Cl_2$ , forms chlorine radicals ( $Cl^\bullet$ ) and peroxides form oxygen radicals.



Radical bond forming reactions (radical couplings) are rather rare processes. The reason is because radicals are normally present at low concentrations in a reaction medium, and it is statistically more likely they will abstract a hydrogen, or undergo another type of a substitution process, rather than reacting with each other by coupling. And as radicals are uncharged, there is little long range coulombic attraction between two radical centers. Radical substitution reactions tend to proceed as chain reaction processes, often with many thousands of identical propagation steps. The propensity for chain reactivity gives radical chemistry a distinct feel compared with polar Lewis acid/base chemistry where chain reactions are less common. Methane can be chlorinated with chlorine to give chloromethane and hydrogen chloride. The reaction proceeds as a chain, radical, substitution mechanism. The process is a little more involved, and three steps are involved: initiation, propagation and termination:

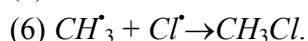
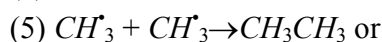


(1) is called chain-initiating step.



then (2), (3), (2), (3), etc, until finally:

(2) and (3) are called chain-propagating steps.



(4), (5) and (6) are called chain-terminating steps.

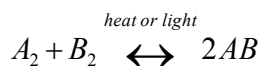
First in the chain of reactions is a chain-initiating step, in which energy is absorbed and a reactive particle generated; in the present reaction it is the cleavage of chlorine into atoms (Step 1). There are one or more chain-propagating steps, each of which consumes a reactive particle and generates another; there they are the reaction of chlorine atoms with methane (Step 2), and of methyl radicals with chlorine (Step 3).

A chlorine radical abstracts a hydrogen from methane to give hydrogen chloride and a methyl radical. The methyl radical then abstracts a chlorine atom (a chlorine radical) from  $Cl_2$  to give methyl chloride and a chlorine radical... which abstracts a hydrogen from methane... and the cycle continues... Finally there are chain-terminating steps, in which reactive particles are consumed but not generated; in the chlorination of methane these would involve the union of two of the reactive particles, or the capture of one of them by the walls of the reaction vessel.

The halogens are all typical non-metals. Although their physical forms differ fluorine and chlorine are gases, bromine is a liquid and iodine is a solid at room temperature, each consists of diatomic molecules;  $F_2, Cl_2, Br_2$  and  $I_2$ . The halogens all react with hydrogen to form gaseous compounds, with the formulas  $HF, HCl, HBr$  and  $HI$  all of which are very soluble in water. The halogens all react with metals to give halides.



The reader will find in [22] a deep discussion of chain reactions and halogens. During chain reaction



there exist all molecules  $A_2, B_2, AB$  and whose fragment parts  $A^*, B^*$  in experiment. The elements of this collection can be combined with each other. All combinational probabilities for the set  $H = \{A^*, B^*, A_2, B_2, AB\}$  to do without energy can be displayed as in Table 1.

**Table 1.** Chain Reactions.

$\oplus$	$A^*$	$B^*$	$A_2$	$B_2$	$AB$
$A^*$	$A^*, A_2$	$A^*, B^*, AB$	$A^*, A_2$	$A^*, B_2, B^*, AB$	$A^*, AB, A_2, B^*$
$B^*$	$A^*, B^*, AB$	$B^*, B_2$	$A^*, B^*, AB, A_2$	$B^*, B_2$	$A^*, B^*, AB, B_2$
$A_2$	$A^*, A_2$	$A^*, B^*, AB, A_2$	$A^*, A_2$	$A^*, B^*, A_2, B_2, AB$	$A^*, B^*, A_2, AB$
$B_2$	$A^*, B^*, B_2, AB$	$B^*, B_2$	$A^*, B^*, A_2, B_2, AB$	$B^*, B_2$	$A^*, B^*, B_2, AB$
$AB$	$A^*, AB, A_2, B^*$	$A^*, B^*, AB, B_2$	$A^*, B^*, A_2, AB$	$A^*, B^*, B_2, AB$	$A^*, B^*, A_2, B_2, AB$

Then,  $(H, \oplus)$  is an  $H_v$ -group [6]. Moreover,  $X = \{A^*, A_2\}$  and  $Y = \{B^*, B_2\}$  are only  $H_v$ -subgroups of  $(H, \oplus)$  [6]. If we consider  $A = H$  and  $B \in \{F, CL, Br, I\}$  (for example  $B = I$ ), the complete reactions table becomes Table 2.

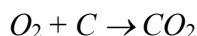
**Table 2.** For  $H$  and  $I$ .

$\oplus$	$H^*$	$I^*$	$H_2$	$I_2$	$HI$
$H^\circ$	$H^*, H_2$	$H^*, I^*, HI$	$H^*, H_2$	$H^*, I_2, I^*, HI$	$H^*, HI, H_2, I^*$
$I^*$	$H^*, I^*, HI$	$I^*, I_2$	$H^*, I^*, HI, H_2$	$I^*, I_2$	$H^*, I^*, HI, I_2$
$H_2$	$H^*, H_2$	$H^*, I^*, HI, I_2$	$H^*, H_2$	$H^*, I^*, H_2, I_2, HI$	$H^*, I^*, H_2, HI$
$I_2$	$H^*, I^*, I_2, HI$	$H^*, I_2$	$H^*, I^*, H_2, I_2, HI$	$H^*, I_2$	$H^*, I^*, I_2, HI$
$HI$	$H^*, HI, H_2, I^*$	$H^*, I^*, HI, I_2$	$H^*, I^*, H_2, HI$	$H^*, I^*, H_2, HI$	$H^*, I^*, H_2, I_2, HI$

### 3.2 DISMUTATION REACTIONS

In a redox reactions or oxidation-reduction reaction, electrons are transferred from one reactant to another. Oxidation refers to the loss of electrons, while reduction refers to the gain of electrons. A substance that has strong affinity for electrons and tends to extract them from other species is called an oxidizing agent or an oxidant. A reducing agent, or reductant, is a reagent that readily donates electrons to another species [26]. A half reaction is a reduction or an oxidation reaction. Two half-reactions are needed to form a whole reaction. Redox reactions have a number of similarities to acid-base reactions. Like acid-base reactions, redox reactions are a matched set; you don't have an oxidation reaction without a reduction reaction happening at the same time. When the change in free energy ( $\Delta G$ ) is negative, a process or chemical reaction proceeds spontaneously in the forward direction. When  $\Delta G$  is positive, the process proceeds spontaneously in reverse. In electrochemical reactions  $\Delta G = -nFE$ , where  $n$ ,  $F$  and  $E$  are number of electrons transferred in the reaction, Faraday constant and cell potential, respectively [26].

The change in the oxidation state of a species lets you know if it has undergone oxidation or reduction. Oxidation is the process in which an atom undergoes an algebraic increase in oxidation number, and reduction is the process in which an atom undergoes an algebraic decrease in oxidation number. On this basis, oxidation-reduction is involved in the reaction;



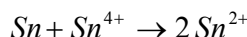
In the reaction, oxidation number of the  $C$  atom increases from zero to +4 whereas, the oxidation number of  $O$  atom decreases from zero to -2. Furthermore, the total increase in the oxidation number equals to the total decrease in oxidation number [23].

Disproportion at ion or dismutation is used to describe two particular types of chemical reaction:

- (1) A chemical reaction of the type  $2A \rightarrow A' + A''$ , where  $A, A'$  and  $A''$  are different chemical pieces [27]. Most but not all are redox reactions. For example  $2H_2 \rightarrow OH_3O^+ + OH^-$  is a *disproportionation*, but is not a redox reaction.
- (2) A chemical reaction in which two or more atoms of the same element originally having the same oxidation state react with other chemical(s) or themselves to give different oxidation numbers. In another word, disproportionation is a reaction in which a species is simultaneously reduced and oxidized to form two different oxidation numbers. The reverse of disproportionation is called *comproportionation*. *Comproportionation* is a chemical reaction where two reactants, each containing the same element but with a different oxidation number, will form a product with an oxidation number intermediate of the two reactants. For example, an element tin in the oxidation states 0 and +4 can comproportionate to the state +2. The standard reduction potentials of all half reactions are:

$$E^\circ_{Sn^{4+}/Sn^{2+}} = 0.154 V, E^\circ_{Sn^{2+}/Sn} = -0.136 V, E^\circ_{Sn^{4+}/Sn} = 0.009 V$$

Therefore, the comproportionation reaction is spontaneous.

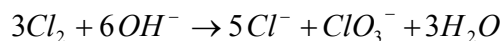


All combinational probability for the set  $S = \{Sn, Sn^{2+}, Sn^{4+}\}$  to do without energy can be displayed as follows. The major products are written in Table 3.

**Table 3.** Dismutation Reactions  $S_n$ .

$\oplus$	$Sn$	$Sn^{2+}$	$Sn^{4+}$
$Sn$	$Sn$	$Sn, Sn^{2+}$	$Sn^{2+}$
$Sn^{2+}$	$Sn, Sn^{2+}$	$Sn^{2+}$	$Sn^{2+}, Sn^{4+}$
$Sn^{4+}$	$Sn^{2+}$	$Sn^{2+}, Sn^{4+}$	$Sn^{4+}$

Then,  $(S, \oplus)$  is weak associative. Also, we can conclude that  $(\{S_n, S_n^{2+}\}, \oplus)$  is a hypergroup and  $(\{Sn^{2+}, Sn^{4+}\}, \oplus)$  is an  $H_v$ -semigroup [7]. Chlorine gas reacts with dilute hydroxide to form chloride, chlorate and water. The ionic equation for this reaction is as follows [19]:



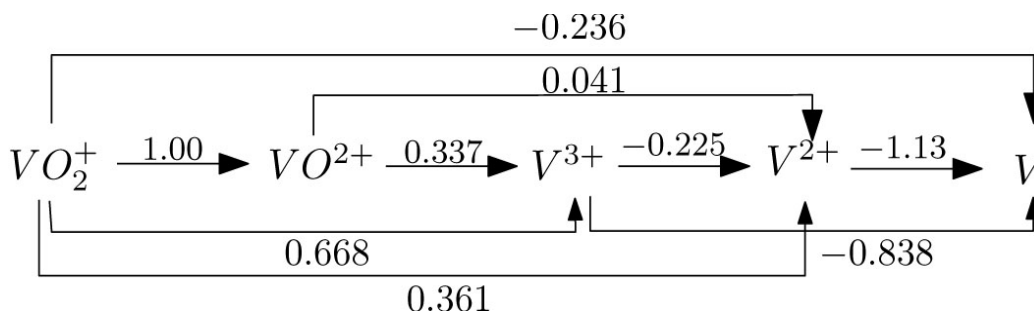
As a reactant, the oxidation number of the elemental chlorine, chloride and chlorate are 0, 1 and +5, respectively. Therefore, chlorine has been oxidized to chlorate whereas; it has been reduced to chloride [19].

Indium has three oxidation states 0,+1 and +3. The standard reduction potentials of all half reactions are:  $E^\circ_{In^{3+}/In^+} = -0.434V$ ,  $E^\circ_{In^+/In} = -0.147V$ ,  $E^\circ_{In^{3+}/In} = -0.338V$ . According to the standard reduction potentials, disproportionation reaction of  $In^+$  is spontaneous. All combinational probability for the set  $S = \{In, In^+, In^{3+}\}$  to do without energy can be displayed as Table 4.

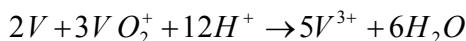
**Table 4.** Dismutation Reactions  $In$ .

$\oplus$	$In$	$In^+$	$In^{3+}$
$In$	$In$	$In, In^+$	$In, In^{3+}$
$In^+$	$In, In^+$	$In, In^{3+}$	$In^+, In^{3+}$
$In^{3+}$	$In, In^{3+}$	$In^+, In^{3+}$	$In^{3+}$

Then,  $(S, \oplus)$  is weak associative. Clearly,  $\oplus$  is commutative. Also, the reproduction axiom holds. Therefore,  $(S, \oplus)$  is a commutative  $H_v$ -group [7]. Vanadium forms a number of different ions including  $V, V^{2+}, V^{3+}, VO^{2+}$  and  $VO_2^+$ . The oxidation states of these species are 0, +2, +3, +4 and +5, respectively. The standard reduction potentials of all corresponding half reactions are:



All combinational probability for the set  $S = \{V, V^{2+}, V^{3+}, VO^{2+}, VO_2^+\}$  to do without energy in acidic media can be displayed as following table. When the reactants are added in appropriate stoichiometric ratios. For example vanadium( $V$ ) reacts with  $VO^{2+}$  as follows:



Then,  $(S, \oplus)$  is a hyperstructure. The hyperstructures

$$(\{V, V^{2+}\}, \oplus), (\{V^{2+}, V^{3+}\}, \oplus), (\{V^{3+}, VO^{2+}\}, \oplus) \text{ and } (\{VO^{2+}, VO_2^+\}, \oplus)$$

are hypergroups [7]. Moreover, we have:

$$(\{V, V^{2+}\}, \oplus) \cong (\{V^{2+}, V^{3+}\}, \oplus) \cong (\{V^{3+}, VO^{2+}\}, \oplus) \cong (\{VO^{2+}, VO_2^+\}, \oplus).$$

The major products between all forms of vanadium are showed in Table 6. It is assumed the reactants are added together in 1 : 1 mole ratios.

**Table 5.** Vanadium.

$\oplus$	$V$	$V^{2+}$	$V^{3+}$	$VO^{2+}$	$VO_2^+$
$V$	$V$	$V, V^{2+}$	$V^{2+}$	$V^{2+}, V^{3+}$	$V^{3+}$
$V^{2+}$	$V, V^{2+}$	$V^{2+}$	$V^{2+}, V^{3+}$	$V^{3+}$	$V^{3+}, VO^{2+}$
$V^{3+}$	$V^{2+}$	$V^{2+}, V^{3+}$	$V^{3+}$	$V^{3+}, V^{2+}$	$VO^{2+}$
$VO^{2+}$	$V^{2+}, V^{3+}$	$V^{3+}$	$V^{3+}, VO^{2+}$	$VO^{2+}$	$VO^{2+}, VO_2^+$
$VO_2^+$	$V^{3+}$	$V^{3+}, VO^{2+}$	$VO^{2+}$	$VO^{2+}, VO_2^+$	$VO_2^+$

**Table 6.** The Major Products between all Forms of Vanadium.

$\oplus$	$V$	$V^{2+}$	$V^{3+}$	$VO^{2+}$	$VO_2^+$
$V$	$V$	$V, V^{2+}$	$V, V^{2+}$	$V^{2+}$	$V^{2+}, V^{3+}$
$V^{2+}$	$V, V^{2+}$	$V^{2+}$	$V^{2+}, V^{3+}$	$V^{3+}$	$V^{3+}, VO^{2+}$
$V^{3+}$	$V, V^{2+}$	$V^{2+}, V^{3+}$	$V^{3+}$	$V^{3+}, VO^{2+}$	$VO^{2+}$
$VO^{2+}$	$V^{2+}$	$V^{3+}$	$V^{3+}, VO^{2+}$	$VO^{2+}$	$VO^{2+}, VO_2^+$
$VO_2^+$	$V^{2+}, V^{3+}$	$V^{3+}, VO^{2+}$	$VO^{2+}$	$VO^{2+}, VO_2^+$	$VO_2^+$

Therefore,  $(S, \oplus)$  is a hyperstructure. The hyperstructures

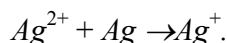
$(\{V, V^{2+}\}, \oplus)$ ,  $(\{V^{2+}, V^{3+}\}, \oplus)$ ,  $(\{V^{3+}, VO^{2+}\}, \oplus)$  and  $(\{VO^{2+}, VO_2^+\}, \oplus)$  are hypergroups. Moreover, we have:

$$(\{V, V^{2+}\}, \oplus) \cong (\{V^{2+}, V^{3+}\}, \oplus) \cong (\{V^{3+}, VO^{2+}\}, \oplus) \cong (\{VO^{2+}, VO_2^+\}, \oplus).$$

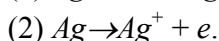
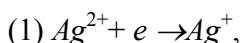
### 3.3 REDOX REACTIONS

Redox (reduction-oxidation) reactions include all chemical reactions in which atoms have their oxidation state changed. This can be either a simple redox process, such as the oxidation of carbon to yield carbon dioxide ( $CO_2$ ) or the reduction of carbon by hydrogen to yield methane ( $CH_4$ ), or a complex process such as the oxidation of glucose ( $C_6H_{12}O_6$ ) in the human body through a series of complex electron transfer processes. Oxidation is the loss of electrons or an increase in oxidation state, and reduction is the gain of electrons or a decrease in oxidation state by an analyte (molecule, atom or ion). There can not be an oxidation reaction without a reduction reaction happening simultaneously. Therefore the oxidation alone and the reduction alone are each called a half-reaction, because two half reactions always occur together to form a whole reaction [23].

Each half-reaction has a standard reduction potential ( $E^0$ ), which is equal to the potential difference at equilibrium under standard conditions of an electrochemical cell in which the cathode reaction is the half-reaction considered, and the anode is a standard hydrogen electrode (SHE). For a redox reaction, the potential of the cell is defined by:  $E^0_{cell} = E^0_{cathode} - E^0_{anode}$ . If the potential of a redox reaction ( $E^0_{cell}$ ) is positive, this reaction will be spontaneous [23]. For example, consider the redox reaction of  $Ag^{2+}$  with  $Ag$ :



We can write two half-reactions for this reaction:



The  $E^0$  of the first reaction ( $E^0_{cathode}$ ) is 1.98 V (vs. SHE) and the  $E^0$  of the second reaction ( $E^0_{anode}$ ) is 0.799 V (vs. SHE) [26]. Therefore, in this case, the  $E^0_{cell} (E^0_{cathode} - E^0_{anode} = 1.181)$  is positive and the above redox reaction between  $Ag^{2+}$  and  $Ag$  is spontaneous. Silver ( $Ag$ ) is a transition metal and has a large number of applications in jewelry, electrical contacts and conductors, catalysis of chemical reactions, disinfectants and microbiocides. Silver plays no known natural biological role in humans and itself is not toxic, but most silver salts are toxic, and some may be carcinogenic.  $Ag$  can be in three oxidation states:  $Ag(0)$ ,  $Ag(I)$  and  $Ag(II)$ . Among  $Ag(I)$  and  $Ag(II)$ ,  $Ag(I)$  is very well characterized and many simple ionic compounds are known containing  $Ag^+$ . However,  $AgF_2$  is known in which  $Ag$  has an oxidation state of  $II$  in it.  $AgF_2$  is strongly oxidizing and a good fluorinating agent. But  $Ag(II)$  is more stable in complex forms. A number of  $Ag(II)$  complexes have been obtained by oxidation of  $Ag(I)$  salts in aqueous solution in the presence of the ligand. For example,  $[Ag(pyridine)_4]^{2+}$  and  $[Ag(bipyridine)_2]^{2+}$  are quite stable. The  $+1$  oxidation state is the best known oxidation state of silver.  $Ag^+$  salts are generally insoluble in water with the exception of nitrate, fluoride and perchlorate. Most stable  $Ag(I)$  complexes have a linear structure [25].

As described above,  $Ag$  species with different oxidation states can react with themselves. All possible products for spontaneous reactions are presented in Table 7.

**Table 7.** Redox Reactions  $Ag$ .

$\oplus$	$Ag^{2+}$	$Ag^+$	$Ag$
$Ag^{2+}$	$Ag^{2+}$	$Ag^+, Ag^{2+}$	$Ag^+$
$Ag^+$	$Ag^+, Ag^{2+}$	$Ag^+$	$Ag, Ag^+$
$Ag$	$Ag^+$	$Ag^+, Ag$	$Ag$

The Table 7 is isomorphic to Table 3 of dismutation reactions. Therefore,  $\oplus$  is weak associative. Also, we conclude that  $(\{Ag^{2+}, Ag^+\}, \oplus)$  and  $(\{Ag^+, Ag\}, \oplus)$  are hypergroups.



Copper (*Cu*) is a ductile metal with very high thermal and electrical conductivity. It is used as a conductor of heat and electricity, a building material, and a constituent of various metal alloys. *Cu* can be in four oxidation states: *Cu* (0), *Cu*(I), *Cu* (II) and *Cu* (III). In nature, copper mainly is as *CuFeS<sub>2</sub>*, with oxidation state of II for *Cu*. Also, *Cu* can be as *Cu<sub>2</sub>S* or *Cu<sub>2</sub>O* with the oxidation state of I. Pure copper is obtained by electrolytic refining using sheets of pure copper as cathode and impure copper as anode. In this process different ions of *Cu*, *Cu*(II) or *Cu*(I), reduced to *Cu*(0) at cathode. *Cu*(III) is generally uncommon, however some of its complexes are known [25].

The standard reduction potential ( $E^0$ ) for conversion of each oxidation state to another are:  $E^0 (Cu^{3+}/Cu^{2+}) = 2.4 V$ ,  $E^0 (Cu^{2+}/Cu^+) = 0.153 V$ ,  $E^0 (Cu^{2+}/Cu) = 0.342 V$  and  $E^0 (Cu^+/Cu) = 0.521 V$ , where potentials are versus SHE [26]. According to these standard potentials, and similar to example of *Ag*, the following reactions are spontaneous:

- (1)  $Cu^{3+} + Cu^+ \rightarrow Cu^{2+}$ ,
- (2)  $Cu^{3+} + Cu \rightarrow Cu^{2+} + Cu^+$ .

Therefore, all possible products in reactions between oxidation states of *Cu* which can be produced spontaneously are listed in Table 8.

**Table 8.** Redox Reactions *Cu*.

$\odot$	<i>Cu</i>	<i>Cu</i> <sup>+</sup>	<i>Cu</i> <sup>2+</sup>	<i>Cu</i> <sup>3+</sup>
<i>Cu</i>	<i>Cu</i>	<i>Cu</i> , <i>Cu</i> <sup>+</sup>	<i>Cu</i> <sup>2+</sup> , <i>Cu</i>	<i>Cu</i> <sup>2+</sup> , <i>Cu</i> <sup>+</sup>
<i>Cu</i> <sup>+</sup>	<i>Cu</i> , <i>Cu</i> <sup>+</sup>	<i>Cu</i> <sup>+</sup>	<i>Cu</i> <sup>2+</sup> , <i>Cu</i> <sup>+</sup>	<i>Cu</i> <sup>2+</sup>
<i>Cu</i> <sup>2+</sup>	<i>Cu</i> , <i>Cu</i> <sup>2+</sup>	<i>Cu</i> <sup>2+</sup> , <i>Cu</i> <sup>+</sup>	<i>Cu</i> <sup>2+</sup>	<i>Cu</i> <sup>2+</sup> , <i>Cu</i> <sup>3+</sup>
<i>Cu</i> <sup>3+</sup>	<i>Cu</i> <sup>+</sup> , <i>Cu</i> <sup>2+</sup>	<i>Cu</i> <sup>2+</sup>	<i>Cu</i> <sup>2+</sup> , <i>Cu</i> <sup>3+</sup>	<i>Cu</i> <sup>3+</sup>

In Table 8, the hyperoperation  $\odot$  is weak associative. Hence, we have an *H*-semigroup. The hyperstructures

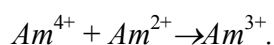
$$(\{Cu, Cu^+\}, \odot), (\{Cu, Cu^{2+}\}, \odot), (\{Cu^+, Cu^{2+}\}, \odot) \text{ and } (\{Cu^{2+}, Cu^{3+}\}, \odot)$$

are hypergroups. Let *H* be a set with three elements. On *H*, we define the following hyperoperation:  $x \star y = \{x, y\}$ , for all  $x, y \in H$ .

It is easy to see that  $\star$  is associative and so (*H*,  $\star$ ) is a hypergroup. Now, we have

$$(\{Cu, Cu^+, Cu^{2+}\}, \odot) \cong (H, \star).$$

Note that  $(\{Cu^+, Cu^{2+}, Cu^{3+}\}, \odot)$  is not semihypergroup. Americium (*Am*) is a transuranic radioactive chemical element in actinide series. It has four oxidation states of 0, 2, 3 and 4. The standard reduction potential ( $E^0$ ) for conversion of each oxidation state to another are:  $E^0 (Am^{4+}/Am^{3+}) = 2.6 V$ ,  $E^0 (Am^{3+}/Am^{2+}) = -2.3 V$ ,  $E^0 (Am^{3+}/Am) = -2.048 V$  and  $E^0 (Am^{2+}/Am) = -1.9 V$ , where potentials are versus SHE [26]. Therefore, the following reaction is spontaneous:



Therefore, all possible combinations for different oxidation states of  $Am$  which can be produced without energy are presented in Table 9.

**Table 9.** Redox Reactions  $Am$ .

$\otimes$	$Am$	$Am^{2+}$	$Am^{3+}$	$Am^{4+}$
$Am$	$Am$	$Am, Am^{2+}$	$Am, Am^{3+}$	$Am, Am^{4+}$
$Am^{2+}$	$Am, Am^{2+}$	$Am^{2+}$	$Am^{2+}, Am^{3+}$	$Am^{3+}$
$Am^{3+}$	$Am, Am^{3+}$	$Am^{2+}, Am^{3+}$	$Am^{3+}$	$Am^{3+}, Am^{4+}$
$Am^{4+}$	$Am, Am^{4+}$	$Am^{3+}$	$Am^{3+}, Am^{4+}$	$Am^{4+}$

Regarding to Table 9, similar to Table 8, we have

$$(\{Am, Am^{2+}, Am^{3+}\}, \otimes) \cong (H, \star).$$

Note that  $(\{Am^{2+}, Am^{3+}, Am^{4+}\}, \otimes)$  is not semihypergroup.

Gold ( $Au$ ) is a dense, soft, shiny, malleable and ductile metal and can be in four oxidation states of  $Au$  (0),  $Au$  (I),  $Au$  (II) and  $Au$  (III).  $Au$  (III) is common for gold compounds and exist as:  $Au_2O_3$ ,  $AuF_3$ ,  $AuCl_3$ ,  $AuBr_3$  and  $Au(OH)_3$ .  $Au$  (I) is much less stable in solution and is stabilized in complexes [25].

The standard reduction potential ( $E^0$ ) for conversion of each oxidation state to another are:  $E^0(Au^{3+}/Au^+) = 1.401 V$ ,  $E^0(Au^{3+}/Au) = 1.498 V$ ,  $E^0(Au^{2+}/Au^+) = 1.8 V$  and  $E^0(Au^+/Au) = 1.692 V$ , where potentials are versus SHE [26]. According to these standard potentials, the following reaction is spontaneous:



Therefore, the major products in reactions between oxidation states of  $Au$  which can be produced spontaneously are listed in Table 10.

**Table 10.** Redox Reactions  $Au$ .

$\cup$	$Au$	$Au^+$	$Au^{2+}$	$Au^{3+}$
$Au$	$Au$	$Au, Au^+$	$Au^+$	$Au, Au^{3+}$
$Au^+$	$Au, Au^+$	$Au^+$	$Au^+, Au^{2+}$	$Au^+, Au^{3+}$
$Au^{2+}$	$Au^+$	$Au^+, Au^{2+}$	$Au^{2+}$	$Au^{2+}, Au^{3+}$
$Au^{3+}$	$Au, Au^{3+}$	$Au^+, Au^{3+}$	$Au^{2+}, Au^{3+}$	$Au^{3+}$

The  $H_v$ -semigroups defined in Tables 9 and 10 are isomorphic.

## REFERENCES

1. S. C. Chung, K. M. Chun, N. J. Kim, S. Y. Jeong, H. Sim, J. Lee and H. Maeng, Chemical hyperalgebras for three consecutive oxidation states of elements, *MATCH Communications in Mathematical and in Computer Chemistry* **72** (2014) 389–402.
2. P. Corsini, Prolegomena of Hypergroup Theory, Second edition, Aviani Editore, 1993.
3. P. Corsini and V. Leoreanu, Applications of Hyperstructures Theory, *Advances in Mathematics, Kluwer Academic Publisher*, 2003.
4. B. Davvaz, Polygroup Theory and Related Systems, World Scientific Publishing Co. Pte. Ltd., Hackensack, NJ, 2013.
5. B. Davvaz, A brief survey of the theory of  $H_V$ -structures, Proc. 8th International Congress on Algebraic Hyperstructures and Applications, 1–9 September, 2002, Samothraki, Greece, *Spanidis Press*, 2003, 39–70.
6. B. Davvaz and A. Dehghan-Nezad, Chemical examples in hypergroups, *Ratio Matematica* **14** (2003) 71–74.
7. B. Davvaz, A. Dehghan-Nezhad and A. Benvidi, Chemical hyperalgebra: dismutation reactions, *MATCH Communications in Mathematical and in Computer Chemistry* **67** (2012) 55–63.
8. B. Davvaz, A. Dehghan-Nezad and A. Benvidi, Chain reactions as experimental examples of ternary algebraic hyperstructures, *MATCH Communications in Mathematical and in Computer Chemistry* **65** (2) (2011) 491–499.
9. B. Davvaz and A. Dehghan-Nezhad, Dismutation reactions as experimental verifications of ternary algebraic hyperstructures, *MATCH Communications in Mathematical and in Computer Chemistry* **68** (2012) 551–559.
10. B. Davvaz, A. Dehghan-Nezad and M. M. Heidari, Inheritance examples of algebraic hyperstructures, *Information Sciences* **224** (2013) 180–187.
11. A. Dehghan-Nezhad, S. M. Moosavi-Nejad, M. Nadjafikhah and B. Davvaz, A physical example of algebraic hyperstructures: Leptons, *Indian Journal of Physics* **86** (11) (2012) 1027–1032.
12. B. Davvaz, A. Dehghan-Nezad and M. Mazloun-Ardakani, Chemical hyperalgebra: Redox reactions, *MATCH Communications in Mathematical and in Computer Chemistry* **71** (2014) 323–331.
13. B. Davvaz, A. Dehghan-Nezad and M. Mazloun-Ardakani, Describing the algebraic hyperstructure of all elements in radiolytic processes in cement medium, *MATCH Communications in Mathematical and in Computer Chemistry* **72** (2) (2014) 375–388.

14. B. Davvaz and V. Leoreanu-Fotea, *Hyperring Theory and Applications*, *International Academic Press*, **115**, Palm Harbor, USA, 2007.
15. B. Davvaz, R. M. Santilli and T. Vougiouklis, Studies of multivalued hyperstructures for the characterization of matter-antimatter systems and their extension, *Algebras Groups and Geometries*, **28** (3) (2011) 105–116.
16. B. Davvaz, R. M. Santilli and T. Vougiouklis, Multi-Valued Hypermathematics for Characterization of Matter and Antimatter Systems, *Journal of Computational Methods in Sciences and Engineering (JCMSE)*, **13** (2013) 37–50.
17. B. Davvaz, R. M. Santilli and T. Vougiouklis, Mathematical prediction of Ying's twin universes, *American Journal of Modern Physics* **4** (3) (2015) 5–9.
18. M. Ghadiri, B. Davvaz and R. Nekouian, Hv-Semigroup structure on  $F_2$ -offspring of a gene pool, *International Journal of Biomathematics* **5** (4) (2012) 1250011 (13 pages).
19. C. Harding, D.A. Johnson, R. Janes, *Elements of the P Block*, Published by Royal Society of Chemistry, 2002.
20. Š. Hošková, J. Chvalina and P. Račková, Transposition hypergroups of Fredholm integral operators and related hyperstructures. *Part I*, *Journal of Basic Science*, **4** (2008) 43–54.
21. Š. Hošková, J. Chvalina and P. Račková, Transposition hypergroups of Fredholm integral operators and related hyperstructures. *Part II*, *G. Journal of Basic Science* **4** (2008) 55–60.
22. R.T. Morrison and R. N. Boyd, *Organic Chemistry*, Sixth Edition, Prentice-Hall Inc., 1992.
23. Mortimer, C. E., *Chemistry: A Conceptual Approach*, 4<sup>th</sup> ed., D. Van Nostrand Co., New York, 1979.
24. R.M. Santilli and T. Vougiouklis, Isotopies, genotopies, hyperstructures and their applications, *New frontiers in hyperstructures*, *New frontiers in hyperstructures* (Molise, 1995), 1–48, Ser. New Front. Adv. Math. Ist. Ric. Base, Hadronic Press, Palm Harbor, FL, 1996.
25. M.S. Sethi and M. Satake, *Chemistry of Transition Elements*, *South Asian Publishers*, New Delhi, 1988.
26. D.A. Skoog D.M. West and F.J. Holler, *Saunders College Publishing*, New York, 1992.
27. International Union of Pure and Applied Chemistry. “disproportionation”. Compendium of Chemical Terminology Internet edition, <http://en.wikipedia.org/wiki/Disproportionation>.

28. T. Vougiouklis, The fundamental relation in hyperrings. The general hyperfield, *Algebraic Hyperstructures and Applications* (Xanthi, 1990), 203–211, World Sci. Publishing, Teaneck, NJ, 1991.
29. T. Vougiouklis, A new class of hyperstructures, *Journal of Combinatorics, Information & System Sciences* **20** (1995) 229–235.
30. T. Vougiouklis,  $H_v$ -groups defined on the same set, *Discrete Mathematics* **155** (1996) 259–265.
31. T. Vougiouklis, Convolutions on WASS hyperstructures, *Combinatorics* (Rome and Montesilvano, 1994). *Discrete Mathematics* **174** (1997) 347–355.
32. T. Vougiouklis, *Hyperstructures and their Representations*, Hadronic Press Inc., **115**, Palm Harbor, 1994.



**ABSTRACTS  
IN  
PERSIAN**





# Type-Itemized Enumeration of RS-Stereoisomers of Octahedral Complexes

SHINSAKU FUJITA

Shonan Institute of Chemoinformatics and Mathematical Chemistry, Kaneko 479-7

Ooimachi, Ashigara-Kami-Kanagawa-Ken, 258-0019 Japan

## شمارش نوع آرایش RS-ایزومرهای فضایی مجتمع‌های هشت‌وجهی

ادیتور(رابط): علی (رضا) اشرفی

### چکیده

ایزومرهای فضایی مجتمع‌های هشت‌وجهی، تحت عمل گروه‌های RS-ایزومتریکی فضایی متناظر با آن، به پنج نوع (نوع I تا نوع V) طبقه‌بندی شده‌اند. شمارش آن‌ها در نوع خاصی انجام می‌شود که در آن، روش پیشرفته فوجیتا، دراصل برای شمارش ترکیبی تحت گروه‌های نقطه‌ای، برای پاسخگویی به نیاز رویکرد پیشرفته فوجیتا گسترش می‌یابد. شاخص چرخه با تناسب آرایش‌بندی فضایی (CL-CF) از گروه نقطه‌ای  $O_h$ ، با در نظر گرفتن CL-CF برای محاسبه‌ی نوع V چهارگانه‌ی موجود در ایزوگرام‌های فضایی مدوله شده است. مدوله CL-CF با CL-CF از حداکثر گروه نقطه‌ای آرایش‌بندی فضایی (O)، یک CL-CF از حداکثر گروه RS-جایگشت، یک CL-CF از گروه بازتاب لیگاند و یک CL-CF از گروه RS-ایزومتریکی فضایی برای تولید CL-CFS برای ارزیابی نوع I به نوع V چهارگانه، ترکیب شده است. با معرفی توابع موجودی لیگاند به CL-CFS، تعداد چهارگانه‌های مجتمع‌های هشت‌وجهی به‌دست آمده و به شکل جداولی نشان داده شده است. چند ایزوگرام فضایی برای مجتمع‌های معمولی به تصویر کشیده شده است. شاخص‌های پیکربندی و توصیف‌گرهای C/A، براساس رویکرد ایزوگرام فضایی فوجیتا مورد بحث قرار گرفته است.

لغات کلیدی: شمارش، ایزوگرام فضایی، مجتمع هشت‌وجهی، گروه RS-ایزومریکی فضایی.

# Half-Century Journey from Synthetic Organic Chemistry to Mathematical Stereochemistry through Chemoinformatics

SHINSAKU FUJITA

ShonanInstitute of Chemoinformatics and Mathematical Chemistry, Kaneko 479-7

OOIMACHI, ASHIGARA-KAMI-GUN, KANAGAWA-KEN, 258-0019 JAPAN

## نیم قرن سفر، از شیمی آلی مصنوعی به ریاضی-شیمی فضایی از طریق شیمی داده‌ورزی

ادیتور رابط: علی رضا اشرفی

### چکیده

نیم قرن سفر من، از شیمی آلی مصنوعی آغاز شد. در مرحله‌ی اول از این سفر، علاقه‌ام به شیمی فضایی از طریق تداخل اثرات فضایی در واسطه‌ی واکنش، سیلوفان‌ها، هتروسیکل‌های فشرده و ترکیبات آلی برای عکاسی آغاز شد. در قسمت دوم از این سیر و سفر علمی در شیمی داده‌ورزی، ساختارهای انتقال موهومی (*ITSs*) را تحت عنوان بازنمایی کامپیوتری از واکنش‌های آلی مطرح کردم. علاقه‌ی من به حمله به شمارش ترکیبیاتی از طریق تحقیق در شمارش زیرگراف‌های *ITSs* تحریک شده بود. در انتهای این سفر، از کنار هم قرار دادن شیمی فضایی و شمارش ترکیبیاتی که از علایق من بوده‌اند، به ریاضی-شیمی فضایی رسیدم. رویکرد شاخص چرخه‌ی فرعی واحد فوجیتا، روش پیشرفته فوجیتا و رویکرد استریایزوگرافی فوجیتا، توسعه یافت به طوری که ادغام روش و انت هوف (نامتقارن، استرس‌زایی) و روش لی بل (عدم تقارن، آرایش‌بندی فضایی) باعث سردرگمی مستمر در تاریخ شیمی فضایی شده است.

لغات کلیدی: کروی، شمارش ترکیبی، استریایزوگرافی، شیمی فضایی.

# *Enumeration of conformers of octahedral $[M(ABC)_6]$ complex on the basis of computational group theory*

HIROSHI SAKYAMA AND ANTSUSHI WAKI

Department of Material and Biological Chemistry, Faculty of Science, Yamagata University, Japan

Department of Mathematical Sciences, Faculty of Science, Yamagata University, Japan

## شمارش سازندگان مجتمع هشتوجهی $[M(ABC)_6]$ بر اساس نظریه‌ی گروه محاسباتی

ادیتوررابطا: مسن یوسفی آذری

### چکیده

سازندگان مجتمع  $[M(ABC)_6]$  براساس نظریه‌ی گروه محاسباتی، برشمرده شده‌اند که در آن،  $M$  فلز اصلی است و  $ABC$  لیگاندی است که به  $M$  از طریق  $A$  محدود شده است. بر اساس 16 سازنده از واحد هسته‌ی  $M(AB)$ ، 7173 سازنده برای مجتمع  $[M(ABC)_6]$  یافت شده است که به 9 گروه نقطه‌ای  $D_{3d}$ ، 1،  $D_3$ ، 4،  $S_6$ ، 4،  $C_{2h}$ ، 5،  $C_3$ ، 7،  $C_2$ ، 182،  $C_s$ ، 15،  $23C_i$  و  $6932C_1$  اختصاص داده شده‌اند.

لغات کلیدی: شمارش، سازنده، مجتمع هشتوجهی  $[M(ABC)_6]$ ، نظریه‌ی گروه محاسباتی.

## *QSPR modeling of heat capacity, thermal energy and entropy of aliphatic Aldehydes by using Topological Indices and MLR method*

A. ALAGHEBANDI<sup>1</sup> AND F. SHAFIEI<sup>\*,2</sup>

Department of Chemistry, Science Faculty, Arak Branch, Islamic Azad University,

Arak, Iran

### مدل سازی ارتباط کمی ساختار-خاصیت ظرفیت گرمایی، انرژی گرمایی و گشتاور آلدئیدهای چربی‌دار با استفاده از شاخص‌های توپولوژیکی و رگرسیون قطعی چندمتغیره

ادیتور رابطا : ایوان گوتمن

#### چکیده

مدل‌های کمی ساختار-خاصیت در فهمیدن ارتباط ساختار شیمیایی با خواص فیزیکی شیمیایی مواد طبیعی و سنتزی مفید می‌باشند. در مطالعه حاضر، کاربرد شاخص‌های توپولوژیکی برای مطالعه ارتباط کمی ساختار-خاصیت 24 آلدئید مورد آزمون قرار گرفته است. شاخص‌های توپولوژیکی مورد استفاده عبارتند از: شاخص راندیک اتصال یک ( $1\chi$ )، بالابان (J)، وینر (W) و هاراری (H). در این مطالعه، ارتباط بین شاخص‌های توپولوژیکی با انرژی گرمایی، ظرفیت گرمایی و گشتاور 24 آلدئید با استفاده از نرم‌افزار گوسین 98 و یکی از روش‌های آغازین، هارتری-فاک و سری پایه 6-31G محاسبه گردید. سپس به منظور مطالعه رابطه کمی ساختار-خاصیت از نرم‌افزار آماری SPSS، روش برگشتی و رگرسیون خطی چند متغیره (MLR) استفاده شد. بدین طریق معین گردید که برای پیشگویی کمیت ظرفیت گرمایی در حجم ثابت (CV) آلدئیدهای مورد مطالعه ترکیبی از سه توصیفگر توپولوژیکی ( $J$ ,  $W$ ,  $1\chi$ )، برای تخمین و پیشگویی کمیت آنتروپی (S) ترکیبی از دو توصیفگر توپولوژیکی ( $J$ ,  $1\chi$ )، و جهت پیشگویی انرژی گرمایی (Eth) شاخص راندیک اتصال یک ( $1\chi$ ) مناسب هستند.

لغات کلیدی: شاخص‌های توپولوژیکی، آلدئیدها، بررسی کمی ساختار-خاصیت، روش رگرسیون خطی چندمتغیره.

## *On the Mark and Markaracter Tables of Finite Groups*

M. GHORBANI

Department of mathematics, Shahid Rajaei Teacher Training University

### جدول نمره و نمرشت گروه‌های متناهی

ادیتور (رابطه): علیرضا اشرفی

#### چکیده

فرض کنید  $G$  یک گروه متناهی باشد و  $C(G)$  یک خانواده از زیرگروه‌های دوبدو غیر مزودج از  $G$  باشد. ماتریسی که درایه  $KH$ -ام آن تعداد نقاط ثابت مجموعه  $G/K$  تحت عمل  $H$  است را جدول نمره  $G$  می‌نامیم که در آن  $H$  و  $K$  عناصر  $C(G)$  هستند. شینساکو فوجیتا برای اولین بار واژه نمرشت را تعریف کرد تا نمره نمایش‌های جایگشتی و سرشت‌های نمایش‌های خطی را همزمان مورد مطالعه قرار دهد. در این مقاله ما این جداول را برای کلاس‌های خاصی از گروه‌های متناهی به دست می‌آوریم.

لغات کلیدی: عمل گروه، گروه خودریختی، جدول نمره، جدول نمرشت.

## *Weak algebraic hyperstructures as a model for interpretation of chemical reactions*

B. DAVVAZ

Department of Mathematics, Yazd University, Yazd, Iran

### ابرساختارهای جبری ضعیف به عنوان یک مدل برای تفسیر واکنش‌های شیمیایی

ادیتور (رابطه): علیرضا اشرفی

#### چکیده

ابرساختارهای جبری ضعیف یا  $H_v$ -ساختارها، تعمیمی از ابرساختارهای جبری شناخته‌شده (نیم‌ابروگروه‌ها، ابرگروه‌ها و ...) هستند. هدف اصلی این مقاله، ارائه یک مقدمه از برخی نتایج، روش‌ها و ایده‌ها درباره مثال‌های شیمیایی ابرساختارهای جبری ضعیف است. در این مقاله، بعد از معرفی تعاریف و نتایج اساسی از ابرساختارهای جبری ضعیف، به مرور مطالب زیر می‌پردازیم:

- (۱) ابرساختارهای جبری ضعیف مرتبط با واکنش‌های زنجیره‌ای
- (۲) ابرساختارهای جبری ضعیف مرتبط با واکنش‌های مصنوعی
- (۳) ابرساختارهای جبری ضعیف مرتبط با واکنش‌های مجدد.

**لغات کلیدی:** ابرساختارهای جبری ضعیف، ابرگروه،  $H_v$ -گروه، واکنش زنجیره‌ای، واکنش مصنوعی، واکنش مجدد.

این نشریه طبق مجوز شماره 89/3/11/104372 مورخه 89/11/27 دارای اعتبار علمی-پژوهشی از وزارت علوم ، تحقیقات و فناوری می باشد. همچنین این مجله در پایگاه اطلاعاتی ISC (Islamic World Science Citation Center) وابسته به وزارت علوم ، تحقیقات و فناوری نمایه می شود.

October 2016

## CONTENTS

Pages

Autobiography of Shinsaku Fujita S. Fujita	111
Type-itemized enumeration of RS-stereoisomers of octahedral complexes S. Fujita	113
Half-century journey from synthetic organic chemistry to mathematical stereochemistry through chemoinformatics S. Fujita	155
Enumeration of conformers of octahedral $[M(ABC)_6]$ complex on the basis of computational group theory H. Sakiyama and K. Waki	223
QSPR modeling of heat capacity, thermal energy and entropy of aliphatic aldehydes by using topological indices and MLR method A. Alaghebandi and F. Shafiei	235
On the mark and markaracter tables of finite groups M. Ghorbani	253
Weak algebraic hyperstructures as a model for interpretation of chemical reactions B. Davvaz	267

ISSN

2 2 2 8 - 6 4 8 9 ( Print Version )

2 0 0 8 - 9 0 1 5 ( Online Version )